Extracellular Vesicles within the Bone Marrow Niche

A novel way of communication between osteoblasts and hematopoietic progenitor cells

Jess Morhayim

ISBN: 9789462954618

Published articles presented in this thesis were adapted with permission from the publishers.

Cover art illustrates a cell secreting a heterogeneous group of extracellular vesicles.

Layout and design by Jess Morhayim
Cover art by Gizem Kuşçu
Printed by Uitgeverij BOXPress || proefschriftmaken.nl

Publication of this thesis was supported by:
Erasmus University Rotterdam

Extracellular Vesicles within the Bone Marrow Niche

A novel way of communication between osteoblasts and hematopoietic progenitor cells

Extracellulaire blaasjes in de beenmerg niche

Een nieuwe wijze van communicatie tussen osteoblasten en hematopoëtische stamcellen

Thesis

to obtain the degree of Doctor at
Erasmus University Rotterdam
on the authority of the
rector magnificus

Prof.dr. H.A.P. Pols

and in accordance with the decision of the Doctorate Board.

The public defence ceremony shall be held on
Wednesday, 7 September 2016 at 09:30 hours

by

Jess Morhayim
born in Istanbul, Turkey

Erasmus University Rotterdam

DOCTORAL COMMITTEE

Supervisors:	Prof.dr. J.P.T.M. van Leeuwen
	Prof.dr. J.J. Cornelissen
Other members:	Prof.dr. W.E. Fibbe
	Prof.dr. G.W. Jenster
	Prof.dr. J.H. Gribnau
Co-supervisor:	Dr.ing. H.J. van de Peppel

The work presented in this thesis was performed in the Departments of Internal Medicine and Hematology, Erasmus University Medical Center, Rotterdam, the Netherlands. This work was financially supported by a grant from the Dutch government to the Netherlands Institute for Regenerative Medicine (FES0908), Erasmus MC Stem Cell and Regenerative Medicine Institute and Erasmus University Medical Center. Next-generation RNA sequencing studies were performed in collaboration with the Department of Orthopedic Surgery at Mayo Clinic, Rochester, MN, USA, with the additional financial support provided by the US National Institutes of Health grants (R01-AR049069 and F32-AR066508).

In dedication to:

My dear parents for making me be who I am,
My loving husband Hugo for supporting me all the way,
And my greatest gift…my little prince Mateo.

TABLE OF CONTENTS

1

General Introduction

This chapter is based on:

"Extracellular vesicles: Specialized bone messengers"

by

Jess Morhayim, Marta Baroncelli and Johannes P. van Leeuwen

Archives of Biochemistry and Biophysics (2014), 561:38-45

1.1. OVERVIEW

Mammalian cells actively secrete factors that contribute to shape their microenvironment. These factors either travel freely or they are enclosed within the lipid bilayer of extracellular vesicles (EVs), and regulate the function of neighboring and distant cells. EVs are secreted by a wide spectrum of cell types and are found in various biological fluids. They convey their message by mediating the horizontal transfer of bioactive molecules, such as proteins, lipids and RNAs, between cells. Recent studies showed the vital roles of EVs in a wide range of physiological and pathophysiological processes. Throughout this chapter, we highlight the recent developments in the newly emerging EV field, including their biogenesis, molecular content and function. Moreover, we discuss the role of EVs in bone biology and their promising applications in diagnosis, drug development and regenerative therapy with particular focus on hematopoietic stem cell (HSC) therapy.

1.2. EXTRACELLULAR VESICLES

Multicellular organisms developed complex communication networks to regulate biological activities, and consequently maintain physiological homeostasis. Interruptions in intercellular communication lead to pathological complications and disease progression. Cells exchange information with each other via immobilized molecules as well as secreted factors. Traditionally, secreted factors include small soluble molecules, such as neurotransmitters, chemokines, cytokines and hormones, which can either act over short distances and affect the neighboring cells in a paracrine manner or travel long distances in an endocrine manner. The last couple of decades have witnessed the unprecedented dedication of scientists to the study of EVs as novel mediators of intercellular communication.

EVs had long been regarded as cellular debris until Wolf and colleagues described their biological significance in coagulation in 1967[1]. Later same year, Anderson and Bonucci reported the discovery of matrix vesicles as specialized EVs involved in biomineralization of the bone matrix[2,3]. Since then, EVs have been described to have a broad range of functions in development, immunology, angiogenesis and stem cell biology, as well as disease progression. EVs are considered to be bioactive organelles that carry genetic information in forms of lipids, proteins and nucleic acids between cells, and have effects on diverse molecular functions, such as signaling and regulation of gene expression of the target cells[4-8]. EVs embrace a heterogeneous group of vesicles, including microvesicles, microparticles, ectosomes, exosomes, shedding vesicles, apoptotic bodies and many others released under different biological circumstances. Even though the different names reflect their diversity in terms of biogenesis, structure, content and function, there are still conflicts over the definition and characterization of different vesicular structures. For simplicity, EVs are often categorized in three classes based on the well-defined processes for EV biogenesis: small vesicles (10-100 nm) released by exocytosis (exosomes, exosome-like vesicles), bigger vesicles (100-1,000 nm) formed by budding from the plasma membrane

(microvesicles, shed vesicles, matrix vesicles) and big vesicles (0.8-5 µm) released from dying cells (apoptotic bodies) (Fig. **1**)[8-10].

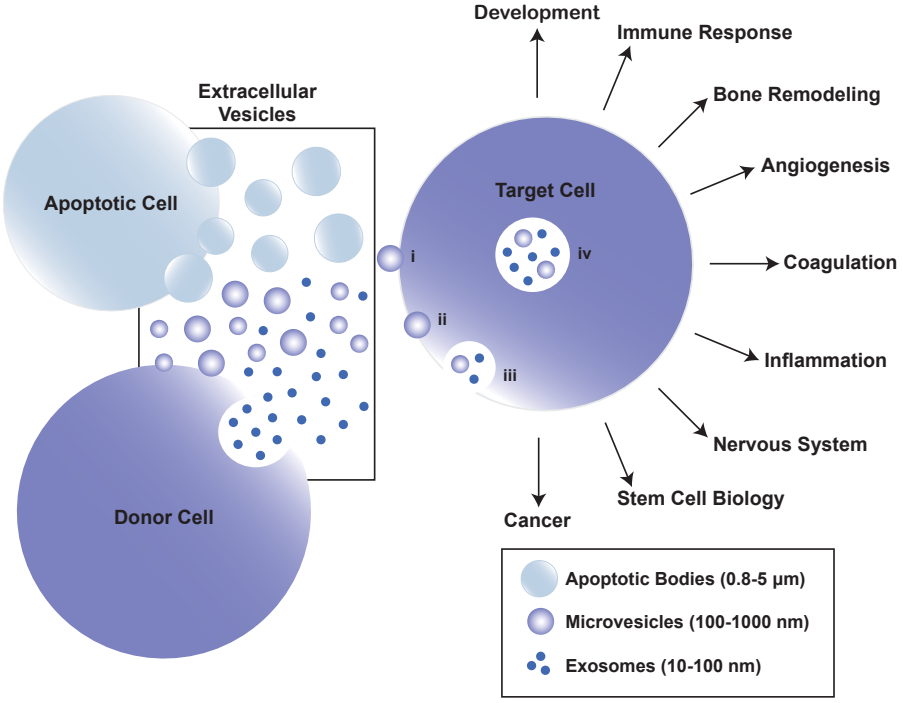

Figure 1. Schematic representation of EV release from donor cells and the interaction with the target cells. EVs are released either by exocytosis of the multivesicular bodies or direct budding from the plasma membrane. Apoptotic bodies are released from the breakdown of the apoptotic cells. EVs interact with their targets via i) signal transduction mediated by docking at the plasma membrane of the target cell and/ or via releasing the bioactive cargo upon ii) fusion or iii-iv) endocytosis followed by fusing with the delimiting membrane of the endosomal compartment. Interaction with target cells leads to a broad range of biological functions. Interaction with the target cell is only shown for microvesicles but exosomes and apoptotic bodies utilize similar mechanisms.

Cells release EVs either constitutively during their growth or upon activation by biological stimuli. Apoptotic and diseased cells also release EVs providing valuable information about the health state of the cell[10,11]. EVs have been detected in all studied cell types so far and most biological fluids, including blood, urine and breast milk[12-14]. Osteoblasts, the bone forming cells, also secrete EVs that have well characterized roles in mineralization[15]. There is increasing knowledge about the biological functions of EVs in other bone-related processes. Particularly, the regenerative role of mesenchymal stem cell-(MSC)-derived EVs makes them promising therapeutic agents for bone regenerative medicine[16-18]. In this chapter, we review the various roles of EVs in diverse aspects of intercellular communication and highlight their function in bone biology.

1.2.1. Isolation and characterization

With the rapid development of EV research, the optimization and standardization of isolation techniques have become of utmost importance to improve the understanding of EV biology. Currently, the most commonly applied EV isolation method relies on differential ultracentrifugation protocol developed by Thery and colleagues in 2006[19]. According to this protocol, biological fluids or the conditioned media from cultured cells are subjected to a series of centrifugation and ultracentrifugation steps to pellet the EVs. Cells break open at high speeds, and as a consequence cellular organelles and big protein complexes are co-isolated with EVs. Therefore, it is very important to start with a low centrifugation speed to remove floating and/ or dead cells, and perform serial centrifugation steps in increasing speeds to remove the contaminants in a step-wise fashion. Furthermore, it is crucial that the purified EV pellet is free of bovine serum contaminants, such as serum proteins and vesicles. For cell cultures it is common to use EV-depleted serum and/or serum-free medium treatment before EV collection. This becomes, indeed, more challenging with biological fluids. The duration and speed of each centrifugation step varies between different protocols based on the EV source. Large microvesicles and apoptotic bodies are commonly pelleted using 10,000g centrifugation, while smaller microvesicles and exosomes require high-speed centrifugation at about 100,000g[6,19]. The crude EV pellet can be subjected to further purification by sucrose density gradient or high performance liquid chromatography to remove possible contaminants. There have been attempts to separate EVs with different sizes based on their sediment density by sucrose density gradient. Recent studies have reported the sediment densities as the following: 1.11-1.21 g/ ml for exosomes[20-22], 1.25-1.30 g/ ml for microvesicles[23], and 1.18-1.28 g/ ml for apoptotic bodies[24]. However, some small microvesicles can have even lighter densities than exosomes making the separation of the different EV populations very difficult using the conventional techniques[6].

Purified EVs are commonly characterized by microscopic, biochemical and fluidic analyses. EVs can be visualized by electron microscopy, which gives clues about their size and morphology (Fig. **2A**). In the past, researchers used electron microscopy to verify the presence of exosomes based on their cup shape morphology; however, it was recently discovered that this was due to dehydration during sample processing[25,26]. Atomic force microscopy, on the other hand, allows samples to be in their native state, and hence it proves to be a better alternative to study the morphology of different EVs (Fig. **2B**)[27]. Other common methods to study EVs include western blot and flow cytometry analyses using known vesicle markers. On-going studies are focusing on identifying markers specific to unique EV classes. A major challenge of EV characterization is the accurate quantification. ELISA and immunoadsorption are possible methods to determine the abundance of EVs using known markers; however, they do not give comprehensive information about the total EV concentration[28]. Conventional flow cytometry is a useful technique to quantify big EVs, while accurate quantification of EVs smaller than 250 nm is difficult. Van der Vlist and colleagues developed a high-resolution flow cytometry-based technique that can be

used to detect smaller EVs based on their fluorescence intensity[29]. Recently, several companies developed techniques that allow multi-parameter analysis of EVs of certain size ranges providing greater accuracy than fluidic-based techniques. Nanoparticle tracking analysis measures concentration and absolute size distribution of particles as small as 50 nm based on their Brownian motion in fluids[27,30]. qNano is another method that uses nanopores to measure size distribution of EVs bigger than 100 nm[31].

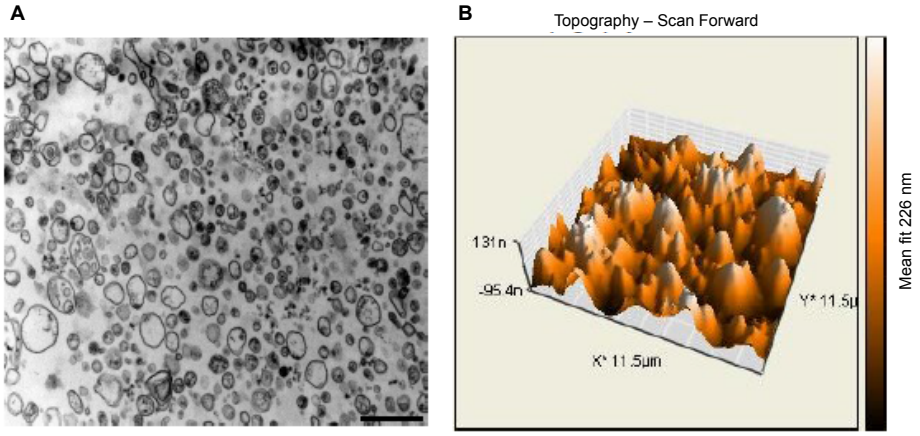

Figure 2. EV morphology and topography. EVs isolated from mineralizing human fetal pre-osteoblasts (SV-HFO cells) were fixed with glutaraldehyde and analyzed by A) transmission electron microscopy, scale bar: 500 nm, and B) atomic force microscopy (non-contact mode), scale bar: 223 nm. Both images show that EVs are heterogeneous in size and have spherical morphology.

1.2.2. Molecular composition

EVs are small cell fractions consisting of a lipid bilayer enclosed lumen that contains vesicular cargo, which is a selective combination of lipids, proteins and nucleic acids essential for EV structure and function. Even though the parent cell and EV biogenesis are the contributing factors to cargo differences, most of the structural cargo is shared among EVs released by different cells. Comprehensive understanding of the molecular composition of different EV populations is crucial to understand their molecular function. Proteomics, lipidomics, microarrays and deep sequencing analyses have been applied to characterize the molecular content of EVs from diverse cellular sources. ExoCarta and EVpedia are the two new databases that list the entire lipid, protein and RNA content of EVs described in the literature[32-37].

1.2.2.1. *Lipids*

EVs are formed by a specific selection of lipids organized in a bilayer membrane that provides structure and protects the bioactive cargo from degradation before they reach

their targets. Most EVs are enriched with structural lipids, such as cholesterol, sphingomyelin and phosphatidylserine, compared to the cellular plasma membrane[38-40]. The mode of biogenesis greatly affects the lipid composition of a given EV class. Exosomes are enriched with endosomal phospholipid bis-monoacylglycero-phosphate, whereas microvesicles contain plasma membrane levels of phosphatidylcholine and are devoid of phospholipid bis-monoacylglycero-phosphate[41,42]. Lipids are not only the structural elements of EVs but they also contribute to their bioactivity. Vesicular lipids play pivotal roles in EV biogenesis, release and interaction with other cells and biological function. Lipid rafts formed by cholesterol and sphingomyelin are shown to be important for clathrin pit formation that mediates exosome biogenesis[43]. These lipid rafts can also act as signaling complexes along with the lipid-associated proteins. Furthermore, exosomes contain prostaglandins and leukotrienes important to mediate cell signaling[44,45]. Transfer of vesicular lipids to recipient cells may lead to changes in cell homeostasis caused by the accumulation of lipids and their associated enzymes. For instance, T cells release EVs that upon uptake by monocytes result in cholesterol accumulation leading to phenotypic alterations[22].

1.2.2.2. *Proteins*

As with lipids, EVs are enriched with proteins that contribute to the biogenesis, structure, motility and the biological function of EVs. The most commonly identified protein cargo includes cytoskeletal proteins, tetraspanins, membrane and nuclear receptors, heat shock proteins, proteases, adhesion molecules, signaling molecules, metabolic enzymes, annexins, transporters and ion channels. Table **1** lists the top 25 identified EV proteins as described by ExoCarta[32,34]. Despite the large number of shared proteins among different EV classes, the mode of biogenesis determines the enrichment of endosomal-associated proteins and plasma membrane proteins in exosomes and microvesicles, respectively[5,46]. Tetraspanins that cluster at the site of exocytosis and plasma membrane budding act as sorting machineries to target proteins into EVs[47,48]. Chaperones, such as heat shock proteins coupled to tetraspanins, also aid in sorting lumen proteins. Cytoskeleton proteins are crucial for EV release, structure, and motility[49]. EVs are particularly enriched in cellular markers based on the cell of origin. For instance, tumor-EVs are enriched with metalloproteinases and other proteolytic enzymes involved in the digestion of extracellular matrix necessary for invasion and tumor progression[50,51].

1.2.2.3. *Nucleic acids*

The discovery of EV-associated nucleic acids with regulatory capacity greatly contributed to understand the role of EVs in gene-based cell communication. In late ‘90s, EVs co-isolated with viruses were already suggested to contain RNA[52]. A decade later, researchers found messenger RNA (mRNA) for chemokines and growth factors in tumor

EVs derived from different cancer cell lines[53]. In 2007, Valadi and colleagues showed that mast cell exosomes are enriched with microRNAs (miRNAs)[20]. Since then there have been a great amount of research demonstrating the presence of functional RNA molecules in EVs derived from cell cultures and biological fluids[54-59]. Bioanalyzer profiles showed that EVs are devoid of the cellular ribosomal RNA peaks, instead they are enriched with small RNAs[20]. Deep sequencing analyses identified mainly the presence of mRNAs and miRNAs but also other small non-coding RNA molecules, such as transfer RNA, Y RNA, vault RNA, small interfering RNA (siRNA), repeat sequences, structural RNA and RNA transcripts overlapping with protein coding regions, within EVs[60,61]. Turchinovich and colleagues demonstrated that miRNAs associated with the outer membrane of EVs also have important implications in EV function[62]. Even though most EV preparations are devoid of DNA, several groups reported the presence of functional DNA in apoptotic bodies secreted by cancer cells as a way of transferring their activated oncogenes[11,63].

Table 1. The most commonly identified EV proteins described in ExoCarta[a].

Protein Family	Gene Symbol
Heat Shock Proteins	*HSPA8* *HSP90AA1* *HSP90AB1*
Tetraspanins	*CD9* *CD63* *CD81*
Metabolic Enzymes	*ALDOA* *ENO1* *GAPDH* *LDHA* *PGK1* *PKM2*
Annexins	*ANXA2* *ANXA5*
Cytoskeletal and Associated Proteins	*ACTB* *ACTG1* *CFL1* *MSN*
Elongation Factors	*EEF1A1* *EEF2*
14-3-3 Family Proteins	*YWHAE* *YWHAZ*
Other	*ALB* *PDCD6IP* *SDCBP*

[a] ExoCarta: http://www.exocarta.org/

1.2.3. Biogenesis and cargo loading

In spite of the recent progress in elucidation of EV biology, the exact process of EV biogenesis and cargo sorting is still not known; however the amount of data is fortunately increasing. EVs are generated via diverse biological mechanisms triggered by microenvironmental stimuli, cellular activation, stress, transformation and programmed cell death. We know at least three distinct mechanisms of EV biogenesis: exocytosis, direct budding from the plasma membrane, and breakdown of dying cells, each leading to the release of distinct EV classes.

Exosomes and exosome-like vesicles are small vesicles (10-100 nm) that originate from exocytosis of multivesicular bodies (MVBs)[64,65]. Vesicle budding into exosomal MVB lumen is still under investigation, nevertheless there are studies suggesting that exosome formation follows a mechanism parallel to endosomal degradation pathway. Cellular cargo destined for degradation in lysosomes are selectively sorted into vesicles that bud into MVB lumen under the control of endosomal sorting complex required for receptor transport (ESCRT) and their associated proteins, such as ALIX and VPS4[66,67]. ESCRT subunits ESCRT-0, -I, and –II recognize and control the destination of ubiquitinated cargo proteins at the endosomal delimiting membrane. Silencing of ESCRT complex components and/or their associated proteins reduce exosome secretion suggesting that ESCRT-mediated sorting plays a role in exosome formation but possibly via a different mechanism than the degradation pathway[68]. Exosomes are also released in a lipid-dependent manner independently from the ESCRT pathway, depending on cell type and stimuli. Trajkovic and colleagues showed that ceramides that are concentrated around lipid-rafts of oligodendroglial cells sort exosomal cargo into vesicles and mediate budding into the MVB lumen[69]. The importance of lipids is further supported by the findings showing that that exosomal MVBs are rich in cholesterol and phosphatidylserine on the outer lipid leaflet, while degradative MVBs are cholesterol poor, but rich in lysobisphosphatidic acid[28]. There is evidence showing that cells can produce exosomes independently of both ESCRT complex and ceramides. For instance, tetraspanins are also suggested to play a role in exosome sorting[48]. The process of MVB fusion with plasma membrane and release of exosomes is still unclear. It is noted that exosome release process is a cytoskeleton dependent and p53-controlled process[70]. Furthermore, ESCRT-III subunit and GTPases, such as RAB5, RAB27 and RAB35, have been implicated to play roles in exosome release[6,71].

The molecular mechanisms of microvesicle and apoptotic body biogenesis are far less understood than exosome biogenesis. Direct budding from the plasma membrane releases a heterogeneous EV population with a size range between 100-1,000 nm[43]. These EVs are commonly referred to as microvesicles as well as shed vesicles, and to a lesser extent microparticles. Microvesicles contain a specific group of plasma membrane proteins suggesting that budding occurs at specific parts of the membrane. As with exosomes, cholesterol-rich lipid rafts enriched with ceramides, cholesterol and other lipids are described to be involved in biogenesis of microvesicles[72,73]. It has been reported that increase in cyto-

solic calcium leads to exposure of phosphatidylserine residues, which in turn causes budding from the plasma membrane[74]. Several reports suggest the involvement of the ESCRT complex indicating that microvesicle budding might be similar to exosome budding into MVBs[75]. Actin-based motors are also proposed to be involved in the detachment of the microvesicle bud from the plasma membrane[76]. Apoptotic bodies, large vesicles with a diameter range between 0.8-5 µm, are released from cellular breakdown of dying cells[10]. These EVs are usually engulfed by phagocytic cells and quickly removed before the contents can be spilled out to the surrounding cells and cause damage. Studies showing their role in intercellular communication suggest that they can escape phagocyte ingestion and target neighboring cells; however, the molecular mechanism of apoptotic body targeting is still unknown[63].

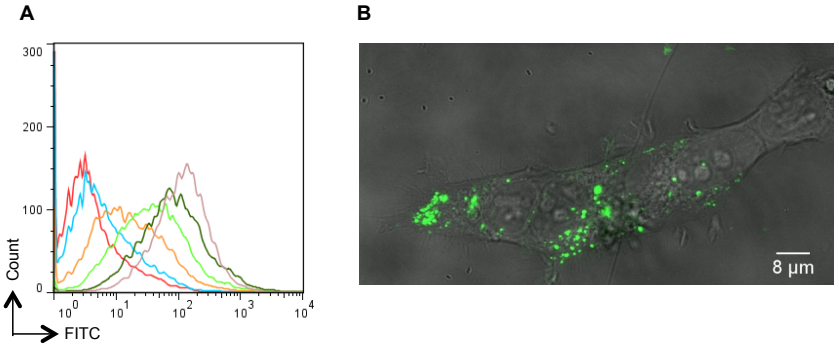

Figure 3. **EV uptake by HEK 293 cells**. A) Flow cytometry histogram shows increasing fluorescence intensity shift of HEK 293 cells treated with different concentrations of PKH67-labeled SV-HFO EVs. EV concentrations: red-1X; blue-2X; orange-5X; light green-10X; dark green-20X; pink-40X. (1X: 0.25% v/v) B) Confocal microscopy image of HEK 293 cells that were treated with the highest dose (40X) of PKH67-labeled SV-HFO EVs shows EV uptake. Analyses were performed after overnight treatment with labeled EVs. Scale bar: 8 µm.

1.2.4. Interactions with target cells

EVs originate from their parent cells, and travel in extracellular space until they interact with their target cells. The literature contains an increasing number of studies verifying the specificity of EV target interaction and subsequent biological effect.[77,78]. Even though the molecular mechanism of EV targeting is not yet well described, it is thought to mainly occur via adhesion (peripheral) and heat shock proteins that interact with the receptors located on the target cell surface[79-82]. Phosphatidylserine lipids also participate in target recognition via interaction with their receptors on the target cell[83]. Upon interaction with the target cells EVs can dock at the plasma membrane and exert their biological function via signal transduction or fuse with the cell membrane and transfer their bioactive cargo[8]. EV membrane fluidity and pH of the environment greatly affects the efficiency of EV fusion. High cholesterol, sphingomyelin, and saturated fatty acid content contribute to EV

rigidity, and prevent fusion at neutral pH. The acidity of the tumor microenvironment increases the efficiency of tumor EV fusion by the target stromal cells[84]. EVs can also be internalized by endocytosis, broken down in lysosomes, and subsequently release their cargo into the lumen of their targets. EV targeting can be monitored via different methods that rely on imaging techniques and fluorescence dyes. Docking can be detected by targeting cell surface proteins with antibodies, while fusion is commonly detected using self-quenching lipophilic dyes (e.g. R18)[59]. Thanks to their tendency to form aggregates *in vitro*, EVs internalized by endocytosis can be easily observed by membrane intercalating dyes, such as PKH dyes (Fig. **3**). EV aggregation is usually explained by the formation of bridges between the anionic phospholipids due to the calcium content of culture media; however, we cannot rule out that aggregation may be important for EV propagation similar to viruses[85].

1.2.5. Biological functions

Only a few decades ago it was commonly accepted that intercellular communication was solely mediated via receptors and small soluble molecules. Vesicular structures secreted to the extracellular space were mainly considered to be cell artifacts as a way of disposing cellular waste. During the '80s, several studies attributed more functions to EVs in antigen-presentation, antitumor activity and immune response[86-89]. Today, EVs have been shown to be involved in many biological functions, such as development, immunity, inflammation, coagulation, cardiovascular function and stem cell biology, as well as cancer and chemotherapy resistance.

EVs are important regulators of coagulation via the exchange of active cargo that promotes vessel formation, angiogenesis, clotting and platelet aggregation[8,89,90]. EVs regulate coagulation by transferring cargo with either anticoagulant activity (e.g. activated protein C) or procoagulant activity (e.g. arachidonic acid) between activated and resting platelets[91-93]. Neuronal EVs are known to play a regulatory role in myelin formation, neuron outgrowth and neuronal survival[94-96]. Neuronal EVs are also essential in recycling receptors and removing potential pathological proteins from the central nervous system[95]. EV production is up-regulated during inflammatory response[5]. Elevated ATP levels caused by cellular injury triggers macrophage EV secretion, which in turn have the capacity to activate other macrophages[97]. EVs also have essential implications in immune response as they are released both by infected cells and immune cells. Hepatitis C infected cells release EVs that contain viral RNA that is transferred to target plasmacytoid dendritic cells, and consequently activate immune response[98]. Ramakrishnaiah and colleagues showed that hepatitis C virus RNA could also evade the immune system by transmitting the infection between human hepatocytes[99]. Recently studies showed that EVs have crucial implications in the regulation of stem cell fate. Ratajczak and colleagues showed that embryonic stem cells stimulate the pluripotency of hematopoietic progenitors via transferring Wnt3 protein[100].

EVs released from apoptotic T cells induce differentiation of leukemic cells towards megakaryocytes via the associated hedgehog morphogen[101]. EVs isolated from the peripheral circulation of pregnant women contain different cargo in different gestation phases, suggesting a role for EVs in morphogenesis during vertebrate development[102]. Several reports showed that EVs carry developmental proteins, such as β-catenin, Wnt proteins and sonic hedgehog, further supporting their involvement during development[103].

EVs also have many implications in cellular pathologies, such as diabetes, coagulopathies, inflammation, infection, autoimmune disease and cancer, being of particular interest in the field[104-108]. Both tumor cells and the surrounding non-malignant cells in the tumor microenvironment produce EVs that contribute to pre-metastatic niche formation, immunosuppression, angiogenesis, invasion, metastasis and tumor progression[109-113]. Tumor EVs generally carry oncogenes and pro-metastatic cargo consisting of metalloproteinases, tetraspanins, plasminogens, integrins, heath shock proteins, growth factors, etc. that promote extracellular matrix degradation, invasion and consequent tumor progression[54]. Several reports showed the role of EVs in priming metastatic niches for enhanced metastatic propensity of the target cells via the exchange of pro-angiogenic factors and chemoattractants[114]. Hood and colleagues reported that melanoma EVs prime the sentinel lymph nodes for melanoma metastasis[115], while Peinado and colleagues reported that melanoma EVs stimulate the bone marrow cells to support metastasis and tumor growth via receptor tyrosine kinases[116]. Interestingly, EVs shed by tumor cells inhibit immune surveillance and promote chemotherapy resistance by expulsion of therapeutic drugs from tumor cells via exchange of ABC transporters and drug metabolizing enzymes[117-119].

1.3. INTERCELLULAR COMMUNICATION IN BONE

Bone, the key structural component of the vertebral endoskeleton that mechanically supports the body, protects the integral organs and enables motility, is a living organ made up of diverse tissues. The primary tissue is the osseous tissue consisting of bone cells, including osteoblast, osteoclasts and osteocytes. The bone cells communicate with each other throughout adult life to regulate the balance between bone resorption and bone formation, which is important to maintain normal bone mass and strength as well as mineral homeostasis[120,121]. Bone also houses the bone marrow tissue forming a complex microenvironment that supports other vital biological functions, including hematopoiesis, adipogenesis and chondrogenesis[122]. Keeping the constant balance of bone homeostasis as well as the efficient regulation of other essential physiological events that occur within the bone microenvironment requires the formation of balanced signaling networks between the resident cells. Elucidation of the regulatory mechanisms involved in EV-mediated cell communication within the bone microenvironment is critical for a deeper understanding of the skeletal system in health and disease.

1.3.1. EV-mediated communication between bone cells

Over the past few years, researchers have shown increasing interest in delineating the role of EVs in bone biology. The work of Anderson and Bonucci not only pioneered the development of EV field but also contributed to study the regulation of bone matrix development, mainly via matrix vesicles secreted by osteoblasts. Matrix vesicles with diameters between 30 and 300 nm originate from the plasma membrane of mineralizing osteoblasts, and are involved in bone matrix mineralization via hydroxyapatite deposition[123]. Matrix vesicles are also released by cartilage during endochondral calcification. Proteome profiles of matrix vesicles obtained from bone and cartilage of different species revealed a large number of shared proteins, such as phosphatases, annexins and ion channels, which contribute to the understanding of mineral formation[124,125]. Studies with hypophosphatasia patients showed that the defects in proper mineral crystal propagation from matrix vesicles lead to improper or complete failure of bone calcification[126]. *In vitro* manipulation of osteoblast mineralization further supported the parallels between matrix vesicle production and mineralization. Inhibition of mineralization by activin A triggers reduced expression of matrix vesicle markers implying deficient or altered matrix vesicles production[127], while vitamin D treatment successfully increases matrix vesicle secretion from osteoblasts leading to higher mineralization rates[128]. Osteocytes also secrete EVs with possible roles in regulation of mineral deposition via communication with osteoblasts and osteoclasts[129,130]. On-going studies have reported preliminary results showing the enrichment of osteocyte EVs with receptor activator of nuclear factor kappa-B ligand, of which the vesicular levels are elevated upon parathyroid hormone treatment, suggestive of a role in promoting osteoclast formation (BoneKEy reports). Recent studies with osteoclasts reported the importance of the miRNAs in osteoclastogenesis[131,132]. Current studies are focusing on elucidating whether miRNAs are transported via EVs secreted by osteoclasts.

1.3.2. EV-mediated communication in the bone microenvironment

EV-mediated signaling in bone is particularly a crucial determining factor for the regulation of essential biological processes other than bone tissue regeneration. The favorable bone microenvironment hosts a great diversity of cells, such as HSCs, fat cells, MSCs, endothelial cells, cartilage and nerves. There are numerous studies highlighting the importance of EV-mediated signaling in the regulation of hematopoietic development[58,100,133]. Moreover, $CD34^+$ hematopoietic stem and progenitor cells (HSPCs) stimulate angiogenesis via miRNA exchange.[134]. MSCs also actively secrete EVs containing selected patterns of mRNA and miRNAs[55,56]. Several studies reported the role of MSC-EVs in tissue damage repair, inflammatory responses, and immune system[135]. MSC-EVs regulate inflammation by inhibiting auto-reactive lymphocyte proliferation and promote secretion of the anti-inflammatory cytokines IL-10 and TGF-β[136]. Ekstrom and colleagues demonstrated that monocyte EVs stimulate osteogenic differentiation of regenerative MSCs during bone inju-

ry at the site of titanium implants[137]. Recently, EVs have been implicated in osteoblast-adipocyte crosstalk via horizontal transfer adipogenic RNAs[138]. Furthermore, the discovery of cartilage-derived EVs made a significant contribution to the understanding of cartilage disease and repair[139].

1.3.3. EVs in bone metastases

In cancer, the favorable bone microenvironment attracts distant bone-metastasizing tumors, in particular breast and prostate tumors. EVs secreted by cancer cells are responsible for stimulating angiogenesis and thereby facilitating the migration of the tumor cells into the bone microenvironment. Remarkably, Renzulli and colleagues showed that prostate tumor cells release EVs that educate the bone cells to act as a pre-metastatic niche[57]. *In vitro* manipulation of pro-metastatic EV cargo resulted in several successful studies where they managed to repress the tumor-induced angiogenesis leading to a reduction in bone metastatic lesions in mice[140,141].

EVs derived from human bone marrow MSCs also have crucial consequences in cancer cell growth and behavior. However, studies show contradictory roles of MSC-EVs in tumor microenvironment. Several groups reported that MSC-EVs favor tumor growth and angiogenesis, while others showed the inhibition of these processes[142-144]. MSC-EVs inhibit cancer cell growth of different cancer cell lines in immunodeficient mice[145]. EVs derived from murine MSCs are shown to significantly down-regulate VEGF expression in breast cancer cells leading to an inhibition of angiogenesis both *in vitro* and *in vivo*[146]. On the other hand, MSC-EVs promote tumor growth *in vivo* by increasing VEGF expression in tumor cells as a result of activating the extracellular signal-regulated kinase 1/2 pathway[143].

1.4. APPLICATIONS IN DIAGNOSTICS AND THERAPY

In the last two decades, significant advances have been made in the characterization of EV content and function leading to their implications in health and disease. Better understanding the role of EVs in bone remodeling and bone microenvironment may provide insights into the complexity of diverse physiological and pathophysiological events. Furthermore, their clinical implementations may open the doors for translational medicine, both in diagnostics and therapy.

1.4.1. Biomarkers and diagnosis

Pathological EVs contain molecular disease signatures, and hence function as excellent molecular biomarkers to be used for diagnosis and prognosis. Particularly, EVs in body fluids can be easily collected making them optimal non-invasive biomarkers to detect

renal disease, obesity and diabetes, and cancer[147-151]. EVs are considered to be promising biomarkers for early diagnosis because they are already released at early stages of the disease and they are very stable and easily detectable. EV-derived miRNAs represent one of the most attractive cancer biomarkers as they provide a miRNA pattern that is different in benign and malignant forms, correlating with different stage of tumors[152]. Altered levels of circulating miRNAs are also proposed to be biomarkers for bone cancers, such as osteosarcoma[153]. However, the involvement of EVs is still not clear. Early diagnosis of metabolic bone diseases is essential for subsequent effective treatment. Currently, the conventional diagnostics techniques rely on the detection of bone turnover biomarkers in patient urine and blood[154,155]. Interestingly, osteoprotegerin containing EVs are detected in elevated levels in the urine of patients with chronic kidney disease suggestive of a role in preventing vascular calcification[156]. Investigating the roles of bone EVs in metabolic bone diseases and inappropriate biological mineral formation is promising to provide novel avenues for early diagnosis.

1.4.2. Regenerative medicine, vaccines and drug delivery

Stem cell-derived EVs have been of increasing interest for their potential use in cell-free therapies in regenerative medicine exploiting their physiological functions mimicking their parental cells. They have been shown to improve cellular function in damaged organs by preventing apoptosis and promoting proliferation and angiogenesis via the horizontal transfer of pro-regenerative factors[157-159]. Several studies reported the potential of MSC-EVs as therapeutic agents for tendon repair[160] and rheumatic diseases based on their anti-fibrotic, anti-apoptotic, anti-inflammatory and pro-regenerative properties[161]. Furthermore, MSC-EVs have been shown to be involved in repairing invertebral disc degeneration via transfer of their membrane components to nucleus pulposus cells[162]. These findings stress their potential in bone regenerative therapy.

Thanks to their immunosuppressive properties, EVs have been proposed as vaccines for immunotherapy[163,164]. Particularly, EVs secreted by tumors have been shown to contain tumor antigens that could have an antitumor activity on other tumors[165]. Remarkably, clinical trials with cancer patients showed that melanoma EVs added to autologous dendritic cells *in vitro* stimulate T cells that induce antitumor effects when injected into the patient[166,167]. EVs have been increasingly seen as physiological drug delivery agents[168]. As opposed to synthetic alternatives, such as liposomes and nanoparticles, EVs occur naturally, exhibit a long half-life and an intrinsic homing ability, and are more efficiently tolerated by the recipient cells. Several reports demonstrated the possibility to load EVs with therapeutic molecules via *in vivo* and *in vitro* manipulations[169]. Wood and colleagues showed that they could use electroporation techniques to load EVs with siRNA that is delivered to target cells resulting in gene regulation[170]. Human MSC-EVs are shown to be promising for drug delivery. Chai Lai and colleagues manipulated MSCs to produce infinite numbers of

EVs from a single clone[171]. Several groups are focusing on developing biomimetic drug delivery vehicles inspired by EVs to effectively deliver the therapeutics to the target site[172,173].

1.5. REGENERATION OF THE BLOOD-FORMING SYSTEM

HSCs are multipotent stem cells that give rise to all blood lineages, including myeloid and lymphoid lineages, while maintaining the ability to self-renew (Fig. **4)**. Their potential to replenish blood has made them attractive for stem cell therapies to treat a broad diversity of hematological disorders. HSC transplantation, where the bone marrow of patients is replenished with the stem cells of healthy donors, is one of the most widely applied stem cell therapies. To date, bone marrow is the most commonly used HSC source but researchers continue to explore alternative strategies to improve therapy.

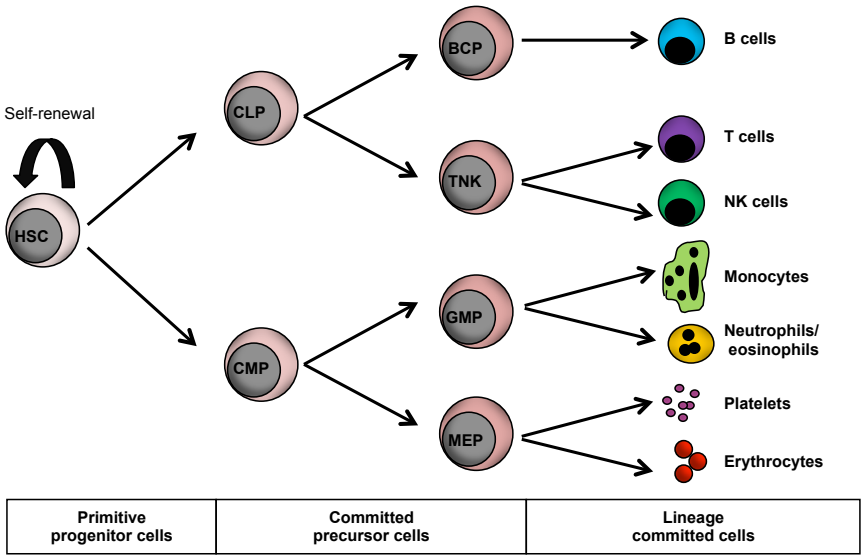

Figure 4. Diagram of hematopoiesis in humans. HSC, hematopoietic stem cell; CLP, common lymphoid progenitor; CMP, common myeloid progenitor; BCP, B cell progenitor; TNK, T/ natural killer cell progenitor; GMP, granulocyte macrophage progenitor; MEP, megakaryocyte erythroid progenitor.

1.5.1. Stem cell transplantations

Pioneer work in early 1950s showed that bone marrow cells from healthy donors when injected intravenously could repopulate the bone marrow of patients with defected hematopoiesis, and regenerate all the blood cells[174]. The first successful European bone marrow transplantation trial was performed to treat patients suffering from leukemia[175]. Since then HSC transplantations have been used to treat patients with hematological malig-

nancies, such as blood cancers and other blood disorders, and non-malignant disorders, such as immune system disorders. Today more than 50,000 transplants are carried out annually worldwide to cure patients where transplantation remains as the last hope for cure.

HSC transplantations can be performed with an autologous (patient) transplant or with an allogeneic (donor) transplant[176]. Allogeneic transplants are typically harvested from the bone marrow or peripheral blood of healthy donors. The stem cells are then infused to the patient whose own HSCs have been impaired or ablated by chemotherapy or radiation. As though it may seem straightforward with numerous success stories, HSC transplantation is a very complicated and risky technique. Successful transplantation relies on optimal donor-recipient compatibility to minimize the likelihood of developing a life-threatening complication called graft-versus-host disease and to maximize the likelihood of sufficient regeneration in a short period of time. Unfortunately, only a small percent of those patients in need for a stem cell transplant have a matching donor. More recently, umbilical cord blood (UCB) has proven to be a great alternative HSC source for patients waiting for an allogeneic transplant without a perfectly matching donor.

1.5.2. Umbilical cord blood as a stem cell source

Since its first application in 1989 to treat a child with Fanconi anemia, the use of UCB as a source of HSCs has increased significantly[177-179]. UCB is a rich source of more primitive HSCs with attractive advantages over bone marrow and peripheral blood. The advantages include ease to harvest with no pain caused to the donor, decreased stringency of human leukocyte antigen matching requirements, and low risk of being attacked from the recipient's immune system leading to relatively lower risk of graft-versus-host disease complications. However, low numbers of progenitor cells deriving from the small UCB volume cause delayed engraftment and immune reconstitution increasing the rate of failure of post-transplantation recovery. This poses difficulties in the clinic, especially for transplantations in adult patients[180].

Currently there is a major interest in developing *ex vivo* expansion technologies to obtain sufficient HSCs for clinical use. Using a cocktail of hematopoietic cytokines, such as stem cell factor, Fms-related tyrosine kinase 3 ligand, thrombopoietin, interleukin 6 and granulocyte-macrophage colony-stimulating factor, scientists successfully managed to stimulate the rapid expansion of $CD34^+$ HSPCs[181,182]. The discovery of small soluble molecules, such as StemRegenin 1, promoted more effective *ex vivo* expansion while maintaining the progenitor cell frequency[183]. The cells expanded by using cytokines, with or without StemRegenin1, could engraft and repopulate immunodeficient mice to replenish the blood *in vivo*. However, challenges still remain as the rapid expansion is often accompanied by the long-term exhaustion of the stem cell pool with true self-renewal and full repopulating capacity as a result of apoptosis or differentiation *in vitro*[184]. Improved culture strategies to promote HSPC expansion while retaining their self-renewal capacity and keeping differen-

tiation at bay are still indispensible. Ultimately, to find the optimal *ex vivo* expansion conditions, researchers have turned their focus on unraveling the soluble and insoluble factors of the bone marrow niche where HSC and HSPC self-renewal is supported.

1.5.3. Bone marrow niche

HSCs reside in special niches, which provide the spatial and mechanical cues necessary to regulate the balance between self-renewal, proliferation and differentiation[185]. Bone marrow, the major location for hematopoiesis in humans, provides a favorable microenvironment composed of niche cells, extracellular matrix, and soluble factors, such as cytokines, chemokines and signaling molecules[186].

There are contrasting studies regarding the identity of true niche cells. Initial reports suggested that endosteal bone surface houses HSCs in close contact with osteoblasts that actively regulate HSCs[187,188]. In contrast, sinusoidal endothelial cells were suggested to regulate primitive HSCs in the perivascular zone[189]. Increasing reports showed the presence of other niche cells, such as CXCL12-abundant reticular cells, adipocytes, MSCs, and nestin-positive cells, which play equally important roles in the HSC niche[190-193]. All these niche cells must work in harmony to maintain the hematopoietic potential of the stem cells located in the bone marrow.

Bone marrow niche cells control HSC function via an intricate network of soluble signals and structural molecules. Signaling molecules, such as WNT proteins, Notch ligands, sonic hedhehog, bone morphogenetic proteins and thrombopoietin, hold fundamental roles to maintain HSC homeostasis[194-196]. CXCL12 secreted by osteoblasts is important for HSC homing to the bone marrow by binding to CXCR4 located on HSC cell surface[197]. Similarly, CaSR and GNAS expressed by HSCs are essential for homing to the niche[198]. Adhesive interactions via ANG1/ TIE2, N-cadherins, integrins, VLA-4, and ANXA2 are critical players of engraftment and mobilization, most likely via binding HSCs to the bone and releasing HSCs into circulation[187,199,200]. Moreover, interactions with the extracellular matrix provide retention cues and mechanical signals, and concentrate growth factors and cytokines[201]. Temporal, metabolic and ambient cues, such as circadian rhythms, prostaglandins, calcium and low oxygen, regulate HSC maintenance directly and indirectly by regulating the niche cells and by targeting production of key cytokines[202-204].

1.5.4. Osteolineage cells

Increasing evidence reports successful *ex vivo* expansion of UCB-derived primitive progenitor cells by targeting the osteolineage cells, such as MSCs, osteoprogenitor cells and osteoblasts[205,206]. Osteoblasts were initially thought to be the major components of the endosteal bone marrow niche; but now it is clear that they are not the only niche cells with that capacity. The current debate over the role of osteoblasts extends into whether

their contribution is absolutely required for HSC regulation in the bone marrow. Nevertheless, several studies demonstrated that the use of osteoblast-derived soluble factors, such as Notch ligands, WNT proteins, angiopoietin-like proteins and bone morphogenetic proteins, promotes HSPC expansion in stroma-free cultures in combination with hematopoietic cytokines[199,207-209]. Similarly, modulation of osteoblast membrane-associated molecules, such as N-cadherin, VLA-4 and VLA-5, results in prolonged survival *in vitro* making it possible to obtain clinically satisfactory expansion to support better engraftment[184]. Modulation of substrate elasticity is also widely applied to mimic the physical and mechanical characteristics of the endosteal bone surface to obtain clinically relevant HSPC numbers.

Currently, we still lack a detailed understanding of the cellular interactions and signals that coordinate normal hematopoietic development. Recent findings have proposed that EVs may be involved in the regulation of stem cell fate in their niches. As we discussed earlier, EVs contain regulatory cargo capable of modulating HSPC reprogramming. Identification of osteoblast-derived EV components critical for the regulation of the cross-talk between osteolineage cells and HSPCs may be exploited clinically to develop improved expansion strategies.

1.6. ABOUT THIS THESIS

EVs are now recognized as biologically significant structures with important roles in cell-to-cell communication. Advancement in the field produced tremendous information that gives insights into the biological role of EVs in many aspects of physiological and pathophysiological events. Due to their signature content and biocompatibility, EVs represent a potential source of diagnostic tools and therapeutic agents. As well, their use might overcome limitations and risks associated with cell-therapy approaches. Further characterization of the EV-mediated modes of communication within the bone microenvironment will not only provide insights into the complexity of bone development and maintenance but also to other biological processes that require the favorable bone microenvironment.

In this thesis, we aim to elucidate the regulatory cargo of human osteoblast-derived EVs and investigate their molecular function in communication within the bone microenvironment, in particular with HSPCs and bone-metastasizing cancer cells. Ultimately, we investigate the therapeutic potency of osteoblast-EVs in regenerative medicine by evaluating their potential in *ex vivo* expansion of human UCB-derived HSPCs for clinical use.

In **Chapter 2**, we present an extensive proteomic characterization of human osteoblast-derived EVs secreted at various time-points during osteoblast differentiation under both mineralizing and non-mineralizing conditions. We also investigate the effect of osteoblast-EVs on human prostate cancer (PC3) cells by microscopic, proteomic and gene expression analyses *in vitro*.

In the remainder of this thesis we focus on EVs deriving from non-mineralizing

osteoblasts. In **Chapter 3**, we present the comparative transcriptome analysis of osteoblasts and their corresponding EVs using next-generation sequencing. Using a bioinformatics workflow, we describe the mRNA species that are selectively incorporated into EVs or depleted from EVs during their biogenesis.

In **Chapter 4**, we characterize the global expression pattern of miRNAs in osteoblast-EVs using next-generation sequencing. Using comparative analyses with the parental osteoblast miRNA profile and *in silico* target prediction analyses we define candidate hematopoietic development pathways affected by EVs. Consequently, we study the functional effect of EVs on UCB-derived HSPCs by gene expression and biochemical analyses.

In **Chapter 5**, we report the therapeutic application of osteoblast-EVs in stem cell therapy by testing their potency to expand UCB-derived HSPCs *ex vivo* in combination with hematopoietic growth factors. We further verify the functionality of the expanded cells *in vivo* by performing xenogeneic transplantation in immunodeficient mice.

In **Chapter 6**, we study the effect of osteoblast-EV treatment on the transcriptome of UCB-derived HSPCs using next-generation sequencing. We use integrated bioinformatics approach to explain the biological mechanism of EV function by showing the direct and indirect molecular relationships between EV cargo (described in chapters 2, 3 and 4) and EV-regulated HSPC genes (this chapter).

Finally in **Chapter 7**, we present the conclusions of the work presented in this thesis. Moreover, this chapter describes the key findings, discusses the potential challenges and gives recommendations for prospective studies.

REFERENCES

1 Wolf, P. The nature and significance of platelet products in human plasma. *British journal of haematology* **13**, 269-288 (1967).

2 Anderson, H. C. Electron microscopic studies of induced cartilage development and calcification. *J Cell Biol* **35**, 81-101 (1967).

3 Bonucci, E. Fine structure of early cartilage calcification. *J Ultrastruct Res* **20**, 33-50 (1967).

4 Gyorgy, B. *et al.* Membrane vesicles, current state-of-the-art: emerging role of extracellular vesicles. *Cell Mol Life Sci* **68**, 2667-2688 (2011).

5 Raposo, G. & Stoorvogel, W. Extracellular vesicles: exosomes, microvesicles, and friends. *J Cell Biol* **200**, 373-383 (2013).

6 Thery, C., Ostrowski, M. & Segura, E. Membrane vesicles as conveyors of immune responses. *Nat Rev Immunol* **9**, 581-593 (2009).

7 Shifrin, D. A., Jr., Demory Beckler, M., Coffey, R. J. & Tyska, M. J. Extracellular vesicles: communication, coercion, and conditioning. *Mol Biol Cell* **24**, 1253-1259 (2013).

8 Cocucci, E., Racchetti, G. & Meldolesi, J. Shedding microvesicles: artefacts no more. *Trends Cell Biol* **19**, 43-51 (2009).

9 Simons, M. & Raposo, G. Exosomes--vesicular carriers for intercellular communication. *Curr Opin Cell Biol* **21**, 575-581 (2009).

10 Hristov, M., Erl, W., Linder, S. & Weber, P. C. Apoptotic bodies from endothelial cells enhance the number and initiate the differentiation of human endothelial progenitor cells in vitro. *Blood* **104**, 2761-2766 (2004).

11 Holmgren, L. *et al.* Horizontal transfer of DNA by the uptake of apoptotic bodies. *Blood* **93**, 3956-3963 (1999).

12 Caby, M. P., Lankar, D., Vincendeau-Scherrer, C., Raposo, G. & Bonnerot, C. Exosomal-like vesicles are present in human blood plasma. *Int Immunol* **17**, 879-887 (2005).

13 Admyre, C. *et al.* Exosomes with immune modulatory features are present in human breast milk. *J Immunol* **179**, 1969-1978 (2007).

14 Gonzales, P. A. *et al.* Isolation and purification of exosomes in urine. *Methods Mol Biol* **641**, 89-99 (2010).

15 Anderson, H. C. Molecular biology of matrix vesicles. *Clin Orthop Relat Res*, 266-280 (1995).

16 Bruno, S. *et al.* Mesenchymal stem cell-derived microvesicles protect against acute tubular injury. *J Am Soc Nephrol* **20**, 1053-1067 (2009).

17 Bruno, S. & Camussi, G. Role of mesenchymal stem cell-derived microvesicles in tissue repair. *Pediatr Nephrol* **28**, 2249-2254 (2013).

18 Lai, R. C. *et al.* Exosome secreted by MSC reduces myocardial ischemia/reperfusion injury. *Stem Cell Res* **4**, 214-222 (2010).

19 Thery, C., Amigorena, S., Raposo, G. & Clayton, A. Isolation and characterization of exosomes from cell culture supernatants and biological fluids. *Curr Protoc Cell Biol* **Chapter 3**, Unit 3 22 (2006).

20 Valadi, H. *et al.* Exosome-mediated transfer of mRNAs and microRNAs is a novel mechanism of genetic exchange between cells. *Nature cell biology* **9**, 654-659 (2007).

21 Bobrie, A., Colombo, M., Raposo, G. & Thery, C. Exosome secretion: molecular mechanisms and roles in immune responses. *Traffic* **12**, 1659-1668 (2011).

22 Zakharova, L., Svetlova, M. & Fomina, A. F. T cell exosomes induce cholesterol accumulation in human monocytes via phosphatidylserine receptor. *J Cell Physiol* **212**, 174-181 (2007).

23 Muller, G., Jung, C., Wied, S., Biemer-Daub, G. & Frick, W. Transfer of the glycosylphosphatidylinositol-anchored 5'-nucleotidase CD73 from adiposomes into rat adipocytes stimulates lipid synthesis. *Br J Pharmacol* **160**, 878-891 (2010).

24 Thery, C. *et al.* Proteomic analysis of dendritic cell-derived exosomes: a secreted subcellular compartment distinct from apoptotic vesicles. *J Immunol* **166**, 7309-7318 (2001).

25 Conde-Vancells, J. *et al.* Characterization and comprehensive proteome profiling of exosomes secreted by hepatocytes. *J Proteome Res* **7**, 5157-5166 (2008).

26 Raposo, G. *et al.* B lymphocytes secrete antigen-presenting vesicles. *The Journal of experimental medicine* **183**, 1161-1172 (1996).

27 van der Pol, E. *et al.* Optical and non-optical methods for detection and characterization of microparticles and exosomes. *J Thromb Haemost* **8**, 2596-2607 (2010).

28 Wubbolts, R. *et al.* Proteomic and biochemical analyses of human B cell-derived exosomes. Potential implications for their function and multivesicular body formation. *The Journal of biological chemistry* **278**, 10963-10972 (2003).

29 van der Vlist, E. J., Nolte-'t Hoen, E. N., Stoorvogel, W., Arkesteijn, G. J. & Wauben, M. H. Fluorescent labeling of nano-sized vesicles released by cells and subsequent quantitative and qualitative analysis by high-resolution flow cytometry. *Nat Protoc* **7**, 1311-1326 (2012).

30 Zheng, Y., Campbell, E. C., Lucocq, J., Riches, A. & Powis, S. J. Monitoring the Rab27 associated exosome pathway using nanoparticle tracking analysis. *Exp Cell Res* **319**, 1706-1713 (2013).

31 Garza-Licudine, E., Deo, D., Yu, S., Uz-Zaman, A. & Dunbar, W. B. Portable nanoparticle quantization using a resizable nanopore instrument - the IZON qNano. *Conf Proc IEEE Eng Med Biol Soc* **2010**, 5736-5739 (2010).

32 Mathivanan, S., Fahner, C. J., Reid, G. E. & Simpson, R. J. ExoCarta 2012: database of exosomal proteins, RNA and lipids. *Nucleic acids research* **40**, D1241-1244 (2012).

33 Simpson, R. J., Kalra, H. & Mathivanan, S. ExoCarta as a resource for exosomal research. *J Extracell Vesicles* **1** (2012).

34 Mathivanan, S. & Simpson, R. J. ExoCarta: A compendium of exosomal proteins and RNA. *Proteomics* **9**, 4997-5000 (2009).

35 Kim, D. K. *et al.* EVpedia: an integrated database of high-throughput data for systemic analyses of extracellular vesicles. *J Extracell Vesicles* **2** (2013).

36 Choi, D. S., Kim, D. K., Kim, Y. K. & Gho, Y. S. Proteomics, transcriptomics and lipidomics of exosomes and ectosomes. *Proteomics* **13**, 1554-1571 (2013).

37 Choi, D. S., Kim, D. K., Kim, Y. K. & Gho, Y. S. Proteomics of extracellular vesicles: Exosomes and ectosomes. *Mass Spectrom Rev* (2014).

38 Laulagnier, K. *et al.* Mast cell- and dendritic cell-derived exosomes display a specific lipid composition and an unusual membrane organization. *Biochem J* **380**, 161-171 (2004).

39 Brouwers, J. F. *et al.* Distinct lipid compositions of two types of human prostasomes. *Proteomics* **13**, 1660-1666 (2013).

40 Subra, C., Laulagnier, K., Perret, B. & Record, M. Exosome lipidomics unravels lipid sorting at the level of multivesicular bodies. *Biochimie* **89**, 205-212 (2007).

41 Bicalho, B., Holovati, J. L. & Acker, J. P. Phospholipidomics reveals differences in glycerophosphoserine profiles of hypothermically stored red blood cells and microvesicles. *Biochim Biophys Acta* **1828**, 317-326 (2013).

42 Mobius, W. *et al.* Immunoelectron microscopic localization of cholesterol using biotinylated and non-cytolytic perfringolysin O. *J Histochem Cytochem* **50**, 43-55 (2002).

43 Al-Nedawi, K., Meehan, B. & Rak, J. Microvesicles: messengers and mediators of tumor progression. *Cell Cycle* **8**, 2014-2018 (2009).

44 Subra, C. *et al.* Exosomes account for vesicle-mediated transcellular transport of activatable phospholipases and prostaglandins. *J Lipid Res* **51**, 2105-2120 (2010).

45 Esser, J. *et al.* Exosomes from human macrophages and dendritic cells contain enzymes for leukotriene biosynthesis and promote granulocyte migration. *J Allergy Clin Immunol* **126**, 1032-1040, 1040 e1031-1034 (2010).

46 van Niel, G., Porto-Carreiro, I., Simoes, S. & Raposo, G. Exosomes: a common pathway for a specialized function. *J Biochem* **140**, 13-21 (2006).

47 Hemler, M. E. Tetraspanin proteins mediate cellular penetration, invasion, and fusion events and define a novel type of membrane microdomain. *Annu Rev Cell Dev Biol* **19**, 397-422 (2003).

48 Perez-Hernandez, D. *et al.* The intracellular interactome of tetraspanin-enriched microdomains reveals their function as sorting machineries toward exosomes. *The Journal of biological chemistry* **288**, 11649-11661 (2013).

49 Hegmans, J. P. *et al.* Proteomic analysis of exosomes secreted by human mesothelioma cells. *Am J Pathol* **164**, 1807-1815 (2004).

50 Dolo, V. *et al.* Matrix-degrading proteinases are shed in membrane vesicles by ovarian cancer cells in vivo and in vitro. *Clin Exp Metastasis* **17**, 131-140 (1999).

51 Taraboletti, G. *et al.* Shedding of the matrix metalloproteinases MMP-2, MMP-9, and MT1-MMP as membrane vesicle-associated components by endothelial cells. *Am J Pathol* **160**, 673-680 (2002).

52 Bess, J. W., Jr., Gorelick, R. J., Bosche, W. J., Henderson, L. E. & Arthur, L. O. Microvesicles are a source of contaminating cellular proteins found in purified HIV-1 preparations. *Virology* **230**, 134-144 (1997).

53 Baj-Krzyworzeka, M. *et al.* Tumour-derived microvesicles carry several surface determinants and mRNA of tumour cells and transfer some of these determinants to monocytes. *Cancer Immunol Immunother* **55**, 808-818 (2006).

54 Skog, J. *et al.* Glioblastoma microvesicles transport RNA and proteins that promote tumour growth and provide diagnostic biomarkers. *Nature cell biology* **10**, 1470-1476 (2008).

55 Chen, T. S. *et al.* Mesenchymal stem cell secretes microparticles enriched in pre-microRNAs. *Nucleic acids research* **38**, 215-224 (2010).

56 Collino, F. *et al.* Microvesicles derived from adult human bone marrow and tissue specific mesenchymal stem cells shuttle selected pattern of miRNAs. *PloS one* **5**, e11803 (2010).

57 Renzulli, J. F., 2nd *et al.* Microvesicle induction of prostate specific gene expression in normal human bone marrow cells. *J Urol* **184**, 2165-2171 (2010).

58 Mittelbrunn, M. *et al.* Unidirectional transfer of microRNA-loaded exosomes from T cells to antigen-presenting cells. *Nature communications* **2**, 282 (2011).

59 Montecalvo, A. *et al.* Mechanism of transfer of functional microRNAs between mouse dendritic cells via exosomes. *Blood* **119**, 756-766 (2012).

60 Bellingham, S. A., Coleman, B. M. & Hill, A. F. Small RNA deep sequencing reveals a distinct miRNA signature released in exosomes from prion-infected neuronal cells. *Nucleic acids research* **40**, 10937-10949 (2012).

61 Nolte-'t Hoen, E. N. *et al.* Deep sequencing of RNA from immune cell-derived vesicles uncovers the selective incorporation of small non-coding RNA biotypes with potential regulatory functions. *Nucleic acids research* **40**, 9272-9285 (2012).

62 Turchinovich, A., Weiz, L., Langheinz, A. & Burwinkel, B. Characterization of extracellular circulating microRNA. *Nucleic acids research* **39**, 7223-7233 (2011).

63 Bergsmedh, A. *et al.* Horizontal transfer of oncogenes by uptake of apoptotic bodies. *Proceedings of the National Academy of Sciences of the United States of America* **98**, 6407-6411 (2001).

64 de Gassart, A., Geminard, C., Hoekstra, D. & Vidal, M. Exosome secretion: the art of reutilizing nonrecycled proteins? *Traffic* **5**, 896-903 (2004).

65 Hurley, J. H. & Odorizzi, G. Get on the exosome bus with ALIX. *Nature cell biology* **14**, 654-655 (2012).

66 Williams, R. L. & Urbe, S. The emerging shape of the ESCRT machinery. *Nat Rev Mol Cell Biol* **8**, 355-368 (2007).

67 Gill, D. J. *et al.* Structural insight into the ESCRT-I/-II link and its role in MVB trafficking. *EMBO J* **26**, 600-612 (2007).

68 Colombo, M. *et al.* Analysis of ESCRT functions in exosome biogenesis, composition and secretion highlights the heterogeneity of extracellular vesicles. *Journal of cell science* (2013).

69 Trajkovic, K. *et al.* Ceramide triggers budding of exosome vesicles into multivesicular endosomes. *Science* **319**, 1244-1247 (2008).

70 Yu, X., Harris, S. L. & Levine, A. J. The regulation of exosome secretion: a novel function of the p53 protein. *Cancer Res* **66**, 4795-4801 (2006).

71 Simpson, R. J., Lim, J. W., Moritz, R. L. & Mathivanan, S. Exosomes: proteomic insights and diagnostic potential. *Expert Rev Proteomics* **6**, 267-283 (2009).

72 Del Conde, I., Shrimpton, C. N., Thiagarajan, P. & Lopez, J. A. Tissue-factor-bearing microvesicles arise from lipid rafts and fuse with activated platelets to initiate coagulation. *Blood* **106**, 1604-1611 (2005).

73 Pilzer, D., Gasser, O., Moskovich, O., Schifferli, J. A. & Fishelson, Z. Emission of membrane vesicles: roles in complement resistance, immunity and cancer. *Springer Semin Immunopathol* **27**, 375-387 (2005).

74 Gonzalez, L. J. *et al.* The influence of membrane physical properties on microvesicle release in human erythrocytes. *PMC Biophys* **2**, 7 (2009).

75 Nabhan, J. F., Hu, R., Oh, R. S., Cohen, S. N. & Lu, Q. Formation and release of arrestin domain-containing protein 1-mediated microvesicles (ARMMs) at plasma membrane by recruitment of TSG101 protein. *Proceedings of the National Academy of Sciences of the United States of America* **109**, 4146-4151 (2012).

76 Muralidharan-Chari, V. *et al.* ARF6-regulated shedding of tumor cell-derived plasma membrane microvesicles. *Curr Biol* **19**, 1875-1885 (2009).

77 Mallegol, J. *et al.* T84-intestinal epithelial exosomes bear MHC class II/peptide complexes potentiating antigen presentation by dendritic cells. *Gastroenterology* **132**, 1866-1876 (2007).

78 Denzer, K., Kleijmeer, M. J., Heijnen, H. F., Stoorvogel, W. & Geuze, H. J. Exosome: from internal vesicle of the multivesicular body to intercellular signaling device. *Journal of cell science* **113 Pt 19**, 3365-3374 (2000).

79 Nolte-'t Hoen, E. N., Buschow, S. I., Anderton, S. M., Stoorvogel, W. & Wauben, M. H. Activated T cells recruit exosomes secreted by dendritic cells via LFA-1. *Blood* **113**, 1977-1981 (2009).

80 Buschow, S. I. *et al.* MHC II in dendritic cells is targeted to lysosomes or T cell-induced exosomes via distinct multivesicular body pathways. *Traffic* **10**, 1528-1542 (2009).

81 Barres, C. *et al.* Galectin-5 is bound onto the surface of rat reticulocyte exosomes and modulates vesicle uptake by macrophages. *Blood* **115**, 696-705 (2010).

82 Klibi, J. *et al.* Blood diffusion and Th1-suppressive effects of galectin-9-containing exosomes released by Epstein-Barr virus-infected nasopharyngeal carcinoma cells. *Blood* **113**, 1957-1966 (2009).

83 Miyanishi, M. *et al.* Identification of Tim4 as a phosphatidylserine receptor. *Nature* **450**, 435-439 (2007).

84 Parolini, I. *et al.* Microenvironmental pH is a key factor for exosome traffic in tumor cells. *The Journal of biological chemistry* **284**, 34211-34222 (2009).

85 Fitzner, D. *et al.* Selective transfer of exosomes from oligodendrocytes to microglia by macropinocytosis. *Journal of cell science* **124**, 447-458 (2011).

86 Anderson, H. C. Mineralization by matrix vesicles. *Scan Electron Microsc*, 953-964 (1984).

87 Ronquist, G. & Brody, I. The prostasome: its secretion and function in man. *Biochim Biophys Acta* **822**, 203-218 (1985).

88 Stegmayr, B. & Ronquist, G. Promotive effect on human sperm progressive motility by prostasomes. *Urol Res* **10**, 253-257 (1982).

89 Bastida, E., Ordinas, A., Escolar, G. & Jamieson, G. A. Tissue factor in microvesicles shed from U87MG human glioblastoma cells induces coagulation, platelet aggregation, and thrombogenesis. *Blood* **64**, 177-184 (1984).

90 Deregibus, M. C. *et al.* Endothelial progenitor cell derived microvesicles activate an angiogenic program in endothelial cells by a horizontal transfer of mRNA. *Blood* **110**, 2440-2448 (2007).

91 Castellana, D., Toti, F. & Freyssinet, J. M. Membrane microvesicles: macromessengers in cancer disease and progression. *Thromb Res* **125 Suppl 2**, S84-88 (2010).

92 Perez-Casal, M. *et al.* Microparticle-associated endothelial protein C receptor and the induction of cytoprotective and anti-inflammatory effects. *Haematologica* **94**, 387-394 (2009).

93 Barry, O. P., Kazanietz, M. G., Pratico, D. & FitzGerald, G. A. Arachidonic acid in platelet microparticles up-regulates cyclooxygenase-2-dependent prostaglandin formation via a protein kinase C/mitogen-activated protein kinase-dependent pathway. *The Journal of biological chemistry* **274**, 7545-7556 (1999).

94 Lachenal, G. *et al.* Release of exosomes from differentiated neurons and its regulation by synaptic glutamatergic activity. *Mol Cell Neurosci* **46**, 409-418 (2011).

95 Von Bartheld, C. S. & Altick, A. L. Multivesicular bodies in neurons: distribution, protein content, and trafficking functions. *Prog Neurobiol* **93**, 313-340 (2011).

96 Turola, E., Furlan, R., Bianco, F., Matteoli, M. & Verderio, C. Microglial microvesicle secretion and intercellular signaling. *Front Physiol* **3**, 149 (2012).

97 Bianco, F. *et al.* Astrocyte-derived ATP induces vesicle shedding and IL-1 beta release from microglia. *J Immunol* **174**, 7268-7277 (2005).

98 Dreux, M. *et al.* Short-range exosomal transfer of viral RNA from infected cells to plasmacytoid dendritic cells triggers innate immunity. *Cell Host Microbe* **12**, 558-570 (2012).

99 Ramakrishnaiah, V. *et al.* Exosome-mediated transmission of hepatitis C virus between human hepatoma Huh7.5 cells. *Proceedings of the National Academy of Sciences of the United States of America* **110**, 13109-13113 (2013).

100 Ratajczak, J. *et al.* Embryonic stem cell-derived microvesicles reprogram hematopoietic progenitors: evidence for horizontal transfer of mRNA and protein delivery. *Leukemia* **20**, 847-856 (2006).

101 Martinez, M. C. *et al.* Transfer of differentiation signal by membrane microvesicles harboring hedgehog morphogens. *Blood* **108**, 3012-3020 (2006).

102 Atay, S., Gercel-Taylor, C., Kesimer, M. & Taylor, D. D. Morphologic and proteomic characterization of exosomes released by cultured extravillous trophoblast cells. *Exp Cell Res* **317**, 1192-1202 (2011).

103 Soleti, R. & Martinez, M. C. Sonic Hedgehog on microparticles and neovascularization. *Vitam Horm* **88**, 395-438 (2012).

104 Mineo, M. *et al.* Exosomes released by K562 chronic myeloid leukemia cells promote angiogenesis in a Src-dependent fashion. *Angiogenesis* **15**, 33-45 (2012).

105 Raimondo, F. *et al.* Urinary exosomes and diabetic nephropathy: a proteomic approach. *Mol Biosyst* **9**, 1139-1146 (2013).

106 Zwicker, J. I., Trenor, C. C., 3rd, Furie, B. C. & Furie, B. Tissue factor-bearing microparticles and thrombus formation. *Arterioscler Thromb Vasc Biol* **31**, 728-733 (2011).

107 Bobryshev, Y. V., Killingsworth, M. C. & Orekhov, A. N. Increased shedding of microvesicles from intimal smooth muscle cells in athero-prone areas of the human aorta: implications for understanding of the predisease stage. *Pathobiology* **80**, 24-31 (2013).

108 Verderio, C. *et al.* Myeloid microvesicles are a marker and therapeutic target for neuroinflammation. *Ann Neurol* **72**, 610-624 (2012).

109 Giusti, I. *et al.* Cathepsin B mediates the pH-dependent proinvasive activity of tumor-shed microvesicles. *Neoplasia* **10**, 481-488 (2008).

110 Higginbotham, J. N. *et al.* Amphiregulin exosomes increase cancer cell invasion. *Curr Biol* **21**, 779-786 (2011).

111 Zhang, H. G. & Grizzle, W. E. Exosomes and cancer: a newly described pathway of immune suppression. *Clin Cancer Res* **17**, 959-964 (2011).

112 Rak, J. Microparticles in cancer. *Semin Thromb Hemost* **36**, 888-906 (2010).

113 Muralidharan-Chari, V., Clancy, J. W., Sedgwick, A. & D'Souza-Schorey, C. Microvesicles: mediators of extracellular communication during cancer progression. *Journal of cell science* **123**, 1603-1611 (2010).

114 Castellana, D., Kunzelmann, C. & Freyssinet, J. M. Pathophysiologic significance of procoagulant microvesicles in cancer disease and progression. *Hamostaseologie* **29**, 51-57 (2009).

115 Hood, J. L., San, R. S. & Wickline, S. A. Exosomes released by melanoma cells prepare sentinel lymph nodes for tumor metastasis. *Cancer Res* **71**, 3792-3801 (2011).

116 Peinado, H. *et al.* Melanoma exosomes educate bone marrow progenitor cells toward a pro-metastatic phenotype through MET. *Nat Med* **18**, 883-891 (2012).

117 Shedden, K., Xie, X. T., Chandaroy, P., Chang, Y. T. & Rosania, G. R. Expulsion of small molecules in vesicles shed by cancer cells: association with gene expression and chemosensitivity profiles. *Cancer Res* **63**, 4331-4337 (2003).

118 Safaei, R. *et al.* Abnormal lysosomal trafficking and enhanced exosomal export of cisplatin in drug-resistant human ovarian carcinoma cells. *Mol Cancer Ther* **4**, 1595-1604 (2005).

119 Bebawy, M. *et al.* Membrane microparticles mediate transfer of P-glycoprotein to drug sensitive cancer cells. *Leukemia* **23**, 1643-1649 (2009).

120 Marks, S. C., Jr. & Popoff, S. N. Bone cell biology: the regulation of development, structure, and function in the skeleton. *Am J Anat* **183**, 1-44 (1988).

121 Proff, P. & Romer, P. The molecular mechanism behind bone remodelling: a review. *Clin Oral Investig* **13**, 355-362 (2009).

122 Leyh, M. *et al.* Subchondral bone influences chondrogenic differentiation and collagen production of human bone marrow-derived mesenchymal stem cells and articular chondrocytes. *Arthritis research & therapy* **16**, 453 (2014).

123 Anderson, H. C., Garimella, R. & Tague, S. E. The role of matrix vesicles in growth plate development and biomineralization. *Frontiers in bioscience : a journal and virtual library* **10**, 822-837 (2005).

124 Balcerzak, M. *et al.* Proteome analysis of matrix vesicles isolated from femurs of chicken embryo. *Proteomics* **8**, 192-205 (2008).

125 Xiao, Z., Blonder, J., Zhou, M. & Veenstra, T. D. Proteomic analysis of extracellular matrix and vesicles. *J Proteomics* **72**, 34-45 (2009).

126 Anderson, H. C., Hsu, H. H., Morris, D. C., Fedde, K. N. & Whyte, M. P. Matrix vesicles in osteomalacic hypophosphatasia bone contain apatite-like mineral crystals. *Am J Pathol* **151**, 1555-1561 (1997).

127 Alves, R. D., Eijken, M., Bezstarosti, K., Demmers, J. A. & van Leeuwen, J. P. Activin A suppresses osteoblast mineralization capacity by altering extracellular matrix (ECM) composition and impairing matrix vesicle (MV) production. *Mol Cell Proteomics* **12**, 2890-2900 (2013).

128 Woeckel, V. J. *et al.* 1Alpha,25-(OH)2D3 acts in the early phase of osteoblast differentiation to enhance mineralization via accelerated production of mature matrix vesicles. *J Cell Physiol* **225**, 593-600 (2010).

129 Webster, D. J., Schneider, P., Dallas, S. L. & Muller, R. Studying osteocytes within their environment. *Bone* **54**, 285-295 (2013).

130 Paic, F. *et al.* Identification of differentially expressed genes between osteoblasts and osteocytes. *Bone* **45**, 682-692 (2009).

131 Kagiya, T. & Nakamura, S. Expression profiling of microRNAs in RAW264.7 cells treated with a combination of tumor necrosis factor alpha and RANKL during osteoclast differentiation. *J Periodontal Res* **48**, 373-385 (2013).

132 Lian, J. B. *et al.* MicroRNA control of bone formation and homeostasis. *Nat Rev Endocrinol* **8**, 212-227 (2012).

133 Rechavi, O. *et al.* Cell contact-dependent acquisition of cellular and viral nonautonomously encoded small RNAs. *Genes & development* **23**, 1971-1979 (2009).

134 Sahoo, S. *et al.* Exosomes from human CD34(+) stem cells mediate their proangiogenic paracrine activity. *Circ Res* **109**, 724-72 (2011).

135 Yu, B., Zhang, X. & Li, X. Exosomes derived from mesenchymal stem cells. *International journal of molecular sciences* **15**, 4142-4157 (2014).

136 Mokarizadeh, A. Microvesicles derived from mesenchymal stem cells: potent organelles for induction of tolerogenic signaling. *Immunol Lett.* **147**, 47-54 (2012).

137 Ekstrom, K. *et al.* Monocyte exosomes stimulate the osteogenic gene expression of mesenchymal stem cells. *PloS one* **8**, e75227 (2013).

138 Martin, P. J. *et al.* Adipogenic RNAs are transferred in osteoblasts via bone marrow adipocytes-derived extracellular vesicles (EVs). *BMC Cell Biol* **16**, 10 (2015).

139 Rosenthal, A. K. *et al.* Autophagy modulates articular cartilage vesicle formation in primary articular chondrocytes. *The Journal of biological chemistry* **290**, 13028-13038 (2015).

140 Thuma, F. & Zoller, M. Outsmart tumor exosomes to steal the cancer initiating cell its niche. *Semin Cancer Biol* **28**, 39-50 (2014).

141 Valencia, K. *et al.* miRNA cargo within exosome-like vesicle transfer influences metastatic bone colonization. *Mol Oncol* **8**, 689-703 (2014).

142 Bruno, S. Microvesicles derived from human bone marrow mesenchymal stem cells inhibit tumor growth. *Stem Cells Dev.* **22**, 758-771 (2013).

143 Zhu, W. *et al.* Exosomes derived from human bone marrow mesenchymal stem cells promote tumor growth in vivo. *Cancer Lett* **315**, 28-37 (2012).

144 Roccaro, A. M. *et al.* BM mesenchymal stromal cell-derived exosomes facilitate multiple myeloma progression. *J Clin Invest* (2013).

145 Bruno, S. *et al.* Microvesicles derived from human bone marrow mesenchymal stem cells inhibit tumor growth. *Stem cells and development* **22**, 758-771 (2013).

146 Lee, J. K. *et al.* Exosomes derived from mesenchymal stem cells suppress angiogenesis by down-regulating VEGF expression in breast cancer cells. *PloS one* **8**, e84256 (2013).

147 Zhou, H. *et al.* Collection, storage, preservation, and normalization of human urinary exosomes for biomarker discovery. *Kidney Int* **69**, 1471-1476 (2006).

148 Mitchell, P. J. *et al.* Can urinary exosomes act as treatment response markers in prostate cancer? *J Transl Med* **7**, 4 (2009).

149 Khan, S. *et al.* Plasma-derived exosomal survivin, a plausible biomarker for early detection of prostate cancer. *PloS one* **7**, e46737 (2012).

150 Szajnik, M. *et al.* Exosomes in Plasma of Patients with Ovarian Carcinoma: Potential Biomarkers of Tumor Progression and Response to Therapy. *Gynecol Obstet (Sunnyvale)* **Suppl 4**, 3 (2013).

151 Michael, A. *et al.* Exosomes from human saliva as a source of microRNA biomarkers. *Oral Dis* **16**, 34-38 (2010).

152 Taylor, D. D. MicroRNA signatures of tumor-derived exosomes as diagnostic biomarkers of ovarian cancer. *Gynecol. Oncol.* **110**, 13–21 (2008).

153 Ouyang, L. *et al.* A three-plasma miRNA signature serves as novel biomarkers for osteosarcoma. *Med Oncol* **30**, 340 (2013).

154 Recht, M., Liel, M. S., Turner, R. T., Klein, R. F. & Taylor, J. A. The bone disease associated with factor VIII deficiency in mice is secondary to increased bone resorption. *Haemophilia* **19**, 908-912 (2013).

155 Bhattacharyya, S., Siegel, E. R., Achenbach, S. J., Khosla, S. & Suva, L. J. Serum biomarker profile associated with high bone turnover and BMD in postmenopausal women. *J Bone Miner Res* **23**, 1106-1117 (2008).

156 Benito-Martin, A. *et al.* Osteoprotegerin in exosome-like vesicles from human cultured tubular cells and urine. *PloS one* **8**, e72387 (2013).

157 Ratajczak, M. Z. *et al.* Pivotal role of paracrine effects in stem cell therapies in regenerative medicine: can we translate stem cell-secreted paracrine factors and microvesicles into better therapeutic strategies? *Leukemia* **26**, 1166-1173 (2012).
158 Katsuda, T., Kosaka, N., Takeshita, F. & Ochiya, T. The therapeutic potential of mesenchymal stem cell-derived extracellular vesicles. *Proteomics* **13**, 1637-1653 (2013).
159 Tetta, C., Bruno, S., Fonsato, V., Deregibus, M. C. & Camussi, G. The role of microvesicles in tissue repair. *Organogenesis* **7**, 105-115 (2011).
160 Tetta, C. The role of microvesicles derived from mesenchymal stem cells in tissue regeneration; a dream for tendon repair? *Muscles Ligaments Tendons J.* **2**, 212-221 (2012).
161 Maumus, M. Mesenchymal stem cells in regenerative medicine applied to rheumatic diseases: Role of secretome and exosomes. *Biochimie* **95**, 2229-2234 (2013).
162 Strassburg, S. Bi-directional exchange of membrane components occurs during co-culture of mesenchymal stem cells and nucleus pulposus cells. *PLoS One.* **7**, e33739 (2012).
163 Chaput, N. *et al.* The potential of exosomes in immunotherapy of cancer. *Blood Cells Mol Dis* **35**, 111-115 (2005).
164 Hao, S., Moyana, T. & Xiang, J. Review: cancer immunotherapy by exosome-based vaccines. *Cancer Biother Radiopharm* **22**, 692-703 (2007).
165 Wolfers, J. *et al.* Tumor-derived exosomes are a source of shared tumor rejection antigens for CTL cross-priming. *Nat Med* **7**, 297-303 (2001).
166 Chaput, N. *et al.* Exosomes as potent cell-free peptide-based vaccine. II. Exosomes in CpG adjuvants efficiently prime naive Tc1 lymphocytes leading to tumor rejection. *J Immunol* **172**, 2137-2146 (2004).
167 Andre, F. *et al.* Exosomes as potent cell-free peptide-based vaccine. I. Dendritic cell-derived exosomes transfer functional MHC class I/peptide complexes to dendritic cells. *J Immunol* **172**, 2126-2136 (2004).
168 van Dommelen, S. M. *et al.* Microvesicles and exosomes: opportunities for cell-derived membrane vesicles in drug delivery. *J Control Release* **161**, 635-644 (2012).
169 Baglio, S. Mesenchymal stem cell secreted vesicles provide novel opportunities in (stem) cell-free therapy. *Front Physiol.* **3**, 359-370 (2012).
170 Alvarez-Erviti, L. *et al.* Delivery of siRNA to the mouse brain by systemic injection of targeted exosomes. *Nat Biotechnol* **29**, 341-345 (2011).
171 Lai, R. C., Yeo, R. W., Tan, K. H. & Lim, S. K. Exosomes for drug delivery - a novel application for the mesenchymal stem cell. *Biotechnol Adv* **31**, 543-551 (2013).
172 Jang, S. C. *et al.* Bioinspired exosome-mimetic nanovesicles for targeted delivery of chemotherapeutics to malignant tumors. *ACS Nano* **7**, 7698-7710 (2013).
173 Kooijmans, S. A., Vader, P., van Dommelen, S. M., van Solinge, W. W. & Schiffelers, R. M. Exosome mimetics: a novel class of drug delivery systems. *Int J Nanomedicine* **7**, 1525-1541 (2012).
174 Thomas, E. D. Bone marrow transplantation from the personal viewpoint. *International journal of hematology* **81**, 89-93 (2005).
175 Jansen, J. The first successful allogeneic bone-marrow transplant: Georges Mathe. *Transfusion medicine reviews* **19**, 246-248 (2005).
176 Thomas, E. D. Landmarks in the development of hematopoietic cell transplantation. *World journal of surgery* **24**, 815-818 (2000).
177 Gluckman, E. *et al.* Hematopoietic reconstitution in a patient with Fanconi's anemia by means of umbilical-cord blood from an HLA-identical sibling. *The New England journal of medicine* **321**, 1174-1178 (1989).

178 Wagner, J. E. *et al.* Successful transplantation of HLA-matched and HLA-mismatched umbilical cord blood from unrelated donors: analysis of engraftment and acute graft-versus-host disease. *Blood* **88**, 795-802 (1996).

179 Barker, J. N. *et al.* Availability of cord blood extends allogeneic hematopoietic stem cell transplant access to racial and ethnic minorities. *Biology of blood and marrow transplantation : journal of the American Society for Blood and Marrow Transplantation* **16**, 1541-1548 (2010).

180 Rocha, V., Gluckman, E., Eurocord-Netcord, r., European, B. & Marrow Transplant, g. Improving outcomes of cord blood transplantation: HLA matching, cell dose and other graft- and transplantation-related factors. *British journal of haematology* **147**, 262-274 (2009).

181 Walenda, T. *et al.* Synergistic effects of growth factors and mesenchymal stromal cells for expansion of hematopoietic stem and progenitor cells. *Experimental hematology* **39**, 617-628 (2011).

182 Wagers, A. J. The stem cell niche in regenerative medicine. *Cell stem cell* **10**, 362-369 (2012).

183 Boitano, A. E. *et al.* Aryl hydrocarbon receptor antagonists promote the expansion of human hematopoietic stem cells. *Science* **329**, 1345-1348 (2010).

184 Hofmeister, C. C., Zhang, J., Knight, K. L., Le, P. & Stiff, P. J. Ex vivo expansion of umbilical cord blood stem cells for transplantation: growing knowledge from the hematopoietic niche. *Bone marrow transplantation* **39**, 11-23 (2007).

185 Schofield, R. The relationship between the spleen colony-forming cell and the haemopoietic stem cell. *Blood cells* **4**, 7-25 (1978).

186 Lund, T. C., Boitano, A. E., Delaney, C. S., Shpall, E. J. & Wagner, J. E. Advances in umbilical cord blood manipulation-from niche to bedside. *Nature reviews. Clinical oncology* **12**, 163-174 (2015).

187 Zhang, J. *et al.* Identification of the haematopoietic stem cell niche and control of the niche size. *Nature* **425**, 836-841 (2003).

188 Calvi, L. M. *et al.* Osteoblastic cells regulate the haematopoietic stem cell niche. *Nature* **425**, 841-846 (2003).

189 Kiel, M. J. *et al.* SLAM family receptors distinguish hematopoietic stem and progenitor cells and reveal endothelial niches for stem cells. *Cell* **121** (2005).

190 Mendez-Ferrer, S. *et al.* Mesenchymal and haematopoietic stem cells form a unique bone marrow niche. *Nature* **466**, 829-834 (2010).

191 Naveiras, O. *et al.* Bone-marrow adipocytes as negative regulators of the haematopoietic microenvironment. *Nature* **460**, 259-263 (2009).

192 Sugiyama, T., Kohara, H., Noda, M. & Nagasawa, T. Maintenance of the hematopoietic stem cell pool by CXCL12-CXCR4 chemokine signaling in bone marrow stromal cell niches. *Immunity* **25**, 977-988 (2006).

193 Ding, L., Saunders, T. L., Enikolopov, G. & Morrison, S. J. Endothelial and perivascular cells maintain haematopoietic stem cells. *Nature* **481**, 457-462 (2012).

194 Reya, T. *et al.* A role for Wnt signalling in self-renewal of haematopoietic stem cells. *Nature* **423**, 409-414 (2003).

195 Gao, J. *et al.* Hedgehog signaling is dispensable for adult hematopoietic stem cell function. *Cell stem cell* **4**, 548-558 (2009).

196 Yoshihara, H. *et al.* Thrombopoietin/MPL signaling regulates hematopoietic stem cell quiescence and interaction with the osteoblastic niche. *Cell stem cell* **1**, 685-697 (2007).

197 Watt, S. M. & Forde, S. P. The central role of the chemokine receptor, CXCR4, in haemopoietic stem cell transplantation: will CXCR4 antagonists contribute to the treatment of blood disorders? *Vox sanguinis* **94**, 18-32 (2008).

198 Adams, G. B. *et al.* Stem cell engraftment at the endosteal niche is specified by the calcium-sensing receptor. *Nature* **439**, 599-603 (2006).

199 Arai, F. *et al.* Tie2/angiopoietin-1 signaling regulates hematopoietic stem cell quiescence in the bone marrow niche. *Cell* **118**, 149-161 (2004).

200 Zhu, J. *et al.* Osteoblasts support B-lymphocyte commitment and differentiation from hematopoietic stem cells. *Blood* **109**, 3706-3712 (2007).

201 Nilsson, S. K. *et al.* Osteopontin, a key component of the hematopoietic stem cell niche and regulator of primitive hematopoietic progenitor cells. *Blood* **106**, 1232-1239 (2005).

202 Ceradini, D. J. *et al.* Progenitor cell trafficking is regulated by hypoxic gradients through HIF-1 induction of SDF-1. *Nat Med* **10**, 858-864 (2004).

203 Mendez-Ferrer, S., Lucas, D., Battista, M. & Frenette, P. S. Haematopoietic stem cell release is regulated by circadian oscillations. *Nature* **452**, 442-447 (2008).

204 North, T. E. *et al.* Prostaglandin E2 regulates vertebrate haematopoietic stem cell homeostasis. *Nature* **447**, 1007-1011 (2007).

205 Pinho, S. *et al.* PDGFRalpha and CD51 mark human nestin+ sphere-forming mesenchymal stem cells capable of hematopoietic progenitor cell expansion. *The Journal of experimental medicine* **210**, 1351-1367 (2013).

206 Greenbaum, A. *et al.* CXCL12 in early mesenchymal progenitors is required for haematopoietic stem-cell maintenance. *Nature* **495**, 227-230 (2013).

207 Varnum-Finney, B., Brashem-Stein, C. & Bernstein, I. D. Combined effects of Notch signaling and cytokines induce a multiple log increase in precursors with lymphoid and myeloid reconstituting ability. *Blood* **101**, 1784-1789 (2003).

208 Bhatia, M. *et al.* Bone morphogenetic proteins regulate the developmental program of human hematopoietic stem cells. *The Journal of experimental medicine* **189**, 1139-1148 (1999).

209 Ko, K. H. *et al.* GSK-3beta inhibition promotes engraftment of ex vivo-expanded hematopoietic stem cells and modulates gene expression. *Stem cells* **29**, 108-118 (2011).

2 Proteome and Function of Osteoblast-Derived Extracellular Vesicles

This chapter is based on:

"Proteomic signatures of extracellular vesicles secreted by non-mineralizing and mineralizing human osteoblasts and stimulation of tumor cell growth"

by

Jess Morhayim, Jeroen van de Peppel, Jeroen A.A. Demmers, Gulistan Kocer, Alex L. Nigg, Marjolein van Driel, Hideki Chiba, and Johannes P. van Leeuwen

FASEB Journal. (2015), 29: 274-285

Beyond forming bone, osteoblasts play pivotal roles in various biological processes, including hematopoiesis and bone metastasis. Extracellular vesicles (EVs) have recently been implicated in intercellular communication via transfer of proteins and nucleic acids between cells. Here, we focused on the proteomic characterization of non-mineralizing (NMOBs) and mineralizing (MOBs) human osteoblast (SV-HFOs) EVs and investigated their effect on human prostate cancer (PC3) cells by microscopic, proteomic and gene expression analyses. Proteomic analysis showed that 97% of the proteins are shared among NMOB- and MOB-EVs, and 30% are novel osteoblast-specific EV proteins. Label-free quantification demonstrated mineralization stage-dependent five-fold enrichment of 59 and 451 EV proteins in NMOBs and MOBs, respectively. Interestingly, bioinformatic analyses of the osteoblast EV proteomes and EV-regulated prostate cancer gene expression profiles showed that they converge on pathways involved in cell survival and growth. This was verified by *in vitro* proliferation assays where osteoblast EV uptake leads to two-fold increase in PC3 cell growth compared to cell-free culture medium-derived vesicle controls. Our findings elucidate the mineralization stage-specific protein content of osteoblast-secreted EVs, show a novel way by which osteoblasts communicate with prostate cancer, and open up innovative avenues for therapeutic intervention.

2.1. INTRODUCTION

Osteoblasts are the bone cells of mesenchymal origin that contribute to the strength of the skeletal system by bone matrix production and mineralization[1,2]. The discovery of various cytokines and chemokines secreted by osteoblasts underlined the importance of paracrine signaling in the establishment of favorable microenvironments that support the regulation of bone homeostasis, as well as growth, survival and maintenance of the neighboring bone marrow cells[3,4]. In cancer, osteoblastic microenvironment acts as a pre-metastatic niche by attracting bone-metastasizing tumors[5,6]. Identifying the regulatory mechanism of osteoblast paracrine signaling network may help us design therapeutics to reduce the risk of bone disorders and metastases.

Extracellular vesicles (EVs) have recently emerged as a novel class of cellular messengers involved in communication via exchange of bioactive cargo, such as lipids, proteins and nucleic acids, among cells[7,8]. EVs are released under physiological and pathological conditions, and are involved in various developmental and biological processes, as well as disease progression[9,10]. Thanks to their bioactive content and biocompatibility, EVs have been of increasing interest for their applications as biomarkers, vaccines and drug delivery agents[11-13]. Although there are no defined terms yet to classify different types of EVs, three processes of EV biogenesis have been well documented. Exocytosis of multivesicular bodies releases small vesicles (10-100 nm) called exosomes and exosomes-like vesicles[14]. Budding from the plasma membrane releases a heterogeneous group of vesicles (100-1000 nm) usually referred to as microvesicles[15]. Cells undergoing apoptosis also release EVs as apoptotic bodies (0.8-5 μm) formed by the breakdown of dying cells[16]. Osteoblasts secrete EVs called matrix vesicles (30-300 nm) mainly involved in mineralization of the newly forming bone matrix via hydroxyapatite deposition[17]. In recent years, reports describing the protein profiles of matrix vesicles secreted by osteoblast cell lines from different species indicated that they contain a broad variety of proteins important for bone mineralization[18-20]. On the other hand, there are a few studies demonstrating that matrix vesicles contain signaling proteins and growth factors, such as BMPs and VEGF, suggestive of a role in intercellular communication[21]. However, comprehensive information about osteoblast-secreted EVs with roles other than mineralization is still lacking.

In this study, we present an extensive characterization of human osteoblast-secreted EVs in terms of size, morphology and protein content, and report their role in communication with bone-metastasizing human prostate cancer cells. We focus on identifying the unique and abundant proteins packaged within EVs secreted at various time-points during osteoblast differentiation under both mineralizing and non-mineralizing conditions. We also delineate the biological function of osteoblast EVs by showing that they enter human prostate cancer (PC3) cells and stimulate their growth *in vitro*. Our findings define a role for osteoblast EVs in intercellular communication, and provide a foundation for the development and utilization of EVs as treatment agents.

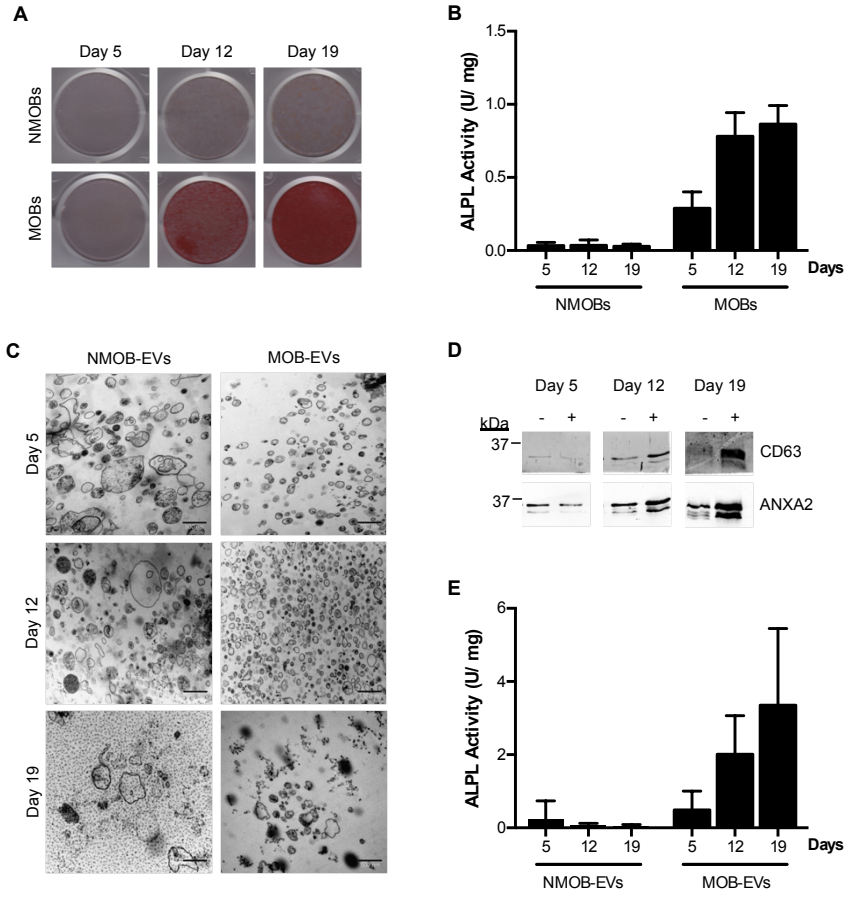

Figure 1. Characterization of EVs secreted by NMOBs and MOBs on day 5, day 12, and day 19 of cultures. A) Alizarin Red S staining of the calcium deposited in the bone matrix, and B) ALPL activity (mean ± SD) of osteoblasts during differentiation. ALPL activity is shown as enzyme unit (U) per milligram (mg) of total protein. C) TEM images (magnification ×28,000) of each EV group. Scale bar: 500 nm. D) Western blot analysis of EV proteins (3 µg/ lane) in NMOB-EVs (-) and MOB-EVs (+) using antibodies against CD63 and ANXA2. E) ALPL activity (mean ± SD) measured in NMOB-EVs and MOB-EVs (N = 3).

2.2. RESULTS

2.2.1. Characterization of human osteoblast-EVs during differentiation and under different mineralization conditions

In this study, we used human pre-osteoblasts (SV-HFOs), which differentiate into mature osteoblasts that produce extracellular matrix and deposit calcium when stimulated with dexamethasone[22]. Throughout this study, dexamethasone-treated and non-dexamethasone-treated osteoblasts were referred to as mineralizing (MOBs) and non-mineralizing (NMOBs) osteoblasts, respectively. To reduce serum-derived EV contamina-

tion we cultured the osteoblasts in medium supplemented with EV-depleted serum followed by serum-free medium for 24 hours before EV isolation. Osteoblasts behave normally under these modified conditions, and undergo proper differentiation and mineralization as shown by Alizarin Red S staining of the calcium deposited in the matrix and alkaline phosphatase (ALPL) activity (Fig. **1A & 1B**).

We isolated EVs secreted by both MOBs and NMOBs on day 5, 12, and 19 of cultures by a series of ultracentrifugation steps, and referred to these six different EV preparations as "EV groups". Transmission electron microscopy (TEM) images show that osteoblast EVs have irregular and spherical structures in wide ranges of diameters depending on the stage of differentiation and mineralization (Fig. **1C**). EVs secreted by NMOBs are more heterogeneous in size (50-1000 nm) than EVs secreted by MOBs (50-250 nm). We further verified the presence of EVs by testing for known EV proteins, such as CD63 and annexin A2 (ANXA2) by western blot (Fig. **1D**)[23]. We confirmed the presence of matrix vesicles within the EV groups derived from MOBs by measuring ALPL activity that is absent in EV groups of NMOBs (Fig. **1E**). These results show that human osteoblasts secrete EVs under both non-mineralizing and mineralizing conditions at different stages of osteoblast differentiation regardless of matrix vesicle activity suggestive of a role not primarily linked to mineralization.

2.2.2. Proteomic profiling of NMOB-EVs and MOB-EVs

EV proteomes of NMOBs and MOBs on day 5, 12 and 19 of culture were analyzed by mass spectrometry, as previously described[24,25]. Briefly, proteins of isolated EVs were separated by SDS-PAGE electrophoresis, in-gel digested and analyzed by LC-MS/MS. Altogether we detected 1,120 proteins, among which 946 proteins (84%) are detected in every EV group despite the morphological differences shown in Figure **1C** (Appendix A, Table A1). These proteins consist of commonly known vesicle proteins, and are mainly annotated to a wide array of vesicle related molecular functions and biological processes (Fig. **2A**). Furthermore, the overlapping proteins include osteoblast-related proteins linked to skeletal development, mesenchymal differentiation, calcium ion binding and phosphatase activity, which can be attributed to the activity of matrix vesicles (Appendix A, Table A2). Figure **2B** shows a schematic representation of the over-represented protein families found in all EV groups.

Next, we combined the protein data from all three time-points for each of the mineralization conditions. The Venn diagram in Figure **3A** shows that 1,090 proteins (97% of the total proteins) are overlapping. 4 and 26 proteins are uniquely detected in NMOB-EVs and MOB-EVs, respectively. Comparison with ExoCarta database[23] shows that the majority of the mineralization condition-specific proteins (3 out of 4 NMOB-EV and 22 out of 26 MOB-EV proteins) as well as 352 overlapping proteins are uniquely detected in our osteoblast EVs at the time of the analysis (Fig. **3A**).

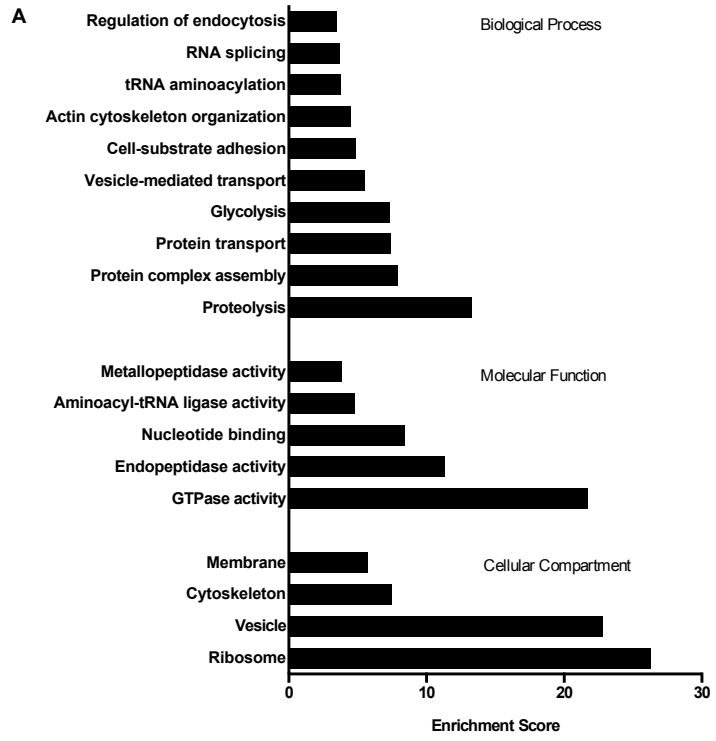

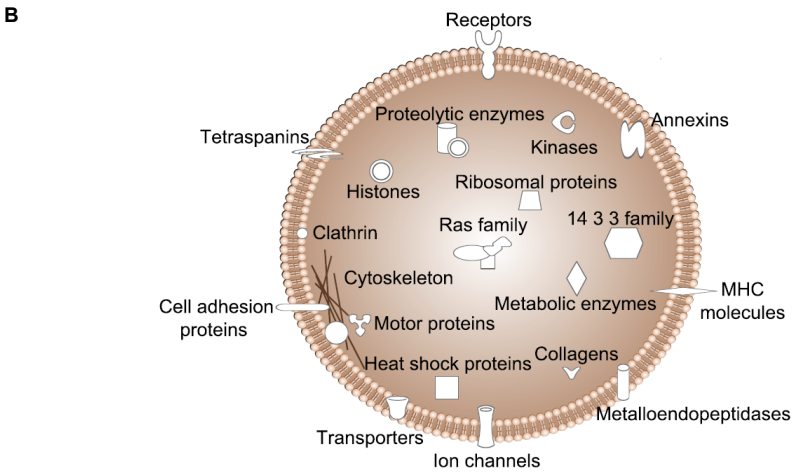

Figure 2. Protein profiling of NMOB-EVs and MOB-EVs on day 5, 12 and 19 of cultures. A) GO annotations for cellular components, molecular functions and biological processes of EV proteins shared across the 6 EV groups (N = 2). Only the highest significantly (Benjamini $P < 0.001$) over-represented terms are shown. B) Schematic representation of the protein families detected in all EVs determined based on literature and IPA.

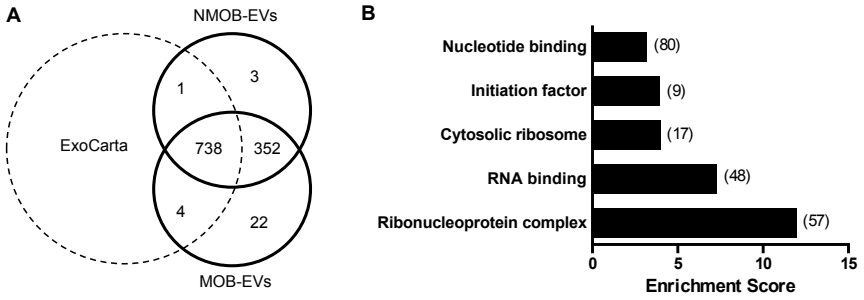

Figure 3. Identification of novel osteoblast-specific EV proteins. A) Venn diagram shows the numbers of proteins in EVs derived from NMOBs and MOBs and comparison with proteins reported in ExoCarta. B) GO annotations of novel osteoblast EV proteins (panel A) not recorded in ExoCarta. Only the highest significantly (Benjamini $P < 0.001$) over-represented terms are shown. The brackets indicate the number of proteins for each term.

Table 1. The list of osteoblast-specific proteins uniquely detected in either NMOB-EVs or MOB-EVs.

Osteoblast	UniProt Accession	Gene Symbol	Description
NMOB-EVs	Q9BUB4	*ADAT1*	tRNA-specific adenosine deaminase 1
	P19784	*CSNK2A2*	Casein kinase II subunit alpha
	Q02539	*HIST1H1A*	Histone H1.1
MOB-EVs	Q8TDN6	*BRIX1*	Ribosome biogenesis protein BRX1 homolog
	P45973	*CBX5*	Chromobox protein homolog 5
	Q7Z7A1	*CNTRL*	Centriolin
	Q9UBL6	*CPNE7*	Copine-7
	Q9NVP1	*DDX18*	ATP-dependent RNA helicase DDX18
	P23743	*DGKA*	Diacylglycerol kinase alpha
	Q9HCE0	*EPG5*	Ectopic P granules protein 5 homolog
	P46976	*GYG1*	Glycogenin-1
	Q13151	*HNRNPA0*	Heterogeneous nuclear ribonucleoprotein A0
	O00425	*IGF2BP3*	Insulin-like growth factor 2 mRNA-binding protein 3
	O43731	*KDELR3*	ER lumen protein retaining receptor 3
	Q6VAB6	*KSR2*	Kinase suppressor of Ras 2
	O15243	*LEPROT*	Leptin receptor gene-related protein
	Q9H0P0	*NT5C3*	Cytosolic 5-nucleotidase 3
	Q8TAD7	*OCC1*	Overexpressed in colon carcinoma 1 protein
	Q5T091	*RER1*	Protein RER1
	Q9GZN7	*ROGDI*	Protein rogdi homolog
	P67812	*SEC11A*	Signal peptidase complex catalytic subunit SEC11A
	P61011	*SRP54*	Signal recognition particle 54 kDa protein
	Q13242	*SRSF9*	Serine/arginine-rich splicing factor 9
	O14787	*TNPO2*	Transportin-2
	P11172	*UMPS*	Uridine 5-monophosphate synthase

GO annotation analysis indicates that these osteoblast-specific proteins are mostly annotated to ribonucleoprotein complex, RNA-binding, ribosome, initiator factor and nucleotide binding (Fig. **3B**). Table **1** shows the list of the osteoblast-specific proteins that are uniquely detected in either NMOB-EVs or MOB-EVs. Together, these findings show that osteoblast EVs are enriched with known vesicular proteins while they also contain unique proteins depending on the mineralization condition.

2.2.3. Label-free quantitative distribution of osteoblast EV proteins

Absolute protein abundances can be estimated by label-free methods based on quantification using the peak intensities of the LC-MS/MS data. We used the iBAQ values from the MaxQuant analysis output to identify the most abundant proteins in each EV group, and compared the protein abundances between the different EV groups[26]. The most abundant EV proteins are the commonly known vesicular proteins, such as ANXA2, GAPDH, CD9, ENO1, PDCD61P, etc. for all EV groups (Fig. **4A**)[23]. Interestingly, all EV groups contain high levels of histones. Multi-scatter plots in Figure **4B** show the strong correlation between the protein content of the different EV groups. EV proteins isolated at different time-points during culture show a higher correlation when compared within a culture condition (i.e. within NMOBs and MOBs) than between the culture conditions. The differences between EVs derived from NMOBs and MOBs become more apparent as the cells start to mineralize on day 12 (Day 5: r=0.959, Day 12: r=0.912, Day 19: r=0.905).

Next, we compared the average intensities of NMOB-EV and MOB-EV proteins isolated on the same day of culture to identify specifically enriched EV proteins. Proteins with more than five-fold increase in iBAQ intensities were regarded as more abundant in either one of the EV groups on that specific day of culture (Fig. **4C- 4E**). In accordance with the scatter plots, the number of abundant MOB-EV proteins shows a strong increase from 46 to 279 and 321 on day 12 (onset of mineralization) and 19 (full mineralization), respectively (Fig. **4D & 4E**). Surprisingly, these proteins are mostly annotated to RNA-binding and processing, and not to matrix vesicle-dependent mineralization. NMOB-EVs are mainly enriched with cell adhesion-associated extracellular matrix proteins and chromosomal proteins. Table **2** shows a representative list of proteins that were detected with more than five-fold abundance in either NMOB-EVs or MOB-EVs. The Venn diagrams in Figures **4F & 4G** show the distribution of the proteins (i.e. those shown in Figures **4C- 4E**) specifically enriched in either NMOB-EVs (Fig. **4F**) or MOB-EVs (Fig. **4G**) over the different culture time-points. HMGA2, PLAU, TNC and HIST1H1C are highly abundant at every time-point in NMOB-EVs. MOB-EVs are enriched with 22 proteins throughout culture, among which ALPL and CD109 show the most striking abundance. These results show that despite the similarity in protein content, osteoblast EVs are enriched with distinct proteins depending on the mineralization condition and the stage of differentiation.

Table 2. Representative list of proteins significantly enriched (> five-fold) in either NMOB-EVs or MOB-EVs.

Osteoblast	UniProt Accession	Gene Symbol	Description
NMOB-EVs			
Extracellular matrix proteins			
	P08253	*MMP2*	72 kDa type IV collagenase
	P00749	*PLAU*	Urokinase-type plasminogen activator
	Q15582	*TGFBI*	Transforming growth factor-beta-induced protein ig-h3
	P35442	*THBS2*	Thrombospondin-2
	P24821	*TNC*	Tenascin
	P13611	*VCAN*	Versican core protein
Chromosomal proteins			
	P07305	*H1F0*	Histone H1.0
	P16403	*HIST1H1C*	Histone H1.2
	P62805	*HIST1H4A*	Histone H4
	P17096	*HMGA1*	High mobility group protein HMG-I
	P52926	*HMGA2*	High mobility group protein HMGI-C
MOB-EVs			
Ribonucleoprotein complexes			
	Q00839	*HNRNPU*	Heterogeneous nuclear ribonucleoprotein U
	Q12906	*ILF3*	Interleukin enhancer-binding factor 3
	P49207	*RPL34*	60S ribosomal protein L34
	P62847	*RPS24*	40S ribosomal protein S24
	Q92616	*GCN1L1*	Translational activator GCN1
RNA-binding proteins			
	Q9NR30	*DDX21*	Nucleolar RNA helicase 2
	Q9Y2L1	*DIS3*	Exosome complex exonuclease RRP44
	P20042	*EIF2S2*	Eukaryotic translation initiation factor 2 subunit 2
	Q01081	*U2AF1*	Splicing factor U2AF 35 kDa subunit
	Q9HAV4	*XPO5*	Exportin-5
Nucleotide binding proteins			
	Q9UN86	*G3BP2*	Ras GTPase-activating protein-binding protein 2
	P54652	*HSPA2*	Heat shock-related 70 kDa protein 2
	O00425	*IGF2BP3*	Insulin-like growth factor 2 mRNA-binding protein 3
	Q14566	*MCM6*	DNA replication licensing factor MCM6
	P22694	*PRKACB*	cAMP-dependent protein kinase catalytic subunit beta
GTPase activity			
	P84085	*ARF5*	ADP-ribosylation factor 5
	Q9NZN4	*EHD2*	EH domain-containing protein 2
	P20591	*MX1*	Interferon-induced GTP-binding protein Mx1
	P61020	*RAB5B*	Ras-related protein Rab-5B
	P08134	*RHOC*	Rho-related GTP-binding protein RhoC
Other			
	Q09666	*AHNAK*	Neuroblast differentiation-associated protein AHNAK
	P05186	*ALPL*	Alkaline phosphatase, tissue-nonspecific isozyme
	Q8ND76	*CCNY*	Cyclin-Y;Cyclin-Y-like protein 2
	Q6YHK3	*CD109*	CD109 antigen
	Q13451	*FKBP5*	Peptidyl-prolyl cis-trans isomerase FKBP5

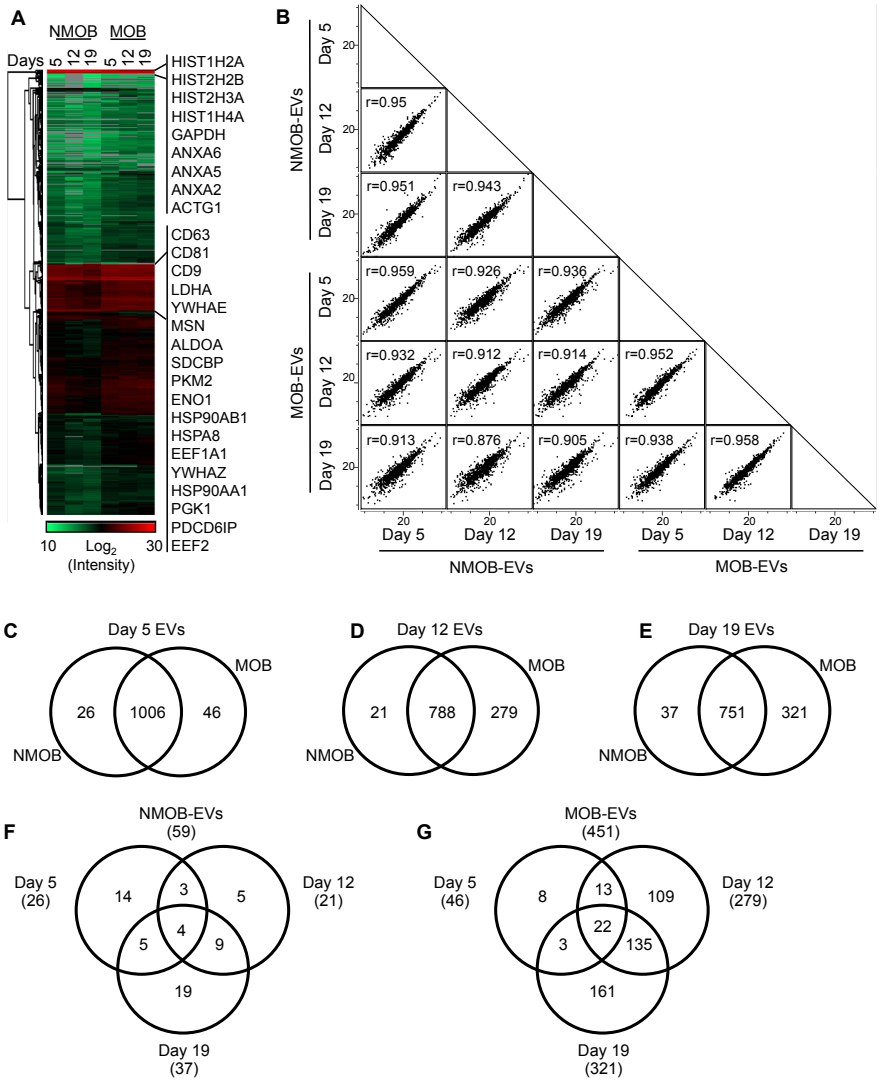

Figure 4. Comparative proteomic analysis of EVs secreted from NMOBs and MOBs during 19 days of culture. A) Heat map shows protein abundances (iBAQ values) across the six EV groups. The most abundant proteins including the top identified EV markers (ExoCarta) are shown next to the heat map. Red, high abundance; green, low abundance; grey, no signal. B) Multi-scatter plots show the strong correlation between NMOB-EV and MOB-EV protein abundances. Venn diagrams C-G) show the number of proteins that are at least five-fold more abundant in either NMOB-EVs or MOB-EVs on (C) day 5, (D) day 12 and (E) day 19, and the distribution of the abundant proteins in (F) NMOB-EVs and (G) MOB-EVs at different stages of differentiation.

2.2.4. Effect of osteoblast EVs on PC3 cell growth

Next, we tested the functionality of EVs in intercellular communication. For this we chose the osteoblast-prostate tumor cell interaction. Proteomics analyses indicated that the EV proteome content of NMOBs and MOBs starts to show greater specificity on day 12

of cultures. Therefore, here we focused on day 12 EVs, and analyzed whether osteoblast EVs regulate PC3 cell growth and survival *in vitro*. First, we evaluated the uptake of osteoblast EVs by PC3 cells using fluorescence labeling. High-resolution 4Pi microscopy analysis confirms that PC3 cells internalize the PKH67-labeled osteoblast EVs within 24 hours (Fig. **5A & 5B**). Flow cytometry analyses indicate that EV uptake is dose-dependent (Fig. **5C**).

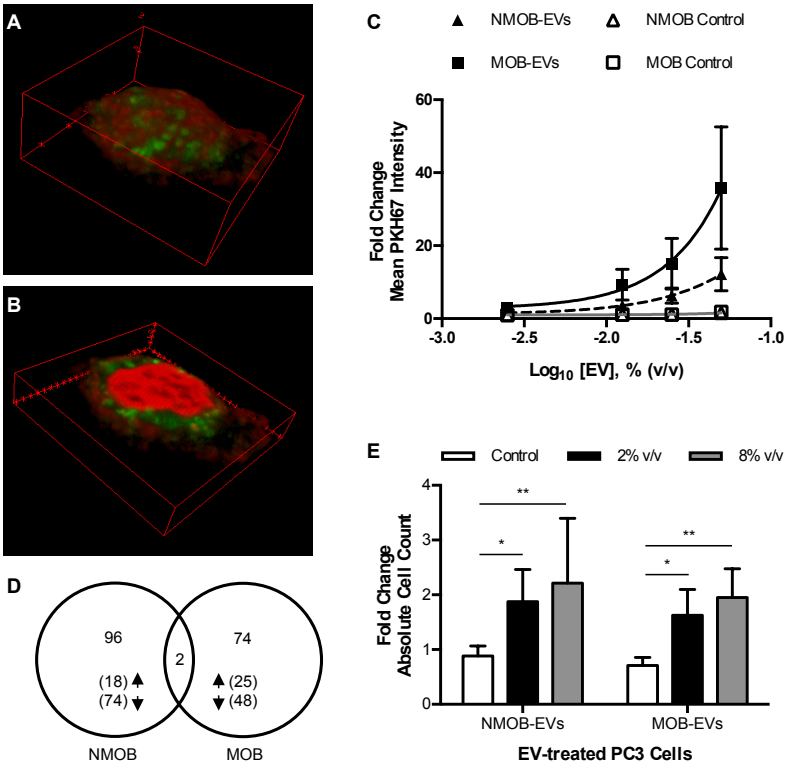

Figure 5. Internalization of day 12 osteoblast EVs and their functional effect on PC3 cells. A-B) 4Pi images show the uptake of PKH67-labeled NMOB-EVs by PC3 cells. Panel (A) shows 3D reconstruction of all confocal stacks; panel (B) shows the half plane showing the EVs inside the cells. Images are representative for MOB-EVs uptake. Red, cell membrane & nucleus; green, PKH67-labeled EVs. See the online manuscript for supplemental movie. C) Flow cytometry analysis shows dose-dependent uptake (mean ± SD) of PKH67-labeled EVs by PC3 cells (N = 2). Fold change is determined relative to untreated cells. D) Venn diagram shows the PC3 genes that were regulated in response to day 12 osteoblast EVs (2.86% v/v) by at least 1.5-fold. The numbers in brackets denote the genes that were up- and down-regulated by the respective EV group. E) Fold change of PC3 cell count (mean ± SD) after 5 days of incubation with different EV doses (N = 3). * $P < 0.05$, ** $P < 0.01$, compared with control by two-way ANOVA. Control: cell-free culture medium processed the same way as the conditioned medium.

Next, we performed microarray analysis to investigate the effect of osteoblast EV treatment on the gene expression profile of PC3 cells. We incubated PC3 cells with day 12

NMOB-EVs and MOB-EVs, and collected RNA after 4, 24 and 48 hours. Interestingly, treatment with the two different EV groups resulted in regulation of different sets of prostate cancer genes (Appendix A, Table A3). We identified 98 and 76 genes that are regulated more than 1.5-fold by NMOB-EVs and MOB-EVs, respectively, compared to the control-treated cells (Fig. **5D**). The two overlapping genes are *FTHL8* and *LOC728499*, and they are down- and up-regulated by both EV groups, respectively. The majority of the genes in both treatment groups are down-regulated (74 out of 96 genes by NMOB-EVs and 48 out of 74 genes by MOB-EVs). Ingenuity Pathway Analysis (IPA) indicated that even though the regulated genes are different they are annotated to similar molecular and cellular functions mainly related to cell growth and survival ($P < 0.05$). We assessed the effect of osteoblast EVs on PC3 cell growth by culturing the tumor cells with different EV concentrations for 5 days. Both NMOB-EVs and MOB-EVs induce two-fold increase of absolute cell numbers compared to control-treated cells (Fig. **5E**).

We used bioinformatics to integrate the proteomics and microarray data, and thus correlate the proteome of day 12 osteoblast EVs to the EV-regulated PC3 genes. We used IPA to build a network showing the direct molecular relationships between the EV proteins and the regulated PC3 genes for each treatment group (**Fig. 6**). 25 out of the 98 NMOB-EV-regulated PC3 genes are mapped with 157 out of 980 day 12 NMOB-EV proteins (Fig. **6A**). Most proteins are annotated to vesicle and ribosomal proteins, and mainly interact with *YWHAG* and *PAK2*. For the MOB-EV treatment 38 out of 76 genes interact with 337 proteins out of 1,079 day 12 MOB-EV proteins (Fig. **6B**). Most of the mapped proteins are ribosomal proteins, and interact predominantly with *RAD21* and *CDK5*. Together these results show that NMOB-EVs and MOB-EVs are both internalized by PC3 cells and regulate the expression of different prostate genes, however, both converging to stimulation of cell growth.

2.3. DISCUSSION

The findings described in this study showed that both NMOBs and MOBs secrete EVs selectively packaged with known vesicle proteins as well as an interesting range of proteins unique to the mineralization and differentiation status of the osteoblasts. Osteoblast EVs enter human prostate cancer cells, regulate the expression of cell growth-related prostate cancer genes, and stimulate their growth *in vitro* demonstrating their active role in intercellular communication.

Osteoblasts actively undergo sequential events of differentiation along the course of their maturation. Previous work in our group showed the importance of studying protein and genetic composition of osteoblasts at different stages of their differentiation[22,25]. Here, we used a well-characterized human pre-osteoblast cell model to isolate EVs at three stages of differentiation to gain a comprehensive understanding of the osteoblast EV proteome: pre-mineralization (day 5), onset of mineralization (day 12) and full mineralization (day

19). We also isolated EVs from NMOBs at the same culture time-points as a comparison to elucidate the EV proteins not primarily linked to mineralization and thus understand their role in cell communication. Interestingly, 84% of the total proteins are shared between all the EV groups, and 97% are detected at least in one of the time-points in both NMOB-EVs and MOB-EVs. This was surprising as the TEM images show clear morphological differences between the EVs secreted by osteoblasts under different mineralization conditions. A large number of the overlapping proteins are novel proteins, primarily associated with ribonucleoproteins, which were not recorded in the EV database ExoCarta at the time of the analysis. Even though we cannot exclude that part of these proteins may be arising from non-specific background, recent studies reporting the presence of vesicle-associated RNA-binding proteins suggest that our osteoblast EVs contain novel proteins linked to known vesicle-related processes[27,28].

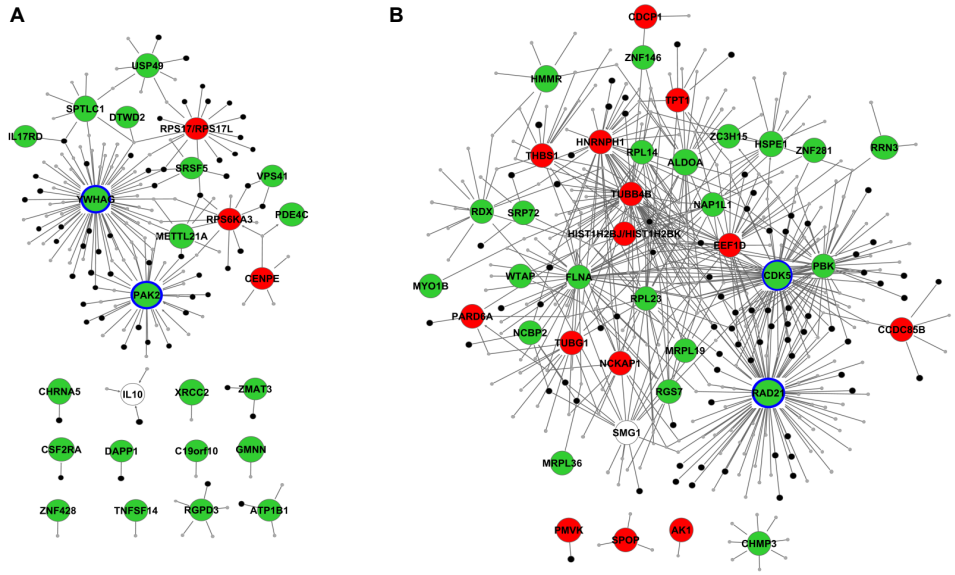

Figure 6. IPA network showing the direct relationship maps between the EV-regulated PC3 genes and day 12 EV proteins for A) NMOB-EV and B) MOB-EV treatments. Green, down-regulated PC3 genes; red, up-regulated PC3 genes; grey, EV proteins; black, EV proteins annotated to vesicles and ribosomes. The most predominantly mapped PC3 genes are highlighted (blue line).

We hypothesized that despite the similarities in cargo the different EV groups are specifically enriched with distinct proteins giving clues to their biological function. Label free quantification is a very useful proteomics tool to compare the relative abundances of proteins across different samples, which leads to a selection of proteins that can be analyzed for molecular function. All of the EV groups described in this study contain abundant levels of the classical vesicle proteins, such as annexins (ANXA2, ANXA6), tetraspanins

(CD9, CD81), and metabolic proteins (GAPDH, LDHA), verifying the robustness of these proteins as vesicle markers. It is interesting to note that histones are also among the highly enriched proteins detected in all EV groups. In fact, we previously showed that histone proteins are among the most abundant proteins in human bone suggesting the likelihood of possessing extranuclear roles[29]. In accordance, there have been increasing number of studies reporting the functionality of circulating nuclear proteins as well as their presence in apoptotic bodies, exosomes and microvesicles[7,30-32]. While the abundances of the predominant proteins are similar across all EV groups, we detected unique group of proteins that are at least five-fold more abundant in EVs secreted by either NMOBs or MOBs at a given culture time-point. Among the bone-related proteins ALPL is significantly enriched in MOB-EVs with an increasing abundance in time, which parallels the vesicular and cellular ALPL activity. Mineralization is indeed one of the most important processes of bone formation with a major role for matrix vesicles. Thus, it is not surprising to observe the high level of vesicular ALPL activity in MOB-EVs compared to the donor cells. However, GO analyses showing over-representation of vesicle-related processes over bone-related processes suggest a role for EVs not primarily linked to mineralization. The most striking differences between the EV groups are the enrichment of adhesion proteins and RNA-binding proteins in NMOB-EVs and MOB-EVs, respectively.

To investigate the role of EVs in intercellular communication we tested EV uptake by prostate cancer cells and their effect on prostate cancer cell growth. Prostate cancer, which is one of the most frequently diagnosed cancers among men, is primarily associated with bone metastasis[33]. Osteoblast microenvironment consisting of a network of receptors and secreted factors acts as an attractive force and regulator of tumor cell growth[34]. We showed that PC3 prostate cancer cells dose-dependently internalize PKH67-labeled EVs derived from both NMOBs and MOBs. The fluorescence intensity of PC3 cells treated with MOB-EVs is higher than those treated with NMOB-EVs at any given EV dose. Due to the challenges of absolute quantification of EVs it is difficult to make an accurate quantitative comparison between the EV groups[35]. Moreover, the mode of internalization may contribute to the difference in fluorescence signal. EVs that are internalized via endocytosis are more likely to retain a stronger PKH67 signal compared to the EVs that transfer their cargo via fusion in host cell's plasma membrane. Here, we observed that osteoblast EVs retain their fluorescence upon overnight cultures. Therefore it seems that endocytosis is involved in their uptake, however, we cannot rule out the involvement of other uptake modes.

Studying the molecular mechanism of cancer survival and growth is an important area of investigation. In particular bone metastasis, which is considered an incurable stage of the disease, is of great interest with clinical significance. Our EV treatment studies demonstrated that both NMOB-EVs and MOB-EVs stimulate the growth of PC3 cells *in vitro*. This shows that osteoblast EVs are not only internalized by the prostate cancer cells but that they are also functional and can stimulate prostate cancer cell growth. This was further supported by PC3 cell gene expression analysis, which revealed the EV-regulated prostate cancer genes are mainly involved in cell survival and growth. It is important to

note that the two EV groups affect the regulation of different sets of prostate cancer genes, which are annotated to similar molecular functions. This is most likely due to the differences in their bioactive cargo that may act via different pathways leading to the same biological outcome.

Proteomic analyses showed that there are differences in protein abundances between day 12 NMOB-EVs and MOB-EVs. When we mapped the EV proteins with the regulated prostate genes in an interaction network we found that the MOB-EV-regulated genes are mostly mapped with ribosomal and RNA-binding proteins. Previous studies showed the role of ribosomal proteins in physiological events, such as proliferation and cell growth, besides the well-known role in protein biosynthesis[36]. Lai and colleagues showed that ribosomal proteins are also involved in cancer progression and metastasis[37]. Particularly, ribosomal proteins have been shown to have elevated expression levels in prostate tumors, and hence play an important role in prostate cancer development[38,39]. NMOB-EV-regulated genes are mostly mapped with known vesicle proteins, mainly consisting of signaling proteins and chaperones, as well as ribosomal proteins that may act via different pathways than the MOB-EV proteins. 14-3-3 family proteins are involved in various signaling cascades and have been shown to be regulators of prostate cancer tumor formation with the exception of 14-3-3σ protein, a tumor suppressor, which is most interestingly not present in osteoblast EVs[40,41]. Chaperones, such as heat shock proteins, have been shown to be negative regulators of apoptosis during prostate tumorigenesis suggesting an anti-apoptotic role for our chaperone-containing osteoblast EVs[42]. With the growing interest in the field, more comprehensive information on EV composition and knowledge on their molecular function in diverse biological and pathological processes is becoming of utmost importance. Alternatively, increasing reports on EV biogenesis, content and targeting may provide the basis for their exploitation as carriers of therapeutic cargo for targeted cancer therapy, cell therapy and tissue engineering[43-45]. In this study, we demonstrated that osteoblast EVs play a role in the crosstalk between osteoblasts and prostate cancer cells highlighting the importance of EV cargo in cancer regulation. We anticipate that deeper investigation of EV function in the bone microenvironment will help us develop preventive or curative therapies for a broad variety of pathological conditions.

In conclusion, our data give insights into the morphology and proteomic composition of osteoblast EVs at different stages of differentiation under mineralizing and non-mineralizing conditions. Proteomic analyses presented here suggest a role for osteoblast EVs in intercellular communication besides a well-characterized role in mineralization. We further demonstrate the existence of an EV-driven interaction between osteoblasts and prostate cancer cells stressing the clinical/pathophysiological significance of our data. Albeit, challenges still remain, as we need optimized tools to quantify and separate different sub-populations of EVs and to interpret the roles of individual proteins in the context of communication. The present study unequivocally demonstrates that osteoblasts produce EVs that can enter other cells and stimulate their proliferation. This provides an additional way by which osteoblasts may regulate their microenvironment, not only metastatic pros-

tate cancer cells, but also the surrounding bone marrow cells, such as hematopoietic stem cells and osteoclasts.

2.4. MATERIALS AND METHODS

Cell cultures. Simian virus 40-immortalized human osteoblast cell line (SV-HFO cells) established from normal human fetal calvaria was cultured as described previously with modifications[22]. Cells were seeded at a density of 5×10^3 cells/ cm^2 and cultured in α-MEM (GIBCO, Paisley, UK) supplemented with 20 mM HEPES, pH 7.5 (Sigma, St. Louis, MO, USA), streptomycin/ penicillin, 1.8 mM $CaCl_2$ (Sigma), 10 mM β-glycerophosphate (Sigma) and 2% depleted (100,000g for 90 minutes at 4°C)-FCS (GIBCO) at 37°C in a humidified atmosphere of 5% CO_2 for up to 19 days. The culture medium was replaced every 2-3 days. SV-HFOs were washed with 1X PBS and refreshed with serum-free medium 24 hours prior to EV isolation. PC3 cells were cultured in α-MEM (GIBCO) supplemented with streptomycin/ penicillin, 1.8 mM $CaCl_2$ (Sigma) and 10% FCS at 37°C in a humidified atmosphere of 5% CO_2. For functional experiments PC3 cell culture medium was supplemented with 2% FCS.

EV isolation. Osteoblast-EVs were isolated from 20 ml conditioned medium by low speed centrifugation (1,500 rpm, 5 minutes; 4,500 rpm, 10 minutes) followed by ultracentrifugation (20,000g, 30 minutes; 100,000g, 1 hour at 4°C) of the supernatant using the SW28 rotor (Beckman Coulter, Fullerton, CA, USA). The 100,000g EV pellet was re-suspended in 20 µl fixative for TEM, 100 µl PBS for biochemical assays and immunoblotting, and 100 µl PC3 culture medium for functional experiments. EVs were labeled with PKH67 (Sigma) according to the manufacturer's instructions. The amount of experimental EV dose was determined as 5% (v/v). Cell- and serum-free SV-HFO culture medium was processes the same way as the conditioned medium, and was used as a control for functional experiments.

Biochemical assays. Alizarin staining, protein concentration, ALPL activity assay, and DNA quantification were performed as described previously[46]. Briefly, mineralization of the bone matrix was monitored by Alizarin Red staining of the calcium matrix. Cells were fixed with 70% ethanol for 60 minutes on ice. After fixation, cells were washed with 1X PBS twice and stained with Alizarin Red solution (saturated Alizarin Red in demineralized water titrated to pH 4.2 with 0.5% ammonium hydroxide) for 10 minutes. Protein concentration was determined using the BCA kit (Pierce Biotechnology, Rockford, IL, USA) following the manufacturer's instructions. ALPL activity of the whole cell lysates and EVs was determined in a colorimetric assay detecting the release of paranitrophenol from paranitrophenyl phosphate upon reaction catalyzed by endogenous ALPL. The activity was displayed as enzyme units per milligrams of total protein. DNA was quantified by spectro-

fluorimetry using ethidium bromide. Samples were analyzed by a microplate reader using an excitation filter of 340 nm and an emission filter of 590 nm.

Immunoblot analysis. Protein samples were prepared by mixing the EVs (in PBS) with 6X reducing sample buffer immediately after isolation. EV proteins (3µg total protein/ sample) were separated by SDS-PAGE at 200 V and transferred onto a nitrocellulose membrane (Hybond-ECL, Amersham Biosciences, Buckinghamshire, UK). After blocking non-specific signal with 5% BSA in TBS/ 0.1% Tween-20, the membrane was incubated with primary antibodies against annexin A2 (rabbit polyclonal, 1:500, Abcam, Cambridge, UK) and CD63 (rabbit polyclonal, 1:1000, SantaCruz, Dallas, TX, USA). Membranes were probed with secondary antibody conjugated with IRDye 800CW (1:5000, goat anti-rabbit, LI-COR, Lincoln, NE, USA) using Odyssey Infrared Imaging System according to the manufacturer's instructions (LI-COR).

Flow cytometry. PC3 cells were incubated with different concentrations (% v/v) of PKH67-labeled day 12 osteoblast EVs and EV control. After overnight culture the mean fluorescence intensity was detected by flow cytometry (BD Accuri C6, BD Biosciences, San Jose, CA, USA) using the FITC channel. Absolute cell counts were determined using counting beads (BD Biosciences).

Transmission electron microscopy. EVs were fixed in 4% formaldehyde (37% solution, Merck, New York, NY, USA) in 1% glutaraldehyde (25% solution, Merck) at 4°C (Trump's fixative). Fixative was removed by incubating the sample in Millonig buffer (NaH2PO4.H2O) (BDH Chemicals, Radnor, PA, USA) for 6 hours followed by post-fixation with 1% osmium tetroxide (4% solution, Electron Microscopy Sciences, Hatfield, PA, USA). The samples were rinsed with distilled water and a series of acetone concentrations (50%, 70%, 90%, 96%, 100%). The EV pellets were incubated on pure epoxy resin for 1 hour at 37°C, and then embedded in fresh epoxy and polymerized for 12 hours at 60°C. The polymerized resin was cut into thin sections (40-60 nm) using ultramicrotome (Leica Ultracut UCT, Wetzlar, Germany) and a diamond knife (Diatome, Hatfield, PA, USA) and mounted on a copper grid. The sample was detected by TEM (Morgagni, Philips/FEI, Hillsboro, OR, USA).

4Pi microscopy. EV uptake by PC3 cells was monitored using 4Pi microscope, which is a confocal fluorescence microscope with an improved axial resolution by a factor of 5-7 over conventional confocal microscopes[47]. PC3 cells were seeded on poly-lysine coated quartz coverslips. After overnight incubation with PKH67-labeled EVs, cells were washed with PBS, fixed with 10% formalin, stained with concanavalin A (Alexa Fluor 647 conjugate, Life Technologies, Carlsbad, CA, USA). The fixed cells were washed 3 times with 0.01 M PBS and then 3 times impregnated with 87% glycerol. The coverslip was mounted on a special 4Pi sample holder and covered with another quartz coverslip, using 87% glycerol as mounting medium giving the whole beam path a refractive index of 1.458[48]. The coverslips

were sealed with 2-component silicon (Twinsil, Picodent, Germany). Images were taken with a Leica 4Pi TCS microscope using two opposing 100X 1.35NA glycerol HCX PL APO objectives. A two-photon Ti-Sapphire laser (Mai Tai, Spectra Physics, Santa Clara, CA, USA) was used for excitation at 800 nm wavelength[49]. Avalanche photo diodes were used for detection of the signals with a 500-550 nm bandpass filter for PKH67 and a 647-703 nm bandpass filter for Alexa647. Images were deconvoluted with Imspector (Max-Planck Innovation, Munich, Germany). Images and the video were generated using ImageJ 3D Viewer plugin.

Mass spectrometry. EV proteins (8 µg protein/ sample) were separated by NuPage Novex 4-12% Bis-Tris gel (Life Technologies), and stained with Coomassie (Bio-Rad, Hercules, CA, USA) for 1 hour and de-stained with water overnight. 1D SDS-PAGE gel lanes were cut into 2-mm slices using an automatic gel slicer and subjected to in-gel reduction with dithiothreitol, alkylation with iodoacetamide (D4, 98%, Cambridge Isotope Laboratories, Inc., Tewksbury, MA, USA) and digestion with trypsin (Promega, sequencing grade, Madison, WI, USA)[50]. Nanoflow LC-MS/MS was performed on a 1100 series capillary LC system (Agilent Technologies, Santa Clara, CA, USA) coupled to an LTQ-Orbitrap XL mass spectrometer (Thermo Scientific, Waltham, MA, USA) operating in positive mode[25]. Peptide mixtures were trapped on a ReproSil C18 reversed phase column (Dr Maisch GmbH; 1.5 cm × 100 µm, packed in-house) at a flow rate of 8 µl/ minute. Peptide separation was performed on ReproSil C18 reversed phase column (Dr. Maisch GmbH, Ammerbuch-Entringen, GE; 15 cm × 50 µm, packed in-house) using a linear gradient from 0 to 80% B (A = 0.1% formic acid; B = 80% (v/v) acetonitrile, 0.1% formic acid) in 170 minutes and at aconstant flow rate of 200 nl/ minute using a splitter. The column eluent was directly sprayed into the ESI source of the mass spectrometer. Mass spectra were acquired in continuum mode, and fragmentation of the peptides was performed in data-dependent mode.

Microarray analysis. PC3 cells were incubated with day 12 osteoblast EVs and their controls for 4, 24 and 48 hours. Total PC3 cell RNA was isolated using TRIzol (Life Technologies) extraction method according to the manufacturer's instructions. RNA samples were prepared for microarray analysis using the Illumina TotalPrep RNA Amplification Kit (Ambion, Life Technologies) according to the manufacturer's instructions. Biotinylated cRNA was hybridized to HumanHT-12 v4 Expression BeadChip (Illumina, San Diego, CA, USA) microarray chips according to the manufacturer's protocol. Data acquisition was performed using iScan (Illumina).

Bioinformatic analysis. The raw MS data were analyzed using the MaxQuant software (version 1.3.0.5)[51]. A false discovery rate of 0.01 for proteins and peptides and a minimum peptide length of 6 amino acids were required. The Andromeda search engine[52] was used to search the MS/MS spectra against the Uniprot database (taxonomy: *Homo sapiens*, release HUMAN_2013_04) concatenated with the reversed versions of all sequences (maximum of two missed cleavages; 0.6 Da fragment mass tolerance, enzyme specificity: trypsin). Only

proteins identified with at least 2 unique peptides and 2 quantitation events were considered for analysis. The data from the replicates were combined as averages of label-free quantification intensity values for each EV group defined by the mineralization condition and the day of culture. Perseus 1.3.0.4 (Max Planck Institute of Biochemistry 2012) was used to generate the heat map and scatter plots based on iBAQ values. DAVID Bionformatics Resources v6.7 was used to categorize the proteins into overrepresented processes using our previously described SV-HFO gene expression dataset as a background[53,54]. ExoCarta database (Release date: 29 May 2012) was used for comparative EV analysis. IPA (Ingenuity® Systems, www.ingenuity.com) was used to analyze the interaction between EV proteome and PC3 genes using the path explorer tool in My Pathway analysis.

Statistics. The results were described as mean ± SD based on at least two independent experiments. Significance was calculated using two-way ANOVA test and P values of < 0.05 were considered significant.

REFERENCES

1 Marks, S. C., Jr. & Popoff, S. N. Bone cell biology: the regulation of development, structure, and function in the skeleton. *Am J Anat* **183**, 1-44 (1988).

2 Chamberlain, G., Fox, J., Ashton, B. & Middleton, J. Concise review: mesenchymal stem cells: their phenotype, differentiation capacity, immunological features, and potential for homing. *Stem cells* **25**, 2739-2749 (2007).

3 Proff, P. & Romer, P. The molecular mechanism behind bone remodelling: a review. *Clin Oral Investig* **13**, 355-362 (2009).

4 Taichman, R. S. Blood and bone: two tissues whose fates are intertwined to create the hematopoietic stem-cell niche. *Blood* **105**, 2631-2639 (2005).

5 Coleman, R. E. Clinical features of metastatic bone disease and risk of skeletal morbidity. *Clin Cancer Res* **12**, 6243s-6249s (2006).

6 Shiozawa, Y. *et al.* Human prostate cancer metastases target the hematopoietic stem cell niche to establish footholds in mouse bone marrow. *J Clin Invest* **121**, 1298-1312 (2011).

7 Thery, C., Ostrowski, M. & Segura, E. Membrane vesicles as conveyors of immune responses. *Nat Rev Immunol* **9**, 581-593 (2009).

8 Morhayim, J., Baroncelli, M. & van Leeuwen, J. P. Extracellular vesicles: specialized bone messengers. *Archives of biochemistry and biophysics* **561**, 38-45 (2014).

9 Raposo, G. & Stoorvogel, W. Extracellular vesicles: exosomes, microvesicles, and friends. *J Cell Biol* **200**, 373-383 (2013).

10 Shifrin, D. A., Jr., Demory Beckler, M., Coffey, R. J. & Tyska, M. J. Extracellular vesicles: communication, coercion, and conditioning. *Mol Biol Cell* **24**, 1253-1259 (2013).

11 Ratajczak, M. Z. *et al.* Pivotal role of paracrine effects in stem cell therapies in regenerative medicine: can we translate stem cell-secreted paracrine factors and microvesicles into better therapeutic strategies? *Leukemia* **26**, 1166-1173 (2012).

12 Katsuda, T., Kosaka, N., Takeshita, F. & Ochiya, T. The therapeutic potential of mesenchymal stem cell-derived extracellular vesicles. *Proteomics* **13**, 1637-1653 (2013).

13 Tetta, C., Bruno, S., Fonsato, V., Deregibus, M. C. & Camussi, G. The role of microvesicles in tissue repair. *Organogenesis* **7**, 105-115 (2011).

14 Ostrowski, M. *et al.* Rab27a and Rab27b control different steps of the exosome secretion pathway. *Nature cell biology* **12**, 19-30; sup pp 11-13 (2010).

15 Al-Nedawi, K., Meehan, B. & Rak, J. Microvesicles: messengers and mediators of tumor progression. *Cell Cycle* **8**, 2014-2018 (2009).

16 Hristov, M., Erl, W., Linder, S. & Weber, P. C. Apoptotic bodies from endothelial cells enhance the number and initiate the differentiation of human endothelial progenitor cells in vitro. *Blood* **104**, 2761-2766 (2004).

17 Anderson, H. C., Garimella, R. & Tague, S. E. The role of matrix vesicles in growth plate development and biomineralization. *Frontiers in bioscience : a journal and virtual library* **10**, 822-837 (2005).

18 Xiao, Z. *et al.* Analysis of the extracellular matrix vesicle proteome in mineralizing osteoblasts. *J Cell Physiol* **210**, 325-335 (2007).

19 Balcerzak, M. *et al.* Proteome analysis of matrix vesicles isolated from femurs of chicken embryo. *Proteomics* **8**, 192-205 (2008).

20 Thouverey, C. *et al.* Proteomic characterization of biogenesis and functions of matrix vesicles released from mineralizing human osteoblast-like cells. *J Proteomics* **74**, 1123-1134 (2011).

21 Nahar, N. N., Missana, L. R., Garimella, R., Tague, S. E. & Anderson, H. C. Matrix vesicles are carriers of bone morphogenetic proteins (BMPs), vascular endothelial growth factor (VEGF), and noncollagenous matrix proteins. *J Bone Miner Metab* **26**, 514-519 (2008).

22 Eijken, M. *et al.* The essential role of glucocorticoids for proper human osteoblast differentiation and matrix mineralization. *Mol Cell Endocrinol* **248**, 87-93 (2006).

23 Mathivanan, S., Fahner, C. J., Reid, G. E. & Simpson, R. J. ExoCarta 2012: database of exosomal proteins, RNA and lipids. *Nucleic acids research* **40**, D1241-1244 (2012).

24 Stoop, M. P. *et al.* The rate of false positive sequence matches of peptides profiled by MALDI MS and identified by MS/MS. *J Proteome Res* **7**, 4841-4847 (2008).

25 Alves, R. D. *et al.* Proteomic analysis of human osteoblastic cells: relevant proteins and functional categories for differentiation. *J Proteome Res* **9**, 4688-4700 (2010).

26 Schwanhausser, B. *et al.* Global quantification of mammalian gene expression control. *Nature* **473**, 337-342 (2011).

27 Collino, F. *et al.* Microvesicles derived from adult human bone marrow and tissue specific mesenchymal stem cells shuttle selected pattern of miRNAs. *PloS one* **5**, e11803 (2010).

28 Meckes, D. G., Jr. *et al.* Modulation of B-cell exosome proteins by gamma herpesvirus infection. *Proceedings of the National Academy of Sciences of the United States of America* **110**, E2925-2933 (2013).

29 Alves, R. D. *et al.* Unraveling the human bone microenvironment beyond the classical extracellular matrix proteins: a human bone protein library. *J Proteome Res* **10**, 4725-4733 (2011).

30 Hosseini-Beheshti, E., Pham, S., Adomat, H., Li, N. & Tomlinson Guns, E. S. Exosomes as biomarker enriched microvesicles: characterization of exosomal proteins derived from a panel of prostate cell lines with distinct AR phenotypes. *Mol Cell Proteomics* **11**, 863-885 (2012).

31 Sun, N. K. & Chao, C. C. The cytokine activity of HMGB1--extracellular escape of the nuclear protein. *Chang Gung Med J* **28**, 673-682 (2005).

32 Bab, I. *et al.* Histone H4-related osteogenic growth peptide (OGP): a novel circulating stimulator of osteoblastic activity. *EMBO J* **11**, 1867-1873 (1992).

33 Roodman, G. D. Mechanisms of bone metastasis. *The New England journal of medicine* **350**, 1655-1664 (2004).

34 Joyce, J. A. & Pollard, J. W. Microenvironmental regulation of metastasis. *Nat Rev Cancer* **9**, 239-252 (2009).

35 Varga, Z. *et al.* Towards traceable size determination of extracellular vesicles. *J Extracell Vesicles* **3** (2014).

36 Wool, I. G. Extraribosomal functions of ribosomal proteins. *Trends Biochem Sci* **21**, 164-165 (1996).

37 Lai, M. D. & Xu, J. Ribosomal proteins and colorectal cancer. *Curr Genomics* **8**, 43-49 (2007).

38 Wang, M., Hu, Y. & Stearns, M. E. RPS2: a novel therapeutic target in prostate cancer. *J Exp Clin Cancer Res* **28**, 6 (2009).

39 Vaarala, M. H. *et al.* Several genes encoding ribosomal proteins are over-expressed in prostate-cancer cell lines: Confirmation of L7a and L37 over-expression in prostate-cancer tissue samples. *International Journal of Cancer* **78**, 27-32 (1998).

40 Oh, S., Shin, S., Lightfoot, S. A. & Janknecht, R. 14-3-3 proteins modulate the ETS transcription factor ETV1 in prostate cancer. *Cancer Res* **73**, 5110-5119 (2013).

41 Urano, T. *et al.* 14-3-3sigma is down-regulated in human prostate cancer. *Biochem Biophys Res Commun* **319**, 795-800 (2004).

42 Ciocca, D. R., Fanelli, M. A., Cuello-Carrion, F. D. & Castro, G. N. Heat shock proteins in prostate cancer: from tumorigenesis to the clinic. *Int J Hyperthermia* **26**, 737-747 (2010).

43 Ohno, S. *et al.* Systemically injected exosomes targeted to EGFR deliver antitumor microRNA to breast cancer cells. *Mol Ther* **21**, 185-191 (2013).

44 Zhang, Y. *et al.* Microvesicle-mediated delivery of transforming growth factor beta1 siRNA for the suppression of tumor growth in mice. *Biomaterials* **35**, 4390-4400 (2014).

45 van Dommelen, S. M. *et al.* Microvesicles and exosomes: opportunities for cell-derived membrane vesicles in drug delivery. *J Control Release* **161**, 635-644 (2012).

46 Bruedigam, C. *et al.* Basic techniques in human mesenchymal stem cell cultures: differentiation into osteogenic and adipogenic lineages, genetic perturbations, and phenotypic analyses. *Curr Protoc Stem Cell Biol* **Chapter 1**, Unit1H 3 (2011).

47 Glaschick, S. *et al.* Axial resolution enhancement by 4Pi confocal fluorescence microscopy with two-photon excitation. *J Biol Phys* **33**, 433-443 (2007).

48 Cappellen van, A. W., Nigg, A. & Houtsmuller, A. B. *Enhancement of optical rsolution by 4pi single and multiphoton confcal fluorescence microscopy*. (Oxford: Academic Press, 2012).

49 Hell, S. & Stelzer, E. H. K. Fundamental Improvement of Resolution with a 4pi-Confocal Fluorescence Microscope Using 2-Photon Excitation. *Opt Commun* **93**, 277-282 (1992).

50 Wilm, M. *et al.* Femtomole sequencing of proteins from polyacrylamide gels by nano-electrospray mass spectrometry. *Nature* **379**, 466-469 (1996).

51 Cox, J. *et al.* A practical guide to the MaxQuant computational platform for SILAC-based quantitative proteomics. *Nat Protoc* **4**, 698-705 (2009).

52 Cox, J. *et al.* Andromeda: a peptide search engine integrated into the MaxQuant environment. *J Proteome Res* **10**, 1794-1805 (2011).

53 Huang da, W., Sherman, B. T. & Lempicki, R. A. Systematic and integrative analysis of large gene lists using DAVID bioinformatics resources. *Nat Protoc* **4**, 44-57 (2009).

54 Eijken, M. *et al.* The activin A-follistatin system: potent regulator of human extracellular matrix mineralization. *FASEB journal : official publication of the Federation of American Societies for Experimental Biology* **21**, 2949-2960 (2007).

3 Messenger RNA Profiling of Osteoblast-Derived Extracellular Vesicles

This chapter is based on:

"Molecular characterization of human osteoblast-derived extracellular vesicle mRNA using next-generation sequencing "

by

Jess Morhayim, Jeroen van de Peppel, Amel Dudakovic, Hideki Chiba, Andre J. van Wijnen, and Johannes P. van Leeuwen

Submitted

Extracellular vesicles (EVs) are membrane-bound intercellular communication vehicles that transport proteins, lipids and nucleic acids with regulatory capacity between cells. RNA profiling using microarrays and sequencing technologies has revolutionized the discovery of EV-RNA content, which is crucial to understand the molecular mechanism of EV function. Recent studies have indicated that EVs are enriched with specific RNAs compared to the originating cells suggestive of an active sorting mechanism. In this study, we present the comparative transcriptome analysis of human osteoblasts and their corresponding EVs using next-generation sequencing. We demonstrate that osteoblast-EVs are specifically depleted of cellular mRNAs that encode proteins involved in basic cellular activities, such as cytoskeletal functions, cell survival and apoptosis. In contrast, EVs are significantly enriched with 254 mRNAs that are associated with protein translation and RNA processing. Moreover, mRNAs enriched in EVs encode proteins important for communication with the surrounding cells, in particular with osteoclasts, adipocytes and hematopoietic stem cells. Strikingly, EVs are particularly enriched with *RAB13* mRNA, which is linked to vesicular trafficking. The latter suggests that EVs may affect vesicle production in target cells. These findings provide the foundation for understanding the molecular mechanism and function of EV-mediated interactions between osteoblasts and the surrounding bone microenvironment.

3.1. INTRODUCTION

Extracellular RNAs have long been utilized as non-invasive tools for early diagnosis of clinical disorders[1,2]. More recently, various studies reported RNA transfer between cells providing cues to their biological significance[3,4]. The majority of the extracellular RNA is found in tight complexes with proteins or lipids, as a protection against the action of RNases present in the circulation[5,6]. The discovery of RNA with regulatory capacity packaged inside extracellular vesicles (EVs) greatly contributed to the understanding of a novel mode of communication between cells[7-9].

EVs are actively secreted small membrane-bound structures consisting of a lipid bilayer enclosing a lumen that contains a bioactive message in forms of lipids, proteins and nucleic acids[10-12]. Extensive studies of EVs present in cell culture media or biological fluids revealed that EVs are very heterogeneous in size (10 nm to 5 μm) and morphology. Most often they are classified in at least three categories, such as exosomes, microvesicles and apoptotic bodies, merely based on their biogenesis. Their specific structure is essential for the protection of the vesicular cargo in the extracellular environment until they reach the target cells, where they regulate a broad range of biological functions[13-15]. Advanced high throughput RNA and protein analysis methods ('omics' technologies) have greatly facilitated the characterization of EV content and our ability to understand EV function. Since the first discovery of EV-associated RNA, many studies have focused on delineating the EV-RNA profile[16-18]. Interestingly, EVs are devoid of cellular ribosomal RNA (rRNA), and instead are enriched with small RNA molecules suggestive of active sorting rather than random incorporation as a by-product from dying cells[8]. Moreover, distinct EV-RNA patterns are evident in EVs from different cellular sources emphasizing the specificity of cargo loading in EVs. Expression profiling studies focusing on mRNA and microRNA (miRNA) analysis by next-generation sequencing or microarray analyses have shown that numerous small non-coding RNA molecules (e.g. small nuclear RNAs, vault RNA, Y RNA) are present inside EVs[19-21]. At present, there is a significant body of evidence indicating that EV-RNAs are important for development, immunology, angiogenesis, stem cell biology, and cancer, among many other biological functions[22-25].

Osteoblasts are specialized bone cells that are responsible for the formation of the mineralized bone tissue. It has been well established that they also play pivotal roles in maintaining cellular homeostasis by regulating the interactions with the surrounding cells[26-28]. In Chapter 2, we showed that osteoblasts secrete EVs packaged with functional proteins that contribute to the complex network of communication with the cells in the osteoblastic microenvironment[29]. The crosstalk is also highly regulated at the level of gene expression. In the present study, we employed next-generation sequencing analysis for in-depth characterization of the mRNA content of EVs that are secreted by human osteoblasts. Using a bioinformatics workflow, we described the mRNA species that are selectively incorporated into EVs or depleted from EVs during their biogenesis, and explored the molecular functions by which osteoblasts may deliver their specific message. Our comprehensive tran-

scriptome profiling represents a versatile resource for diverse biomedical applications ranging from biomarker discovery to gene therapy.

3.2. RESULTS

3.2.1. Osteoblasts secrete RNA containing EVs

To characterize the transcriptome of EVs, we isolated RNAs present in EVs released by human osteoblastic cells (SV-HFOs) at day 12-14 of their maturation. EVs were isolated from the conditioned medium by a series of ultracentrifugation steps and characterized by microscopy before EV-RNA isolation. Transmission electron microscopy (Fig. **1A**) and nanoparticle tracking analysis (Fig. **1B**) show the heterogeneous morphology and size distribution of the EV population with an average size of 158 nm.

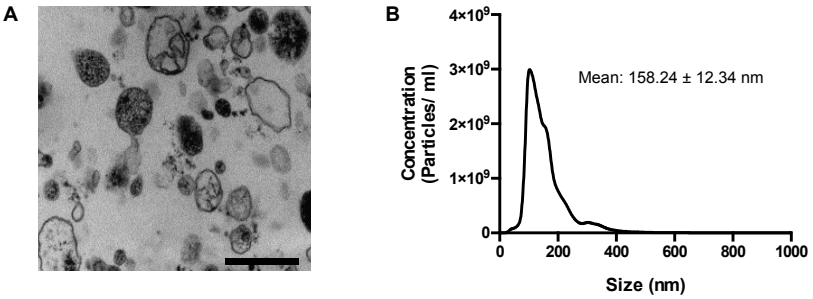

Figure 1. Size and morphology of osteoblast-EVs. A) Representative transmission electron microscope image (× 28,000) of EVs isolated from human osteoblasts. Scale bar: 500 nm. B) Nanoparticle tracking analysis shows EV size distribution and concentration. (N = 3).

Next, we isolated total EV-RNA using the TRIzol® extraction method. Quality control of RNA samples revealed that the yield is consistent between the independent EV preparations, with an average of 2.6 µg EV-RNA deriving from 80 ml of culture medium (Appendix A, Table A4). In parallel, we also isolated total RNA from the same osteoblasts to permit a direct comparison of RNA content. Representative Bioanalyzer electropherograms show expected differences in the RNA size distribution profiles for osteoblasts and their corresponding EVs (Fig. **2A & 2B**). EVs mainly contain small RNAs with a size range between 25 and 1,000 nucleotides, and lack the intact rRNA peaks characteristic of cellular 18S and 28S rRNAs. These findings emphasize the robustness of our isolation techniques and clearly demonstrate the distinctiveness of EV-RNA content compared to their parental cells.

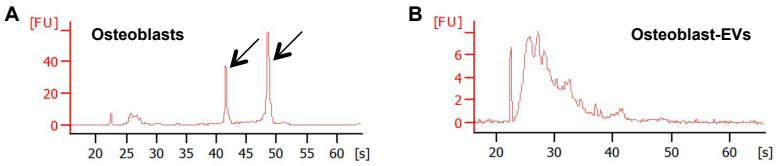

Figure 2. RNA profiling of human osteoblasts and osteoblast-EVs. A-B) Representative Agilent Bioanalyzer electropherograms show the size distribution of total RNA extracted from (A) osteoblasts and (B) osteoblast-EVs (N = 3). Arrows show the characteristic cellular 18S (*left)* and 28S (r*ight*) rRNA peaks. FU, fluorescent units.

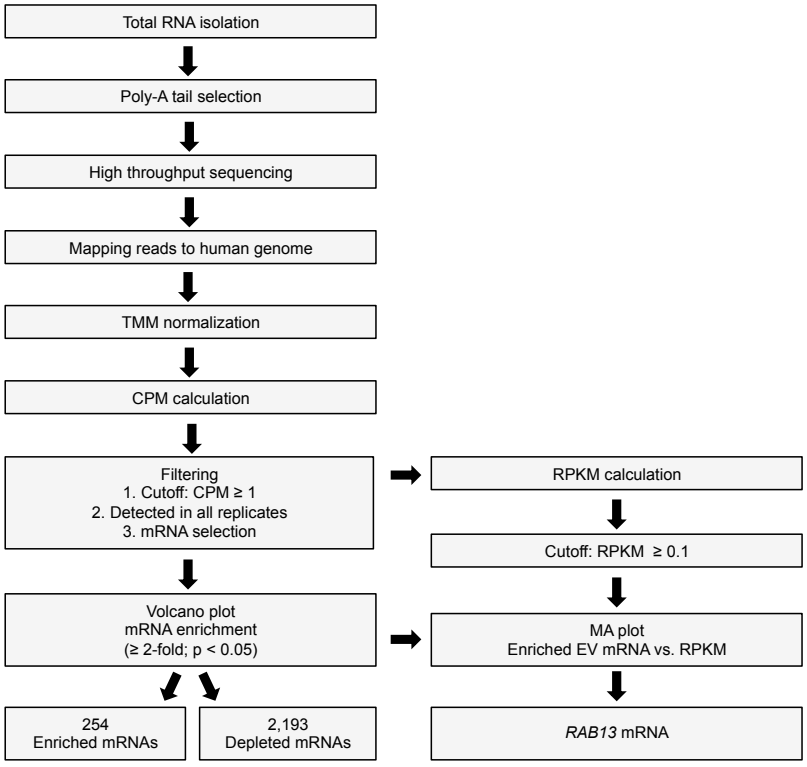

Figure 3. Flowchart of the mRNA-sequencing data analysis. Total cellular and EV-RNA was isolated using TRIzol® extraction method, and after poly-A tail selection with oligo(dT) primers the RNA was sequenced via high throughput next-generation sequencing (N = 3). Initially, the reads were mapped to human genome and then the read counts were normalized and converted to counts per million mapped reads (CPM), which were subsequently converted to reads per kilobase per million (RPKM) mapped reads using Edge R. The reads were further filtered to remove low quality reads (CPM ≤ 1 and RPKM ≤ 0.1). Only the transcripts that mapped to mRNAs, which were detected in all replicates were considered for further analysis. Highly abundant mRNA transcripts that were enriched in EVs compared to the donor osteoblasts were studied via volcano plot and MA plot analyses.

3.2.2. EV-mRNA profiling using next-generation sequencing

We investigated the EV-mRNA profile at high resolution by next-generation sequencing. We constructed sequencing libraries from three independent osteoblast cultures and their derived EVs, and analyzed the data using an established bioinformatics workflow (Figure **3**).

The detected RNA read counts are robust and reproducible between the sequencing libraries, indicating a consistent distribution across independent preparations (Appendix A, Table A5). Scatter plot in Figure **4A** shows a fairly strong positive correlation between cellular RNA and EV-RNA (R^2: 0.731, $P < 0.0001$). As expected, the majority of the transcripts are mapped to mRNA sequences for both osteoblasts (11,629 mRNAs) and EVs (11,714 mRNAs) (Fig. **4B**). Classification of cellular- and EV-mRNAs shows a high diversity of biochemical functions (Fig. **4C**).

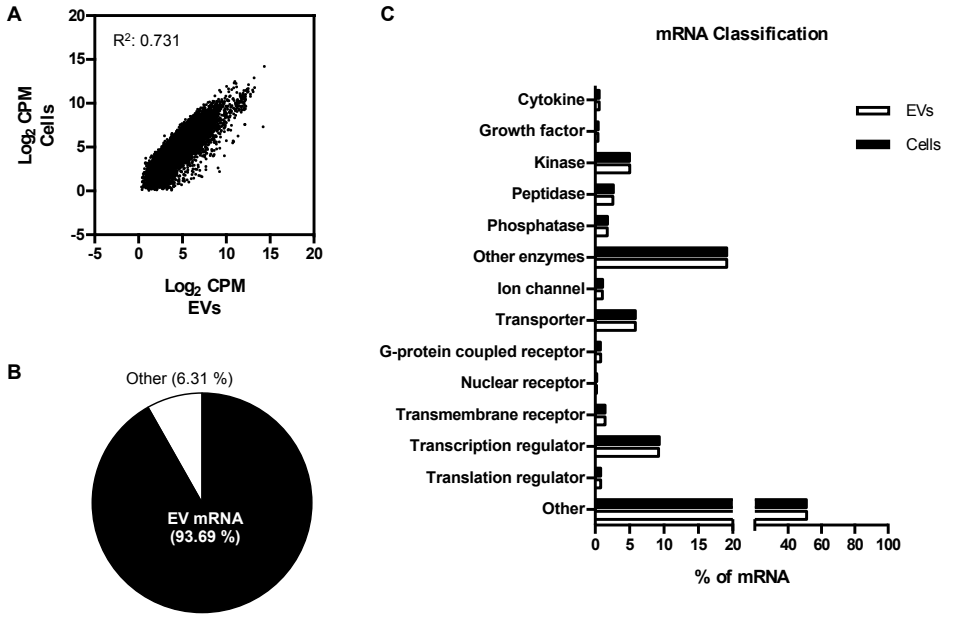

Figure 4. Next-generation sequencing mRNA profiling of osteoblast-EVs. A) Scatter plot shows the correlation (R^2: 0.731) of normalized read counts (average CPM) between cellular and EV transcripts (N = 3). B) Pie chart shows the fraction of transcripts that were mapped to protein-coding mRNAs in EVs (dark gray). Cellular mRNA percentage is shown in brackets. C) Functional classification of the detected cellular and EV-mRNAs.

As it is evident from the scatter plot, the majority of the mRNAs are shared between osteoblasts and their derived EVs. Yet, a small but significant fraction of mRNAs is exclusive to either osteoblasts or EVs [5.9% (693 mRNAs) and 5.2% (608 mRNAs), re-

spectively] (Fig. **5A**). These exclusive mRNAs are expressed at relatively low levels and represent a small fraction of total cellular- and EV-mRNA read counts (0.16% and 0.17%, respectively). Interestingly, the top 100 highly expressed genes account for 58.25% of all mapped EV-mRNA read counts, whereas only 34.04% account for the top 100 mapped mRNAs in the cells (Fig. **5B**). This result suggests a specific enrichment of biologically significant mRNAs in EVs. The majority of these mRNAs (78 mRNAs) appear in both the top 100 of either the cellular- or EV-derived transcriptome, and many encode rather ubiquitous ribosomal proteins (Fig. **5C**). The remaining top EV-mRNAs (22 mRNAs) are mostly associated with oxidative phosphorylation and protein transport (Fig. **5D**). In contrast, the cellular transcriptome is enriched with mRNAs required for essential cellular functions, such as glycolysis, cell motion and regulation of apoptosis (Fig. **5E**). Taken together, these results indicate that even though EV-mRNA content mirrors the transcriptome of their donor cells, EVs exhibit a distinct pattern in distribution of mRNA abundance. These findings clearly indicate that mRNAs are selectively sorted into EVs, rather than randomly incorporated during vesicular trafficking and extracellular release.

3.2.3. EVs are selectively enriched with a subset of mRNAs

We assessed the relative abundance of mRNAs in cells and EVs to determine the types of mRNAs that are specifically enriched in EVs. Volcano plotting shows that 254 mRNAs are significantly ($P < 0.05$) more abundant ($\geq$ two-fold) in EVs compared to the cells (Fig. **6A**, Appendix A, Table A6). The most highly enriched EV-mRNAs ("Top 10") are *RAB13*, *ARRDC4*, *NEFM*, *IGIP*, *NET1*, *RASSF3*, *HMGN5*, *TRAK2*, *ESF1* and *ZEB1*, in descending order of fold enrichment. Bioinformatic analysis using the Ingenuity Pathway Analysis (IPA) revealed that cellular processes, such as RNA post-transcriptional modification, gene expression and cell-to-cell signaling and interaction, are strongly overrepresented in EV-mRNAs. On the other hand, the transcriptome of EVs is depleted of 2,192 cellular mRNAs that are selectively linked to essential cellular processes, such as cell death and survival and cellular growth and proliferation. Strikingly, EVs preferentially contain mRNAs that encode proteins involved in cell-to-cell communication in the bone and bone marrow microenvironment. These include the genes involved in the recruitment of osteoclasts (*NFKBIB*, *PGF*), priming of adipose cells (*FGF1*), as well as self-renewal and proliferative expansion of hematopoietic stem and progenitor cells (*FLT3LG*, *IL18*, *HOXB7*, *CCND1*, *CCND2*) (Fig. **6B**).

Among the 254 enriched EV-mRNAs, osteoblast-EVs contain 49 unique mRNAs that have not been previously detected in EVs secreted by other cells or present in body fluids (Fig. **6C**)[30]. These unique mRNAs are mostly annotated to zinc ion-binding (*AGAP2*, *ZNF677*, *ZNF846*), regulation of transcription (*BDP1*, *SOX11*, *TAF7L*) and kinase activity (*LPAR1*, *MAP3K13*, *ZEB2*). Furthermore, we compared the enriched EV-mRNA dataset to the protein content of the corresponding osteoblast-derived EVs described in Chapter 2. For

a limited number of mRNAs (18 mRNAs), osteoblast-EVs contain the corresponding protein (Fig. **6D**). Two of these are derived from osteoblast-EV specific mRNAs (*HIST1H1E* and *LPAR1*), whereas the remaining 16 proteins include ribonucleoproteins (*HNRNPA1*, *HNRNPA3*, *HNRNPH3*), translation initiation factors (*EIF3A*, *EIF5B*), histones (*HIST1H2BH*, *HIST1H2BO*) and others (*MAP4K4*, *NAP1L1*, *NCL*, *PABPC1*, *SEPT7*, *SET*, *ST13*, *YES1*).

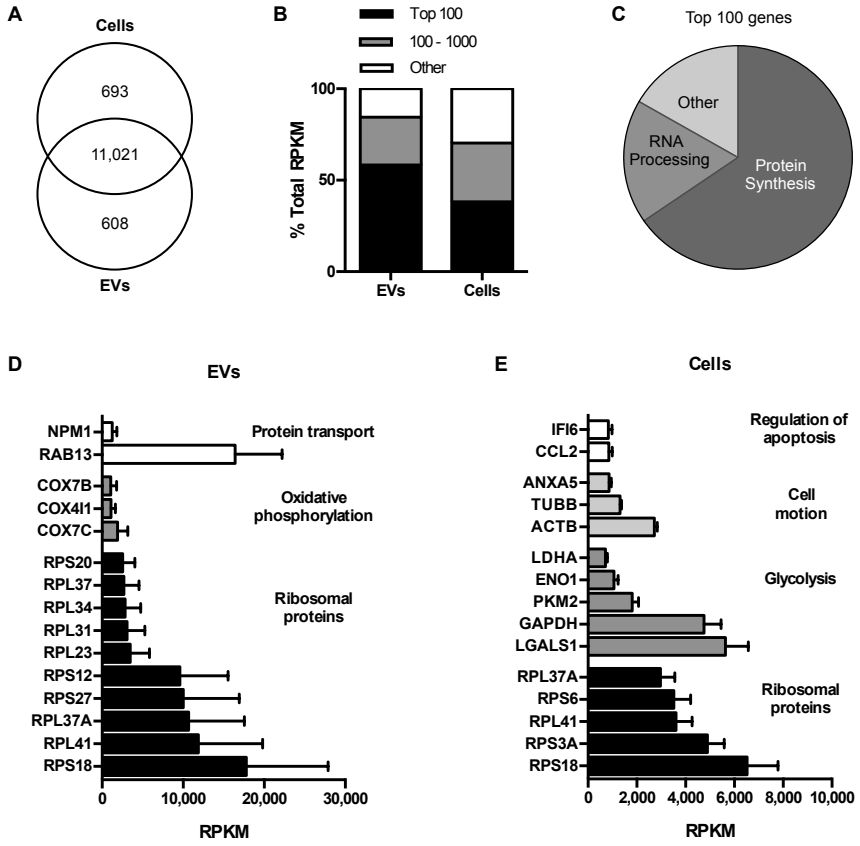

Figure 5. The most abundant cellular and EV-mRNAs. A) Venn diagram shows the distribution of mRNAs between osteoblast and EVs. B) Top 100 most abundant mRNAs make up more than 50% of the total RPKM values for EVs. C) Top 100 EV-mRNAs are mostly annotated to genes encoding for proteins involved in protein synthesis and RNA processing. D-E) RPKM values of the representative top 100 (D) EV-mRNAs and (E) cellular RNAs.

Next, we visualized log ratios of the normalized read counts for mRNAs from EVs versus cells relative to their mean abundance. The resulting MA plot compares the expression levels of the 254 mRNAs enriched by at least two-fold in EVs. Remarkably, *RAB13* is both the most highly enriched and most abundant EV-mRNA that is selectively incorpo-

rated in EVs compared to the EV-producing osteoblasts (Fig. **7A**). Furthermore, it is the only member of the Rab GTPase family with such a striking selective abundance in EVs, strongly suggesting that *RAB13* is specifically enriched in EVs (Fig. **7B**). We evaluated the expression levels of *RAB13* along with *ATP5E*, which show similar cellular and vesicular abundances in sequencing analysis (Fig. **7C**). Quantitative real-time PCR results confirm the significant enrichment of *RAB13* in EVs, consistent with the sequencing data (Fig. **7D**).

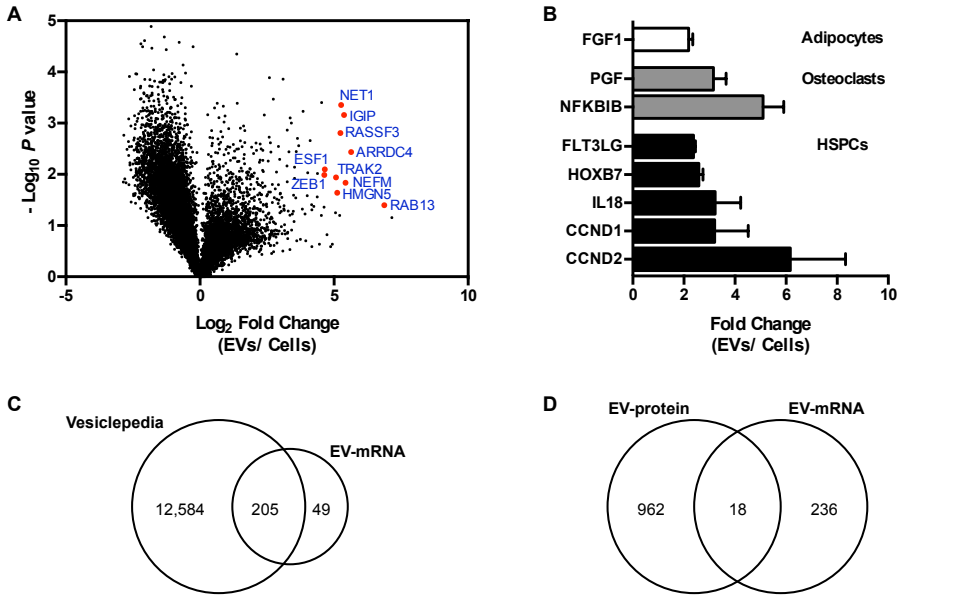

Figure 6. Selectively enriched EV-mRNAs. A) Volcano plot (significance versus fold change) shows the significantly ($P < 0.05$, compared with osteoblasts by Student's *t*-test) abundant (≥ two-fold; 254 mRNAs) and depleted (≤ 0.5-fold; 2192 mRNAs) EV-mRNAs based on CPM values. The top 10 most enriched EV-mRNAs are highlighted in blue. B) Fold change distribution of selected genes annotated to overrepresented biological processes, such as induction of proliferation and expansion of hematopoietic stem and progenitor cells (HSPCs), recruitment of osteoclasts, and priming of adipocytes. C) Venn diagram shows the number of unique mRNAs detected in osteoblast-EVs in comparison with Vesiclepedia. D) Venn diagram shows the overlap between the EV-protein and -mRNA content.

Using IPA, we investigated the molecular functions and canonical pathways associated with the RAB13 protein (Fig. **7E**). We identified 26 proteins that are directly or indirectly coupled to the activity of RAB13. These proteins have molecular and cellular functions related to DNA replication, recombination and repair, cellular growth and proliferation, cellular assembly and organization, cell movement, and cell morphology. The main canonical pathways in which RAB13 participates are TGF-β signaling, cell cycle control of chromosomal replication and nucleotide excision repair pathway. In addition, several of these RAB13 associated proteins regulate the proliferation of stromal cells, chondrocytes, blood cells and tumor cells, which are precisely the potential target cells that physiological-

ly interact with osteoblasts in the bone microenvironment. Taken together, our study is consistent with the broader concept that osteoblasts communicate with their surrounding cells by generating EVs that are actively loaded with specific bioactive molecules. This molecular cargo encompasses a selective group of mRNAs capable of providing defined regulatory signals to recipient cells.

3.3. DISCUSSION

The discovery of extracellular RNA (e.g. circulating RNA, EV-RNA) with regulatory functions has tremendous ramifications for both medical sciences and clinical applications. In this study, we reported the extensive profiling of mRNAs incorporated within EVs released by human osteoblasts. We showed that EVs to some degree contain the mRNA signature of their host cells while being selectively enriched with a unique set of mRNAs that may support intercellular communication. Our findings provide a major advancement in our understanding of EVs as a newly discovered mode of communication between osteoblasts and the surrounding microenvironment.

We previously showed that osteoblasts secrete EVs containing a specific set of proteins important for their communication with their target cells[29]. Here, we investigated the mRNA profile of osteoblast-EVs to further characterize and discover the role of EVs in intercellular communication. Currently, the EV field is still challenged by variation in the reliability and procedural differences in EV-RNA isolation protocols[31,32]. In our study, we reproducibly obtained satisfactory RNA yields with robust size distributions that were consistent between the different preparations. Bioanalyzer profiles of our total RNA preparations show that osteoblast-EVs lack the typical cellular rRNAs and are enriched with small RNAs that range from 25 to 1,000 nucleotides, in accordance with other EV-RNA studies[33-35]. Diverse cell types secrete small EV-RNAs that mainly consist of miRNAs and other small non-coding RNA molecules. Yet, there is increasing evidence showing the presence of functional mRNA specifically packaged inside EVs. However, intact mammalian mRNAs typically range between 400 and 12,000 nucleotides in length[36]. The smaller size range of EV-derived RNAs inevitably leads to the question whether EVs are enriched with full-length mRNAs of intermediate size or merely with mRNA fragments. A report by Batagov and colleagues presented data indicating that EVs contain fragments derived from the 3'-untranslated regions (3'-UTR) of certain mRNAs to protect the target mRNA against miRNA degradation[37]. On the other hand, several other studies reported the transfer of full-length EV-mRNA between cells with subsequent translation into functional proteins by the recipient cells[38-40]. It is conceivable that cells may transmit both full-length mRNAs and 3'-UTR fragments as a two-pronged strategy that, first, instructs translation of proteins in the recipient cell, and second, relieves miRNA-mediated translation inhibition by competition with 3'-UTRs containing relevant miRNA binding sequences.

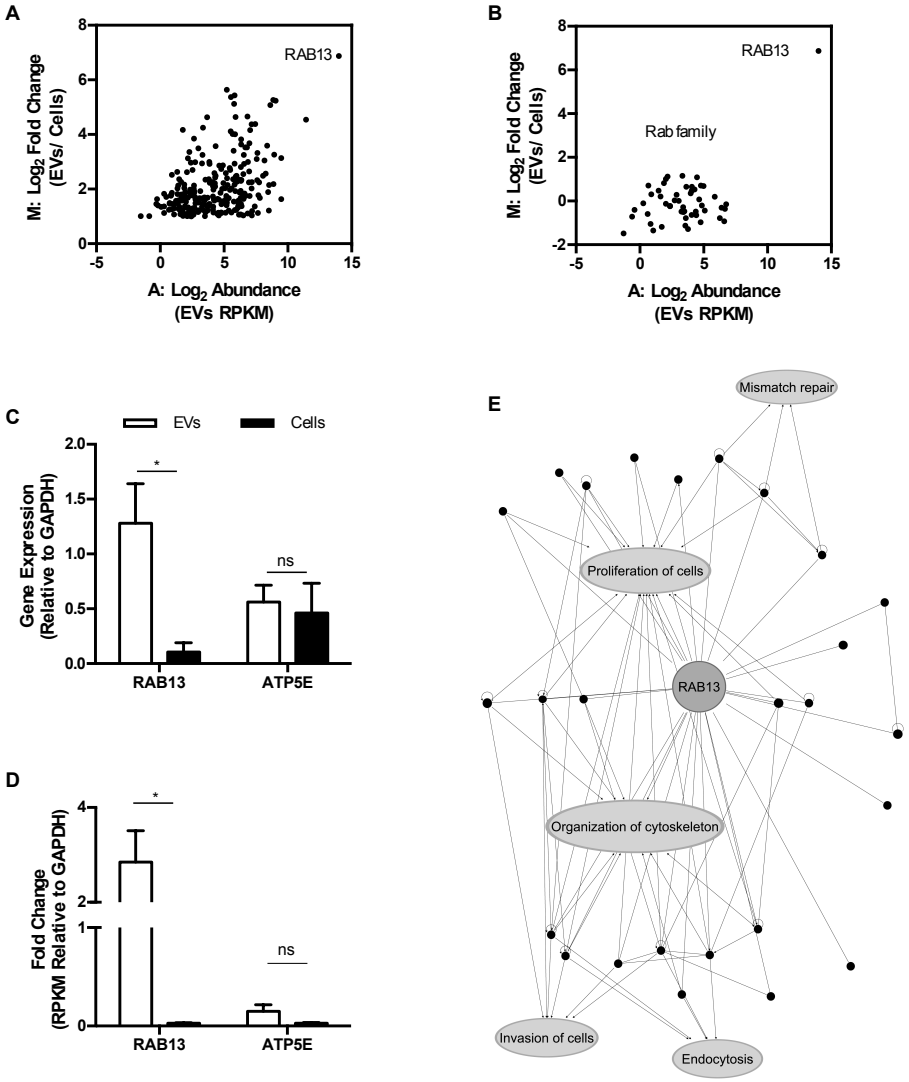

Figure 7. EVs are selectively enriched with *RAB13* mRNA. A) MA plot (fold change versus abundance) shows the RPKM values of the significantly enriched EV-mRNAs. *RAB13*, which is both the most enriched and abundant mRNA detected in EVs, is highlighted blue. B) MA plot of the Rab family mRNAs detected in both cells and EVs. *RAB13* is the only Rab family mRNA that is highly enriched in EVs compared to the donor osteoblasts. C-D) Relative expressions of *RAB13* and *ATP5E* in EVs and cells by (C) qPCR (N = 6) and (D) mRNA-sequencing (N = 3). The qPCR results are normalized to average *GAPDH* expression. The mRNA-sequencing results are shown as average fold change of RPKM values relative to *GAPDH*. E) IPA interaction network shows the predicted biological functions (grey) associated with the downstream targets (black) of RAB13 protein. * $P < 0.05$, compared with cells by Student's *t*-test; ns, not significant.

Next-generation sequencing technologies have permitted comprehensive analyses of whole transcriptomes with single nucleotide resolution and quantitative assessments of

RNA levels. We applied next-generation sequencing to identify RNA reads that correspond to 11,714 EV-mRNAs. The content and abundance profile of this mRNA set mirrors the mRNAs detected in donor cells. Because EVs may form by budding from the plasma membrane or exocytosis of multivesicular bodies, it is possible that cellular components are non-specifically incorporated into EVs during their biogenesis. Indeed, many mRNAs present in EVs are similarly abundant in the cells that produce them suggesting that they are simply stochastically distributed into EVs. For example, mRNAs for ribosomal proteins are highly abundant in cells and also found in top 100 in EV-mRNAs. Nevertheless, there are a number of mRNAs that are either selectively enriched or depleted in EVs compared to the producing cells. The quantitative and qualitative differences in the transcriptome of EVs versus cells clearly suggest that at least some mRNAs may be specifically sorted and packaged into EVs to support cell–cell communication.

Comparative transcriptome analyses reveal selective enrichment and depletion of particular mRNAs that are significantly overrepresented (254 mRNAs) or underrepresented (2,193 mRNAs) in EVs when compared to the producing cells. EVs appear to be specifically depleted of mRNAs required for vital cellular functions, yet many enriched EV-mRNAs encode proteins that directly or indirectly mediate mRNA translation by supporting the biogenesis of ribosomes (e.g., enzymes that mediate rRNA processing or structural ribosomal proteins). Because 18S and 28S rRNAs, which are two major constituents of the ribosome, are not detected in the total RNA distribution of EVs compared to that of cells and the abundance of mRNAs encoding a particular subset of ribosomal proteins may suggest a specific role in vesicular function. Consistent with our findings, previous studies reported that EVs contain mRNAs encoding ribosomal proteins, as well as elongation and translation factors[8,41]. Furthermore, Jenjaroenpun and colleagues suggested that these genes upon translation in the recipient cells may provide essential ribosomal components to support the translation of other EV-mRNAs[42]. Regardless of the possibility that EV-mRNAs may be involved in very common cellular activities, the most interesting mRNA species are those that are less abundant, as well as fairly unique to EVs and not represented in the recipient cell.

Crosstalk between osteoblasts and the surrounding bone microenvironment is critical to maintain essential biological processes, such as osteoclastogenesis, hematopoiesis and adipogenesis. Hence, a major objective of our studies is to identify unique mRNAs in EVs that could affect the biological state of the recipient cell. The majority of the mRNAs enriched in osteoblast-EVs are also detected in EV preparations from other cells and body fluids, suggesting that some of these mRNAs may have common functions related to generic activities of EVs, rather than specific biological roles linked to the bone microenvironment. However, a substantial subset (~20%) of the enriched mRNAs is uniquely detected in osteoblast-EVs and thus can be attributed to a specific osteoblast-related and EV-mediated function. Enriched osteoblast-EV-mRNAs include those that encode proteins capable of regulating the fate of target neighboring cells in the bone microenvironment. Therefore, it is intriguing that such regulatory mRNAs are selectively sorted into osteoblast-EVs. We

anticipate that further investigation of EV-specific mRNAs will permit delineation of the EV-mediated mechanisms by which osteoblasts communicate and control an intricate cell-to-cell interaction network in the bone microenvironment.

The most strikingly overrepresented EV-mRNA is *RAB13*, because it is exceptionally abundant in EVs compared to the cells. RAB13 protein is a member of the Rab family of small GTPases, which are primarily involved in vesicle trafficking, including vesicle production and fusion at the target cell membrane[43]. Furthermore, even though our studies yielded very few examples in which mRNAs and their encoded proteins are co-packaged in EVs, osteoblasts-EVs not only contain *RAB13* mRNA but also the RAB13 protein. RAB13 protein may have a role in EV biogenesis and cargo sorting at the donor cell membrane[29]. However, the enrichment of this mRNA in osteoblast-EVs and its putative transfer into recipient cells could represent a regulatory mechanism by which osteoblasts control EV production in their target cells. Beyond the latter possibility, Rab proteins also regulate cytoskeleton organization and assembly of tight junctions, and thereby regulate cell adhesion necessary for cell growth[44,45]. Accordingly, our network analysis predicted potential RAB13 targets that play important roles in the proliferation of chondrocytes, stromal, blood and tumor cells, indicative of a possible role in communication between osteoblasts and the target cells within the bone microenvironment.

Osteoblasts are known to communicate with osteoclasts to coordinate tissue mineralization and resorption during bone remodeling. Intriguingly, Rab family proteins have essential roles in osteoclastic membrane trafficking required for bone resorption[46,47]. RAB13, in particular, has been shown to be upregulated during osteoclast differentiation where it engages in vesicular trafficking events unrelated to bone resorption[48]. The possibility arises that osteoblasts could deliver RAB13 to immature osteoclasts via EVs to alter the osteoclast phenotype and perhaps provoke secondary extracellular signals emanating from osteoclasts. A number of follow-up studies will be required to identify potential target cells of osteoblast-EVs, establish how EVs unload their cargo and determine how EVs affect the biological properties of recipient cells.

In conclusion, in this study we present a comprehensive analysis of the EV transcriptome that suggests new mechanistic concepts. Our studies suggests a model in which EVs produced by osteoblasts may be part of a paracrine signaling system that coordinates the biological functions of both skeletal and hematopoietic cells in the bone microenvironment. Our results provide the molecular basis for understanding the biological significance of EV-mRNAs in the context of bone related processes. It remains to be elucidated whether EV-mRNAs are translated and consequently are rendered functional upon delivery into the target cells. Finally, EV transcriptome-profiling offers a potent avenue for discovery of non-invasive diagnostics for various diseases and facilitates the development of cell-free strategies for regenerative therapy.

3.4. MATERIALS AND METHODS

Cell cultures and EV isolation. Human osteoblast cells (SV-HFO cells) were cultured as described in Chapter 2[29]. Osteoblast-EVs were isolated from 20 ml conditioned medium by low speed centrifugation (1,500 rpm, 5 minutes; 4,500 rpm, 10 minutes) followed by ultracentrifugation (20,000g, 30 minutes; 100,000g, 1 hour at 4°C) of the supernatant using the SW32Ti rotor (Beckman Coulter, Fullerton, CA, USA). Transmission electron microscopy images were taken as previously described in Chapter 2. EV size distribution and concentration was measured with NanoSight LM10 (Nanosight Ltd., Amesbury, UK) equipped with a 405 nm laser. Each sample was tracked for 60 seconds with 3 repetitions. The data was processed by NTA 2.3 software.

RNA isolation and quantitative real-time PCR. Total cellular and EV-RNA was isolated using the TRIzol® reagent (Thermo Fisher Scientific, Waltham, MA, USA) according to the manufacturer's instructions. RNA concentration was determined using Nanodrop (Thermo Fisher Scientific) and size distribution was checked on an Agilent Bioanalyzer RNA 6000 Nano chip (Thermo Fisher Scientific). Quantitative real-time PCR was performed using the SYBR™ Green kit (Eurogentec, Seraing, Belgium) according to the manufacturer's instructions. The primer sequences are listed in Appendix C.

Next-generation sequencing and bioinformatics analysis. RNA sequencing and bioinformatic analysis was performed as previously described[49]. In brief, sequencing RNA libraries were prepared with the TruSeq RNA Sample Prep Kit v2 (Illumina, San Diego, CA, USA) according to the manufacturer's instructions. The concentration and size distribution of the libraries was determined on an Agilent Bioanalyzer DNA 1000 chip (Thermo Fisher Scientific), and verified with Qubit fluorometry (Thermo Fisher Scientific). Libraries were loaded onto flow cells at concentrations of 8–10 pM to generate cluster densities of 700,000/ mm^2 following the standard protocol for the Illumina cBot and cBot Paired-end cluster kit version 3. Flow cells were sequenced as 51 × 2 paired end reads on an Illumina HiSeq 2000 using TruSeq SBS sequencing kit version 3 and HCS v2.0.12 data collection software. Base-calling was performed using Illumina's RTA version 1.17.21.3. The sequencing data was analyzed using CAP-miRSeq v1.1. Normalization (counts per million mapped reads, CPM; and reads per kilobasepair per million mapped reads, RPKM) analysis was performed using edgeR 2.6.2. The data from the replicates were combined as averages of the normalized read values, and only transcripts with CPM ≥ 1 for all replicates were included in the analysis. Comparative analyses of the EV data were obtained by querying the Vesiclepedia plugin provided by FunRich functional enrichment analysis tool (V2.1.2, 29 April 2015). IPA (Ingenuity® Systems, www.ingenuity.com) was used to classify the mRNA categories and predict target pathways and genes. DAVID Bionformatics Resources v6.7 was used to categorize the genes into overrepresented processes using human genome as a background[50].

Statistics. The data provided were based on multiple independent experiments. The results were described as mean ± SD. Significance was calculated using paired Student's *t*-test, and *P* values of < 0.05 were considered significant.

REFERENCES

1 Wieczorek, A. J. *et al.* Diagnostic and prognostic value of RNA-proteolipid in sera of patients with malignant disorders following therapy: first clinical evaluation of a novel tumor marker. *Cancer Res* **47**, 6407-6412 (1987).

2 Kopreski, M. S., Benko, F. A., Kwak, L. W. & Gocke, C. D. Detection of tumor messenger RNA in the serum of patients with malignant melanoma. *Clin Cancer Res* **5**, 1961-1965 (1999).

3 Kolodny, G. M. Evidence for transfer of macromolecular RNA between mammalian cells in culture. *Exp Cell Res* **65**, 313-324 (1971).

4 Galand, P. & Ledoux, L. Uptake of exogenous ribonucleic acid by ascites tumor cells. II. Relations between RNA uptake and the cellular metabolism. *Exp Cell Res* **43**, 391-397 (1966).

5 Arroyo, J. D. *et al.* Argonaute2 complexes carry a population of circulating microRNAs independent of vesicles in human plasma. *Proceedings of the National Academy of Sciences of the United States of America* **108**, 5003-5008 (2011).

6 Fleischhacker, M. Biology of circulating mRNA: still more questions than answers? *Annals of the New York Academy of Sciences* **1075**, 40-49 (2006).

7 Ceccarini, M. *et al.* Biochemical and NMR studies on structure and release conditions of RNA-containing vesicles shed by human colon adenocarcinoma cells. *International journal of cancer. Journal international du cancer* **44**, 714-721 (1989).

8 Valadi, H. *et al.* Exosome-mediated transfer of mRNAs and microRNAs is a novel mechanism of genetic exchange between cells. *Nature cell biology* **9**, 654-659 (2007).

9 Montecalvo, A. *et al.* Mechanism of transfer of functional microRNAs between mouse dendritic cells via exosomes. *Blood* **119**, 756-766 (2012).

10 Thery, C., Ostrowski, M. & Segura, E. Membrane vesicles as conveyors of immune responses. *Nat Rev Immunol* **9**, 581-593 (2009).

11 Shifrin, D. A., Jr., Demory Beckler, M., Coffey, R. J. & Tyska, M. J. Extracellular vesicles: communication, coercion, and conditioning. *Mol Biol Cell* **24**, 1253-1259 (2013).

12 Morhayim, J., Baroncelli, M. & van Leeuwen, J. P. Extracellular vesicles: specialized bone messengers. *Archives of biochemistry and biophysics* **561**, 38-45 (2014).

13 Cocucci, E., Racchetti, G. & Meldolesi, J. Shedding microvesicles: artefacts no more. *Trends Cell Biol* **19**, 43-51 (2009).

14 Gyorgy, B. *et al.* Membrane vesicles, current state-of-the-art: emerging role of extracellular vesicles. *Cell Mol Life Sci* **68**, 2667-2688 (2011).

15 Raposo, G. & Stoorvogel, W. Extracellular vesicles: exosomes, microvesicles, and friends. *J Cell Biol* **200**, 373-383 (2013).

16 Bellingham, S. A., Coleman, B. M. & Hill, A. F. Small RNA deep sequencing reveals a distinct miRNA signature released in exosomes from prion-infected neuronal cells. *Nucleic acids research* **40**, 10937-10949 (2012).

17 Huang, X. *et al.* Characterization of human plasma-derived exosomal RNAs by deep sequencing. *BMC genomics* **14**, 319 (2013).

18 Eirin, A. *et al.* MicroRNA and mRNA cargo of extracellular vesicles from porcine adipose tissue-derived mesenchymal stem cells. *Gene* **551**, 55-64 (2014).

19 Nolte-'t Hoen, E. N. *et al.* Deep sequencing of RNA from immune cell-derived vesicles uncovers the selective incorporation of small non-coding RNA biotypes with potential regulatory functions. *Nucleic acids research* **40**, 9272-9285 (2012).

20 Miranda, K. C. *et al.* Massively parallel sequencing of human urinary exosome/microvesicle RNA reveals a predominance of non-coding RNA. *PloS one* **9**, e96094 (2014).

21 Guzman, N. *et al.* Breast Cancer-Specific miR Signature Unique to Extracellular Vesicles Includes "microRNA-like" tRNA Fragments. *Molecular cancer research : MCR* **13**, 891-901 (2015).

22 Ratajczak, J. *et al.* Embryonic stem cell-derived microvesicles reprogram hematopoietic progenitors: evidence for horizontal transfer of mRNA and protein delivery. *Leukemia* **20**, 847-856 (2006).

23 Baj-Krzyworzeka, M. *et al.* Tumour-derived microvesicles carry several surface determinants and mRNA of tumour cells and transfer some of these determinants to monocytes. *Cancer Immunol Immunother* **55**, 808-818 (2006).

24 Skog, J. *et al.* Glioblastoma microvesicles transport RNA and proteins that promote tumour growth and provide diagnostic biomarkers. *Nature cell biology* **10**, 1470-1476 (2008).

25 Ekstrom, K. *et al.* Characterization of mRNA and microRNA in human mast cell-derived exosomes and their transfer to other mast cells and blood CD34 progenitor cells. *J Extracell Vesicles* **1** (2012).

26 Peng, S. *et al.* The cross-talk between osteoclasts and osteoblasts in response to strontium treatment: involvement of osteoprotegerin. *Bone* **49**, 1290-1298 (2011).

27 Muruganandan, S., Roman, A. A. & Sinal, C. J. Adipocyte differentiation of bone marrow-derived mesenchymal stem cells: cross talk with the osteoblastogenic program. *Cell Mol Life Sci* **66**, 236-253 (2009).

28 Calvi, L. M. *et al.* Osteoblastic cells regulate the haematopoietic stem cell niche. *Nature* **425**, 841-846 (2003).

29 Morhayim, J. *et al.* Proteomic signatures of extracellular vesicles secreted by nonmineralizing and mineralizing human osteoblasts and stimulation of tumor cell growth. *FASEB journal : official publication of the Federation of American Societies for Experimental Biology* **29**, 274-285 (2015).

30 Pathan, M. *et al.* FunRich: An open access standalone functional enrichment and interaction network analysis tool. *Proteomics* **15**, 2597-2601, doi:10.1002/pmic.201400515 (2015).

31 Eldh, M., Lotvall, J., Malmhall, C. & Ekstrom, K. Importance of RNA isolation methods for analysis of exosomal RNA: evaluation of different methods. *Molecular immunology* **50**, 278-286 (2012).

32 Van Deun, J. *et al.* The impact of disparate isolation methods for extracellular vesicles on downstream RNA profiling. *J Extracell Vesicles* **3** (2014).

33 Palanisamy, V. *et al.* Nanostructural and transcriptomic analyses of human saliva derived exosomes. *PloS one* **5**, e8577 (2010).

34 Lasser, C. *et al.* Human saliva, plasma and breast milk exosomes contain RNA: uptake by macrophages. *J Transl Med* **9**, 9 (2011).

35 Kesimer, M. *et al.* Characterization of exosome-like vesicles released from human tracheobronchial ciliated epithelium: a possible role in innate defense. *FASEB journal : official publication of the Federation of American Societies for Experimental Biology* **23**, 1858-1868 (2009).

36 Ravasi, T. *et al.* Experimental validation of the regulated expression of large numbers of non-coding RNAs from the mouse genome. *Genome research* **16**, 11-19 (2006).

37 Batagov, A. O. & Kurochkin, I. V. Exosomes secreted by human cells transport largely mRNA fragments that are enriched in the 3'-untranslated regions. *Biology direct* **8**, 12 (2013).

38 Deregibus, M. C. *et al.* Endothelial progenitor cell derived microvesicles activate an angiogenic program in endothelial cells by a horizontal transfer of mRNA. *Blood* **110**, 2440-2448 (2007).

39 Bruno, S. *et al.* Mesenchymal stem cell-derived microvesicles protect against acute tubular injury. *J Am Soc Nephrol* **20**, 1053-1067 (2009).

40 Zomer, A. *et al.* In Vivo imaging reveals extracellular vesicle-mediated phenocopying of metastatic behavior. *Cell* **161**, 1046-1057 (2015).

41 Graner, M. W. *et al.* Proteomic and immunologic analyses of brain tumor exosomes. *FASEB journal : official publication of the Federation of American Societies for Experimental Biology* **23**, 1541-1557 (2009).

42 Jenjaroenpun, P. *et al.* Characterization of RNA in exosomes secreted by human breast cancer cell lines using next-generation sequencing. *PeerJ* **1**, e201 (2013).

43 Hutagalung, A. H. & Novick, P. J. Role of Rab GTPases in membrane traffic and cell physiology. *Physiological reviews* **91**, 119-149 (2011).

44 Marzesco, A. M. *et al.* The small GTPase Rab13 regulates assembly of functional tight junctions in epithelial cells. *Mol Biol Cell* **13**, 1819-1831 (2002).

45 Nishimura, N. & Sasaki, T. Rab family small G proteins in regulation of epithelial apical junctions. *Frontiers in bioscience* **14**, 2115-2129 (2009).

46 Coxon, F. P. *et al.* Phosphonocarboxylate inhibitors of Rab geranylgeranyl transferase disrupt the prenylation and membrane localization of Rab proteins in osteoclasts in vitro and in vivo. *Bone* **37**, 349-358 (2005).

47 Pavlos, N. J. *et al.* Rab3D regulates a novel vesicular trafficking pathway that is required for osteoclastic bone resorption. *Molecular and cellular biology* **25**, 5253-5269 (2005).

48 Hirvonen, M. J. *et al.* Rab13 is upregulated during osteoclast differentiation and associates with small vesicles revealing polarized distribution in resorbing cells. *J Histochem Cytochem* **60**, 537-549 (2012).

49 Dudakovic, A. *et al.* High-resolution molecular validation of self-renewal and spontaneous differentiation in clinical-grade adipose-tissue derived human mesenchymal stem cells. *Journal of cellular biochemistry* **115**, 1816-1828 (2014).

50 Huang da, W., Sherman, B. T. & Lempicki, R. A. Systematic and integrative analysis of large gene lists using DAVID bioinformatics resources. *Nat Protoc* **4**, 44-57 (2009).

4 MicroRNA Profiling of Osteoblast-Derived Extracellular Vesicles

This chapter is based on:

"Osteoblasts secrete miRNA-containing extracellular vesicles that enhance expansion of human umbilical cord blood cells"

by

Jess Morhayim, Jeroen van de Peppel, Eric Braakman, Elwin W. J. C. Rombouts, Mariette N. D. ter Borg, Amel Dudakovic, Hideki Chiba, Bram C. J. van der Eerden, Marc H. Raaijmakers, Andre J. van Wijnen, Jan J. Cornelissen, and Johannes P. van Leeuwen

Submitted

Osteolineage cells represent one of the critical bone marrow niche components that support maintenance of hematopoietic stem and progenitor cells (HSPCs). Recent studies demonstrate that extracellular vesicles (EVs) regulate stem cell development via horizontal transfer of bioactive lipids, proteins and RNA, including non-coding microRNAs (miRNAs). We hypothesize that the miRNAs in osteoblast-derived EVs may control the expression of key regulatory genes that mediate HSPC development. We performed next-generation sequencing to characterize global expression of miRNAs in human osteoblast-EVs, and investigated the role of EVs in crosstalk with human umbilical cord blood (UCB)-derived $CD34^+$ HSPCs. Osteoblast-EVs contain a set of highly abundant miRNAs specifically enriched in EVs, including critical regulators of hematopoietic proliferation (e.g., miR-29a). EV treatment of UCB derived $CD34^+$ cells down-regulated the expression of candidate miRNA targets, such as *HBP1*, *BCL2* and *PTEN*. Furthermore, EVs stimulate cell cycle progression and thereby enhance proliferation of $CD34^+$ cells. These discoveries reveal a novel osteoblast-derived EV-mediated mechanism for regulation of HSPC proliferation and warrant consideration of EV-miRNAs for the development of therapeutic strategies to treat hematological disorders.

4.1. INTRODUCTION

Extracellular vesicles (EVs) are secreted nano-sized cellular compartments that carry a specific biochemical cargo encompassing bioactive proteins, lipids and nucleic acids to regulate the function of recipient cells[1-3]. Circulating microRNAs (miRNAs), which are short non-coding RNAs of 21-25 nucleotides in length, are present in EVs and function as potent post-transcriptional regulators of gene expression[4-6]. EV-mediated miRNA transfer regulates various fundamental biological processes, including cell differentiation, proliferation and apoptosis[7-10]. Recent studies indicate that EV-miRNAs have biological roles in the hematopoietic system indicating the importance of EV-mediated paracrine signalling in hematopoiesis[11,12].

Hematopoietic stem cells (HSCs) are multipotent cells responsible for constant blood supply by undergoing tightly regulated self-renewal, proliferation and differentiation into different mature blood cell types. In adult humans, hematopoiesis mainly occurs in the bone marrow niche, which provides a supportive network of cells that orchestrate HSC fate[13,14]. Osteolineage cells, ranging from primitive mesenchymal cells to bone-forming mature osteoblasts, are thought to be important to maintain hematopoietic stem and progenitor cells (HSPCs)[15-19]. The molecular mechanisms that control the crosstalk between osteolineage cells and HSPCs in humans remain largely unexplored. Comparative gene expression profiling identified a number of molecules ranging from adhesion molecules to secreted factors, such as growth factors and cytokines, which may be essential for hematopoietic activity[20,21].

Even though there is no direct evidence yet, EVs may participate in the regulation of HSPC maintenance. We previously reported the protein content of human osteoblast-derived EVs at different stages of differentiation and mineralization[22]. Beyond protein cargo, it has become increasingly clear that miRNAs play a pivotal role in the regulation of HSPC fate[23-25]. Therefore, characterization of the miRNA content of osteoblast-EVs is necessary for appreciating the complexity of the HSPC-osteolineage-cell crosstalk and may open new avenues for clinical applications. In this chapter, we elucidate the miRNA profile of EVs secreted from human pre-osteoblasts using next-generation sequencing. Based on *in silico* target prediction analyses and *in vitro* biochemical analyses we define candidate hematopoietic development pathways affected by osteoblast-EVs. Our findings provide a foundation for the utilization of EVs as novel tools to modulate hematopoiesis for the development of suitable strategies to treat hematological disorders.

4.2. RESULTS

4.2.1. Human osteoblasts secrete EVs that contain small RNAs

To characterize osteoblast-derived EVs, SV-HFO cells were cultured for 12-14 days, and EV-RNA was isolated from the conditioned medium by a series of ultracentrifu-

gation steps followed by TRIzol total RNA extraction. Agilent Bioanalyzer RNA profiles show that osteoblast-EVs lack the typical cellular rRNAs, and instead are enriched with small RNAs (Fig. **1A**). The EV-RNA peak is retained when the EVs are treated with RNase A prior to RNA isolation (Fig. **1B**), verifying that the majority of the detected RNA is indeed present inside the EVs.

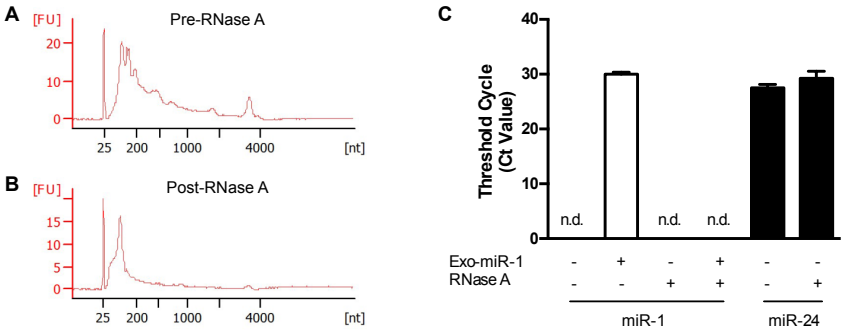

Figure 1. RNA analysis of osteoblast-derived EVs. A-B) Representative Agilent Bioanalyzer (Pico) RNA profiles of osteoblast-EVs (A) before and (B) after RNase A treatment (100 ng/ ml, 30 minutes at 37°C). FU, fluorescent units. (N = 3). C) Quantification of vesicular human miR-24 and miR-1 levels by qPCR in the presence or absence of exogenous synthetic miR-1 and RNase A. Data is presented as raw threshold cycle numbers (Ct values) (mean ± SD) (N = 3). n.d. denotes Ct values above 35 or not detectable.

To demonstrate that small EV-RNAs comprise miRNAs, we performed quantitative real-time PCR (qPCR) of the widely expressed human miR-1 and miR-24. As shown in Figure **1C**, osteoblast-EVs are devoid of miR-1 (*left panel*) while they contain relatively high amounts of miR-24 (*right panel*). Interestingly, RNase A treatment does not significantly alter the miR-24 level, confirming the presence of nuclease-resistant miR-24 inside the EVs. In contrast, exogenously added synthetic miR-1 was immediately degraded when spiked into the sample. Collectively, these data demonstrate that miRNAs are present in the heterogeneous population of osteoblast-EVs.

4.2.2. Osteoblast EVs contain the signature miRNA content of the donor cells

To evaluate the miRNA profile of osteoblast-EVs, we performed next-generation sequencing using total RNA from three independent osteoblast cultures and their corresponding EVs. The majority of the miRNAs yielded similar read counts in cells and EVs (Fig. **2A**). In total, we identified 761 mature miRNAs, of which 496 miRNAs are shared between cells and EVs and listed in ExoCarta (Fig. **2B**)[26,27]. Notably, all miRNAs exclusively present in cells (82 miRNAs) or EVs (92 miRNAs) are typically of low abundance. Only 185 EV-miRNAs are significantly abundant with levels above 100 normalized reads per million. This set encompasses 183 miRNAs that are among the 496 common miRNAs in both cells and EVs, as well as 2 miRNAs that are not yet listed in ExoCarta. The top 15

of miRNAs present in EVs produce ~75% of all the EV-miRNA reads, and more than half of the reads belong to just three major miRNA families related to miR-21-5p, miR-100-5p and let-7 (let-7f-5p, let-7i-5p, let-7g-5p, let-7a-5p) (Fig. **2C**). Figure **2D** shows the qPCR validation of selected abundant EV-miRNAs. These findings demonstrate that osteoblast-EVs contain miRNA profile of their donor cells as well as EV-miRNA markers, suggesting a conserved and preferential cargo export into EVs across all tissues.

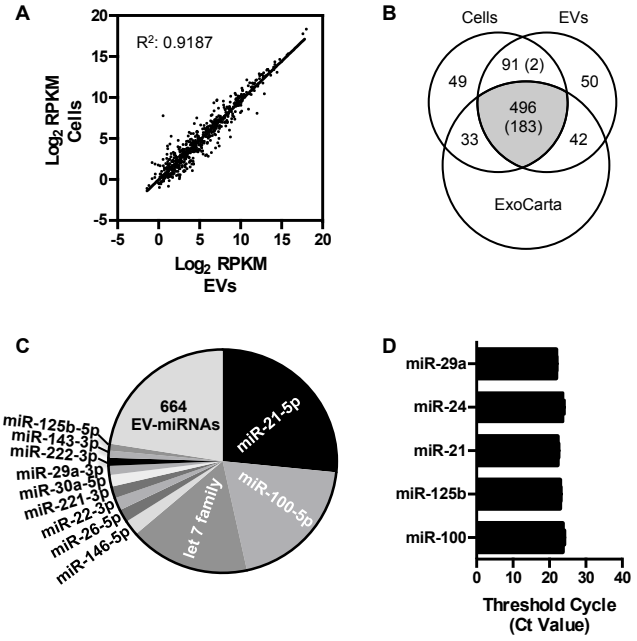

Figure 2. Next-generation sequencing miRNA profiling of osteoblast-EVs. A) Scatter plot shows the strong correlation (R^2: 0.9187) of normalized read counts (average RPKM) between cellular and vesicular miRNAs (N = 3). B) Venn diagram shows the number of miRNAs detected in osteoblasts and EVs in comparison with ExoCarta. Numbers in brackets denote the number of highly abundant miRNAs with reads greater than 100 RPKM among all EV miRNAs. C) Pie chart shows the normalized read count proportions of all EV-miRNAs. Only the top 15 most abundant EV-miRNAs, including let-7f-5p, let-7i-5p, let-7g-5p and let-7a-5p grouped as let7 family, are displayed. D) Validation of highly abundant EV miRNAs by TaqMan qPCR miRNA assay. Data is presented as raw Ct values (mean ± SD) (N = 3).

4.2.3. Osteoblast-EVs contain a specific set of abundant miRNAs

Next, we performed relative quantitation of cellular and vesicular miRNAs to assess whether a unique set of miRNAs is enriched in EVs. The Volcano plot in Figure **3A** shows all EV-miRNAs with statistical significance ($P < 0.05$) and differential abundance (≥ two-fold enrichment); the low abundance miRNAs unique to EVs and cells were excluded from this analysis. The results essentially reveal that EVs are preferentially loaded with 82

miRNAs (*red dots*) and depleted of 38 miRNAs (*green dots*). Table **1** shows the highly abundant and enriched 33 miRNAs with normalized reads above 100. Among these miRNAs, miR-146a-5p and miR-29a-3p are the most abundant, while miR-1246 and miR-1290 are most enriched (> 10-fold) in EVs (Fig. **3B**). Interestingly, 21 out of 33 enriched EV-miRNAs have not been previously reported as EV markers that are most commonly detected across all tissues and body fluids[28]. Hence, these 21 miRNAs may reflect selective sorting into osteoblast-EVs.

Table 1. The list of highly abundant (RPKM > 100) EV-miRNAs significantly ($P < 0.05$) enriched (≥ two-fold) in osteoblast-EVs compared to the cells.

Mature miRNAs	EVs (RPKM)	Cells (RPKM)	Fold Change	*P* value (< 0.05)
miR-146a-5p	22222.93	8704.45	2.6	0.00007
miR-29a-3p	13142.2	6705.16	2.0	0.00023
miR-23a-3p	7703.92	1420.23	5.7	0.00183
miR-181a-5p	6769.81	3463.81	2.0	0.0115
miR-1246	4118.99	271.75	16.1	0.02431
miR-574-5p	1984.81	383.66	5.6	0.01881
miR-374b-5p	1113.04	322.55	3.6	0.00283
miR-495-3p	1048.32	537.18	2.0	0.00033
miR-23b-3p	1018.65	290.86	3.6	0.00047
miR-197-3p	658.81	310.78	2.2	0.02496
miR-574-3p	625.27	164.21	4.0	0.00979
miR-34a-5p	575.65	202.6	3.0	0.0171
miR-19b-3p	529.06	261.05	2.0	0.00993
miR-106b-5p	521.13	218.05	2.4	0.00096
miR-214-3p	479.95	171.42	2.8	0.00111
miR-193b-3p	472.47	129.99	3.7	0.01471
miR-1290	432.46	36.65	13	0.0375
miR-30b-5p	400.98	65.07	6.4	0.00734
miR-29b-3p	338.76	130.27	2.6	0.0324
miR-15b-5p	318.36	148.02	2.4	0.04894
miR-320b	294.83	92.36	3.2	0.01741
miR-365a-3p	282.92	127.6	2.5	0.03148
miR-365b-3p	282.92	127.6	2.5	0.03148
miR-487b	204.27	88.43	2.3	0.00437
miR-130a-3p	172.66	84.39	2.1	0.00158
miR-485-5p	170.74	75.44	2.3	0.00023
miR-193a-3p	168.1	17.09	9.8	0.00266
miR-331-3p	166.59	32.65	5.2	0.00393
miR-181d	158.26	57.68	2.8	0.00281
miR-320c	147.98	22.5	6.7	0.01261
miR-664a-3p	123.31	14.54	8.7	0.00022
miR-299-5p	122.54	43.88	2.9	0.00022
miR-132-3p	112.94	47.1	2.5	0.01702

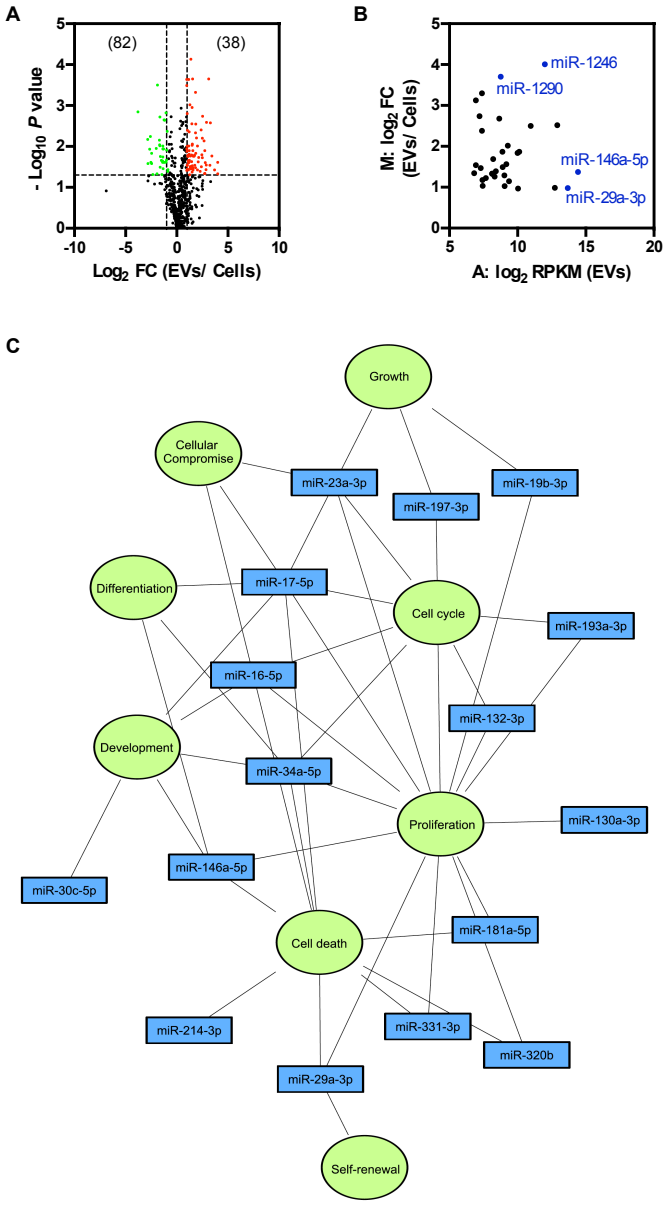

Figure 3. The analysis of the overrepresented EV-miRNAs. A) Volcano plot (significance versus fold change) shows the significantly ($P < 0.05$, compared with osteoblasts by Student's *t*-test) abundant (≥ 2-fold; red) and depleted (≤ 0.5-fold; green) miRNAs in EVs. Numbers in brackets denote the number of differentially expressed miRNAs. FC, fold change. B) MA plot (fold change versus EV abundance) shows the expression levels of the selectively enriched EV-miRNAs. The most highly abundant miRNAs are shown in blue. C) IPA network map shows the predicted biological functions significantly targeted by some of the highly abundant (RPKM > 100) enriched EV miRNAs. Blue, EV miRNAs; Green, biological functions.

Ingenuity Pathway Analysis (IPA) was performed to predict the impact of enriched EV-miRNAs on target cell gene expression and phenotype. The most significantly annotated molecular functions are cellular development, cellular growth and proliferation, cell cycle, cell death and survival and cellular compromise (Fig. **3C**). Together, our comparative analyses revealed overrepresentation of a selective group of miRNAs in osteoblast-EVs, indicating specific packaging of biologically functional regulatory molecules as EV cargo.

4.2.4. Osteoblast-EVs are enriched with miRNAs crucial for hematopoiesis

Each stage of hematopoietic differentiation is characterized by a specific miRNA signature[29]. We analyzed the osteoblast-EV-miRNA content for known regulators of hematopoiesis to find cues for EV-mediated HSPC-osteolineage-cell crosstalk. Indeed, a number of miRNAs that may control distinct stages of hematopoietic development are detected in high abundance in EVs (Fig. **4A**). Hence, we investigated whether treatment of HSPCs with osteoblast-EVs would alter expression of specific mRNAs that are targeted by miRNAs enriched in osteoblast-EVs.

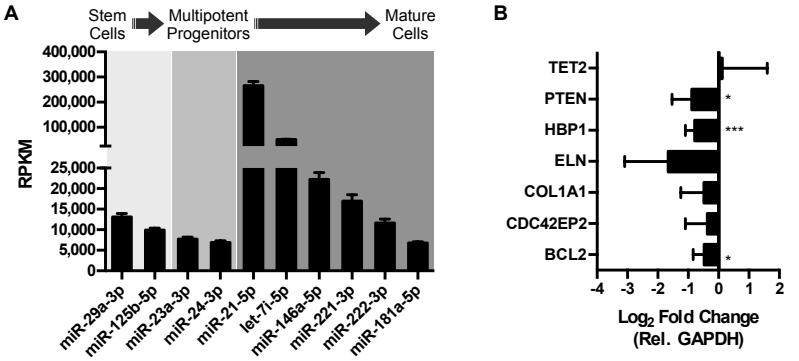

Figure 4. Osteoblast-EVs downregulate miR-29a target genes in UCB-derived CD34$^+$ cells. A) RPKM values (mean ± SD) of osteoblast-EV miRNAs known to be involved in different phases of hematopoiesis. B) Expression levels (mean ± SD) of candidate mRNA targets of miR-29a in human UCB-derived CD34$^+$ cells after 24 hours of incubation in the absence (control) or presence of osteoblast-EVs (N = 5). Fold change is determined compared to control and normalized to average *GAPDH* expression. * $P < 0.05$, *** $P < 0.005$, compared with control by Student's *t*-test.

We focused initially on miR-29a, which is significantly enriched in osteoblast-EVs, because it is known to be involved in early stages of hematopoiesis as a regulator of self-renewal, survival and proliferation of HSCs and HSPCs[30]. *In silico* target prediction analysis by TargetScan combined with supervised literature searches refined the large list of potential targets to a defined list of validated miR-29a target genes relevant to HSPCs.

By qPCR analysis we evaluated the expression level of miR-29a target genes involved in proliferation (*TET2*, *PTEN*), apoptosis (*BCL2*), cell cycle regulation (*HBP1*, *CDC42EP2*) and extracellular matrix adhesion (*COL1A1*, *ELN*) of HSPCs[30-32]. Osteoblast-EVs reduce the expression of all selected target genes, except *TET2*, in human UCB-derived $CD34^+$ HSPCs (Fig. **4B**). EVs significantly down-regulate the expression of *HBP1*, *BCL2* and *PTEN*, suggesting that osteoblast-EVs control proliferation of the recipient HSPCs. Proliferation assays that monitor Ki-67 staining (Fig. **5A**) and cell cycle analysis based on DNA content (Fig. **5B**) establish that osteoblast-EVs stimulate proliferation and cell cycle progression of the $CD34^+$ cells 24 hours after treatment. Thus, the integrated results of both *in silico* and *in vitro* approaches indicate that osteoblast-EVs are enriched with miRNAs involved in signaling cascades that regulate HSPC proliferation.

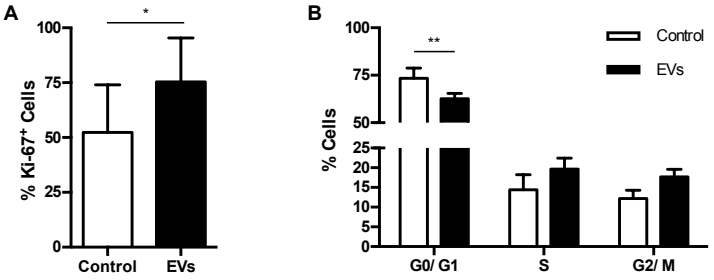

Figure 5. Osteoblast-EVs stimulate proliferation and cell cycle progression of UCB-derived $CD34^+$ cells. A) Proliferation assay, determined by the % of Ki-67^+ $CD34^+$ cells (mean ± SD), after 24 hours incubation in the absence (control) or presence of osteoblast-EVs (N = 3). * $P < 0.05$, compared with control by Student's *t*-test. B) Cell cycle distribution, using propidium iodide (PI) staining of $CD34^+$ cells (mean ± SD), after 24 hours incubation in the absence (control) or presence of osteoblast-EVs (N = 3). ** $P < 0.01$, compared with control by two-way ANOVA.

4.3. DISCUSSION

EV-mediated intercellular communication is an exciting new area of research that is rapidly evolving thanks to the emergence of powerful tools that enable characterization of their bioactive cargo. We used next-generation sequencing to study the miRNA profile of human osteoblast-derived EVs. Based on the overrepresented EV-miRNAs we delineated the targeted biological functions associated with hematopoiesis and verified *in silico* predictions with *in vitro* results. We showed that osteoblast-EVs stimulate the cell cycle progression and proliferation of UCB-derived $CD34^+$ HSPCs. Our findings provide a fundamental description of the biological roles of EVs in mediating crosstalk between osteolineage cells and HSPCs. Equally important, osteoblast-derived EVs may present potential value in clinical applications to treat hematopoietic disorders.

There is considerable interest in understanding circulating miRNAs as potential disease markers for early diagnosis[33]. These regulatory miRNAs mostly circulate entrapped

in protein complexes that protect them from degradation by circulating nucleases[34,35]. Recent studies show that they also exert their effect in a paracrine manner via EV-mediated delivery to the target tissue[4]. The hematopoietic bone marrow niche consists of a tightly regulated network of numerous cell types, including osteoblasts, mesenchymal stromal-, endothelial- and neuronal cells and hematopoietic progenitors. Characterization of the EV-mediated intercellular communication within the bone marrow niche may contribute to the understanding of this complex network.

We performed high throughput analysis of miRNAs to assess whether human osteoblast-EVs utilize small RNAs to communicate with HSPCs in the bone marrow niche. As expected, the EV-miRNA profile mirrors that of the osteoblastic donor cell, but we also detected a large number of miRNAs that appear to be enriched in EVs. Importantly, we identified a number of miRNAs that are abundant in osteoblast-EVs and are known regulators of hematopoiesis. We focused on miR-29a because it controls early steps of hematopoiesis and is enriched in EVs compared to the donor cells. Our study shows that osteoblast-EVs are capable of down-regulating the expression of cell cycle- and growth-related miR-29 target genes in $CD34^+$ cells. We further demonstrate that osteoblast-EVs stimulate proliferation and cell cycle progression of $CD34^+$ cells, in accordance with the expression profile of down-regulated target genes.

Stem cells are special cells with remarkable regenerative abilities, which make them very attractive for the development of cell-based therapies. A complex network of environmental cues tightly regulates stem cell fate determination, including self-renewal and differentiation. Ratajczak and colleagues were one of the firsts to report the role of EVs in stem cell regulation[36]. They showed that embryonic stem cells released EVs containing regulatory proteins and mRNA capable of reprogramming HSCs. Since then numerous studies reported the role of EVs in stem cell biology with a major focus on miRNA transfer, suggesting a critical paracrine role for EVs in stem cell niches[37-40]. We previously showed that osteoblast-EVs induced proliferation of bone-metastasizing prostate cancer cells[22]. Recent studies indicate that prostate cancer cells compete with HSCs for the bone marrow niche, emphasizing the importance of EVs in the regulation of HSC growth and survival[41]. Hematopoietic differentiation is characterized by specific miRNA signatures, which act in each step of linage decision to ensure proper hematopoiesis[25,29]. The osteoblast-EV-miRNA profile we described here provides further insights into the complexities of the HSPC-osteolineage-cell crosstalk.

In conclusion, our findings provide a new paradigm for the role of EVs in the regulation of stem cell niches. We propose that EVs contain a signature miRNA profile that participates in the HSPC-osteolineage-cell crosstalk. It remains to be determined whether EV-miRNAs act in concert with other regulatory EV cargo, such as mRNAs and proteins, which may contribute to the proliferative effect of osteoblast-EVs. Identification of such critical EV components opens up avenues to be exploited clinically to develop novel approaches not only for the treatment hematological disorders but in a broader context also for use in regenerative medicine.

4.4. MATERIALS AND METHODS

Cell cultures. Human osteoblast cells (SV-HFO cells) were cultured as described in Chapter 2[22]. UCB was collected in several hospitals using Stemcare®/CB collection blood bag system (Fresenius Kabi Norge AS, Halden, Norway). Approval for collection was obtained from the Medical Ethical Committee of the Erasmus University Medical Centre (MEC-2009-410) and written informed consent from the mother was obtained prior to UCB donation. Within 48 hours after collection, mononuclear cells were isolated using ficoll (Lymphoprep™, Fresenius Kabi Norge AS). $CD34^+$ cells were isolated as described previously[42]. 20,000 $CD34^+$ cells were cultured in serum-free Glycostem Basic Growth Medium (GBGM; Glycostem, Oss, the Netherlands) supplemented with stem cell factor (SCF; 50 ng/ ml, Cellgenix, Freiburg, Germany) and Fms-related tyrosine kinase 3 ligand (Flt3L; 50 ng/ ml, Cellgenix), with or without osteoblast-EVs at 37°C in a humidified atmosphere of 5% CO_2.

EV isolation and characterization. Osteoblast-EVs were isolated from 20 ml conditioned medium by low speed centrifugation (1,500 rpm, 5 minutes; 4,500 rpm, 10 minutes) followed by ultracentrifugation (20,000g, 30 minutes; 100,000g, 1 hour at 4°C) of the supernatant using the SW32Ti rotor (Beckman Coulter, Fullerton, CA, USA). EVs were prepared as 100 µl suspensions, and the amount of experimental EV dose was determined as 5% (v/v).

RNA isolation and quantitative real-time PCR. The purified EV pellet was incubated with or without RNase A (100 mM) and synthetic miR-1 (20 pM) at 37°C for 30 minutes, and total RNA was isolated using the TRIzol reagent (Thermo Fisher Scientific, Waltham, MA, USA) according to the manufacturer's instructions. RNA concentration was determined using Nanodrop (Thermo Fisher Scientific) and size distribution was checked on an Agilent Bioanalyzer RNA 6000 Pico chip (Thermo Fisher Scientific). RNA from $CD34^+$ cells was isolated using NucleoSpin RNA XS kit (Macherey-Nagel, Duren, Germany) according to the manufacturer's instructions. Quantitative real-time PCR for mRNAs and miRNAs were performed using the SYBR™ Green (Eurogentec, Seraing, Belgium) and Taqman® kits (Thermo Fisher Scientific), respectively, according to the manufacturer's instructions. The primer sequences are listed in Appendix C.

Next-generation sequencing and bioinformatic analysis of miRNAs. Sequencing of miRNAs was performed by Illumina HiSeq with samples prepared with the NEBNext Small RNA library preparation kit. We used the CAP-miRSeq bioinformatic pipeline for mapping of miRNA reads data analysis[43]. In brief, adaptor sequences were removed from 50bp reads using Cutadapt[44] and sequences of sufficient size (>17 nucleotides in length) were aligned to the hg19 reference genome and miRBase 19 reference sequences using Bowtie[45]. Quantitative analysis of known and predicted miRNAs was performed using

miRDeep2[46]. Comparative analyses of the EV data were obtained by querying the ExoCarta (V5, 29 July 2015) database. IPA (Ingenuity® Systems, www.ingenuity.com) and TargetScan (Release 7.0) were used to predict target pathways and genes.

Flow cytometry. Analysis of proliferation and cell cycle progression of $CD34^+$ cells was performed using flow cytometry by monitoring the proliferation marker Ki-67 relative to DNA content. Cells were incubated with or without EVs for 24 hours, and stained with Alexa Fluor® 488-conjugated Ki-67 antibody (BD Biosciences, San Jose, CA, USA) followed by the addition of propidium iodide (BD Biosciences) according to the manufacturers instructions. All samples were immediately analyzed using BD Accuri™ C6 flow cytometry (BD Biosciences), and the data was analyzed using C6 software.

Statistics. The results were described as mean ± SD based on at least two independent experiments performed with independent EV isolations and/ or different UCB donors. Significance was calculated using Student's *t*-test and two-way ANOVA test, and *P* values of < 0.05 were considered significant.

REFERENCES

1 Raposo, G. & Stoorvogel, W. Extracellular vesicles: exosomes, microvesicles, and friends. *J Cell Biol* **200**, 373-383 (2013).

2 Thery, C., Ostrowski, M. & Segura, E. Membrane vesicles as conveyors of immune responses. *Nat Rev Immunol* **9**, 581-593 (2009).

3 Morhayim, J., Baroncelli, M. & van Leeuwen, J. P. Extracellular vesicles: specialized bone messengers. *Archives of biochemistry and biophysics* **561**, 38-45 (2014).

4 Valadi, H. *et al.* Exosome-mediated transfer of mRNAs and microRNAs is a novel mechanism of genetic exchange between cells. *Nature cell biology* **9**, 654-659 (2007).

5 Collino, F. *et al.* Microvesicles derived from adult human bone marrow and tissue specific mesenchymal stem cells shuttle selected pattern of miRNAs. *PloS one* **5**, e11803 (2010).

6 Bartel, D. P. MicroRNAs: genomics, biogenesis, mechanism, and function. *Cell* **116**, 281-297 (2004).

7 Chen, X., Liang, H., Zhang, J., Zen, K. & Zhang, C. Y. Horizontal transfer of microRNAs: molecular mechanisms and clinical applications. *Protein & cell* **3**, 28-37 (2012).

8 Kosaka, N. *et al.* Secretory mechanisms and intercellular transfer of microRNAs in living cells. *The Journal of biological chemistry* **285**, 17442-17452 (2010).

9 Muralidharan-Chari, V., Clancy, J. W., Sedgwick, A. & D'Souza-Schorey, C. Microvesicles: mediators of extracellular communication during cancer progression. *Journal of cell science* **123**, 1603-1611 (2010).

10 Pegtel, D. M. *et al.* Functional delivery of viral miRNAs via exosomes. *Proceedings of the National Academy of Sciences of the United States of America* **107**, 6328-6333 (2010).

11 Mittelbrunn, M. *et al.* Unidirectional transfer of microRNA-loaded exosomes from T cells to antigen-presenting cells. *Nature communications* **2**, 282 (2011).

12 Rechavi, O. *et al.* Cell contact-dependent acquisition of cellular and viral nonautonomously encoded small RNAs. *Genes & development* **23**, 1971-1979 (2009).

13 Taichman, R. S. Blood and bone: two tissues whose fates are intertwined to create the hematopoietic stem-cell niche. *Blood* **105**, 2631-2639 (2005).

14 Bianco, P. Bone and the hematopoietic niche: a tale of two stem cells. *Blood* **117**, 5281-5288 (2011).

15 Zhang, J. *et al.* Identification of the haematopoietic stem cell niche and control of the niche size. *Nature* **425**, 836-841 (2003).

16 Calvi, L. M. *et al.* Osteoblastic cells regulate the haematopoietic stem cell niche. *Nature* **425**, 841-846 (2003).

17 Visnjic, D. *et al.* Hematopoiesis is severely altered in mice with an induced osteoblast deficiency. *Blood* **103**, 3258-3264 (2004).

18 Pinho, S. *et al.* PDGFRalpha and CD51 mark human nestin+ sphere-forming mesenchymal stem cells capable of hematopoietic progenitor cell expansion. *The Journal of experimental medicine* **210**, 1351-1367 (2013).

19 Greenbaum, A. *et al.* CXCL12 in early mesenchymal progenitors is required for haematopoietic stem-cell maintenance. *Nature* **495**, 227-230 (2013).

20 Taichman, R. S. & Emerson, S. G. Human osteoblasts support hematopoiesis through the production of granulocyte colony-stimulating factor. *The Journal of experimental medicine* **179**, 1677-1682 (1994).

21 Shiozawa, Y. & Taichman, R. S. Getting blood from bone: an emerging understanding of the role that osteoblasts play in regulating hematopoietic stem cells within their niche. *Experimental hematology* **40**, 685-694 (2012).
22 Morhayim, J. *et al.* Proteomic signatures of extracellular vesicles secreted by nonmineralizing and mineralizing human osteoblasts and stimulation of tumor cell growth. *FASEB journal : official publication of the Federation of American Societies for Experimental Biology* **29**, 274-285 (2015).
23 Chen, C. Z., Li, L., Lodish, H. F. & Bartel, D. P. MicroRNAs modulate hematopoietic lineage differentiation. *Science* **303**, 83-86 (2004).
24 Lu, J. *et al.* MicroRNA-mediated control of cell fate in megakaryocyte-erythrocyte progenitors. *Developmental cell* **14**, 843-853 (2008).
25 Bissels, U., Bosio, A. & Wagner, W. MicroRNAs are shaping the hematopoietic landscape. *Haematologica* **97**, 160-167 (2012).
26 Mathivanan, S. & Simpson, R. J. ExoCarta: A compendium of exosomal proteins and RNA. *Proteomics* **9**, 4997-5000 (2009).
27 Mathivanan, S., Fahner, C. J., Reid, G. E. & Simpson, R. J. ExoCarta 2012: database of exosomal proteins, RNA and lipids. *Nucleic acids research* **40**, D1241-1244 (2012).
28 Kalra, H. *et al.* Vesiclepedia: a compendium for extracellular vesicles with continuous community annotation. *PLoS biology* **10**, e1001450 (2012).
29 Montagner, S., Deho, L. & Monticelli, S. MicroRNAs in hematopoietic development. *BMC immunology* **15**, 14 (2014).
30 Han, Y. C. *et al.* microRNA-29a induces aberrant self-renewal capacity in hematopoietic progenitors, biased myeloid development, and acute myeloid leukemia. *The Journal of experimental medicine* **207**, 475-489 (2010).
31 Wang, X. S. *et al.* MicroRNA-29a and microRNA-142-3p are regulators of myeloid differentiation and acute myeloid leukemia. *Blood* **119**, 4992-5004 (2012).
32 Cheng, J. *et al.* An extensive network of TET2-targeting MicroRNAs regulates malignant hematopoiesis. *Cell reports* **5**, 471-481 (2013).
33 Williams, Z. *et al.* Comprehensive profiling of circulating microRNA via small RNA sequencing of cDNA libraries reveals biomarker potential and limitations. *Proceedings of the National Academy of Sciences of the United States of America* **110**, 4255-4260 (2013).
34 Wang, K., Zhang, S., Weber, J., Baxter, D. & Galas, D. J. Export of microRNAs and microRNA-protective protein by mammalian cells. *Nucleic acids research* **38**, 7248-7259 (2010).
35 Turchinovich, A., Weiz, L., Langheinz, A. & Burwinkel, B. Characterization of extracellular circulating microRNA. *Nucleic acids research* **39**, 7223-7233 (2011).
36 Ratajczak, J. *et al.* Embryonic stem cell-derived microvesicles reprogram hematopoietic progenitors: evidence for horizontal transfer of mRNA and protein delivery. *Leukemia* **20**, 847-856 (2006).
37 Yuan, A. *et al.* Transfer of microRNAs by embryonic stem cell microvesicles. *PloS one* **4**, e4722 (2009).
38 Chen, T. S. *et al.* Mesenchymal stem cell secretes microparticles enriched in pre-microRNAs. *Nucleic acids research* **38**, 215-224 (2010).
39 Nair, R. *et al.* Extracellular vesicles derived from preosteoblasts influence embryonic stem cell differentiation. *Stem cells and development* **23**, 1625-1635 (2014).

40 Quesenberry, P. J. & Aliotta, J. M. The paradoxical dynamism of marrow stem cells: considerations of stem cells, niches, and microvesicles. *Stem cell reviews* **4**, 137-147 (2008).

41 Yu, C. *et al.* Prostate cancer and parasitism of the bone hematopoietic stem cell niche. *Critical reviews in eukaryotic gene expression* **22**, 131-148 (2012).

42 Duinhouwer, L. E. *et al.* Wnt3a protein reduces growth factor-driven expansion of human hematopoietic stem and progenitor cells in serum-free cultures. *PloS one* **10**, e0119086 (2015).

43 Sun, Z. *et al.* CAP-miRSeq: a comprehensive analysis pipeline for microRNA sequencing data. *BMC genomics* **15**, 423 (2014).

44 Martin, M. Cutadapt removes adapter sequences from high-throughput sequencing reads. *EMBnet.journal* **17**, 10-12 (2011).

45 Langmead, B., Trapnell, C., Pop, M. & Salzberg, S. L. Ultrafast and memory-efficient alignment of short DNA sequences to the human genome. *Genome biology* **10**, R25 (2009).

46 Friedlander, M. R. *et al.* Discovering microRNAs from deep sequencing data using miRDeep. *Nat Biotechnol* **26**, 407-415 (2008).

5 Expansion of Human Umbilical Cord Blood Cells Using Extracellular Vesicles

This chapter is based on:

"Osteoblasts secrete miRNA-containing extracellular vesicles that enhance expansion of human umbilical cord blood cells"

by

Jess Morhayim, Jeroen van de Peppel, Eric Braakman, Elwin W. J. C. Rombouts, Mariette N. D. ter Borg, Amel Dudakovic, Hideki Chiba, Bram C. J. van der Eerden, Marc H. Raaijmakers, Andre J. van Wijnen, Jan J. Cornelissen, and Johannes P. van Leeuwen

Submitted

Umbilical cord blood (UCB) is increasingly used as an important source of hematopoietic stem cells to treat a number of hematological malignancies. The major obstacle to the widespread use of UCB is the insufficient amount of progenitor cells to sustain therapy. Culturing UCB cells with osteolineage cells or in the presence of osteolineage-cell-derived secreted factors have helped the development of successful expansion protocols for clinical use. Extracellular vesicles (EVs) are secreted cellular compartments that carry regulatory cargo between cells. In this chapter, we investigated the capacity of human osteoblast-derived EVs to expand human UCB-derived $CD34^+$ hematopoietic stem and progenitor cells (HSPCs). Osteoblast-EVs enhance proliferation of $CD34^+$ HSPCs and their immature subsets ($Lin^-CD34^+CD38^{low}CD45RA^{low}CD90^+$ cells) in hematopoietic growth factor-driven *ex vivo* expansion cultures. Importantly, EV-expanded cells retain their differentiation capacity *in vitro* and successfully engraft *in vivo*. In conclusion, our findings demonstrate the potency of using osteoblast-EVs in development of novel clinically relevant expansion strategies. Further investigation of EV content as well as their role in HSPC proliferation described in previous chapters is critical to unravel key factors useful for therapeutic applications.

5.1. INTRODUCTION

Hematopoietic stem cells (HSCs), multipotent cells that give rise to all blood lineages, are widely used in stem cell transplantations that have saved many lives where other cures are no longer possible[1]. Umbilical cord blood (UCB) is a rich source of HSCs and an attractive alternative to bone marrow due to its rapid availability and less stringent human leucocyte antigen match requirement. However, UCB grafts contain a low number of hematopoietic stem and progenitor cells (HSPCs) that poses as a limiting factor for proper engraftment, which leads to delayed hematopoietic recovery and patient morbidity and mortality[2,3].

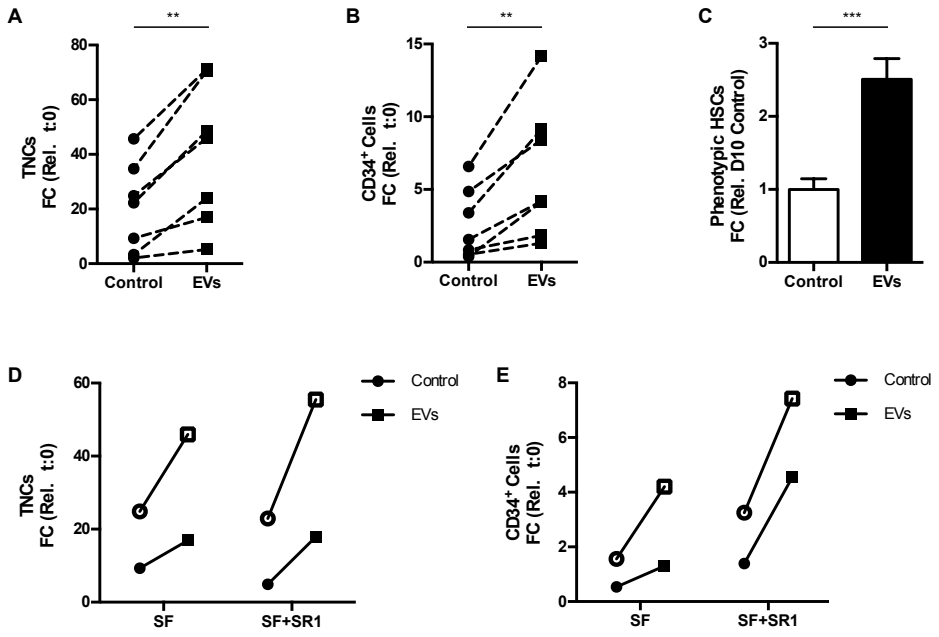

Figure 1. Osteoblast-EVs enhance ex vivo expansion of UCB-derived CD34$^+$ cells. A-B) Osteoblast-EVs increase the expansion of (A) total nucleated cells (TNCs) and (B) CD34$^+$ cells after 10 days of expansion with SCF and Flt3L compared to cells cultured in the absence of EVs (control) (N = 7). Expansion is shown as fold change (FC) increase in total cell number compared to input. ** $P < 0.01$, compared with control by Student's *t*-test. C) Osteoblast-EVs increase the number (mean ± SD) of phenotypic HSCs ($Lin^-CD34^+CD38^{low}CD45RA^{low}CD90^+$) compared to control on day 10 (N = 3). *** $P < 0.005$, compared with control by Student's *t*-test. D-E) Osteoblast-EVs increase the numbers of (D) TNCs and (E) CD34$^+$ cells after 10 days of expansion with SCF, Flt3L and SR1 compared to control (N = 2). Empty and full shapes show the different donors.

Over the past few decades, studies have been focusing on the establishment of *ex vivo* culture systems to expand UCB-derived HSPCs for improved engraftment and post-transplantation recovery[4]. Culture systems supplemented with growth factor cocktails, in-

cluding stem cell factor (SCF), Fms-related tyrosine kinase 3 ligand (Flt3L), thrombopoietin (TPO), granulocyte-macrophage colony stimulating factor (GM-CSF) and interleukin 6 (IL-6), successfully stimulate the expansion of the HSPCs, though at the expense of long-term repopulating HSCs[5]. Recent studies reported the success of improved expansion by mimicking the bone marrow niche, where HSC fate determination is tightly regulated[6,7]. Osteolineage cells represent one of the critical niche components that support self-renewal and proliferation of HSCs *in vivo*[8-13]. Osteolineage-cell-derived secreted factors and adhesion molecules yield robust *in vitro* proliferation of HSPCs with long-term repopulation ability stressing the importance of discovering other osteolineage cell components that can support the growth factor-based expansion culture systems[12-17].

Extracellular vesicles (EVs) are small cellular compartments that alter the function of their targets by transferring bioactive lipids, proteins and RNA between cells[18-21]. Increasing studies report the role of EV-mediated intercellular communication within the hematopoietic system[22-25]. A pivotal study by Ratajczak and colleagues highlighted the importance of EV cargo on the regulation of HSC fate[26]. In Chapter 4, we showed that human osteoblast-derived EVs stimulate the proliferation of UCB-derived $CD34^+$ HSPCs *in vitro*. In this chapter, we take this further and evaluate in greater detail the proliferative capacity of human osteoblast-EVs and the opportunity to exploit them to expand human UCB-derived $CD34^+$ HSPCs in SCF- and Flt3L-driven serum-free *ex vivo* expansion cultures. We further verify the functionality of the expanded cells *in vivo* by performing xenogeneic transplantation in sub-lethally irradiated immunodeficient NOD.Cg-*Prkdc*^{scid} *Il2rg*^{tm1Wjl}/SzJ (NSG) mice. Taken together our findings demonstrate that EVs prove to be powerful tools to expand HSPCs *ex vivo* suitable for clinical use.

5.2. RESULTS

5.2.1. Human osteoblasts secrete EVs that promote *ex vivo* expansion of $CD34^+$ HSPCs

In this study, we used EVs derived from human pre-osteoblasts (SV-HFO cell line) cultured for 12-14 days. We evaluated the capacity of osteoblast-EVs to promote the *ex vivo* expansion of human UCB-derived $CD34^+$ cells in growth factor (SCF and Flt3L)-driven serum-free expansion cultures. Osteoblast-EVs induce a two-fold expansion of both total number of viable nucleated cells (TNCs) ($P < 0.01$) and $CD34^+$ cells ($P < 0.01$) in 10 days as compared to the control cultures (Fig. **1A & 1B**). The expansion potential of EVs is not masked even in the presence of additional expansion growth factors, such as TPO (Appendix A, Fig. A1). We also assessed the presence of the most immature $CD34^+$ cell subset in the expanded cells by multicolor flow cytometry using markers for primitive HSPCs ($Lin^-CD34^+CD38^{low}CD45RA^{low}CD90^+$), referred to as phenotypic HSCs (Appendix A, Fig. A2). EV treatment also increases the number of phenotypic HSCs more than two-fold ($P < 0.005$) compared to the control on day 10 (Fig. **1C**). Interestingly, the expansion

potential of EVs remains clearly evident even in the presence of highly effective expansion factors, such as StemRegenin 1 (SR1) (Fig. **1D & 1E**)[27]. These findings demonstrate the potency of osteoblast-EVs to promote growth factor-driven HSPC expansion.

5.2.2. EV-expanded cells retain their differentiation capacity *in vitro*

We evaluated the functional characteristics of the *ex vivo* expanded $CD34^+$ cells *in vitro* and *in vivo*. Initially, we investigated whether the $CD34^+$ cells that were expanded *ex vivo* using EVs retain their differentiation capacity *in vitro* by performing colony-forming unit (CFU) assay. EV-expanded cells exhibit a higher clonogenicity, most likely due to the increased number of viable and functional $CD34^+$ cells after expansion (Fig. **2A**). However, frequencies between control and EV treatment remain comparable suggesting similar capacities for the preservation of primitive HSCs and their progenitors.

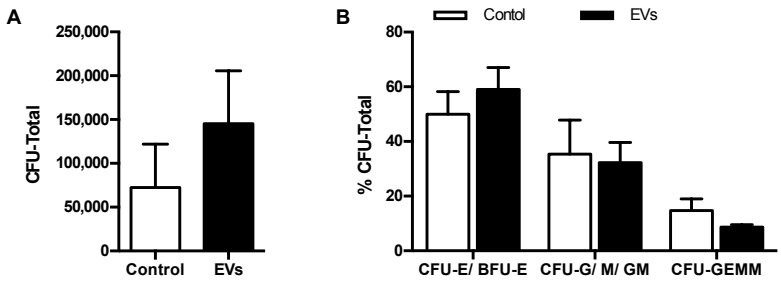

Figure 2. EV-expanded $CD34^+$ cells retain their differentiation capacity *in vitro*. A) Total CFUs (mean ± SD) in EV-expanded cells (N = 3). B) The frequencies of the myeloid and erythroid lineages. Control denotes cells expanded in the absence of EVs.

Next, we investigated whether EV-treatment alters the ability of the HSPCs to differentiate and give rise to colonies of different mature blood cells by enumerating the classes of myeloid and erythroid progenitor cells (Fig. **2B**). Interestingly, frequencies of multilineage progenitors (CFU-GEMM), erythroid progenitors (CFU-E/ BFU-E) and granulocyte/macrophage progenitors (CFU-G/ M/ GM) remain comparable to the control, indicating that EVs promote expansion but do not favor specific hematopoietic lineages. These findings demonstrate that EV-expanded HSPCs retain the pool of progenitor cells that give rise to erythrocytes and myeloid cells *in vitro*.

5.2.3. Osteoblast-EV-expanded cells retain *in vivo* engraftment potential

To assess the impact on engraftment and hematopoietic repopulating ability of the *ex vivo* expanded cells, sublethally irradiated immunodeficient NSG mice were transplant-

ed with $CD34^+$ progeny cells derived from 10^5 seeded cells after expansion with or without EVs for 10 days (Appendix A, Fig. A3). Engraftment was defined as at least 0.1% human chimerism in the peripheral blood. All mice show similar levels of human chimerism (~20%) in both control and EV treatment groups at 19 weeks after transplantation (Fig. **3A**).

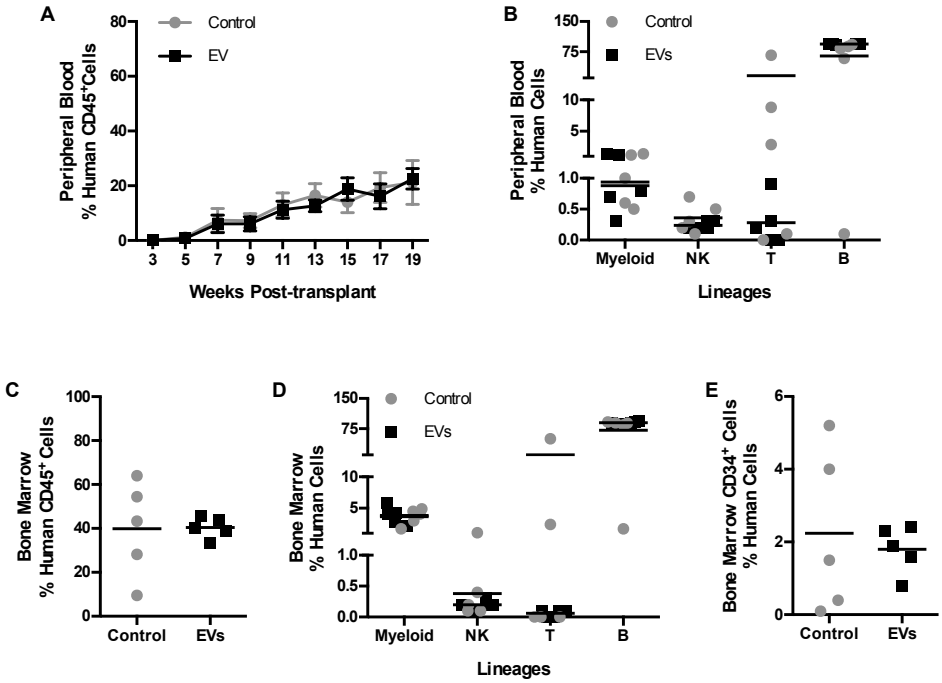

Figure 3. EV-expanded $CD34^+$ cells successfully engraft and re-populate NSG mice. A) Human chimerism level (% human $CD45^+$ cells) (mean ± SD) in peripheral blood at several time-points after transplantation of $CD34^+$ cells expanded in the absence (control) and presence of EVs (N = 5 mice/ group). B) The frequencies of human lymphoid and myeloid lineages in peripheral blood after 19 weeks. C) Human chimerism level in the bone marrow after 21 weeks. C_V (coefficient of variation) is 54.13% and 11.74% for control and EVs, respectively. D) The frequencies of human lymphoid and myeloid lineages in bone marrow after 21 weeks. E) The frequencies of human $CD34^+$ progenitors within the human $CD45^+$ fraction in the bone marrow after 21 weeks. C_V is 100.75% and 35.79% for control and EVs, respectively.

EV treatment does not alter the speed and quality of recovery of different human lymphoid and myeloid lineages in NSG mice. The predominant human cell population after engraftment consists of $CD19^+$ B-cells, as well as very low levels of other lymphoid (NK and T-cells) and myeloid cells (Fig. **3B**). Moreover, both control and the EV treatment groups exhibit similar levels of $CD45^+$ human chimerism in recipient bone marrow at 21 weeks after transplantation (Fig. **3C**). Similar to the peripheral blood, the majority of human cells in the bone marrow expressed the B-cell marker CD19 (Fig. **3D**). As expected, only a small (2%) fraction of human cells is positive for CD34 (Fig. **3E**). We note that the

mice in the control group show a high degree of variability (C_V: 54.13%, Fig. 3C; C_V: 100.75%, Fig. 3E) of chimerism in the bone marrow, possibly explained by the lower number of total transplanted cells after expansion. Taken together, these findings clearly demonstrate that *ex vivo* EV treatment retains the engraftment potential of human cells in NSG mice.

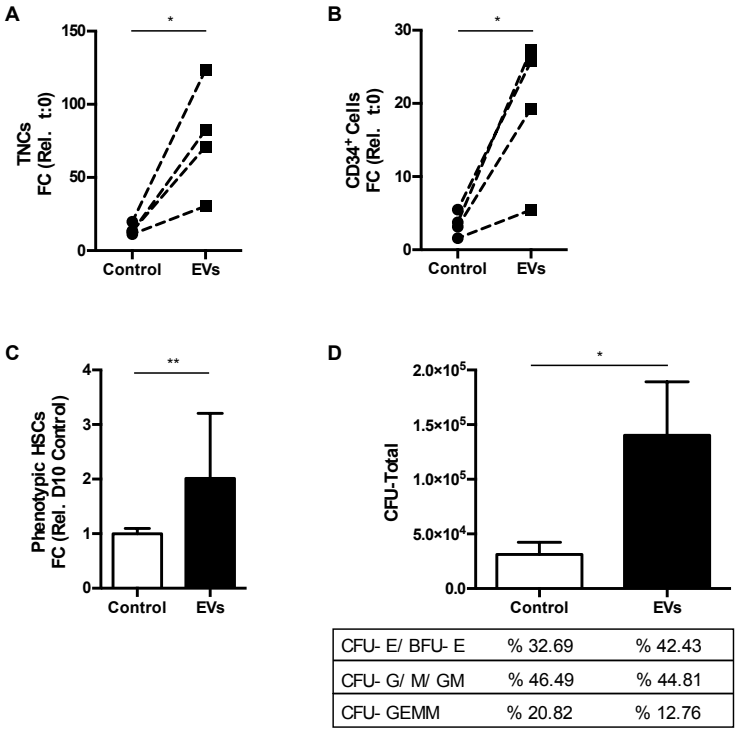

CFU- E/ BFU- E	% 32.69	% 42.43
CFU- G/ M/ GM	% 46.49	% 44.81
CFU- GEMM	% 20.82	% 12.76

Figure 4. Osteoblast-EVs enhance *ex vivo* expansion of sorted phenotypic HSCs. A-B) Osteoblast-EVs improve the expansion capacity of (A) TNCs and (B) $CD34^+$ progenitors after 10 days of expansion with SCF and Flt3L compared to cells cultured in the absence of EVs (control) (N = 4). Expansion is shown as fold change increase in total cell number compared to input. * $P < 0.05$, compared with control by Student's *t*-test. C) Osteoblast-EVs increase the number (mean ± SD) of phenotypic HSCs compared to control on day 10 (N = 4). ** $P < 0.01$, compared with control by Student's *t*-test. D) EV-expanded immature UCB cells retain their differentiation capacity in CFU assay (mean ± SD) (N = 3). The frequencies of the myeloid and erythroid lineages are shown in the table. * $P < 0.05$, compared with control by Student's *t*-test.

5.2.4. Osteoblast-EVs stimulate the proliferation of immature cells

Most conventional expansion protocols, which provide short-term robust proliferation of the $CD34^+$ progenitor cells, are accompanied by concomitant differentiation and result in loss of primitive HSC sub-populations[4,28,29]. To study the effect of EVs on immature stem cells, we sorted phenotypic HSCs as a starting population. Osteoblast-EV treat-

ment of phenotypic HSCs significantly induces the expansion of TNCs (Fig. **4A**), $CD34^+$ cells (Fig. **4B**) and phenotypic HSCs (Fig. **4C**) after 10 days. Corroborating these results, CFU assays reveal an increase in the number of the immature cells while retaining the frequency of the different lineages (Fig. **4D**).

To determine the effect of osteoblast-EVs on the maintenance of CD34 and CD90 expression after successive cell divisions of phenotypic HSCs, we used CellTrace™ Violet staining. Cells that were grown in the presence of osteoblast-EVs undergo a higher number of cell divisions while keeping their stem cell phenotype after 5 days compared to control (Fig. **5A & 5B**). Figures **5C & 5D** show the fraction of cells that have divided up to 4 times within the $CD34^+$ cell population in the absence or presence of EVs. Our data show that EVs stimulate the cell division kinetics of the immature cells, resulting in an increased number of $CD34^+$ cells.

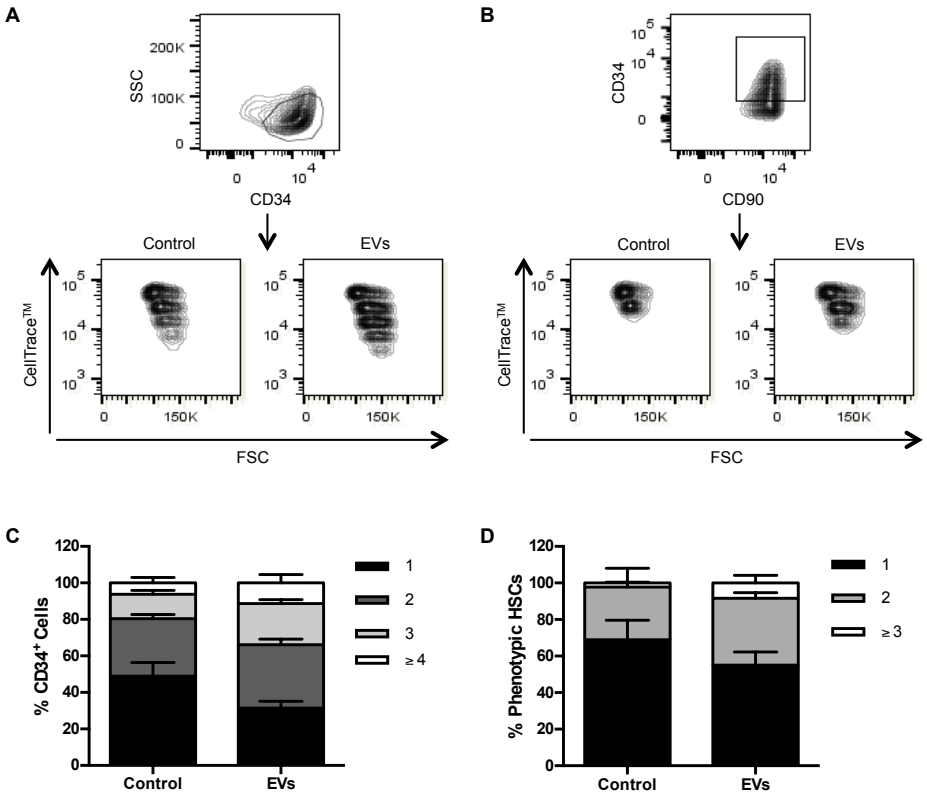

Figure 5. Osteoblast-EVs stimulate the proliferation of the immature cells. A-B) Sorted phenotypic HSCs were loaded with CellTrace™ Violet and incubated in the absence (control) or presence of osteoblast-EVs for 5 days. Flow cytometry plots show the distribution of the progeny of (A) $CD34^+$ progenitors and (B) $CD90^+$ phenotypic HSCs. C-D) The percentages (mean ± SD) of cells that have divided 1 – 4 times within (C) $CD34^+$ progenitors and (D) $CD90^+$ phenotypic HSCs (N = 2).

5.3. DISCUSSION

The ability of EVs to transfer functional cargo between cells brings exciting possibilities for therapeutic applications. In this chapter, we demonstrated that human osteoblast-derived EVs enhance HSPC proliferation leading to the *ex vivo* expansion of UCB-derived CD34$^+$ cells, including the most immature subsets in growth factor-driven serum-free expansion cultures. Importantly, the EV-expanded cells retain their differentiation capacity *in vitro* and successfully engraft and re-populate NSG mice *in vivo*.

The current expansion protocols primarily focus on the use of a cocktail of hematopoietic growth factors, which are successful to stimulate rapid self-renewal of human HSPCs[30]. Combination of SCF and Flt3L with other growth factors, such as TPO, IL-6 and GM-CSF, successfully stimulate the expansion of CD34$^+$ progenitors in matter of a few weeks[31,32]. Here, we limited the use of growth factors to SCF and Flt3L, which are necessary for the minimum required potency, to better study the EV effect[33]. SCF and Flt3L alone lead to an average 2.5-fold expansion of UCB-derived CD34$^+$ HSPCs in 10 days. Remarkably, the addition of osteoblast-EVs significantly increases the number of CD34$^+$ HSPCs by at least two-fold in every UCB donor despite substantial variability among individual donors typical to UCB *ex vivo* expansion. However, EV-treatment does not affect the CD34$^+$ cell frequency demonstrating that the expansion of progenitor cells is accompanied by concomitant differentiation (determined by TNC counts) in both conditions. Growth factor-based expansion culture protocols are often challenged by the difficulty of maintaining human HSPCs *in vitro* due to the fact that the cues to maintain self-renewal and differentiation can only be partially controlled[34,35]. Nonetheless, flow cytometry-based phenotypic HSC and CFU counts demonstrated that EVs also enhance the expansion of the most primitive subset of the progenitor cells compared to the control. Interestingly, we observed similar effects when we started with the sorted immature population. In accordance with cell cycle analyses presented in Chapter 4, we showed that the EVs enhance the division rate of both phenotypic HSCs and CD34$^+$ cells leading to increased proliferation compared to control. These findings clearly demonstrate that despite the accompanied differentiation, EVs stimulate the proliferation and maintenance of HSPCs in short-term cultures. It is therefore critical to test the effect of osteoblast-EVs in the long-term maintenance of the stem cells *in vitro*.

Increasing knowledge on key players of the bone marrow niche, where HSC self-renewal is supported, greatly contributed to the establishment of optimized expansion conditions to promote the proliferation of the stem cells with true self-renewal and full repopulating capacity[36]. Co-cultures with primary or immortalized stromal cells as well as secreted or membrane associated factors support the survival and self-renewal of HSPCs *in vitro*[37-40]. Engineered ligands of Notch pathway, chromatin modifying agents and metals are also used to prevent differentiation and thereby promote large expansion of the repopulating cells[41-43]. Combinatorial screens identified small molecules with promising expansion potential. SR1, a purine derivative that acts as an aryl hydrocarbon receptor antagonist,

has been reported to promote immense expansion of $CD34^+$ cells while maintaining the primitive stem cell pool[27]. Interestingly, the addition of SR1 in our cultures promotes more effective EV-mediated *ex vivo* expansion while maintaining the progenitor cell frequency. Based on these results we speculate that EVs act as a tool to relieve the initial stress of differentiation on HSPCs *in vitro*, most likely by contributing to prolonged survival. Future studies focusing on the discovery of molecules that work cooperatively with osteoblast-EVs are of great importance to develop improved expansion strategies.

Successful HSC transplantation relies on the proper homing of HSPCs with full repopulation capacity to their niches in the bone marrow. Therefore, it is critical that the *ex vivo* expansion cultures do not produce lineage-biased cells. CFU experiments showed that the EV-expanded cells are not skewed into a specific lineage as they have a similar capacity to generate myeloid and erythroid lineages as the control. We then assessed the *in vivo* hematopoietic function of the expanded cell populations by performing transplantations in immunodeficient NSG mice. We demonstrated that important measures, such as engraftment and B-lymphoid lineage reconstituting ability, are not altered as a result of *ex vivo* culture, showing that EV-expanded cells hold the capacity for clonogenicity *in vivo*. Currently, the combination of flow cytometric analysis and the repopulating ability in NSG mice provide the best pre-clinical estimate for the utilization potential of expanded HSPCs. Secondary transplantation experiments are then necessary to provide critical information to determine the long-term multi-lineage repopulation potential of HSPCs for clinical applications in humans.

In conclusion, we propose osteoblast-EVs as novel powerful tools to expand HSPCs for use in regenerative therapy. Based on our findings presented in this chapter, we suggest a role for EVs in HSPC cell proliferation; however, the molecular mechanisms behind EV-mediated expansion still remain to be explored. Proteomic and genomic analyses presented in previous chapters offer a rich osteoblast-EV cargo repository of great value to unravel candidate components that can be modulated to increase expansion capacity that will meet the clinical need.

5.4. MATERIALS AND METHODS

Mice. *In vivo* studies were performed using young NSG mice (8 to 10 weeks old, female). All mice were handled under sterile conditions and housed in ventilated micro-isolation cages with filter tops. Mice were fed *ad libitum*.

Cell cultures. Human osteoblast cells (SV-HFO cells) were cultured for 12-14 days, as described in Chapter 2. UCB-derived $CD34^+$ cells were isolated as described in Chapter 4. Viable $DAPI^-Lin^-CD34^+CD38^{low}CD45RA^{low}CD90^+$ cells were isolated as described previously[44]. 20,000 $CD34^+$ cells and 10,000 $CD34^+CD90^+$ cells were cultured in serum-free Glycostem Basic Growth Medium (GBGM; Glycostem, Oss, the Netherlands) supplement-

ed with SCF (50 ng/ ml, Cellgenix, Freiburg, Germany) and Flt3L (50 ng/ ml, Cellgenix), with or without osteoblast-EVs at 37°C in a humidified atmosphere of 5% CO_2. Cells were refreshed every 2-3 days with fresh culture medium supplemented with newly isolated EVs. In some experiments, TPO (50 ng/ ml; Cellgenix) and SR1 (1μM; Cellagen Technology, San Diego, CA, USA) were added. In some experiments, cells were labeled with CellTrace^{TM} Violet (Thermo Fisher Scientific, Waltham, MA, USA) according to the manufacturer's instructions.

EV isolation. Osteoblast-EVs were isolated from 20 ml conditioned medium as described in Chapter 3. EVs were prepared as 100 μl suspensions, and the amount of experimental EV dose was determined as 5% (v/v).

Flow cytometry. Flow cytometry was used to examine subpopulations of CD34$^+$ cells. Absolute numbers of viable human CD34$^+$ cells were determined by a single platform flow cytometric assay using anti-FITC-CD45, anti-CD34-PE, fluorescence reference counting beads (Beckman Coulter, Fullerton, CA, USA) and DAPI (Sigma Aldrich, St. Louis, MO, USA). The frequencies of human phenotypic HSCs were determined using anti-Lin-FITC, anti-CD38-APC, anti-CD90-PE (eBiosciences, Vienna, Austria), anti-CD34-PE-Cy7, anti-CD45RA-APC-H7 (BD Biosciences, San Jose, CA, USA); and DAPI. Human chimerism in mice blood and bone marrow was determined using anti-mouse CD45-eFluor450, (eBioscience) and anti-human CD45-APC-Cy7 (BioLegend, London, UK). The human lymphoid and myeloid lineages were analyzed by staining with anti-CD19-PE, anti-CD3-APC, anti-CD33-PerCP-eFluor710, anti-CD56-PE-Cy7, and anti-CD15-BV510. All samples were analyzed using BD FACSCantoII (BD Biosciences), and the data was analyzed using FlowJo software (Tree Star, Inc., Ashland, OR, USA).

CFU assays. Suspensions of 300 expanded CD34$^+$ cells in MethoCult™ medium (MethoCult™ GF H4434, Stemcell Technologies, Vancouver, BC, Canada), were incubated in standard culture dishes for 11 days at 37°C in a humidified atmosphere of 5% CO_2. The colonies were counted using an inverted light microscope, and the different lineages were evaluated by morphology.

Transplantation. Transplantation experiments were approved by the Committee on the Ethics of Animal Experiments of the Erasmus University Medical Center, Rotterdam, the Netherlands. NSG mice were sub-lethally irradiated (3 Gy), and intravenously transplanted with the progeny generated from CD34$^+$ cells cultured with or without EVs for 10 days. Peripheral blood was collected at 2 weeks intervals starting at 3 weeks post-transplantation through a small incision in the tail vein. At 21 weeks post-transplantation, the mice were sacrificed by cervical dislocation, and the bone marrow was harvested from the femurs as previously described[45].

Statistics. The results were described as mean ± SD based on at least two independent experiments performed with independent EV isolations and/ or different UCB donors. Significance was calculated using Student's *t*-test and two-way ANOVA test, and *P* values < 0.05 were considered significant.

REFERENCES

1 Kondo, M. *et al.* Biology of hematopoietic stem cells and progenitors: implications for clinical application. *Annu Rev Immunol* **21**, 759-806 (2003).

2 Rocha, V. *et al.* Transplants of umbilical-cord blood or bone marrow from unrelated donors in adults with acute leukemia. *The New England journal of medicine* **351**, 2276-2285 (2004).

3 Brunstein, C. G. *et al.* Allogeneic hematopoietic cell transplantation for hematologic malignancy: relative risks and benefits of double umbilical cord blood. *Blood* **116**, 4693-4699 (2010).

4 Sauvageau, G., Iscove, N. N. & Humphries, R. K. In vitro and in vivo expansion of hematopoietic stem cells. *Oncogene* **23**, 7223-7232 (2004).

5 Walenda, T. *et al.* Synergistic effects of growth factors and mesenchymal stromal cells for expansion of hematopoietic stem and progenitor cells. *Experimental hematology* **39**, 617-628 (2011).

6 Martinez-Agosto, J. A., Mikkola, H. K., Hartenstein, V. & Banerjee, U. The hematopoietic stem cell and its niche: a comparative view. *Genes & development* **21**, 3044-3060 (2007).

7 Su, Y. H., Cai, H. B., Ye, Z. Y. & Tan, W. S. BMP-7 improved proliferation and hematopoietic reconstitution potential of ex vivo expanded cord blood-derived CD34 cells. *Hum Cell* (2014).

8 Taichman, R. S. & Emerson, S. G. Human osteoblasts support hematopoiesis through the production of granulocyte colony-stimulating factor. *The Journal of experimental medicine* **179**, 1677-1682 (1994).

9 Zhang, J. *et al.* Identification of the haematopoietic stem cell niche and control of the niche size. *Nature* **425**, 836-841 (2003).

10 Calvi, L. M. *et al.* Osteoblastic cells regulate the haematopoietic stem cell niche. *Nature* **425**, 841-846 (2003).

11 Visnjic, D. *et al.* Hematopoiesis is severely altered in mice with an induced osteoblast deficiency. *Blood* **103**, 3258-3264 (2004).

12 Pinho, S. *et al.* PDGFRalpha and CD51 mark human nestin+ sphere-forming mesenchymal stem cells capable of hematopoietic progenitor cell expansion. *The Journal of experimental medicine* **210**, 1351-1367 (2013).

13 Greenbaum, A. *et al.* CXCL12 in early mesenchymal progenitors is required for haematopoietic stem-cell maintenance. *Nature* **495**, 227-230 (2013).

14 Varnum-Finney, B., Brashem-Stein, C. & Bernstein, I. D. Combined effects of Notch signaling and cytokines induce a multiple log increase in precursors with lymphoid and myeloid reconstituting ability. *Blood* **101**, 1784-1789 (2003).

15 Arai, F. *et al.* Tie2/angiopoietin-1 signaling regulates hematopoietic stem cell quiescence in the bone marrow niche. *Cell* **118**, 149-161 (2004).

16 Bhatia, M. *et al.* Bone morphogenetic proteins regulate the developmental program of human hematopoietic stem cells. *The Journal of experimental medicine* **189**, 1139-1148 (1999).

17 Ko, K. H. *et al.* GSK-3beta inhibition promotes engraftment of ex vivo-expanded hematopoietic stem cells and modulates gene expression. *Stem cells* **29**, 108-118 (2011).

18 Morhayim, J., Baroncelli, M. & van Leeuwen, J. P. Extracellular vesicles: specialized bone messengers. *Archives of biochemistry and biophysics* **561**, 38-45 (2014).

19 Raposo, G. & Stoorvogel, W. Extracellular vesicles: exosomes, microvesicles, and friends. *J Cell Biol* **200**, 373-383 (2013).
20 Thery, C., Ostrowski, M. & Segura, E. Membrane vesicles as conveyors of immune responses. *Nat Rev Immunol* **9**, 581-593 (2009).
21 De Jong, O. G., Van Balkom, B. W., Schiffelers, R. M., Bouten, C. V. & Verhaar, M. C. Extracellular vesicles: potential roles in regenerative medicine. *Front Immunol* **5**, 608 (2014).
22 Yuan, A. *et al.* Transfer of microRNAs by embryonic stem cell microvesicles. *PloS one* **4**, e4722 (2009).
23 Chen, T. S. *et al.* Mesenchymal stem cell secretes microparticles enriched in pre-microRNAs. *Nucleic acids research* **38**, 215-224 (2010).
24 Nair, R. *et al.* Extracellular vesicles derived from preosteoblasts influence embryonic stem cell differentiation. *Stem cells and development* **23**, 1625-1635 (2014).
25 Quesenberry, P. J. & Aliotta, J. M. The paradoxical dynamism of marrow stem cells: considerations of stem cells, niches, and microvesicles. *Stem cell reviews* **4**, 137-147 (2008).
26 Ratajczak, J. *et al.* Embryonic stem cell-derived microvesicles reprogram hematopoietic progenitors: evidence for horizontal transfer of mRNA and protein delivery. *Leukemia* **20**, 847-856 (2006).
27 Boitano, A. E. *et al.* Aryl hydrocarbon receptor antagonists promote the expansion of human hematopoietic stem cells. *Science* **329**, 1345-1348 (2010).
28 Goff, J. P., Shields, D. S. & Greenberger, J. S. Influence of cytokines on the growth kinetics and immunophenotype of daughter cells resulting from the first division of single CD34(+)Thy-1(+)lin- cells. *Blood* **92**, 4098-4107 (1998).
29 Ivanovic, Z. *et al.* Clinical-scale cultures of cord blood CD34(+) cells to amplify committed progenitors and maintain stem cell activity. *Cell transplantation* **20**, 1453-1463 (2011).
30 Murray, L. J. *et al.* Thrombopoietin, flt3, and kit ligands together suppress apoptosis of human mobilized CD34+ cells and recruit primitive CD34+ Thy-1+ cells into rapid division. *Experimental hematology* **27**, 1019-1028 (1999).
31 Mayani, H., Dragowska, W. & Lansdorp, P. M. Characterization of functionally distinct subpopulations of CD34+ cord blood cells in serum-free long-term cultures supplemented with hematopoietic cytokines. *Blood* **82**, 2664-2672 (1993).
32 Wagers, A. J. The stem cell niche in regenerative medicine. *Cell stem cell* **10**, 362-369 (2012).
33 Curti, A., Fogli, M., Ratta, M., Tura, S. & Lemoli, R. M. Stem cell factor and FLT3-ligand are strictly required to sustain the long-term expansion of primitive CD34+DR- dendritic cell precursors. *J Immunol* **166**, 848-854 (2001).
34 Glettig, D. L. & Kaplan, D. L. Extending human hematopoietic stem cell survival in vitro with adipocytes. *BioResearch open access* **2**, 179-185 (2013).
35 Hofmeister, C. C., Zhang, J., Knight, K. L., Le, P. & Stiff, P. J. Ex vivo expansion of umbilical cord blood stem cells for transplantation: growing knowledge from the hematopoietic niche. *Bone marrow transplantation* **39**, 11-23 (2007).
36 Lund, T. C., Boitano, A. E., Delaney, C. S., Shpall, E. J. & Wagner, J. E. Advances in umbilical cord blood manipulation-from niche to bedside. *Nature reviews. Clinical oncology* **12**, 163-174 (2015).

37 Fei, X. M. *et al.* Co-culture of cord blood CD34(+) cells with human BM mesenchymal stromal cells enhances short-term engraftment of cord blood cells in NOD/SCID mice. *Cytotherapy* **9**, 338-347 (2007).

38 Himburg, H. A. *et al.* Pleiotrophin regulates the expansion and regeneration of hematopoietic stem cells. *Nat Med* **16**, 475-482 (2010).

39 Renstrom, J. *et al.* Secreted frizzled-related protein 1 extrinsically regulates cycling activity and maintenance of hematopoietic stem cells. *Cell stem cell* **5**, 157-167 (2009).

40 Zhang, C. C., Kaba, M., Iizuka, S., Huynh, H. & Lodish, H. F. Angiopoietin-like 5 and IGFBP2 stimulate ex vivo expansion of human cord blood hematopoietic stem cells as assayed by NOD/SCID transplantation. *Blood* **111**, 3415-3423 (2008).

41 Delaney, C. *et al.* Notch-mediated expansion of human cord blood progenitor cells capable of rapid myeloid reconstitution. *Nat Med* **16**, 232-236 (2010).

42 Walasek, M. A. *et al.* The combination of valproic acid and lithium delays hematopoietic stem/progenitor cell differentiation. *Blood* **119**, 3050-3059 (2012).

43 Araki, H. *et al.* Expansion of human umbilical cord blood SCID-repopulating cells using chromatin-modifying agents. *Experimental hematology* **34**, 140-149 (2006).

44 Duinhouwer, L. E. *et al.* Wnt3a protein reduces growth factor-driven expansion of human hematopoietic stem and progenitor cells in serum-free cultures. *PloS one* **10**, e0119086 (2015).

45 Delhanty, P. J. *et al.* Genetic manipulation of the ghrelin signaling system in male mice reveals bone compartment specificity of acylated and unacylated ghrelin in the regulation of bone remodeling. *Endocrinology* **155**, 4287-4295 (2014).

6 Identification of Hematopoietic Regulatory Networks Controlled by Osteoblast-Derived Extracellular Vesicles

by

Jess Morhayim, Jeroen van de Peppel, Eric Braakman, Amel Dudakovic, Hideki Chiba, Andre J. van Wijnen, Jan J. Cornelissen, and Johannes P. van Leeuwen

In Progress

Cells communicate with each other by secreting extracellular vesicles (EVs) as carriers of regulatory information in forms of proteins, RNA and lipids. Osteoblasts secrete EVs that play a role in hematopoiesis by stimulating the proliferation of hematopoietic stem and progenitor cells (HSPCs). Here, we performed next-generation sequencing to study the effects of osteoblast-EVs on the transcriptome of human umbilical cord-derived $CD34^+$ HSPCs. We identified 33 significantly regulated HSPC genes, including genes with known roles in HSPC cell proliferation. Using an integrative bioinformatics approach, we connected the gene expression data with our previously identified protein, messenger RNA (mRNA) and microRNA (miRNA) content of osteoblast-EVs to delineate the potentially targeted biological functions/ pathways during HSPC proliferation. Our analyses reveal a set of candidate EV components, such as signaling proteins, cell cycle related mRNAs and miRNAs involved in HSPC self-renewal. In conclusion, our findings demonstrate that osteoblast-EVs affect the gene expression of HSPCs, and the transcriptome data in combination with bioinformatics analyses serve as a useful resource to unveil the fundamental roles of EVs in HSPC-osteolineage-cell crosstalk.

.

6.1. INTRODUCTION

The secretion of extracellular vesicles (EVs) is an evolutionarily conserved form of communication among cells. All living cells secrete EVs selectively packaged with regulatory cargo necessary to alter the function of their target cells[1-4]. Proteomic, transcriptomic and lipidomic analyses allowed the elucidation of biologically relevant EV cargo from diverse types of cells and biological fluids[5-11]. Advancement of systematic and comprehensive studies further helped us understand the role of EV cargo in various biological functions.

Hematopoietic stem cells (HSCs) have the capacity to self-renew and replenish the entire blood system in a tightly regulated manner. Properly controlled gene expression ensures to maintain a fine balance between the number of stem cells and their differentiated progeny[12,13]. Hematopoiesis is mainly restricted to the unique favorable microenvironment provided by the bone tissue in adult humans[14]. Among many others, osteolineage cells are one of the main bone residents that provide essential regulatory and stimulatory signals critical to support survival and differentiation of hematopoietic stem and progenitor cells (HSPCs)[15-21]. In Chapter 5, we showed that human osteoblasts secrete EVs that stimulate the growth and expansion of human umbilical cord blood (UCB)- derived $CD34^+$ HSPCs *in vitro*. We speculate that the selective EV cargo is responsible for the interaction between osteoblasts and HSPCs. If osteoblast-derived EVs are indeed important regulators of HSPC-osteolineage-cell crosstalk, then exploring the biological pathways that are stimulated by EVs is critical to understand the complexity of the molecular programs underlying HSPC cell proliferation.

In this chapter, we used bioinformatics analytical tools to gain a comprehensive insight into the molecular mechanism of EV action in HSPC fate regulation. Initially, we studied the effect of osteoblast-EVs on the gene expression of UCB-derived $CD34^+$ HSPCs by next-generation sequencing. Next, we used our previously characterized EV cargo datasets and employed comprehensive integrative bioinformatics analyses to define/ propose biological pathways that are dynamically regulated by EV cargo[11]. The proteogenomics approach used in this study is a valuable tool to identify powerful EV cargo candidates, which can be used as potential therapeutic agents.

6.2. RESULTS

6.2.1. Osteoblast-EVs alter the gene expression of $CD34^+$ HSPCs

In this study, we investigated the effect of EVs isolated from human osteoblasts (SV-HFOs) on the gene expression of human UCB-derived $CD34^+$ HSPCs. We performed next-generation sequencing to define the alterations on the transcriptome profiling of $CD34^+$ cells after 24 hours treatment with osteoblast-EVs. To ensure that the genetic differ-

ences are less likely due to different cellular composition at the time of RNA isolation, we verified that cells did not lose their CD34$^+$ phenotype after 24 hours of culture with or without EVs (Fig. **1**). Osteoblast-EV treatment does not alter the expression of the majority of the CD34$^+$ HSPC genes (Fig. **2A**). We identified a small percentage (2.3%) of expressed genes that are exclusively detected or absent in EV-treated cells (Fig. **2B**). Interestingly, these are mostly genes encoding for glycoproteins (108 out of 294 genes) suggesting a link to cell adhesion and signalling. We identified 33 known CD34$^+$ HSPC genes, of which 17 genes are up-regulated and 16 genes down-regulated more than 1.5-fold ($P < 0.05$) by osteoblast-EVs compared to the control (Fig. **2C**, Table **1**).

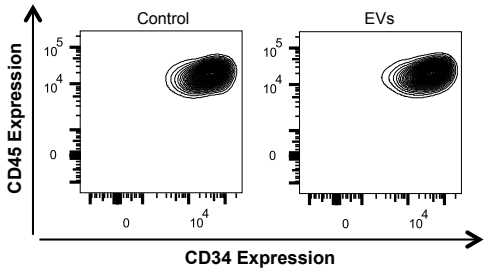

Figure 1. Phenotypic analysis of osteoblast-EV-treated CD34$^+$ HSPCs.
Flow cytometry plots show the expression of CD45 and CD34 after 24 hours culture in the absence (control, *left panel*) and presence (*right panel*) of osteoblast-EVs.

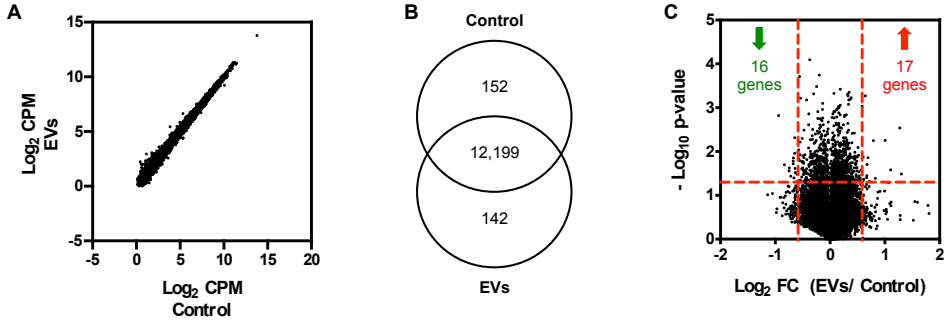

Figure 2. Osteoblast-EVs alter the expression of CD34$^+$ HSPC genes. A) Scatter plot shows the strong correlation (R^2: 0.9882) of normalized read counts (average counts per million, CPM) between the expressions of CD34$^+$ HSPC genes after 24 hours culture in the absence (control) and presence of osteoblast-EVs (N = 2). B) Venn diagram indicates the distribution of CD34$^+$ HSPC transcripts between control and EV treatment groups. C) Volcano plot (significance versus fold change) shows the CD34$^+$ HSPC genes that are significantly ($P < 0.05$, compared with control by Student's *t*-test) regulated in response to osteoblast-EVs by at least 1.5-fold. Numbers in brackets denote the number of up-regulated (red, 17 genes) and down-regulated (green, 16 genes). FC, fold change.

Next, we analyzed the patterns of change in the expression levels of the 33 regulated CD34$^+$ HSPC genes between control and EV-treated cells compared to the expression levels at the starting time-point (t: 0). We identified four different expression profiles: en-

hanced up-regulation (Fig. **3A**), lowered up-regulation (Fig. **3B**), enhanced down-regulation (Fig. **3C**), and lowered down-regulation (Fig. **3D**) of endogenous (control) gene expression as a response to EV-treatment in 24 hours. For the majority of the genes, EV-treatment enhances the endogenous up- or down-regulation (Fig. **3A & 3C**). For a small number of genes, however, osteoblast-EVs alter gene expression by lowering the extent of endogenous up-regulation of *MAOA* and *NFIB* and *TGFB1I1* (Fig. **3B**), and down-regulation of *BCL3*, *PHLDB2*, *PIM1* and *S100A9* (Fig. **3D**).

Table 1. The list of $CD34^+$ HSPC genes significantly ($P < 0.05$) up- or down-regulated (≥ 1.5-fold) in response to osteoblast-EV treatment for 24 hours.

Up-regulated		**Down-regulated**	
Gene Symbols	**Fold Change**	**Gene Symbols**	**Fold Change**
ABI3	2.47	*ITGAX*	-1.92
GLYATL2	2.42	*NFIB*	-1.78
PAQR5	2.15	*SLC15A1*	-1.68
S100A9	2.01	*HIST1H2AL*	-1.67
PIM1	1.78	*TGFB1I1*	-1.64
FAM64A	1.73	*NSUN7*	-1.60
PTRH1	1.65	*CYSLTR2*	-1.59
MAP3K6	1.62	*DYNC2H1*	-1.58
DUSP3	1.60	*FAT4*	-1.57
SPR	1.60	*EGR1*	-1.56
C7orf10	1.59	*OVGP1*	-1.55
BCL3	1.56	*ZNF286B*	-1.55
MRPL27	1.53	*ABCA10*	-1.52
PRTFDC1	1.52	*DUSP8*	-1.51
PHLDB2	1.52	*MAOA*	-1.51
ANKRD35	1.50	*CYP2W1*	-1.50
CACNA1H	1.50		

According to Gene Ontology analysis the 33 regulated genes are mostly ($P < 0.05$) annotated to MAPK signalling pathway (*CACNA1H*, *DUSP3*, *DUSP8*, *MAP3K6*). Further investigation using Ingenuity Pathway Analysis (IPA) indicates that EVs modulate the expression of $CD34^+$ HSPC genes mostly annotated ($P < 0.05$) to cellular development, cellular growth and proliferation, cell-to-cell signaling and interaction, small molecule biochemistry and cell cycle. Molecular and cellular functions annotated to these genes are listed in Table **2**. A set of genes, including *BCL3*, *EGR1*, *ITGAX*, *CYSLTR2*, *PIM1* and *S100A9*, are of particular interest as they are mainly related to the expansion of blood cells, in accordance with our results presented in Chapter 5. We confirmed the differential expression of selected genes by qPCR as shown in Figure **4**. Despite the donor-related variation, on average gene expression is in the same direction as determined by sequencing for all the tested

genes. These findings showed that osteoblast-EVs are capable of altering the expression pattern of cellular growth-related CD34$^+$ HSPC genes, supporting our previous studies reporting the proliferative effect of EV cargo.

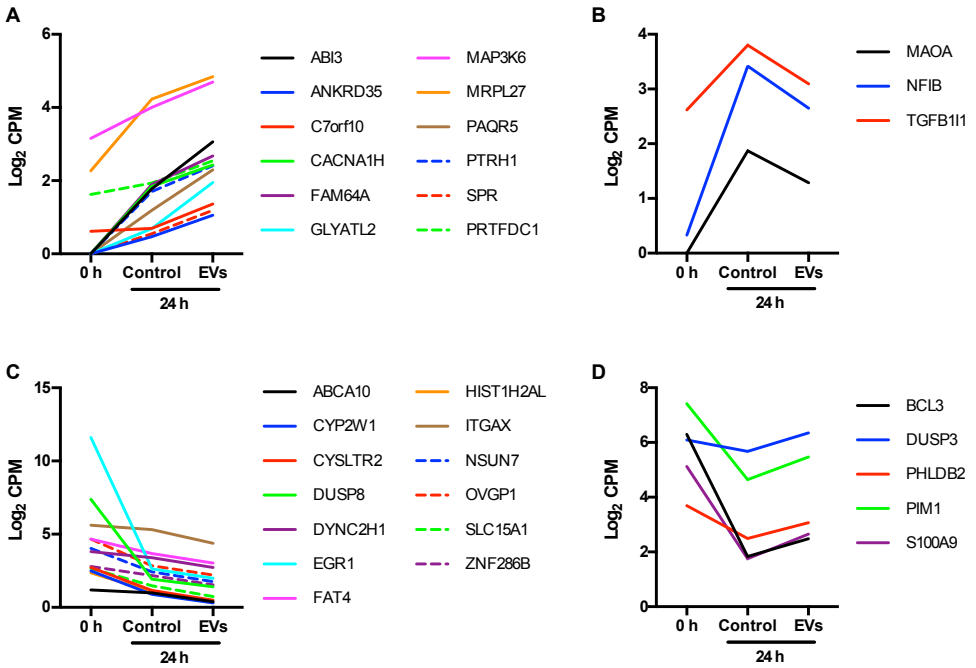

Figure 3. Expression profiles of differentially expressed CD34$^+$ HSPC genes. A-C) Expression profiles show the temporal pattern of gene expression defined by normalized read counts (CPM). Osteoblast-EVs enhance the (A) up-regulation and (C) down-regulation of CD34$^+$ HSPC genes by control alone in 24 hours. EVs lower the control-induced (B) up-regulation and (D) down-regulation of CD34$^+$ HSPC genes by control alone in 24 hours.

Table 2. The list of the osteoblast-EV-regulated CD34$^+$ HSPC genes significantly ($P < 0.05$) annotated to representative molecular and cellular functions.

Molecular and Cellular Functions	# Genes	Gene Symbols
Cellular development	11	*BCL3*, *CACNA1H*, *CYSLTR2*, *DUSP8*, *EGR1*, *ITGAX*, *MAOA*, *NFIB*, *PIM1*, *S100A9*, *TGFB1I1*
Cellular growth and proliferation	10	*BCL3*, *CYSLTR2*, *DUSP8*, *EGR1*, *ITGAX*, *MAOA*, *NFIB*, *PIM1*, *S100A9*, *TGFB1I1*
Cell-to-cell signaling and interaction	10	*BCL3*, *CYSLTR2*, *DUSP3*, *EGR1*, *ITGAX*, *MAOA*, *PIM1*, *S100A9*, *SPR*, *TGFB1I1*
Small molecule biochemistry	7	*BCL3*, *CACNA1H*, *CYSLTR2*, *EGR1*, *MAOA*, *SPR*, *TGFB1I1*
Cell cycle	3	*BCL3*, *EGR1*, *PIM1*

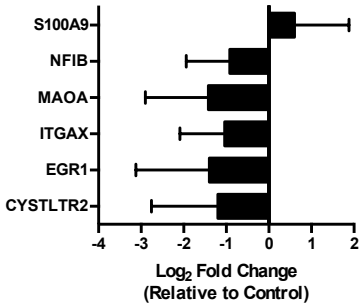

Figure 4. Verification of differentially expressed CD34$^+$ HSPC genes by qPCR. Expression levels (mean ± SD) of selected CD34$^+$ HSPC genes after 24 hours of incubation in the presence of osteoblast-EVs (N = 3). Fold change is determined compared to control and normalized to average *GAPDH* expression. The donors used for qPCR analysis are different than the ones used for mRNA sequencing.

6.2.2. Candidate key molecular players of EV function

To investigate the molecular basis of EV-mediated gene regulation in CD34$^+$ HSPCs we correlated the cargo of osteoblast-EVs to the EV-regulated CD34$^+$ HSPC genes using an integrative bioinformatics approach. We used IPA to build a network showing the tentative direct molecular relationships between the EV cargo, such as protein, messenger RNA (mRNA) and microRNA (miRNA), and the regulated CD34$^+$ HSPC genes (Fig. **5**). It is important to note that, here we only considered the highly abundant EV-miRNAs and EV-mRNAs with normalized read counts above 100, and correlated the EV-miRNAs only to the down-regulated CD34$^+$ HSPC genes. More than half (19 out of the 33) of the EV-regulated CD34$^+$ HSPC genes are mapped with a small number (68 out of 980) of EV-proteins. 11 genes are mapped with 16 (out of 809) EV-mRNAs, and 14 down-regulated genes are mapped with 65 (out of 185) EV-miRNAs. Overall, *NFIB* and *EGR1* are the CD34$^+$ HSPC genes targeted by the highest number of EV cargo. While, *NFIB* is targeted mostly by EV-miRNAs (36 miRNAs and 1 mRNA), *EGR1* shows interaction with at least one biomolecule of each cargo type (12 proteins, 8 miRNAs and 4 mRNAs).

The mapped EV-proteins are mostly annotated to EV markers (ANXA2, HSP90AA1, ITGB1, YWHAZ, BSG), as well as proteins involved in cell cycle (HDAC2, SFN, MAPK1) and protein transport (AP2A1, CLTA, IPO7). The EV-proteins interact predominantly with *EGR1* and *S100A9*. The small group of mapped EV-mRNAs consists of genes mostly encoding proteins annotated to cell cycle (CDC20, CDKN1A/2A, UBC), and interacts predominantly with *PIM1*. *NFIB*, on the other hand, is the most common putative target of the EV-miRNAs. Remarkably, a significant number (16 out of 65) of the mapped EV-miRNAs are among the highly enriched EV-miRNAs speculated to exert most of EV-miRNA-mediated functional effect, as described in Chapter 4. These also include the known regulators of hematopoiesis, such as miR23a-3p, miR-29a-3p and miR-181a-5p.

Combined analysis of the mapped EV cargo indicates that cell cycle, as well as related processes, such as proliferation, are strongly overrepresented in EVs. Particularly, a sizeable set of EV cargo is annotated to the proliferation of blood cells and showed interac-

tion with the above-mentioned six HSPC genes (*BCL3*, *EGR1*, *ITGAX*, *CYSLTR2*, *PIM1*, *S100A9*) with known roles in proliferation during hematopoietic development. These EV components consist of interesting EV-proteins, including signaling proteins (CAV1, CDC42, CTNBB1, PRKCB, STAT1, SFN), DNA-binding proteins (HMGA1, HNRNPA2B1), transporters (SLC3A2) and inflammatory cytokines (MIF), which predominantly interact with *EGR1* and *S100A9*.

We also evaluated the horizontal transfer of EV-mRNAs between osteoblasts and $CD34^+$ HSPCs. First, we questioned whether the increased expression levels of the HSPC genes are due to the accumulation of EV-mRNA inside HSPCs after 24 hours of treatment with osteoblast-EVs. Interestingly, none of the up-regulated HSPC genes are among the significantly ($P < 0.05$) enriched ($\geq$ two-fold) EV-mRNAs reported in Chapter 3. This holds true also for the down-regulated HSPC genes. Then, we checked the expression profiles of the top 10 enriched EV-mRNAs in $CD34^+$ HSPCs (Fig. **6A**). Remarkably, *RAB13* shows a trend for down-regulation upon EV treatment, which was also confirmed by qPCR analysis (Fig. **6B**). Comparison with the expression levels at the starting time-point (0 h) indicates that EV treatment lowers the endogenous up-regulation of *RAB13* in 24 hours. *In silico* analysis, using TargetScan algorithms, revealed that *RAB13* is the predicted target of EV-miRNAs, such as miR-19a-3p, miR-19b-3p and miR-194-5p, which might have key roles in the down-regulation of *RAB13*. Together these analyses link the EV cargo to the regulation of $CD34^+$ HSPC gene expression, enabling valuable insights into the molecular complexity of EV-mediated HSPC-osteolineage-cell crosstalk.

6.3. DISCUSSION

The findings described in this chapter demonstrate that osteoblast-EVs regulate expression of $CD34^+$ HSPC genes encoding for proteins particularly important for proliferation and cell cycle. Using integrative bioinformatics we unified our osteoblast-EV cargo repositories with $CD34^+$ HSPC sequencing data for the extraction of critical knowledge towards deeper understanding of the underlying key players and molecular mechanisms of EV-mediated HSPC-osteolineage-cell crosstalk.

A tightly regulated transcriptional program plays a major role in defining the different stages of hematopoiesis. In previous chapters, we showed the effect of osteoblast-EVs on HSPC proliferation and expansion *in vitro*. Here, we investigated the molecular mechanisms by which EVs may affect the gene expression of $CD34^+$ HSPCs in the early steps of hematopoiesis. In accordance with our previous functional studies, the differentially expressed HSPC genes are mostly annotated to cell growth related processes, Moreover, some of the genes are also annotated to MAPK pathway, which has recently been demonstrated to play a key role in the regulation of HSPC self-renewal and homeostasis[22]. An important study by Oostendorp and colleagues showed that hematopoietic growth factor-

driven stimulation of UCB-derived cells activates MAPK signaling and rapidly induces proliferation[23].

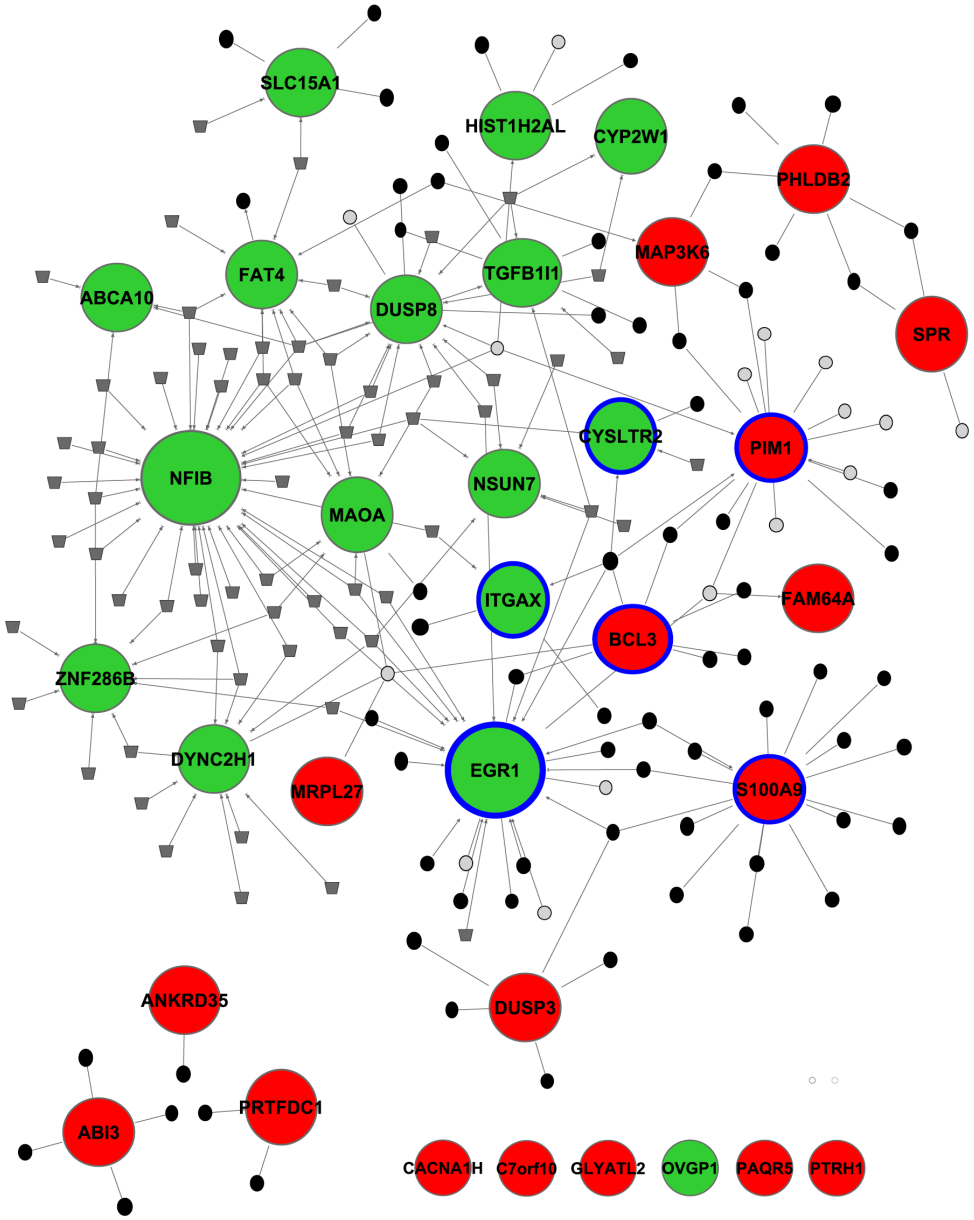

Figure 5. IPA network showing the direct relationship maps between the EV-cargo and 33 EV-regulated CD34$^+$ HSPC genes. Green, down-regulated CD34$^+$ HSPC genes; red, up-regulated CD34$^+$ HSPC genes; black circles, EV-proteins; grey circles, EV-mRNAs; dark grey trapezoids, EV-miRNAs. CD34$^+$ HSPC genes with known roles in proliferation during hematopoietic development are highlighted with blue lines.

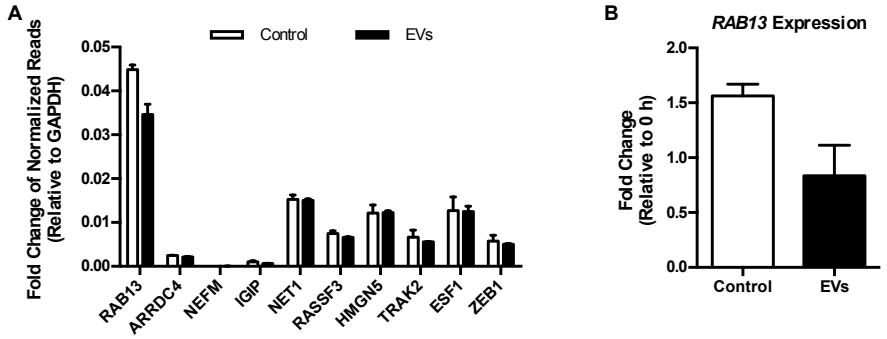

Figure 6. Expression profiles of CD34$^+$ HSPCs mRNAs specifically enriched in osteoblast-EVs. A) Expression profiles of top 10 enriched EV-mRNAs in CD34$^+$ HSPCs. Expression levels are shown as average fold change of normalized reads (RPKM) relative to *GAPDH* (N = 3). B) Relative expression of *RAB13* in CD34$^+$ HSPCs in the absence (control) and presence of EVs using qPCR (N = 2). Expression levels are relative to the starting time-point (0 h) and normalized to average *GAPDH* expression. The donors used for qPCR analysis are different than the ones used for mRNA sequencing.

UCB-based stem cell therapies rely on the development of protocols that support robust expansion of immature stem cells in culture. In recent years, studies reported the use of various hematopoietic factors that improve *ex vivo* expansion mainly via regulating the expression patterns of key players of HSPC self-renewal[24-26]. Interestingly, osteoblast-EV treatment alters the expression of such genes (*BCL3*, *EGR1*, *ITGAX*, *CYSLTR2*, *PIM1*, *S100A9*) with important roles in the regulation of proliferation of HSPCs. Recent reports showed that *S100A9* expression is up-regulated during HSC maturation. Here, *S100A9* levels are down-regulated by osteoblast-EVs, suggestive of an effort for EVs to maintain the cells in more immature state[27]. *EGR1*, on the other hand, encodes for a transcription factor that plays a key role in the regulation of hematopoietic homeostasis. Previous studies showed that *EGR1* levels are high in quiescent cells and they are dramatically down-regulated upon cell division[28]. Accordingly, we demonstrate that *EGR1* levels drop after 24 hours as the HSPCs progress into cell cycle. Interestingly, the down-regulation is further enhanced in the presence of EVs most likely due to the ability of EVs to drive the cell division kinetics of HSPCs.

Despite increasing evidence reporting single factors that influence cell fate decisions, it is indisputable that complex transcriptional regulatory networks are the key players. The remarkable power of active sorting mechanism renders EVs with unique combinations of EV cargo that act in concert to modulate the expression levels of their target genes. Understanding the role of EVs in hematopoiesis, therefore, requires unraveling the way EV regulators interact with each other to regulate transcriptional networks. Thanks to the rapid rise of high-throughput technologies we formed comprehensive osteoblast-EV cargo repositories useful to delineate a specific set of candidate components that give insights into the biological functions. Using an integrative bioinformatics approach, we investigated the tentative molecular relationships between the EV cargo and the regulated HSPC genes con-

trolling proliferation and cell cycle. Surprisingly, the above-mentioned genes with known roles in the proliferation of blood cells are among the predominantly targeted HSPC genes, such as *EGR1*, *S100A9* and *PIM1*. In particular, the targeting EV-proteins mainly consist of an interesting set of signaling proteins, including STAT1, CTNBB1 and CDC42, as potential candidates for further investigation[29-33]. Moreover, *NFIB* is the target of the majority of EV-miRNAs. The down-regulation of *NFIB* has been shown to be critical during the transition of the immature HSCs to the multipotent progenitors[34]. In previous chapters, we demonstrated that osteoblast-EVs stimulate the expansion of the progenitor cells while maintaining the immature stem cell pool. Although it is tempting to speculate a role for *NFIB* targeting in the expansion of the progenitors, further functional studies are needed to investigate the detailed molecular mechanisms.

In Chapter 3, we demonstrated that *RAB13* mRNA is exceptionally highly abundant in osteoblast-EVs compared to the parental cells suggestive of an essential role in EV-mediated communication. Contrary to increasing evidence reporting the detection of a variety of EV-mRNAs in the target cells[35,36]; it is striking to discover the down-regulation of the most enriched osteoblast-EV-mRNA in HSPCs upon EV treatment. We speculate that the alteration of *RAB13* in HSPCs is most likely connected to other osteoblast cargo, such as miRNAs. However, we cannot rule out the possibility of EV-mRNA in regulating gene expression in the target cell via an alternative biological mechanism. There are studies reporting that EVs contain the 3'-untranslated regions of certain mRNAs to protect the target mRNA from miRNA degradation[37]. As well, EV-mRNAs may function by stimulating cellular mRNA degradation by protecting the EV-miRNAs until they reach their target mRNAs in the recipient cells. Furthermore, the biological function of *RAB13* down-regulation in HSPCs still remains to be explored. Network analysis in Chapter 3 suggested a role for *RAB13* in proliferation of blood cells, which requires further investigation in the context of EV-mediated crosstalk between HSPCs and osteolineage cells.

In conclusion, in this chapter we present an extensive valuable resource for the functional exploration of EV-mediated regulation of HSPC-osteolineage crosstalk. We identified critical EV-driven molecular mechanisms that trigger transcriptional programs and signaling cascades that define HSPC proliferation. However, it is still challenging to assess the extent to which individual or combinations of cargo contribute to these effects. Elucidating the precise molecular functions regulated by osteoblast-EV cargo is promising to provide the basis for the development of effective stem cells therapies.

6.4. MATERIALS AND METHODS

Cell cultures and EV isolation. Human osteoblast cells (SV-HFO cells) were cultured for 12-14 days, and EVs were isolated from the conditioned medium using the SW32Ti rotor (Beckman Coulter, Fullerton, CA, USA) as described in Chapter 2[11]. EVs were prepared as 100 µl suspensions, and the amount of experimental EV dose was determined as 5% (v/v).

UCB-derived $CD34^+$ HSPCs were isolated as described in Chapter 4[38]. The purity of the $CD34^+$ HSPCs was verified using BD FACSCantoII (BD Biosciences) flow cytometer as described in Chapter 4. 20,000 $CD34^+$ cells were cultured in serum-free Glycostem Basic Growth Medium (GBGM; Glycostem, Oss, the Netherlands) supplemented with SCF (50 ng/ ml, Cellgenix, Freiburg, Germany) and Flt3L (50 ng/ ml, Cellgenix), with or without osteoblast-EVs at 37°C in a humidified atmosphere of 5% CO_2 for 24 hours.

RNA isolation and quantitative real-time PCR. RNA from $CD34^+$ cells was isolated using NucleoSpin RNA XS kit (Macherey-Nagel, Duren, Germany) according to the manufacturer's instructions. RNA concentration was determined using Nanodrop (Thermo Fisher Scientific, Waltham, MA, USA) and size distribution was checked on an Agilent Bioanalyzer RNA 6000 Nano chip (Thermo Fisher Scientific). Quantitative real-time PCR were performed using the SYBR™ Green kit (Eurogentec, Seraing, Belgium) according to the manufacturer's instructions. The primer sequences are listed in Appendix C.

Next-generation sequencing and bioinformatic analysis. RNA sequencing and bioinformatic analysis was performed as described in Chapter 3[39]. Normalization of the read counts was performed using edgeR 2.6.2. DAVID Bionformatics Resources v6.7 was used to categorize the proteins into overrepresented GO annotations using the human expression dataset as a background[40,41]. IPA (Ingenuity® Systems. www.ingenuity.com) was used to predict target pathways and analyze the interaction between EV cargo and $CD34^+$ HSPC genes using the path explorer tool in My Pathway analysis. TargetScan (Release 7.0) was used for miRNA target prediction analysis.

Statistics. The results were described as mean ± SD based on at least two independent experiments performed with independent EV isolations and/ or different UCB donors. Significance was calculated using Student's *t*-test, and P values < 0.05 were considered significant.

REFERENCES

1 Raposo, G. & Stoorvogel, W. Extracellular vesicles: exosomes, microvesicles, and friends. *J Cell Biol* **200**, 373-383 (2013).

2 Colombo, M., Raposo, G. & Thery, C. Biogenesis, secretion, and intercellular interactions of exosomes and other extracellular vesicles. *Annu Rev Cell Dev Biol* **30**, 255-289 (2014).

3 Yanez-Mo, M. *et al.* Biological properties of extracellular vesicles and their physiological functions. *J Extracell Vesicles* **4**, 27066 (2015).

4 Morhayim, J., Baroncelli, M. & van Leeuwen, J. P. Extracellular vesicles: specialized bone messengers. *Archives of biochemistry and biophysics* **561**, 38-45 (2014).

5 Kreimer, S. *et al.* Mass-spectrometry-based molecular characterization of extracellular vesicles: lipidomics and proteomics. *J Proteome Res* **14**, 2367-2384 (2015).

6 van Balkom, B. W., Eisele, A. S., Pegtel, D. M., Bervoets, S. & Verhaar, M. C. Quantitative and qualitative analysis of small RNAs in human endothelial cells and exosomes provides insights into localized RNA processing, degradation and sorting. *J Extracell Vesicles* **4**, 26760 (2015).

7 Nolte-'t Hoen, E. N. *et al.* Deep sequencing of RNA from immune cell-derived vesicles uncovers the selective incorporation of small non-coding RNA biotypes with potential regulatory functions. *Nucleic acids research* **40**, 9272-9285 (2012).

8 Huang, X. *et al.* Characterization of human plasma-derived exosomal RNAs by deep sequencing. *BMC genomics* **14**, 319 (2013).

9 Subra, C., Laulagnier, K., Perret, B. & Record, M. Exosome lipidomics unravels lipid sorting at the level of multivesicular bodies. *Biochimie* **89**, 205-212 (2007).

10 Hegmans, J. P. *et al.* Proteomic analysis of exosomes secreted by human mesothelioma cells. *Am J Pathol* **164**, 1807-1815 (2004).

11 Morhayim, J. *et al.* Proteomic signatures of extracellular vesicles secreted by nonmineralizing and mineralizing human osteoblasts and stimulation of tumor cell growth. *FASEB journal : official publication of the Federation of American Societies for Experimental Biology* **29**, 274-285 (2015).

12 Zhu, J. & Emerson, S. G. Hematopoietic cytokines, transcription factors and lineage commitment. *Oncogene* **21**, 3295-3313 (2002).

13 Liu, X. L., Yuan, J. Y., Zhang, J. W., Zhang, X. H. & Wang, R. X. Differential gene expression in human hematopoietic stem cells specified toward erythroid, megakaryocytic, and granulocytic lineage. *Journal of leukocyte biology* **82**, 986-1002 (2007).

14 Taichman, R. S. Blood and bone: two tissues whose fates are intertwined to create the hematopoietic stem-cell niche. *Blood* **105**, 2631-2639 (2005).

15 Calvi, L. M. *et al.* Osteoblastic cells regulate the haematopoietic stem cell niche. *Nature* **425**, 841-846 (2003).

16 Zhu, J. *et al.* Osteoblasts support B-lymphocyte commitment and differentiation from hematopoietic stem cells. *Blood* **109**, 3706-3712 (2007).

17 Visnjic, D. *et al.* Hematopoiesis is severely altered in mice with an induced osteoblast deficiency. *Blood* **103**, 3258-3264 (2004).

18 Taichman, R. S. & Emerson, S. G. Human osteoblasts support hematopoiesis through the production of granulocyte colony-stimulating factor. *The Journal of experimental medicine* **179**, 1677-1682 (1994).

19 Zhang, J. *et al.* Identification of the haematopoietic stem cell niche and control of the niche size. *Nature* **425**, 836-841 (2003).

20 Pinho, S. *et al.* PDGFRalpha and CD51 mark human nestin+ sphere-forming mesenchymal stem cells capable of hematopoietic progenitor cell expansion. *The Journal of experimental medicine* **210**, 1351-1367 (2013).
21 Greenbaum, A. *et al.* CXCL12 in early mesenchymal progenitors is required for haematopoietic stem-cell maintenance. *Nature* **495**, 227-230 (2013).
22 Geest, C. R. & Coffer, P. J. MAPK signaling pathways in the regulation of hematopoiesis. *Journal of leukocyte biology* **86**, 237-250 (2009).
23 Oostendorp, R. A. *et al.* Oncostatin M-mediated regulation of KIT-ligand-induced extracellular signal-regulated kinase signaling maintains hematopoietic repopulating activity of Lin-CD34+CD133+ cord blood cells. *Stem cells* **26**, 2164-2172 (2008).
24 Walenda, T. *et al.* Synergistic effects of growth factors and mesenchymal stromal cells for expansion of hematopoietic stem and progenitor cells. *Experimental hematology* **39**, 617-628 (2011).
25 Sauvageau, G., Iscove, N. N. & Humphries, R. K. In vitro and in vivo expansion of hematopoietic stem cells. *Oncogene* **23**, 7223-7232 (2004).
26 Ko, K. H. *et al.* GSK-3beta inhibition promotes engraftment of ex vivo-expanded hematopoietic stem cells and modulates gene expression. *Stem cells* **29**, 108-118 (2011).
27 Kerkhoff, C. *et al.* Binding of two nuclear complexes to a novel regulatory element within the human S100A9 promoter drives the S100A9 gene expression. *The Journal of biological chemistry* **277**, 41879-41887 (2002).
28 Min, I. M. *et al.* The transcription factor EGR1 controls both the proliferation and localization of hematopoietic stem cells. *Cell stem cell* **2**, 380-391 (2008).
29 Louria-Hayon, I. Signal, transduction, and the hematopoietic stem cell. *Rambam Maimonides medical journal* **5**, e0033 (2014).
30 Ward, A. C., Touw, I. & Yoshimura, A. The Jak-Stat pathway in normal and perturbed hematopoiesis. *Blood* **95**, 19-29 (2000).
31 Datta, S. *et al.* Replenishment of the B cell compartment after doxorubicin-induced hematopoietic toxicity is facilitated by STAT1. *Journal of leukocyte biology* **95**, 853-866 (2014).
32 Ruiz-Herguido, C. *et al.* Hematopoietic stem cell development requires transient Wnt/beta-catenin activity. *The Journal of experimental medicine* **209**, 1457-1468 (2012).
33 Yang, L. *et al.* Rho GTPase Cdc42 coordinates hematopoietic stem cell quiescence and niche interaction in the bone marrow. *Proceedings of the National Academy of Sciences of the United States of America* **104**, 5091-5096 (2007).
34 Notta, F. *et al.* Isolation of single human hematopoietic stem cells capable of long-term multilineage engraftment. *Science* **333**, 218-221 (2011).
35 Deregibus, M. C. *et al.* Endothelial progenitor cell derived microvesicles activate an angiogenic program in endothelial cells by a horizontal transfer of mRNA. *Blood* **110**, 2440-2448 (2007).
36 Zomer, A. *et al.* In Vivo imaging reveals extracellular vesicle-mediated phenocopying of metastatic behavior. *Cell* **161**, 1046-1057 (2015).
37 Batagov, A. O. & Kurochkin, I. V. Exosomes secreted by human cells transport largely mRNA fragments that are enriched in the 3'-untranslated regions. *Biology direct* **8**, 12 (2013).
38 Duinhouwer, L. E. *et al.* Wnt3a protein reduces growth factor-driven expansion of human hematopoietic stem and progenitor cells in serum-free cultures. *PloS one* **10**, e0119086 (2015).

39 Dudakovic, A. *et al.* High-resolution molecular validation of self-renewal and spontaneous differentiation in clinical-grade adipose-tissue derived human mesenchymal stem cells. *Journal of cellular biochemistry* **115**, 1816-1828 (2014).

40 Huang da, W., Sherman, B. T. & Lempicki, R. A. Systematic and integrative analysis of large gene lists using DAVID bioinformatics resources. *Nat Protoc* **4**, 44-57 (2009).

41 Eijken, M. *et al.* The activin A-follistatin system: potent regulator of human extracellular matrix mineralization. *FASEB journal : official publication of the Federation of American Societies for Experimental Biology* **21**, 2949-2960 (2007).

7 General Discussion

7.1. OVERVIEW

For decades, scientists across the world have observed extracellular vesicles (EVs) in their biological systems without realizing that EV-mediated intercellular communication is a universally shared biological process[1-11]. It was not until 2006 that scientists discovered EV-associated RNA, which triggered interest in the field and thereafter studies started increasing exponentially[12-15]. The establishment of an EV society (International Society of Extracellular Vesicles, ISEV) in 2011 brought in so many scientists from various fields ranging from prokaryotes to eukaryotes, immunology to stem cell biology, cancer to autoimmune diseases, highlighting the uniformity of the EV-mediated intercellular communication.

Throughout this thesis, we investigated the role of osteoblast-derived EVs in communication with the neighboring cells residing in the surrounding bone microenvironment. In **Chapters 2**, **3** and **4**, we presented a comprehensive analysis of EV protein, messenger RNA (mRNA) and microRNA (miRNA) cargo, respectively. In **Chapters 2**, **4**, **5** and **6**, we showed the role of EVs mediating communication between osteoblasts and prostate cancer cells as well as hematopoietic stem and progenitor cells (HSPCs). In **Chapter 5**, we investigated possible therapeutic applications of EVs in the field of hematology. In this chapter, we discuss the main findings of this thesis with relevance to the current state of the field. Furthermore, we discuss the strengths and limitations of our research, and propose suggestions for future studies.

7.2. DOES EV CARGO HAVE A BIOLOGICAL MEANING?

The existence of EVs in bone has been known for many years. Already back in 1967, Anderson and colleagues reported the discovery of osteoblast-derived matrix vesicles as specialized EVs involved in biomineralization of the bone matrix[3,4]. They showed that bone mineral crystal is formed with the coordinated activity of matrix vesicle proteins, such as phosphatases, calcium-binding proteins and transporters. However, over the past years it has become clear that beyond forming bone, osteoblasts play a role in various biological processes, including immune cell development, regulation of hematopoietic niche, and cancer metastasis to bone. With this in mind, we aimed to investigate the role of osteoblasts in EV-mediated regulation of essential physiological functions.

7.2.1. Exploring the EV cargo

EVs are actively loaded with a specific repertoire of proteins and RNA molecules that are necessary to convey their intercellular message. We employed various large-scale analysis technologies, such as proteomics and next-generation sequencing, and used com-

munity resources, such as EVpedia, and ExoCarta, to perform comparative studies to unravel the osteoblast-specific regulatory EV cargo[16,17].

EVs commonly contain structural cargo important for essential vesicle functions, such as biogenesis, sorting, motility and targeting. In **Chapter 2**, we demonstrated that EVs secreted by osteoblasts contain the classical EV marker proteins, such as adhesion molecules (FN1, ITGB1), annexins (ANXA2, ANXA6), cytoskeletal proteins (ACTB, MSN), heat shock proteins (HSPA8, HSP90AA1), metabolic enzymes (GAPDH, LDHA) and tetraspanins (CD9, CD81). The parental cell type, mode of biogenesis and environmental stimuli are among the factors that influence the nature and abundance of EV cargo[18]. Accordingly, we showed that osteoblasts secrete EVs that differ in morphology and proteomic composition depending on the stage of differentiation and mineralization condition. EVs secreted by mineralizing osteoblasts are enriched with biomineralization-related proteins indicating an activity associated with matrix vesicles. However, these EVs are also highly abundant in proteins involved in RNA binding and processing, suggestive of the presence of an EV subgroup with a role in intercellular communication. EVs secreted by non-mineralizing osteoblasts, on the other hand, are specifically enriched with cell adhesion-associated extracellular matrix proteins and chromosomal proteins with regulatory potential. To study communication and avoid the cross contamination of matrix vesicle activity, in the reminder of this thesis we focused on non-mineralizing osteoblast-derived EVs that we often referred to as "osteoblast-EVs".

Comparative analyses demonstrated that EV content is not just a reflection of the parental cell composition, but rather a unique set of molecules packaged within the vesicular structure via a conserved and preferential sorting mechanism. In fact, when compared to the cellular RNA distribution, osteoblast-EVs are enriched with small RNAs (25-1,000 nucleotides), and lack the characteristic cellular 18S and 28S ribosomal RNAs. In **Chapter 3**, we showed that EV-mRNAs mostly consist of genes encoding for proteins with ribosomal activities, while they lack the genes important to carry out vital cellular processes. EVs are particularly enriched with *RAB13* mRNA as it is standing out among the overrepresented EV-mRNAs. Rab family of small GTPases, have been implicated to play roles in EV release and transport[19,20]. Assuming that the EV-mRNA is translated upon delivery, we speculate that *RAB13* is likely to regulate EV biogenesis in the recipient cells. In **Chapter 4**, we presented a selective group of miRNAs that are overrepresented in osteoblast-EVs. These are mostly miRNAs involved in molecular functions related to growth and proliferation. Among these, we were particularly interested miR-29a, which is a well-characterized regulator of early hematopoiesis[21].

Taken together, our combined *omics* data analysis identified overrepresented pathways and biological processes important for cellular development and growth of target cells. The enrichment of ribosomal proteins and mRNAs that encode for ribosomal proteins brings diverse speculations on their role of stabilizing the miRNA cargo or transferring of ribosomal parts to facilitate gene expression in the target cells. At this stage, it is still challenging to distinguish the role of individual EV cargo. In light of our findings, we can con-

clude that the EV cargo consists of a combination of functionally diverse structural and regulatory biomolecules that must work in concert to convey the final message.

7.2.2. EV-mediated interaction with the microenvironment

Osteoblasts produce a network of receptors and secreted factors that provide the means of communication with the surrounding cells in the immediate microenvironment [22-25]. Based on our EV cargo analyses and functional studies, we demonstrated that osteoblast-EVs represented one of the critical components of this favorable microenvironment necessary to support vital biological processes. We performed bioinformatics analyses to delineate a candidate list of regulatory EV cargo predicted to target neighboring cells, such as osteoclasts, adipocytes, chondrocytes and hematopoietic stem cells (HSCs).

To investigate the biological meaning of EV-mediated communication, we studied the role of osteoblast-EVs in HSPC-osteolineage-cell crosstalk. In **Chapter 4**, we demonstrated that EV treatment induces the proliferation of HSPCs by stimulating cell cycle progression *in vitro*. In **Chapter 2**, we showed that EVs also stimulate the growth of bone-metastasizing prostate cancer cells, which have been known to compete with HSPCs for the interaction with osteolineage cells. It is critical to note the versatility of the manner in which EVs influence the behavior of different target cells. Through transcriptomics studies in **Chapters 2 & 6** we discovered that EVs alter the expression of different sets of HSPC and prostate cancer genes. Furthermore, we showed that the regulated genes are targeted by different sets of predicted EV cargo. Remarkably, both the altered genes and the predicted cargo are eventually annotated to the same pathway, "cell growth", in accordance with the functional studies. It is important to keep in mind that osteoblast-EVs consist of several types of vesicles that most likely differ in content and function. Therefore, we speculate that EVs exert extrinsic control of their target cells through different EV subgroups that activate different signaling cascades, which eventually converge to the same phenotype.

7.3. THERAPEUTIC POTENTIAL

Stem cell therapies using umbilical cord blood (UCB)-derived $CD34^+$ HSPCs are successful treatment options for patients with disrupted hematopoiesis. Increasing reports on the molecular mechanisms of HSC maintenance and self-renewal enabled the development of *ex vivo* culture systems to expand HSPCs for improved engraftment and post-transplantation recovery[26-29]. As mentioned, osteoblast-EVs showed the potency to stimulate HSPC proliferation *in vitro* making them suitable therapeutic candidates for expansion studies. In **Chapter 5**, we demonstrated that EVs cooperate with hematopoietic growth factors not only to promote proliferation but also to preserve the repopulating activity of UCB-derived $CD34^+$ HSPCs. The latter is especially important to ensure a constant turnover of new blood cells necessary for accelerated hematopoietic recovery. We successfully

showed the ability of the EV-expanded UCB cells to engraft *in vivo* and re-populate immunodeficient mice. These *in vitro* and *in vivo* evaluations indicate the power of an osteoblast-EV-based novel strategy for clinically relevant *ex vivo* expansion of UCB cells. With increasing knowledge on EV biology, we believe that it will not be long before EVs will be used as therapeutic tools for the treatment of a broad range of disorders.

7.4. CHALLENGES IN THE EV FIELD

Currently, there are still major unsolved problems, such as phenotyping, sizing and enumerating EVs, which delay our ability to truly understand EV biology. The main limitation that we frequently faced was the difficulty of distinguishing the different EV subgroups, such as exosomes, microvesicles and apoptotic bodies. Even though the recent standardization of EV nomenclature has greatly facilitated the EV research, there is growing evidence that the subgroups may have distinct functions[30]. The discovery of widely accepted morphological or structural markers might help us distinguish the different EVs, and consequently study the content and interpret the function more precisely. The lack of optimized tools to accurately quantify EVs pose another challenge, especially for functional studies [31]. Actually, using nanoparticle tracking analysis we managed to obtain consistent counts between independent isolations[32]. However, this method is still troublesome as it misses the small EVs, which may attribute to functionally significant differences between isolations.

It is also worth drawing attention to the challenges of interpreting the EV content in relevance to the *in vivo* function. As mentioned, external factors can affect the EV content. Therefore it is very important to consider these aspects with the particular research question in mind. Furthermore, our limited knowledge on the fate of EV cargo once they are delivered to the target cells strictly restricts our ability to study their biochemistry. This is especially difficult when analyzing the mRNA data. Whether the mRNAs are translated using the target cell's machinery or have a regulatory role still remain to be answered. Regarding sequencing studies, the comparison of expression levels across different samples and experiments is often difficult and requires complicated normalization methods. This is further challenged by the lack of well-established housekeeping RNAs for the comparison of cellular versus vesicular mRNAs and miRNAs. Unfortunately, these limitations are faced by most studies conducted on EVs, which fortunately brings together many groups to join forces to overcome these obstacles in the near future.

7.5. CONCLUSIONS & OUTLOOK

The discovery of specialized EVs carrying regulatory molecules between cells has been the hallmark of a recently discovered novel form of intercellular communication. Using comparative proteomics, genomics and bioinformatics analyses we showed that osteo-

blasts secrete EVs containing the signature content of their parental cells while being selectively enriched with a unique set of bioactive cargo. With carefully designed studies, we showed that EVs regulate the expression of cell growth-related HSPC and bone-metastasizing prostate cancer genes, and stimulate their growth *in vitro*. However, the molecular mechanisms behind EV-mediated crosstalk still remain to be explored. Thorough integrated biochemical and genetic analyses are necessary to identify the biologically active EV components and study their physiological relevance *in vivo*.

The increasing knowledge on EV biology has brought along therapeutic opportunities to be exploited clinically. We principally investigated the possibility of using osteoblast-EVs in stem cell therapies, and consequently demonstrated their potency for *ex vivo* expansion of UCB-derived HSPCs suitable for transplantations. However, this approach comes with a caveat: EVs stimulate the proliferation and maintenance of HSPCs in short-term cultures. Our current knowledge on EV content coupled with further investigation on the key molecular mechanism that stimulate HSPC proliferation may give us clues to manipulate EVs to stimulate long-term maintenance of the stem cells *in vitro*. This is especially important to develop improved expansion strategies that will meet the clinical need. Moreover, understanding the key players that regulate HSPC fate holds the promise of using EVs to manipulate other types of stem cells for various regenerative medicine applications in the future.

The comprehensive EV data presented throughout this thesis serves as an extensive osteoblast-EV cargo repository that offers a great source for non-invasive diagnostics as well as facilitates the development of cell-free strategies for therapeutic applications. We showed that the osteoblast-EV protein content is greatly dependent on the stage of mineralization. Therefore, EVs pose as perfect candidates for biomarker discovery useful for the early detection of bone diseases. Furthermore, thanks to their endogenous and biocompatible nature EVs are ideal virus-free vector alternatives for safer gene therapy applications. We anticipate that an elaborate understanding of the mechanism of EV cargo loading will enable us to develop tailored EVs containing therapeutic cargo to treat a broad variety of pathological conditions.

With increasing number of studies deciphering the complexity of EV biology, this newly emerging scientific field rapidly advances beyond basic science. In this thesis, we presented our *in vitro* efforts to uncover the intricate interactions networks that underlie the function of EVs secreted by osteoblasts. To move forward, we need to identify new research strategies and invest in developing optimized technologies that enhances our knowledge required to bring osteoblast-EVs towards clinical applications.

REFERENCES

1 Chargaff, E. & West, R. The biological significance of the thromboplastic protein of blood. *The Journal of biological chemistry* **166**, 189-197 (1946).

2 Wolf, P. The nature and significance of platelet products in human plasma. *British journal of haematology* **13**, 269-288 (1967).

3 Anderson, H. C. Electron microscopic studies of induced cartilage development and calcification. *J Cell Biol* **35**, 81-101 (1967).

4 Bonucci, E. Fine structure of early cartilage calcification. *J Ultrastruct Res* **20**, 33-50 (1967).

5 Anderson, H. C. Mineralization by matrix vesicles. *Scan Electron Microsc*, 953-964 (1984).

6 Stegmayr, B. & Ronquist, G. Promotive effect on human sperm progressive motility by prostasomes. *Urol Res* **10**, 253-257 (1982).

7 Anderson, H. C. Molecular biology of matrix vesicles. *Clin Orthop Relat Res*, 266-280 (1995).

8 Raposo, G. *et al.* B lymphocytes secrete antigen-presenting vesicles. *The Journal of experimental medicine* **183**, 1161-1172 (1996).

9 Bess, J. W., Jr., Gorelick, R. J., Bosche, W. J., Henderson, L. E. & Arthur, L. O. Microvesicles are a source of contaminating cellular proteins found in purified HIV-1 preparations. *Virology* **230**, 134-144 (1997).

10 Denzer, K., Kleijmeer, M. J., Heijnen, H. F., Stoorvogel, W. & Geuze, H. J. Exosome: from internal vesicle of the multivesicular body to intercellular signaling device. *Journal of cell science* **113 Pt 19**, 3365-3374 (2000).

11 Thery, C. *et al.* Proteomic analysis of dendritic cell-derived exosomes: a secreted subcellular compartment distinct from apoptotic vesicles. *J Immunol* **166**, 7309-7318 (2001).

12 Baj-Krzyworzeka, M. *et al.* Tumour-derived microvesicles carry several surface determinants and mRNA of tumour cells and transfer some of these determinants to monocytes. *Cancer Immunol Immunother* **55**, 808-818 (2006).

13 Ratajczak, J. *et al.* Embryonic stem cell-derived microvesicles reprogram hematopoietic progenitors: evidence for horizontal transfer of mRNA and protein delivery. *Leukemia* **20**, 847-856 (2006).

14 Valadi, H. *et al.* Exosome-mediated transfer of mRNAs and microRNAs is a novel mechanism of genetic exchange between cells. *Nature cell biology* **9**, 654-659 (2007).

15 Colombo, M. *et al.* Analysis of ESCRT functions in exosome biogenesis, composition and secretion highlights the heterogeneity of extracellular vesicles. *Journal of cell science* (2013).

16 Kim, D. K. *et al.* EVpedia: a community web portal for extracellular vesicles research. *Bioinformatics* **31**, 933-939 (2015).

17 Keerthikumar, S. *et al.* ExoCarta: A Web-Based Compendium of Exosomal Cargo. *Journal of molecular biology* (2015).

18 Yanez-Mo, M. *et al.* Biological properties of extracellular vesicles and their physiological functions. *J Extracell Vesicles* **4**, 27066 (2015).

19 Thery, C., Ostrowski, M. & Segura, E. Membrane vesicles as conveyors of immune responses. *Nat Rev Immunol* **9**, 581-593 (2009).

20 Simpson, R. J., Lim, J. W., Moritz, R. L. & Mathivanan, S. Exosomes: proteomic insights and diagnostic potential. *Expert Rev Proteomics* **6**, 267-283 (2009).
21 Han, Y. C. *et al.* microRNA-29a induces aberrant self-renewal capacity in hematopoietic progenitors, biased myeloid development, and acute myeloid leukemia. *The Journal of experimental medicine* **207**, 475-489 (2010).
22 Shiozawa, Y. & Taichman, R. S. Getting blood from bone: an emerging understanding of the role that osteoblasts play in regulating hematopoietic stem cells within their niche. *Experimental hematology* **40**, 685-694 (2012).
23 Shiozawa, Y. *et al.* Human prostate cancer metastases target the hematopoietic stem cell niche to establish footholds in mouse bone marrow. *J Clin Invest* **121**, 1298-1312 (2011).
24 Phan, T. C., Xu, J. & Zheng, M. H. Interaction between osteoblast and osteoclast: impact in bone disease. *Histology and histopathology* **19**, 1325-1344 (2004).
25 Liu, Y. *et al.* Intracellular VEGF regulates the balance between osteoblast and adipocyte differentiation. *J Clin Invest* **122**, 3101-3113 (2012).
26 Curti, A., Fogli, M., Ratta, M., Tura, S. & Lemoli, R. M. Stem cell factor and FLT3-ligand are strictly required to sustain the long-term expansion of primitive CD34+DR- dendritic cell precursors. *J Immunol* **166**, 848-854 (2001).
27 Delaney, C. *et al.* Notch-mediated expansion of human cord blood progenitor cells capable of rapid myeloid reconstitution. *Nat Med* **16**, 232-236 (2010).
28 Fei, X. M. *et al.* Co-culture of cord blood CD34(+) cells with human BM mesenchymal stromal cells enhances short-term engraftment of cord blood cells in NOD/SCID mice. *Cytotherapy* **9**, 338-347 (2007).
29 Lund, T. C., Boitano, A. E., Delaney, C. S., Shpall, E. J. & Wagner, J. E. Advances in umbilical cord blood manipulation-from niche to bedside. *Nature reviews. Clinical oncology* **12**, 163-174 (2015).
30 Witwer, K. W. *et al.* Standardization of sample collection, isolation and analysis methods in extracellular vesicle research. *J Extracell Vesicles* **2** (2013).
31 van der Pol, E. *et al.* Optical and non-optical methods for detection and characterization of microparticles and exosomes. *J Thromb Haemost* **8**, 2596-2607 (2010).
32 Dragovic, R. A. *et al.* Sizing and phenotyping of cellular vesicles using Nanoparticle Tracking Analysis. *Nanomedicine* **7**, 780-788 (2011).

Appendix A

Supplementary Figures & Tables

Appendix B

Abbreviations

Appendix C

Primer Sequences

Appendix A

Table A1. LS-MS/MS data. EV proteins are defined by their UniProt accessions. x denotes present in a given sample.

	NMOB-EV			MOB-EV				NMOB-EV			MOB-EV				NMOB-EV			MOB-EV				NMOB-EV			MOB-EV		
Accession	**5**	**12**	**19**	**5**	**12**	**19**	**Accession**	**5**	**12**	**19**	**5**	**12**	**19**	**Accession**	**5**	**12**	**19**	**5**	**12**	**19**	**Accession**	**5**	**12**	**19**	**5**	**12**	**19**
A0AVT1	x	x	x	x	x	x	O43324	x	x	x	x	x	x	O95394	x	x	x	x	x	x	P05455	x	x	x	x	x	x
O00154	x	x	x	x	x	x	O43504	x	x	x	x	x	x	O95772	x	x	x	x	x	x	P05556	x	x	x	x	x	x
O00159	x	x	x	x	x	x	O43592	x	x	x	x	x	x	O95782	x	x	x	x	x	x	P05771	x	x	x	x	x	x
O00186	x	x	x	x	x	x	O43633	x	x	x	x	x	x	O95807			x			x	P06493	x	x	x	x	x	x
O00194	x		x	x		x	O43657	x	x	x	x	x	x	O95816			x	x	x	x	P06576	x		x	x	x	x
O00231	x	x	x	x	x	x	O43684	x	x	x	x	x	x	O95819	x	x	x	x	x	x	P06703	x	x	x	x	x	x
O00232	x	x	x	x	x	x	O43707	x	x	x	x	x	x	O95832	x	x	x	x	x	x	P06733	x	x	x	x	x	x
O00299	x	x	x	x	x	x	O43731						x	O95865	x		x	x	x	x	P06737	x	x	x	x	x	x
O00303	x	x	x	x	x	x	O43776	x	x	x	x	x	x	P00338	x	x	x	x	x	x	P06744	x	x	x	x	x	x
O00338			x	x	x		O43795	x	x	x	x	x	x	P00387	x	x	x	x	x	x	P06748	x	x	x	x	x	x
O00410	x	x	x	x	x	x	O43854	x	x	x	x	x	x	P00441	x	x	x	x	x	x	P06753	x	x	x	x	x	x
O00425					x	x	O60488	x	x	x	x	x	x	P00491	x	x	x	x	x	x	P06756	x	x	x	x	x	x
O00429	x	x	x	x	x	x	O60506	x	x	x	x	x	x	P00492	x	x	x	x	x	x	P06899	x	x	x	x	x	x
O00443			x	x	x	x	O60565	x	x	x	x	x	x	P00505	x	x	x	x	x	x	P07195	x	x	x	x	x	x
O00468	x	x	x	x	x	x	O60610	x	x	x	x	x	x	P00533	x	x	x	x	x	x	P07237	x	x	x	x	x	x
O00487	x	x	x	x	x	x	O60637	x	x	x	x	x	x	P00558	x	x	x	x	x	x	P07305	x	x	x	x	x	x
O00560	x	x	x	x	x	x	O60701	x	x	x	x	x	x	P00749	x	x	x	x		x	P07339	x	x	x	x	x	x
O00567	x	x	x	x	x	x	O60763	x	x	x	x	x	x	P00966	x	x	x	x	x	x	P07355	x	x	x	x	x	x
O00592	x	x	x	x	x		O60841	x	x	x	x	x	x	P01031	x	x		x	x	x	P07384	x	x	x	x	x	x
O00764	x	x	x	x	x	x	O60884	x	x	x	x	x	x	P01111	x	x	x	x	x	x	P07437	x	x	x	x	x	x
O14672;	x	x	x	x	x	x	O75083	x	x	x	x	x	x	P01112	x	x	x	x	x	x	P07741	x	x	x	x	x	x
O14744	x	x	x	x	x	x	O75131	x	x	x	x	x	x	P01892	x	x	x	x	x	x	P07814	x	x	x	x	x	x
O14787					x	x	O75165	x	x	x	x	x	x	P02452	x	x	x	x	x	x	P07900	x	x	x	x	x	x
O14817	x	x	x	x	x	x	O75340	x	x	x	x	x	x	P02545	x	x	x	x	x	x	P07910	x	x	x	x	x	x
O14818	x	x	x	x	x	x	O75347	x		x	x	x		P02649	x	x	x	x	x	x	P07942	x	x	x	x	x	x
O14828	x	x	x	x	x	x	O75351	x	x	x	x	x	x	P02751	x	x	x	x	x	x	P07947	x	x	x	x	x	x
O14929	x	x	x	x	x	x	O75367	x	x	x	x	x	x	P02786	x	x	x	x	x	x	P08107	x	x	x	x	x	x
O14936	x	x	x	x	x	x	O75368	x	x	x			x	P04075	x	x	x	x	x	x	P08123	x	x	x	x	x	x
O14964	x	x	x	x	x	x	O75369	x	x	x	x	x	x	P04080	x	x	x	x	x	x	P08133	x	x	x	x	x	x
O14980	x	x	x	x	x	x	O75390	x	x	x	x	x	x	P04083	x	x	x	x	x	x	P08134			x	x	x	x
O15031	x	x	x	x	x	x	O75396	x	x	x	x	x	x	P04179	x	x	x	x	x	x	P08195	x	x	x	x	x	x
O15067	x	x	x	x	x	x	O75436	x	x	x	x	x	x	P04216	x	x	x	x	x	x	P08237	x	x	x	x	x	x
O15118	x	x	x	x	x	x	O75531	x	x	x	x	x	x	P04350	x	x	x	x	x	x	P08238	x	x	x	x	x	x
O15143	x	x	x	x	x	x	O75643	x	x	x	x	x	x	P04406	x	x	x	x	x	x	P08253	x	x	x	x		x
O15144	x	x	x	x	x	x	O75695	x	x	x	x	x	x	P04632	x	x		x	x	x	P08473	x	x	x	x	x	x
O15145	x	x	x	x	x	x	O75787			x	x	x	x	P04792	x	x	x	x	x	x	P08590	x	x	x	x	x	x
O15162	x	x	x	x	x	x	O75874	x	x	x	x	x	x	P04843	x	x	x	x	x	x	P08648	x	x	x	x	x	x
O15230	x	x	x		x	x	O75923	x	x	x	x	x	x	P04844	x	x	x	x	x	x	P08670	x	x	x	x	x	x
O15243					x	x	O75954	x	x	x	x	x	x	P04899	x	x	x	x	x	x	P08708	x	x	x	x	x	x
O15371	x	x	x	x	x	x	O75955	x	x	x	x	x	x	P05023	x	x	x	x	x	x	P08754	x	x	x	x	x	x
O15372	x	x	x	x	x	x	O76021	x	x	x	x	x	x	P05026	x	x	x	x	x	x	P08758	x	x	x	x	x	x
O15427	x	x	x	x	x	x	O76094	x	x	x	x	x	x	P05106	x	x	x	x	x	x	P08865	x	x	x	x	x	x
O15484	x	x	x	x	x		O94760	x	x	x	x	x	x	P05121	x	x	x	x	x	x	P08962	x	x	x	x	x	x
O15511	x	x	x	x	x	x	O94973	x	x	x	x	x	x	P05161	x	x	x	x	x	x	P09104	x	x	x	x	x	x
O15523	x	x	x	x	x	x	O95084	x	x	x	x	x	x	P05186	x	x	x	x	x	x	P09132	x	x	x	x	x	x
O19617	x	x	x	x	x	x	O95183	x	x	x	x	x	x	P05198	x	x	x	x	x	x	P09211	x	x	x	x	x	x
O43143	x	x	x	x	x	x	O95197	x	x	x	x	x	x	P05362	x	x	x	x	x	x	P09382	x	x	x	x	x	x
O43169	x		x	x	x	x	O95340	x	x	x	x	x	x	P05386	x	x	x	x	x	x	P09496	x	x	x	x	x	x
O43242	x	x	x	x	x	x	O95347	x	x	x	x	x	x	P05387	x	x	x	x	x	x	P09525	x	x	x	x	x	x
O43264	x	x	x	x	x	x	O95373	x	x	x	x	x	x	P05388	x	x	x	x	x	x	P09543	x	x	x	x	x	x

	NMOB-EV			MOB-EV				NMOB-EV			MOB-EV				NMOB-EV			MOB-EV				NMOB-EV			MOB-EV		
Accession	**5**	**12**	**19**	**5**	**12**	**19**	**Accession**	**5**	**12**	**19**	**5**	**12**	**19**	**Accession**	**5**	**12**	**19**	**5**	**12**	**19**	**Accession**	**5**	**12**	**19**	**5**	**12**	**19**
P09619	x	x	x	x	x	x	P13489	x	x	x	x	x	x	P17987	x	x	x	x	x	x	P24821	x	x	x			x
P09651	x	x	x	x	x	x	P13611	x	x	x	x	x	x	P18077	x	x	x	x	x	x	P25205	x	x	x	x	x	x
P09874	x	x	x	x	x	x	P13612	x	x	x	x	x	x	P18084	x	x	x	x	x	x	P25391	x	x	x	x	x	x
P09914	x	x	x	x	x	x	P13639	x	x	x	x	x	x	P18085	x	x	x	x	x	x	P25398	x	x	x	x	x	x
P09936	x	x	x	x	x	x	P13667	x	x	x	x	x	x	P18124	x	x	x	x	x	x	P25445	x	x	x	x	x	x
P09960	x	x	x	x	x	x	P13726	x	x			x		P18206	x	x	x	x	x	x	P25786	x	x	x	x	x	x
P09972	x	x	x	x	x	x	P13797	x	x	x	x	x	x	P18564	x	x	x	x	x	x	P25787	x	x	x	x	x	x
P0C0S5	x	x	x	x	x	x	P13798	x	x	x	x	x	x	P18621	x	x	x	x	x	x	P25788	x	x	x	x	x	x
P0C0S8	x	x	x	x	x	x	P13861	x	x	x	x	x	x	P18669	x	x	x	x	x	x	P25789	x	x	x	x	x	x
P0DJG4		x	x		x	x	P13987	x	x	x	x	x	x	P19105	x	x	x	x	x	x	P26006	x	x	x	x	x	x
P10114			x			x	P14174	x	x	x	x	x	x	P19338	x	x	x	x	x	x	P26022	x	x	x	x	x	x
P10124	x	x	x	x	x	x	P14209			x		x	x	P19623	x		x	x	x	x	P26038	x	x	x	x	x	x
P10301	x	x	x	x	x	x	P14324	x	x	x	x	x	x	P19784	x		x				P26373	x	x	x	x	x	x
P10319	x	x	x	x	x	x	P14384	x	x	x	x	x	x	P20020	x	x	x	x	x	x	P26639	x	x	x	x	x	x
P10321	x	x	x	x	x	x	P14543	x	x	x	x		x	P20042			x		x	x	P26640	x	x	x	x	x	x
P10412	x	x	x	x	x	x	P14550	x	x	x	x	x	x	P20073	x	x	x	x	x	x	P26641	x	x	x	x	x	x
P10599	x	x	x	x	x	x	P14618	x	x	x	x	x	x	P20339	x	x	x	x	x	x	P27105	x	x	x	x	x	x
P10644	x	x	x	x	x	x	P14625	x	x	x	x	x	x	P20340	x	x	x	x	x	x	P27348	x	x	x	x	x	x
P10768	x	x	x	x	x	x	P14735	x	x	x	x	x	x	P20591	x	x	x	x	x	x	P27449	x	x	x	x	x	x
P10809	x		x	x	x	x	P14866	x	x	x	x	x	x	P20594	x		x	x	x	x	P27487	x	x	x	x	x	x
P10915	x	x	x	x	x	x	P14868	x	x	x	x	x	x	P20618	x	x	x	x	x	x	P27635	x	x	x	x	x	x
P11021	x	x	x	x	x	x	P15121	x	x	x	x	x	x	P20645	x	x	x	x	x	x	P27694	x		x	x	x	x
P11047	x	x	x	x	x	x	P15144	x	x	x	x	x	x	P20936			x			x	P27695	x	x	x	x	x	x
P11142	x	x	x	x	x	x	P15151	x	x	x	x	x	x	P21281	x	x	x	x	x	x	P27701	x	x	x	x	x	x
P11166	x	x	x	x	x	x	P15170	x	x	x	x	x	x	P21333	x	x	x	x	x	x	P27708	x	x	x	x	x	x
P11169	x	x	x	x	x	x	P15311	x	x	x	x	x	x	P21399	x	x	x	x	x	x	P27797	x	x	x	x	x	x
P11172						x	P15529	x	x	x	x	x	x	P21589	x	x	x	x	x	x	P27824	x	x	x	x	x	x
P11216	x	x	x	x	x	x	P15531	x	x	x	x	x	x	P21741	x				x	x	P28062	x	x	x	x	x	x
P11217		x	x		x	x	P15880	x	x	x	x	x	x	P21926	x	x	x	x	x	x	P28065	x	x	x	x	x	x
P11233	x	x	x	x	x	x	P15924	x	x	x			x	P21980	x	x	x	x	x	x	P28066	x	x	x	x	x	x
P11279	x	x	x	x	x	x	P16070	x	x	x	x	x	x	P22087	x	x	x	x	x	x	P28070	x	x	x	x	x	x
P11387	x	x	x	x	x	x	P16152	x	x	x	x	x	x	P22234	x	x	x	x	x	x	P28072	x	x	x	x	x	x
P11388	x	x	x	x	x	x	P16189	x	x	x	x	x	x	P22314	x	x	x	x	x	x	P28074	x	x	x	x	x	x
P11413	x	x	x	x	x	x	P16190	x	x	x	x	x	x	P22626	x	x	x	x	x	x	P28482	x	x	x	x	x	x
P11586	x	x	x	x	x	x	P16401	x	x	x	x	x	x	P22694			x	x	x	x	P28838	x	x	x	x	x	x
P11717	x	x	x	x	x	x	P16403	x	x	x	x	x	x	P23229	x	x	x	x	x	x	P29144	x	x	x	x	x	x
P11766	x	x	x	x	x	x	P16442	x		x	x	x	x	P23246	x	x	x	x	x	x	P29317	x	x	x	x	x	x
P11908	x	x	x	x	x	x	P17066	x	x	x	x	x	x	P23258	x	x	x	x	x	x	P29323	x	x	x	x	x	x
P11940	x	x	x	x	x	x	P17096	x	x	x	x	x	x	P23284	x	x	x	x	x	x	P29401	x	x	x	x	x	x
P12004	x	x	x	x	x	x	P17174	x	x	x	x	x	x	P23381	x	x	x	x	x	x	P29692	x	x	x	x	x	x
P12109	x	x	x	x	x	x	P17301	x	x	x	x	x	x	P23396	x	x	x	x	x	x	P29728	x		x	x	x	x
P12110	x	x	x	x	x	x	P17302	x	x	x	x	x	x	P23526	x	x	x	x	x	x	P29966	x	x	x	x	x	x
P12111	x	x	x	x	x	x	P17612	x	x	x	x	x	x	P23528	x	x	x	x	x	x	P29992	x	x	x	x	x	x
P12268	x	x	x	x	x	x	P17655	x	x	x	x	x	x	P23634	x	x	x	x	x	x	P30041	x	x	x	x	x	x
P12429	x	x	x	x	x	x	P17693	x	x	x	x	x	x	P23743						x	P30043	x		x	x	x	x
P12814	x	x	x	x	x	x	P17812	x	x	x	x	x	x	P23921	x	x	x	x	x	x	P30044	x	x	x	x	x	x
P12955	x	x	x	x	x	x	P17813	x	x	x	x	x	x	P23942	x	x	x	x	x	x	P30046	x	x	x	x	x	x
P12956	x	x	x	x	x	x	P17844	x	x	x	x	x	x	P24390	x		x	x	x	x	P30048	x	x	x	x	x	x
P13010	x	x	x	x	x	x	P17858	x	x	x	x	x	x	P24534	x	x	x	x	x	x	P30050	x	x	x	x	x	x
P13473	x	x	x	x	x	x	P17980	x	x	x	x	x	x	P24666	x	x	x	x	x	x	P30086	x	x	x	x	x	x

Appendix A

	NMOB-EV			MOB-EV				NMOB-EV			MOB-EV				NMOB-EV			MOB-EV				NMOB-EV			MOB-EV		
Accession	**5**	**12**	**19**	**5**	**12**	**19**	**Accession**	**5**	**12**	**19**	**5**	**12**	**19**	**Accession**	**5**	**12**	**19**	**5**	**12**	**19**	**Accession**	**5**	**12**	**19**	**5**	**12**	**19**
P30101	x	x	x	x	x	x	P37837	x	x	x	x	x	x	P48637	x	x	x	x	x	x	P53396	x	x	x	x	x	x
P30153	x	x	x	x	x	x	P38606	x	x	x	x	x	x	P48643	x	x	x	x	x	x	P53618	x	x	x	x	x	x
P30408		x	x		x	x	P38646	x	x	x	x	x	x	P48739	x	x	x	x	x	x	P53621	x	x	x	x	x	x
P30453	x	x	x	x	x	x	P38919	x	x	x	x	x	x	P48960	x	x	x	x	x	x	P53675	x	x	x	x	x	x
P30499	x	x	x	x	x	x	P39019	x				x	x	P49006	x	x	x	x	x	x	P53680	x	x	x	x	x	x
P30566	x	x	x	x	x	x	P39023	x	x	x	x	x	x	P49189	x	x	x	x	x	x	P53985	x	x	x	x	x	x
P30626	x	x	x	x	x	x	P40121	x	x	x	x	x	x	P49207	x	x	x	x	x	x	P53990	x	x	x	x	x	x
P30740	x	x	x	x	x	x	P40227	x	x	x	x	x	x	P49327	x	x	x	x	x	x	P54136	x	x	x	x	x	x
P30825	x	x	x	x	x	x	P40261	x	x	x	x	x	x	P49368	x	x	x	x	x	x	P54289	x	x	x	x	x	x
P31150	x	x	x	x	x	x	P40306	x	x	x	x	x	x	P49419	x	x	x	x	x	x	P54578	x	x	x	x	x	x
P31153			x		x	x	P40429	x	x	x	x	x	x	P49588	x	x	x	x	x	x	P54652	x		x	x	x	x
P31350	x	x	x	x	x	x	P40925	x	x	x	x	x	x	P49589	x		x	x	x	x	P54687	x	x	x	x	x	x
P31689	x	x	x	x	x	x	P40926	x	x	x	x	x	x	P49591	x	x	x	x	x	x	P54709	x	x	x	x	x	x
P31939	x	x	x	x	x	x	P41091	x	x	x	x	x	x	P49720	x	x	x	x	x	x	P54852	x	x	x	x	x	x
P31942	x	x	x	x	x	x	P41250	x	x	x	x	x	x	P49721	x	x	x	x	x	x	P54920	x	x	x	x	x	x
P31943	x	x	x	x	x	x	P41252	x	x	x	x	x	x	P49736	x		x	x	x	x	P55010	x	x	x	x	x	x
P31946	x	x	x	x	x	x	P42224	x	x	x	x	x	x	P49755	x		x	x	x	x	P55060	x	x	x	x	x	x
P31947	x	x	x	x	x	x	P42345	x		x	x	x	x	P49770	x	x	x	x	x	x	P55072	x	x	x	x	x	x
P31948	x	x	x	x	x	x	P42677	x	x	x	x	x	x	P49773	x	x	x	x	x	x	P55209	x	x	x	x	x	x
P31949	x	x	x	x	x	x	P42766	x	x	x	x	x	x	P49915	x	x	x	x	x	x	P55263	x	x	x	x	x	x
P32119	x	x	x	x	x	x	P42892	x	x	x	x	x	x	P50148	x	x	x	x	x	x	P55268	x		x			x
P32455	x	x	x	x	x	x	P43007	x	x	x	x	x	x	P50281	x	x	x	x	x	x	P55290	x	x	x	x	x	x
P32969	x	x	x	x	x	x	P43034	x	x	x	x	x	x	P50395	x	x	x	x	x	x	P55735	x	x	x	x	x	x
P33176	x	x	x	x	x	x	P43121	x	x	x	x	x	x	P50454	x	x	x	x	x	x	P55769	x		x	x	x	x
P33991	x	x	x	x	x	x	P43487	x	x	x	x	x	x	P50502	x	x	x	x	x	x	P55786	x	x	x	x	x	x
P33992	x	x	x	x	x	x	P43490	x	x	x	x	x	x	P50570	x		x	x	x	x	P55854	x	x	x	x	x	x
P33993	x	x	x	x	x	x	P43686	x	x	x	x	x	x	P50748	x		x	x	x	x	P55884	x		x			x
P34897	x	x	x	x	x	x	P45973						x	P50914	x	x	x	x	x	x	P56192	x	x	x	x	x	x
P34932	x	x	x	x	x	x	P45974	x	x	x	x	x	x	P50990	x	x	x	x	x	x	P56199	x	x	x	x	x	x
P35030	x	x	x	x	x	x	P46063	x	x	x	x	x	x	P50991	x	x	x	x	x	x	P56537	x	x	x	x	x	x
P35080	x	x	x	x	x	x	P46459	x		x	x	x	x	P50995	x	x	x	x	x	x	P58546	x	x	x	x	x	x
P35221	x	x	x	x	x	x	P46776	x	x	x	x	x	x	P51148	x	x	x	x	x	x	P59998	x	x	x	x	x	x
P35222	x	x	x	x	x	x	P46777	x	x	x	x	x	x	P51149	x	x	x	x	x	x	P60033	x	x	x	x	x	x
P35237	x	x	x	x	x	x	P46778	x	x	x	x	x	x	P51153	x	x	x	x	x	x	P60174	x	x	x	x	x	x
P35241	x	x	x	x	x	x	P46779	x	x	x	x	x	x	P51178	x	x	x	x	x	x	P60228	x	x	x	x	x	x
P35268	x	x	x	x	x	x	P46781	x	x	x	x	x	x	P51571	x		x	x	x	x	P60520	x	x	x	x	x	x
P35442	x	x	x	x	x		P46782	x	x	x	x	x	x	P51572	x		x		x	x	P60660	x	x	x	x	x	x
P35579	x	x	x	x	x	x	P46783	x	x	x	x	x	x	P51665	x	x	x	x	x	x	P60842	x	x	x	x	x	x
P35606	x	x	x	x	x	x	P46926	x	x	x	x	x	x	P51991	x	x	x	x	x	x	P60866	x	x	x	x	x	x
P35613	x	x	x	x	x	x	P46934	x	x	x	x	x	x	P52209	x	x	x	x	x	x	P60900	x	x	x	x	x	x
P35659	x	x	x	x	x	x	P46940	x	x	x	x	x	x	P52272	x	x	x	x	x	x	P60953	x	x	x	x	x	x
P35998	x	x	x	x	x	x	P46976				x	x	x	P52292	x	x	x	x	x	x	P60981	x	x	x	x	x	x
P36383	x	x	x	x	x	x	P47755	x	x	x	x	x	x	P52306	x	x	x	x	x	x	P60983	x	x	x	x	x	x
P36406	x	x	x	x	x	x	P47756	x	x	x	x	x	x	P52565	x	x	x	x	x	x	P61006	x	x	x	x	x	x
P36543	x	x	x	x	x	x	P47813	x	x	x	x	x	x	P52597	x			x	x	x	P61011						x
P36578	x	x	x	x	x	x	P47914	x	x	x	x	x	x	P52788	x	x	x	x	x	x	P61019	x	x	x	x	x	x
P36871				x			P48059	x	x	x	x	x	x	P52888	x	x	x	x	x	x	P61020	x	x	x	x	x	x
P36873	x	x	x	x	x	x	P48147	x	x	x	x	x	x	P52907	x	x	x	x	x	x	P61026	x	x	x	x	x	x
P37108	x	x	x	x	x	x	P48444	x	x	x	x	x	x	P52926	x	x	x	x	x		P61077	x	x	x	x	x	x
P37802	x	x	x	x	x	x	P48509	x	x	x	x	x	x	P53004	x	x	x	x	x	x	P61081	x	x	x	x	x	x

	NMOB-EV			MOB-EV				NMOB-EV			MOB-EV				NMOB-EV			MOB-EV				NMOB-EV			MOB-EV		
Accession	**5**	**12**	**19**	**5**	**12**	**19**	**Accession**	**5**	**12**	**19**	**5**	**12**	**19**	**Accession**	**5**	**12**	**19**	**5**	**12**	**19**	**Accession**	**5**	**12**	**19**	**5**	**12**	**19**
P61088	x	x	x	x	x	x	P62714	x	x	x	x	x	x	P83731	x	x	x	x	x	x	Q12765	x	x	x	x	x	x
P61106	x	x	x	x	x	x	P62745						x	P84085	x	x	x	x	x	x	Q12768	x	x	x	x	x	x
P61158	x	x	x	x	x	x	P62750	x	x	x	x	x	x	P84095	x	x	x	x	x	x	Q12846	x	x	x	x	x	x
P61160	x	x	x	x	x	x	P62753	x	x	x	x	x	x	P84098	x	x	x	x	x	x	Q12884	x	x	x	x	x	x
P61163	x	x	x	x	x	x	P62805	x	x	x	x	x	x	P84103	x	x	x	x	x	x	Q12905	x	x	x	x	x	x
P61201	x	x	x	x	x	x	P62820	x	x	x	x	x	x	P98095	x	x	x	x		x	Q12906	x	x	x	x	x	x
P61204	x	x	x	x	x	x	P62826	x	x	x	x	x	x	P98160	x	x	x	x	x	x	Q12907	x	x	x	x	x	x
P61221	x	x	x	x	x	x	P62829	x	x	x	x	x	x	P99999	x	x	x	x	x	x	Q12959	x	x		x	x	x
P61224	x	x	x	x	x	x	P62841	x	x	x	x	x	x	Q00526	x	x	x	x	x		Q12965	x		x	x	x	x
P61225	x	x	x	x	x	x	P62847	x	x	x	x	x	x	Q00610	x	x	x	x	x	x	Q13045	x		x	x		x
P61247	x	x	x	x	x	x	P62851	x	x	x	x	x	x	Q00688	x		x	x	x	x	Q13085	x		x	x	x	x
P61254	x	x	x	x	x	x	P62854	x	x	x	x	x	x	Q00765	x	x	x	x	x	x	Q13126	x	x	x	x	x	x
P61313	x	x	x	x	x	x	P62857	x		x	x	x	x	Q00839	x	x	x	x	x	x	Q13144	x	x	x	x	x	x
P61353	x	x	x	x	x	x	P62861			x	x	x	x	Q01081	x	x	x	x	x	x	Q13151						x
P61421	x	x	x	x	x	x	P62873	x	x	x	x	x	x	Q01082	x	x	x	x	x	x	Q13200	x	x	x	x	x	x
P61513	x	x	x	x	x	x	P62879	x	x	x	x	x	x	Q01105	x	x	x	x	x	x	Q13242					x	
P61586	x	x	x	x	x	x	P62888	x	x	x	x	x	x	Q01469	x	x	x	x	x	x	Q13263			x	x	x	x
P61604	x		x		x	x	P62899	x	x	x	x	x	x	Q01518	x	x	x	x	x	x	Q13308	x	x	x	x	x	x
P61764	x	x	x	x	x	x	P62906	x	x	x	x	x	x	Q01628	x	x	x	x	x	x	Q13347	x	x	x	x	x	x
P61769	x	x	x	x	x	x	P62910	x	x	x	x	x	x	Q01650	x	x	x	x	x	x	Q13409	x	x	x	x	x	x
P61803	x	x	x	x	x	x	P62913	x	x	x	x	x	x	Q01813	x	x	x	x	x	x	Q13418	x	x	x	x	x	x
P61923	x	x	x	x	x	x	P62917	x	x	x	x	x	x	Q01995	x	x	x	x	x	x	Q13425	x	x	x	x	x	x
P61978	x	x	x	x	x	x	P62937	x	x	x	x	x	x	Q02413	x	x	x	x	x	x	Q13443	x	x	x	x	x	x
P61981	x	x	x	x	x	x	P62942	x	x	x	x	x	x	Q02539			x				Q13451			x	x	x	x
P62070	x	x	x	x	x	x	P62979	x	x	x	x	x	x	Q02543	x	x	x	x	x	x	Q13492	x		x	x	x	x
P62079	x	x	x	x	x	x	P62995	x	x	x	x	x	x	Q02790	x	x	x	x	x	x	Q13509	x	x	x	x	x	x
P62081	x	x	x	x	x	x	P63000	x	x	x	x	x	x	Q02878	x	x	x	x	x	x	Q13557	x	x	x		x	x
P62136	x	x	x	x	x	x	P63010	x	x	x	x	x	x	Q03135	x	x	x	x	x	x	Q13576	x				x	
P62140	x	x	x	x	x	x	P63096	x	x	x	x	x	x	Q03405	x	x	x	x	x	x	Q13617	x		x	x	x	x
P62158	x	x	x	x	x	x	P63104	x	x	x	x	x	x	Q04446	x	x	x	x	x	x	Q13620	x	x	x	x	x	x
P62191	x	x	x	x	x	x	P63167	x		x	x	x	x	Q04760	x	x	x	x	x	x	Q13642	x	x	x	x	x	x
P62195	x	x	x	x	x	x	P63173	x		x	x	x	x	Q04837	x	x	x	x	x	x	Q13683	x	x	x	x	x	x
P62241	x	x	x	x	x	x	P63208	x	x	x	x	x	x	Q04917	x	x	x	x	x	x	Q13740	x	x	x	x	x	x
P62244	x	x	x	x	x	x	P63220	x		x	x	x	x	Q04941	x	x	x	x	x	x	Q13765	x	x	x	x	x	x
P62249	x	x	x	x	x	x	P63241	x	x	x	x	x	x	Q06210	x	x	x	x	x	x	Q13813	x	x	x	x	x	x
P62258	x	x	x	x	x	x	P63244	x	x	x	x	x	x	Q06323	x	x	x	x	x	x	Q13838	x	x	x	x	x	x
P62263	x	x	x	x	x	x	P63261	x	x	x	x	x	x	Q06830	x	x	x	x	x	x	Q13867	x	x	x	x	x	x
P62266	x	x	x	x	x	x	P67809	x	x	x	x	x	x	Q07020	x	x	x	x	x	x	Q13885	x		x	x	x	x
P62269	x	x	x	x	x	x	P67812					x	x	Q07021	x	x	x	x	x	x	Q13907	x	x	x	x	x	x
P62277	x	x	x	x	x	x	P67936	x	x	x	x	x	x	Q07866	x	x	x	x	x	x	Q14019	x	x	x	x	x	x
P62280	x	x	x	x	x	x	P68032	x	x	x	x	x	x	Q07954	x	x	x	x	x	x	Q14103	x	x	x	x	x	x
P62304	x	x	x	x	x	x	P68104	x	x	x	x	x	x	Q07955	x	x	x	x	x	x	Q14108	x	x	x	x	x	x
P62314	x	x	x	x	x	x	P68371	x	x	x	x	x	x	Q07960	x		x	x	x	x	Q14152	x	x	x	x	x	x
P62316	x	x	x	x	x	x	P68400	x		x	x	x	x	Q08211	x	x	x	x	x	x	Q14192	x	x	x	x	x	x
P62318	x	x	x	x	x	x	P68402	x	x	x	x	x	x	Q08380	x	x	x	x	x	x	Q14203	x		x	x	x	x
P62330	x	x	x	x	x	x	P68431	x		x				Q08431	x	x	x	x	x	x	Q14204	x	x	x	x	x	x
P62333	x	x	x	x	x	x	P78371	x	x	x	x	x	x	Q08722	x	x	x	x	x	x	Q14254	x	x	x	x	x	x
P62424	x	x	x	x	x	x	P78417	x	x	x	x	x	x	Q08945			x				Q14258	x		x	x	x	x
P62491	x	x	x	x	x	x	P78527	x	x	x	x	x	x	Q09666	x	x	x	x	x	x	Q14315	x	x	x	x	x	x
P62701	x	x	x	x	x	x	P80723	x	x	x	x	x	x	Q10471	x	x	x	x	x	x	Q14344	x	x	x	x	x	x

Appendix A

	NMOB-EV			MOB-EV				NMOB-EV			MOB-EV				NMOB-EV			MOB-EV				NMOB-EV			MOB-EV		
Accession	**5**	**12**	**19**	**5**	**12**	**19**	**Accession**	**5**	**12**	**19**	**5**	**12**	**19**	**Accession**	**5**	**12**	**19**	**5**	**12**	**19**	**Accession**	**5**	**12**	**19**	**5**	**12**	**19**
Q14517	x	x	x	x	x	x	Q53TN4	x	x	x	x	x	x	Q8IWA5	x	x	x	x	x	x	Q96CW1	x	x	x	x	x	x
Q14566			x	x	x	x	Q562R1	x	x	x	x	x	x	Q8IWB7	x	x	x	x	x	x	Q96EK6	x		x	x	x	x
Q14699	x	x	x	x	x	x	Q58FF8	x	x	x	x	x	x	Q8IXQ6	x		x	x	x	x	Q96EY5	x	x	x	x	x	x
Q14764	x	x	x	x	x	x	Q5JWF2	x	x	x	x	x	x	Q8IY67	x	x	x	x	x	x	Q96F07	x		x	x	x	
Q14847	x	x	x	x	x	x	Q5QNW6	x	x	x	x	x	x	Q8IYT4	x	x	x	x	x	x	Q96F85	x	x	x	x	x	x
Q14974	x	x	x	x	x	x	Q5SSJ5	x	x	x	x	x	x	Q8IZ83	x	x	x	x	x	x	Q96FN4	x	x	x	x	x	x
Q15008	x	x	x	x	x	x	Q5SZU1	x	x	x	x	x	x	Q8N357	x	x		x	x	x	Q96FZ7	x	x	x	x	x	x
Q15012	x	x	x	x	x	x	Q5T091						x	Q8N8Y2	x	x	x	x	x	x	Q96G03	x	x	x	x	x	x
Q15019	x	x	x	x	x	x	Q5T1M3	x	x	x	x	x	x	Q8NBI5	x	x	x	x	x	x	Q96KP4	x	x	x	x	x	x
Q15029	x	x	x	x	x	x	Q5T4S7	x	x	x	x	x	x	Q8NC51					x		Q96P70	x	x	x	x	x	x
Q15043	x	x	x	x	x	x	Q5T749	x	x	x	x	x	x	Q8ND76	x		x	x	x	x	Q96QD8	x	x	x	x	x	x
Q15058	x	x	x	x	x	x	Q5T750	x	x	x	x	x	x	Q8NG11	x	x	x	x	x	x	Q96QK1	x	x	x	x	x	x
Q15084	x	x	x	x	x	x	Q5T7F0	x	x	x	x	x	x	Q8TAD7					x		Q96S44	x		x	x	x	x
Q15149	x	x	x	x	x	x	Q5T8U7	x		x	x	x	x	Q8TB61	x					x	Q96S86	x	x	x	x	x	
Q15181	x	x	x	x	x	x	Q5T9B7		x	x	x	x	x	Q8TDN6					x		Q96S97	x	x	x	x	x	x
Q15185	x	x	x	x	x	x	Q5TZA2	x	x	x	x	x	x	Q8TF09			x	x	x	x	Q96T76	x			x		x
Q15233	x	x	x	x	x	x	Q5VW32	x	x	x	x	x	x	Q8WUM4	x	x	x	x	x	x	Q96TA1	x	x	x	x	x	x
Q15286	x	x	x	x	x	x	Q5VYK3	x	x	x	x	x	x	Q8WUN7	x		x	x	x	x	Q99426	x			x	x	x
Q15363		x	x	x	x	x	Q5W0H4	x	x	x	x	x	x	Q8WV92	x	x	x	x	x	x	Q99436	x	x	x	x	x	x
Q15365	x	x	x	x	x	x	Q6DD88	x	x	x	x	x		Q8WWI5	x	x	x	x	x	x	Q99460	x	x	x	x	x	x
Q15369			x	x	x	x	Q6NZI2	x	x	x	x	x	x	Q8WXH0	x	x	x	x	x	x	Q99497	x	x	x	x	x	x
Q15370	x	x	x	x	x	x	Q6P1R4	x	x	x	x	x	x	Q92499	x	x	x	x	x	x	Q99523	x		x	x	x	x
Q15382	x	x	x	x	x	x	Q6P2Q9	x	x	x	x	x	x	Q92520	x	x		x	x	x	Q99536	x	x	x	x	x	x
Q15393	x	x	x	x	x	x	Q6TDU7	x	x	x	x	x	x	Q92522	x	x	x	x	x	x	Q99584			x			x
Q15404	x	x	x	x	x	x	Q6UVK1	x	x	x	x	x	x	Q92542	x	x	x	x	x	x	Q99613	x	x	x	x	x	x
Q15436	x	x	x	x	x	x	Q6UXN9			x		x	x	Q92598	x	x	x	x	x	x	Q99685	x	x	x	x	x	x
Q15582	x	x	x	x			Q6VAB6						x	Q92608			x		x	x	Q99729	x	x	x	x	x	x
Q15631	x	x	x	x	x	x	Q6YHK3	x	x	x	x	x	x	Q92616	x		x	x	x	x	Q99733	x	x	x	x	x	x
Q15758	x	x	x	x	x	x	Q6ZS74	x	x	x	x	x	x	Q92626	x	x	x	x	x	x	Q99805	x	x	x	x	x	x
Q15819	x	x	x	x	x	x	Q6ZUX7	x	x	x	x	x	x	Q92633	x	x	x	x	x	x	Q99808	x	x	x	x	x	x
Q15836	x	x	x	x	x	x	Q71DI3	x	x	x	x	x	x	Q92734	x	x	x	x	x	x	Q99816	x	x	x	x	x	x
Q16181	x	x	x	x	x	x	Q71U36	x	x	x	x	x	x	Q92743	x	x	x	x	x	x	Q99829	x	x	x	x	x	x
Q16401	x	x	x	x	x	x	Q71UM5	x	x	x	x	x	x	Q92769	x	x	x	x	x	x	Q99832	x	x	x	x	x	x
Q16531	x	x	x	x	x	x	Q75T13	x	x	x	x	x	x	Q92783	x		x	x	x	x	Q99873	x	x	x	x	x	x
Q16543	x	x	x	x	x	x	Q7KYR7	x	x	x	x	x	x	Q92841	x	x	x	x	x	x	Q99973	x		x	x		
Q16555	x	x	x	x	x	x	Q7KZF4	x	x	x	x	x	x	Q92896	x	x	x	x	x	x	Q9BPX3	x	x	x	x	x	x
Q16576	x	x	x	x	x	x	Q7L1Q6	x		x	x	x	x	Q92900	x		x	x	x		Q9BQE3	x	x	x	x	x	x
Q16629	x	x	x	x	x	x	Q7L2H7	x	x	x	x	x	x	Q92930	x	x	x	x	x	x	Q9BRF8	x	x	x	x	x	x
Q16643			x			x	Q7L576	x	x	x	x	x	x	Q92973	x	x	x	x	x	x	Q9BSJ2	x	x	x	x	x	x
Q16658	x	x	x	x	x	x	Q7L5D6	x		x	x	x	x	Q92982	x	x	x	x	x	x	Q9BSJ8	x	x	x	x	x	x
Q16666	x			x	x	x	Q7L9L4	x			x	x	x	Q93008	x	x	x	x	x	x	Q9BTW9	x		x	x	x	
Q16851	x	x	x	x	x	x	Q7LBR1		x	x		x	x	Q969E2	x	x	x	x	x	x	Q9BUB4	x					
Q1KMD3	x		x	x	x	x	Q7Z304	x		x	x		x	Q969P0	x	x	x	x	x	x	Q9BUF5	x	x	x	x	x	x
Q29963	x	x	x	x	x	x	Q7Z406	x	x	x	x	x	x	Q969Q0	x	x	x	x	x	x	Q9BVK6	x	x	x	x	x	x
Q2L7G6	x	x	x	x	x	x	Q7Z5G4	x	x	x	x	x	x	Q969X1	x	x	x	x	x	x	Q9BWD1	x	x	x	x	x	x
Q2M389	x	x	x	x	x	x	Q7Z7A1						x	Q96A72	x	x	x	x	x	x	Q9BX67	x	x	x	x	x	
Q32Q12	x	x	x	x	x	x	Q7Z7G0	x	x	x	x	x	x	Q96AC1	x	x	x	x	x	x	Q9BYE4	x	x	x	x	x	
Q3ZCM7	x	x	x	x	x	x	Q86VP6	x	x	x	x	x	x	Q96AK3	x		x	x	x	x	Q9BYT8	x		x	x	x	x
Q53EZ4	x	x	x	x	x	x	Q8IUE6	x	x	x	x	x	x	Q96AM1	x	x	x	x	x	x	Q9BZG1	x	x	x	x	x	x
Q53FA7	x	x	x	x	x	x	Q8IVF7	x	x	x	x	x	x	Q96BY6	x	x	x	x	x	x	Q9BZQ8	x	x	x	x	x	x

	NMOB-EV			MOB-EV		
Accession	**5**	**12**	**19**	**5**	**12**	**19**
Q9C0H2	x	x	x	x	x	x
Q9GZN7				x		
Q9H0H5				x	x	x
Q9H0P0						x
Q9H0U4	x	x	x	x	x	x
Q9H1C7	x	x	x	x	x	x
Q9H223	x	x	x	x	x	x
Q9H444	x	x	x	x	x	x
Q9H4A4	x	x	x	x	x	x
Q9H4G4	x	x	x	x	x	x
Q9H4M9	x	x	x	x	x	x
Q9H5V8	x	x	x	x	x	x
Q9H8M9	x	x	x	x	x	x
Q9H9H4			x	x	x	x
Q9HA64	x	x	x	x	x	x
Q9HAV0	x	x	x	x	x	x
Q9HAV4	x		x	x	x	x
Q9HB71	x	x	x	x	x	x
Q9HC07	x	x	x	x	x	x
Q9HC38	x	x	x	x	x	x
Q9HCE0						x
Q9HD42					x	x
Q9HD45		x	x		x	x
Q9NP72	x	x	x	x	x	x
Q9NP79	x	x	x	x	x	x
Q9NPA8			x		x	x
Q9NPD3	x		x	x	x	x
Q9NQC3	x	x	x	x	x	x
Q9NQW7	x	x	x	x	x	x
Q9NR30	x	x	x	x	x	x
Q9NR31	x	x	x	x	x	x
Q9NR45	x	x	x	x	x	x
Q9NRN7	x	x		x		
Q9NRV9	x	x	x	x	x	x
Q9NRY6	x	x	x	x	x	x
Q9NSD9	x	x	x	x	x	x
Q9NTJ3	x	x	x	x	x	x
Q9NTK5	x	x	x	x	x	x
Q9NUQ9	x	x	x	x	x	x
Q9NVA2	x	x	x	x	x	x
Q9NVJ2	x	x	x	x	x	x
Q9NVP1						x
Q9NX76	x	x	x	x	x	x
Q9NY33	x		x	x	x	
Q9NZM1	x	x	x	x	x	x
Q9NZN4	x	x	x	x	x	x
Q9P003	x		x	x	x	x
Q9P1F3	x	x	x	x	x	x
Q9P225	x	x	x	x	x	x
Q9P265	x	x	x	x	x	x

	NMOB-EV			MOB-EV		
Accession	**5**	**12**	**19**	**5**	**12**	**19**
Q9P273	x	x	x	x	x	x
Q9P2B2	x	x	x	x	x	x
Q9P2J5	x	x	x	x	x	x
Q9P2R3	x	x	x	x	x	x
Q9UBG0	x	x	x	x	x	x
Q9UBG3	x	x	x	x	x	x
Q9UBI1	x		x	x	x	x
Q9UBI6	x	x	x	x	x	x
Q9UBL6				x	x	x
Q9UBQ0	x	x	x	x	x	x
Q9UBQ5	x	x	x	x	x	x
Q9UBQ7	x	x	x	x	x	x
Q9UBV8	x	x	x	x	x	x
Q9UDY4	x		x	x	x	x
Q9UGI0		x			x	
Q9UHB9	x	x	x	x	x	x
Q9UHD8	x	x	x	x	x	x
Q9UIA9	x	x	x	x	x	x
Q9UIQ6	x	x	x	x	x	x
Q9UIW2	x	x	x	x	x	x
Q9UJ70	x	x	x	x	x	x
Q9UK41	x	x	x	x	x	x
Q9UKD2	x		x	x	x	x
Q9UKK3	x	x	x	x	x	x
Q9UKK9	x	x	x	x	x	x
Q9UKS6	x	x	x	x	x	x
Q9UL25	x	x	x	x	x	x
Q9UL26	x		x	x	x	x
Q9UL46	x	x	x	x	x	x
Q9ULC3	x	x	x	x	x	x
Q9ULV4	x	x	x	x	x	x
Q9UMS4	x	x	x	x	x	x
Q9UN37	x	x	x	x	x	x
Q9UN86			x	x	x	x
Q9UNF0	x	x	x	x	x	x
Q9UNM6	x	x	x	x	x	x
Q9UPR3			x	x	x	x
Q9UQ80	x	x	x	x	x	x
Q9UQE7	x	x	x	x	x	x
Q9UQN3	x	x	x	x	x	x
Q9Y230	x	x	x	x	x	x
Q9Y262	x	x	x	x	x	x
Q9Y265	x	x	x	x	x	x
Q9Y281	x	x	x	x	x	x
Q9Y285	x	x	x	x	x	x
Q9Y287	x		x	x	x	x
Q9Y2A7	x	x	x	x	x	x
Q9Y2E4			x			x
Q9Y2L1			x	x	x	x
Q9Y2X3	x	x	x	x	x	x

	NMOB-EV			MOB-EV		
Accession	**5**	**12**	**19**	**5**	**12**	**19**
Q9Y315	x		x	x	x	x
Q9Y376	x	x	x	x	x	x
Q9Y3E7	x	x	x	x	x	x
Q9Y3F4	x	x	x	x	x	x
Q9Y3I0	x	x	x	x	x	x
Q9Y3L5	x	x	x	x	x	x
Q9Y3U8	x	x	x	x	x	x
Q9Y3Z3	x	x	x	x	x	x
Q9Y490	x	x	x	x	x	x
Q9Y4F1	x	x	x	x	x	x
Q9Y5B9	x	x	x	x	x	x
Q9Y5K8	x	x	x	x	x	x
Q9Y5P6	x	x	x	x	x	x
Q9Y5S9	x	x	x	x	x	x
Q9Y5X1			x	x	x	x
Q9Y624	x	x	x	x	x	x
Q9Y639	x	x	x	x	x	x
Q9Y696	x	x	x	x	x	x
Q9Y6C2	x	x	x	x	x	x
Q9Y6K5	x	x	x	x	x	x

Appendix A

Table A2. The list of osteoblast-related GO annotations based on the EV proteins shared by all EV groups.

GO Term	Count[a)]	Gene Symbol[b)]
Calcium ion binding (GO:0005509)	64	*ANXA2* *S100A6* *CANX*
Extracellular matrix (GO:0031012)	23	*COL1A1* *FN1* *LAMB1*
Skeletal system development (GO:0001501)	16	*ALPL* *COL1A* *EGFR*
Phosphatase activity (GO:0016791)	11	*CYCS* *PPP1CC* *ALPL*
Steroid hormone receptor signaling pathway (GO:0030518)	7	*DNAJA1* *FHL2* *CALR*
Vitamin binding (GO:0019842)	7	*PDXK* *GOT1/2* *FASN*
Mesenchymal cell differentiation (GO:0048762)	3	*CDL1* *CTNNB1* *HNRNPAB*
Collagen metabolic process (GO:0032963)	3	*PEPD* *COL1A1* *BASP1*

[a)] The total number of proteins annotated to the given GO term. [b)] Official gene symbols of exemplary proteins for each GO term.

Table A3. The list of up- and/or down-regulated (≥ 1.5-fold) PC3 genes in response to day 12 NMOB-EVs or MOB-EVs.

NMOB-EV Regulated PC3 Genes	**Up-regulated PC3 Genes**
	ALPP[a, b], *C14ORF153*, *C7ORF54*, *CENPE*, *DMC1*, *GUSBL1*, *HS.276854*, *HS.553301*, *HS.555252*, *HS.579631*, *LOC100128266*, *LOC23117*, *LOC728499*, *LOC728888*, *LOC729978*, *LOC92755*, *NBPF20*, *RPS17*, *RPS6KA3*
	Down-regulated PC3 Genes
	ATP1B1, *BMS1P5*, *C14ORF85*, *C19ORF10*, *C2ORF69*, *CATSPER2*, *CCBE1*, *CHRNA5*, *CSF2RA*, *DAPP1*, *DEM1*, *DTWD2*, *FAM119A*, *FCF1*, *FLJ36131*, *FLJ46309*, *FTHL12*, *FTHL8*, *GMNN*, *HS.544637*, *IL17RD*, *KCNH6*, *LMOD3*, *LOC100008588*, *LOC100128062*, *LOC100128098*, *LOC100128505*, *LOC100129362*, *LOC100130445*, *LOC100131718*, *LOC100132394*, *LOC100132585*, *LOC100133516*, *LOC100133649*, *LOC100133772*, *LOC100134159*, *LOC100134364*, *LOC100190938*, *LOC389517*, *LOC389765*, *LOC399900*, *LOC644745*, *LOC645452*, *LOC646786*, *LOC648210*, *LOC653086*, *LOC653489*, *LOC728809*, *LOC728903*, *LOC729090*, *LOC730278*, *LOC90586*, *MCART1*, *PAK2*, *PDE4C*, *PPA2*, *RRP1*, *SDHALP1*, *SFRS5*, *SLC44A4*, *SLC4A5*, *SPTLC1*, *SULT1A1*, *TDP1*, *TMEM17*, *TNFSF14*, *TRMT2B*, *USP49*, *VPS41*, *XRCC2*, *YWHAG*, *ZMAT3*, *ZNF428*, *ZNF486*, *ZNF682*
	Up-and-down-regulated PC3 Genes
	C15ORF63, *IL10*, *C21ORF58*, *CDKN2AIPNL*
MOB-EV Regulated PC3 Genes	**Up-regulated PC3 Genes**
	AK1, *ALDOA*, *C14ORF4*, *CCDC85B*, *CDCP1*, *CDK5*, *CXORF64*, *EEF1D*, *GAMT*, *HIST1H2BK*, *HNRNPH1*, *LOC100134265*, *LOC645058*, *LOC652595*, *LOC728188*, *LOC728499*, *LRFN3*, *NCKAP1*, *OPN3*, *PARD6A*, *PMVK*, *SPOP*, *THBS1*, *TPT1*, *TUBB2C*, *TUBG1*
	Down-regulated PC3 Genes
	DBI, *FLNA*, *FTHL8*, *HMMR*, *HS.535360*, *HSPE1*, *LOC100128410*, *LOC100129028*, *LOC100129379*, *LOC100129685*, *LOC100130070*, *LOC100131205*, *LOC391833*, *LOC392285*, *LOC402644*, *LOC440595*, *LOC441481*, *LOC644799*, *LOC645979*, *LOC646688*, *LOC648210*, *LOC649009*, *LOC651202*, *LOC653156*, *LOC728481*, *LOC728553*, *LOC728590*, *LOC91561*, *MRPL19*, *MRPL36*, *MYO1B*, *NAP1L1*, *NCBP2*, *PBK*, *RAD21*, *RDX*, *RGS7*, *RPL14*, *RPL23*, *RRN3*, *SRP72*, *STAG3L3*, *TSPAN13*, *UAP1*, *VPS24*, *WTAP*, *ZC3H15*, *ZNF146*, *ZNF281*
	Up-and-down-regulated PC3 Genes
	SMG1

[a] Official gene symbols. [b] PC3 genes that show different regulation pattern after 4, 24 and 48 hours of EV treatment.

Appendix A

Table A4. EV-RNA yield expressed as relative RNA amount (ng) per mL of conditioned medium (CM) or relative RNA amount (pg) per 10^6 cells seeded on day 0 (N = 3).

Sample	RNA Yield (ng/ mL CM)	RNA Yield (pg/ 10^6 cells)
EV_A	30.47	2.44
EV_B	37.20	2.98
EV_C	30.68	2.45

Table A5. Correlation analysis. Coefficients of determination (R^2) show the strength of the correlation between the replicates.

Sample	R^2	Sample	R^2	Sample	R^2
EV_A - EV_B	0.8058	OB_A - OB_B	0.9732	EV_A - OB_A	0.7113
EV_A - EV_C	0.8415	OB_A - OB_C	0.9747	EV_B - OB_B	0.7449
EV_B - EV_C	0.8704	OB_B - OB_C	0.9695	EV_C - OB_C	0.8142

Table A6. The list of EV-mRNAs significantly ($P < 0.05$) enriched (≥ two-fold) in osteoblast-EVs compared to the cells. FC, fold change.

GeneID	FC	*P* value	GeneID	FC	*P* value	GeneID	FC	*P* value	GeneID	FC	*P* value
RAB13	117.19	0.03989	EPB41L4A	10.27	0.00079	PNN	5.84	0.00549	SAP18	4.44	0.02514
ARRDC4	49.85	0.00366	PTPN11	9.98	0.00363	NBPF16	5.74	0.02479	HIRIP3	4.42	0.01210
NEFM	43.09	0.01461	HNRNPH3	9.56	0.01398	SYNJ2BP	5.62	0.04265	WDR60	4.38	0.01422
IGIP	41.36	0.00070	NSRP1	9.55	0.00137	CWC27	5.61	0.02645	ZNF850	4.38	0.04640
NET1	38.48	0.00044	EFCAB2	9.50	0.00685	MAP4K4	5.60	0.03780	NEXN	4.32	0.00341
RASSF3	37.72	0.00155	TAF15	8.82	0.04099	KIF3B	5.52	0.03980	MYEF2	4.27	0.00243
HMGN5	34.79	0.02288	MYOZ3	8.72	0.04723	CYP1B1	5.37	0.01694	SYNM	4.12	0.04630
TRAK2	33.71	0.01144	EIF5B	8.57	0.00014	PRPF38B	5.28	0.00069	SREK1	4.10	0.02771
ESF1	25.28	0.00798	TCEAL4	8.29	0.02830	HIST1H2BO	5.15	0.04023	RNF20	4.07	0.00946
ZEB1	24.95	0.01027	TCEAL3	7.99	0.02340	UPF3A	5.15	0.00883	CRTAP	4.07	0.04272
PITPNM3	24.81	0.04366	TCEAL2	7.97	0.02409	APOBEC3D	5.14	0.03880	PAIP2B	4.06	0.03262
ANP32B	23.28	0.00039	TTLL11	7.91	0.04326	NFKBIB	5.10	0.01806	HMHA1	4.05	0.01920
ARHGAP11A	20.81	0.00968	NEFL	7.83	0.00507	LPAR1	5.10	0.00340	HES4	4.01	0.00392
GDF11	20.68	0.02750	KCNK6	7.69	0.03190	FAIM	5.08	0.00532	HIST1H4H	3.94	0.04654
CGNL1	19.04	0.04207	SAMD4A	7.62	0.01601	RBM25	5.05	0.00832	CDK11A	3.94	0.01097
CACNG8	18.02	0.04924	GPATCH4	7.61	0.00286	EIF3A	5.03	0.01457	PPP1R3C	3.92	0.02899
BCL2L2	17.93	0.03936	SCG5	7.57	0.03706	CHAF1A	4.94	0.02494	LUC7L3	3.83	0.01093
LACC1	17.29	0.00220	ZBTB47	7.29	0.03058	HTATSF1	4.85	0.00318	WWTR1	3.81	0.00295
C7orf41	16.18	0.00934	TRAF3IP1	7.25	0.00905	HIST1H2BH	4.81	0.01648	PHF14	3.80	0.01003
NUDT16	16.05	0.02621	CHCHD7	7.00	0.01920	ZNF677	4.80	0.03522	METTL8	3.78	0.02957
ERG	14.37	0.00059	CA11	6.82	0.02844	ANP32A	4.79	0.02467	DNASE1	3.72	0.01570
TP53INP2	14.14	0.04779	GXYLT1	6.68	0.00034	CDK11B	4.76	0.04841	SET	3.71	0.01088
ASPHD1	12.85	0.00275	CCDC34	6.51	0.03558	PALLD	4.74	0.00254	HIST1H3D	3.67	0.00793
UACA	12.44	0.00199	FAM18B2	6.50	0.01580	HNRNPA3	4.73	0.00526	SLC9A3R2	3.66	0.01959
DYNC1LI2	12.05	0.00357	ANP32E	6.26	0.00367	TCEANC2	4.68	0.02317	FAM101B	3.64	0.00769
HIST1H1E	11.88	0.02896	SNX22	6.18	0.00242	ZEB2	4.66	0.00583	SLC25A34	3.63	0.04629
PKP4	11.51	0.01196	CCND2	6.17	0.02208	TAF3	4.64	0.03071	ROM1	3.63	0.01222
PSMC3IP	11.51	0.00725	ARRDC2	6.01	0.00013	NAP1L1	4.54	0.01574	RAI14	3.59	0.03388
CCDC148	11.28	0.02561	UPF3B	5.98	0.00188	PARD3B	4.50	0.04720	RNF207	3.56	0.02501
ZNF326	10.62	0.00100	CENPB	5.92	0.02211	MAP1B	4.50	0.01578	NANOS1	3.52	0.00915

GeneID	FC	*P* value	GeneID	FC	*P* value	GeneID	FC	*P* value
LRRC34	3.49	0.03804	CDO1	2.79	0.01827	PTPN2	2.25	0.04113
ANKRD18B	3.46	0.01034	POMC	2.78	0.01149	APOL3	2.23	0.03320
APOL2	3.44	0.00894	RHOD	2.77	0.02006	UPF2	2.22	0.00913
ANKDD1A	3.43	0.02275	KTN1	2.77	0.00871	UFM1	2.22	0.01933
HNRNPA1	3.43	0.04890	C2orf63	2.75	0.01346	RASSF7	2.21	0.02186
MESP1	3.41	0.02638	DNAJC21	2.75	0.01956	MIIP	2.20	0.03658
METAP2	3.39	0.01961	AQP3	2.74	0.00559	CCAR1	2.20	0.00531
ZNF585B	3.37	0.02610	KIAA1377	2.74	0.01723	FBXO32	2.19	0.03563
TSR2	3.37	0.01228	LARP7	2.73	0.04883	RINL	2.19	0.03102
TAF7L	3.36	0.02204	ZNF814	2.72	0.01280	KRT10	2.19	0.03254
ACBD3	3.36	0.00909	C18orf56	2.71	0.02864	PPDPF	2.19	0.02935
GADD45A	3.34	0.00927	KATNAL1	2.70	0.00318	FGF1	2.18	0.01238
ZNF707	3.33	0.01155	NUDT14	2.67	0.03389	PPIG	2.18	0.01174
TTC25	3.33	0.01837	AGAP2	2.64	0.00559	XDH	2.18	0.00295
SRSF12	3.28	0.04205	ENAH	2.63	0.04736	ST13	2.15	0.03153
CDKL3	3.27	0.04774	HABP4	2.62	0.00041	BFSP1	2.14	0.01275
TREM2	3.27	0.04236	MFAP1	2.59	0.01479	RAB4A	2.13	0.03136
MSX1	3.25	0.03556	SEPT7	2.59	0.01236	ATXN3	2.12	0.03498
IL18	3.23	0.04630	HOXB7	2.59	0.00004	SIRT4	2.11	0.00965
CEP19	3.22	0.04448	CALD1	2.58	0.00320	MAFF	2.10	0.00128
CCND1	3.20	0.04860	IL17RE	2.57	0.01686	ADSSL1	2.10	0.02055
WDR43	3.20	0.00240	GGPS1	2.57	0.04253	FRAT2	2.09	0.02667
ARMCX3	3.18	0.00140	FRA10AC1	2.55	0.03590	PSIP1	2.09	0.00388
BDP1	3.18	0.00624	SOX11	2.54	0.04741	ZNF880	2.08	0.02382
PGF	3.15	0.00411	FGFBP3	2.54	0.01106	IK	2.06	0.00835
DNAJC2	3.13	0.02260	SBSN	2.53	0.04817	PPID	2.05	0.01439
PINK1	3.12	0.00496	AP4S1	2.52	0.01915	OPTN	2.05	0.00289
NCL	3.10	0.03721	CFDP1	2.51	0.04925	CD3EAP	2.04	0.04628
SLC16A12	3.10	0.03821	LMOD1	2.48	0.00475	MAP3K13	2.02	0.02914
CCDC152	3.08	0.03877	LYRM7	2.46	0.02442	ABCA10	2.02	0.01909
DDX46	3.08	0.00113	HAGHL	2.46	0.02701	TNFAIP8L1	2.02	0.03529
ZNF283	3.07	0.03048	SLC4A5	2.45	0.00351	GTPBP10	2.01	0.03033
SLTM	3.06	0.02966	EPM2A	2.43	0.02194	CNTNAP2	2.01	0.02551
GOLGA4	3.06	0.02651	ZNF487P	2.39	0.03670	CCDC66	2.00	0.02740
ZNHIT6	3.05	0.04097	CEP63	2.38	0.01549			
RPGR	3.00	0.00865	FLT3LG	2.37	0.00260			
RRP15	3.00	0.03886	ORMDL3	2.37	0.01343			
HDGFRP3	2.99	0.01516	ISY1	2.37	0.04690			
YTHDC1	2.99	0.03663	ZNF790	2.37	0.00477			
ZCWPW1	2.98	0.04469	CHCHD10	2.35	0.03256			
ZNF846	2.98	0.00288	DGCR6	2.35	0.00986			
FAM82B	2.94	0.02289	SOCS4	2.33	0.01827			
IFI44L	2.92	0.01260	ENHO	2.33	0.01452			
NPAS1	2.90	0.00757	CEBPZ	2.32	0.03277			
YES1	2.87	0.03825	PABPC1	2.32	0.01825			
IFT74	2.85	0.00223	CCDC91	2.32	0.01536			
CEP70	2.85	0.00125	KIN	2.32	0.03838			
TNNT1	2.83	0.02187	GPS2	2.30	0.01134			
MALL	2.81	0.01170	CCDC41	2.30	0.04670			
RBM17	2.80	0.02804	HSBP1L1	2.28	0.00973			

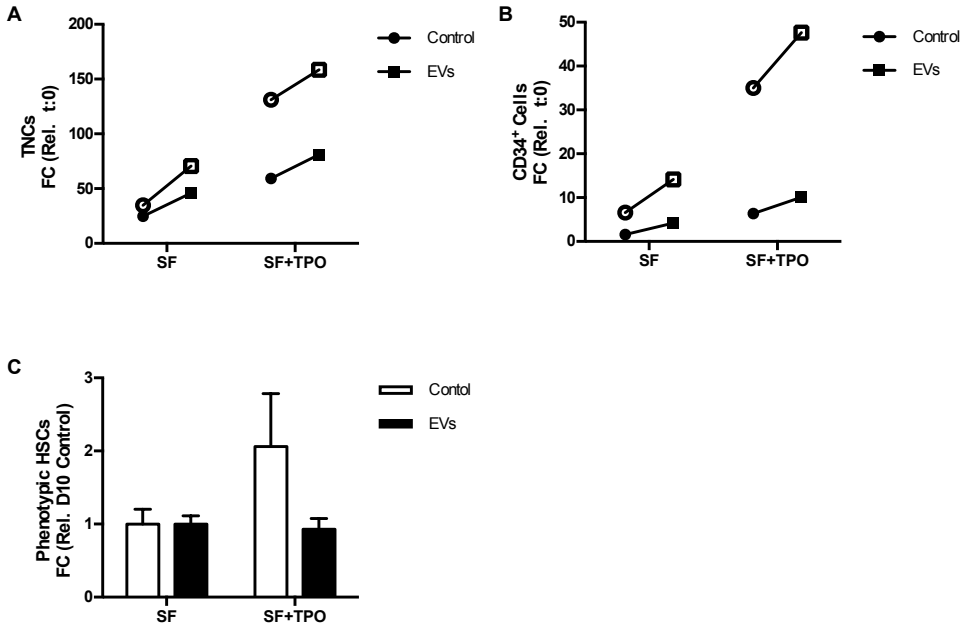

Figure A1. A-B) Osteoblast-EVs increase the *ex vivo* expansion of (A) TNCs and (B) $CD34^+$ cells after 10 days of expansion with SCF, Flt3L and TPO compared to control (N = 2). Expansion is shown as fold change (FC) increase in total cell number compared to input. Empty and full shapes show the different donors. C) The fold change (mean ± SD) of phenotypic HSCs compared to control on day 10 (N = 2).

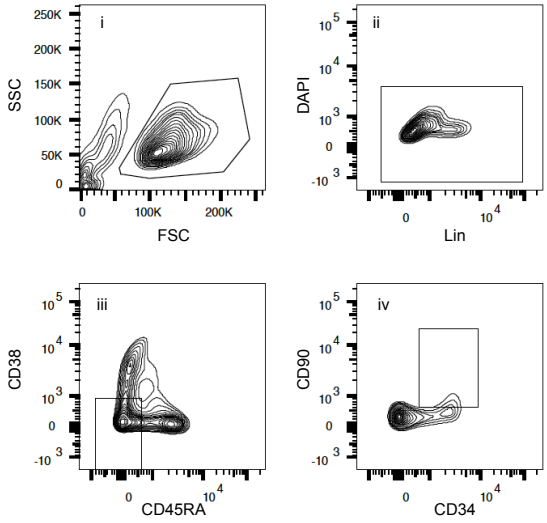

Figure A2. Flow cytometric gating strategy for phenotypic HSCs.

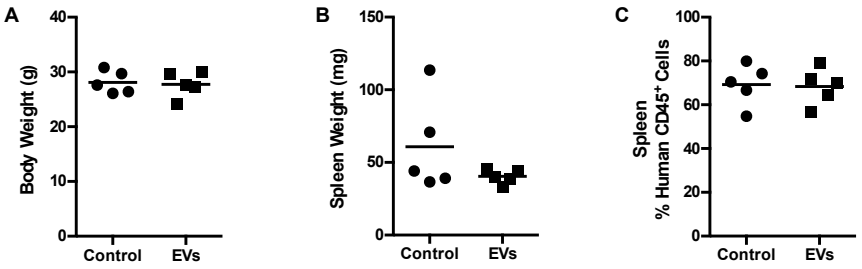

Figure A3. A-B) Analysis of mice (A) body and (B) spleen weight 21 weeks post-injection. C) Human chimerism level in the spleen after 21 weeks (N = 5 mice/ group).

Appendix B

ABBREVIATION INDEX

AFM	Atomic force microscopy
ALPL	Alkaline phosphatase, liver/bone/kidney
α-MEM	Alpha- Minimum Essential Medium
ANXA2	Annexin A2
ATP5E	ATP synthase subunit epsilon, mitochondrial
BCL2	B-cell lymphoma 2
BCL3	B-cell lymphoma 3-encoded protein
BCP	B-cell progenitor
BSA	Bovine serum albumin
CD	Cluster of differentiation
CDC42EP2	Cdc42 effector protein 2
CFU	Colony forming unit
CMP	Common myeloid progenitor
CLP	Common lymphoid progenitor
COL1A1	Collagen type I alpha 1
CPM	Counts per million
CT	Cycle threshold
CV	Coefficient of variance
CYSLTR2	Cysteinyl leukotriene receptor 2
DAPI	4’,6-diamidino-2-phenylindole
DAVID	Database for Annotation, Visualization and Integrated Discovery
DNA	Deoxyribonucleic acid
EGR1	Early growth response protein 1
ELN	Elastin
EDTA	Ethylenediaminetetraacetic acid
ESCRT	Endosomal sorting complex required for receptor transport
EVs	Extracellular vesicles
FACS	Fluorescence-activated cell sorting
FC	Fold change
FCS	Fetal calf serum
FDR	False discovery rate
FITC	Fluorescein isothiocyanate
Flt3L	Fms-related tyrosine kinase 3 ligand
FU	Fluorescence units
GAPDH	Glyceraldehyde 3-phosphate dehydrogenase
GBGM	Glycostem Basic Growth Medium
GM-CSF	Granulocyte-macrophage colony-stimulating factor
GMP	Granulocyte–macrophage progenitor
GO	Gene Ontology
GVHD	Graft-versus-host disease
HBP1	HMG-box transcription factor 1
HEK 293	Human Embryonic Kidney 293 cells
HSCs	Hematopoietic stem cells
HSPCs	Hematopoietic stem and progenitor cells
iBAQ	Intensity-based absolute quantification
IL-6	Interleukin 6
IPA	Ingenuity pathway analysis
ITGAX	Integrin, alpha X
kDa	Kilodalton
LC-MS	Liquid chromatography–mass spectrometry

LFQ	Label-free quantification
MAOA	Monoamine oxidase A
MEP	Megakaryocyte erythroid progenitor
mRNA	Messenger RNA
miRNA	MicroRNA
MOBs	Mineralizing osteoblasts
MSCs	Mesenchymal stem cells
MVs	Matrix vesicles
MVBs	Multivesicular bodies
NFIB	Nuclear factor 1 B-type
NMOBs	Non-mineralizing osteoblasts
NSG	Next-generation sequencing
NTA	Nanoparticle tracking analysis
OBs	Osteoblasts
PBS	Phosphate-buffered saline
PC3	Human prostate cancer cell lines
PI	Propidium iodide
PTEN	Phosphatase and tensin homolog
qPCR	Quantitative polymerase chain reaction
RAB13	Ras-related protein Rab-13
RNA	Ribonucleic acid
RNase	Ribonuclease
RPKM	Reads per kilobase of transcript per million mapped reads
RPM	Revolutions per minute
rRNA	Ribosomal RNA
S100A9	S100 calcium-binding protein A9
SCF	Stem cell factor
SD	Standard deviation
SDS-PAGE	Sodium dodecyl sulfate polyacrylamide gel electrophoresis
snoRNA	Small nucleolar RNAs
SR1	StemRegenin 1
SV-HFOs	Simian virus 40-immortalized human osteoblast cell line
TBS	Tris-buffered saline
TEM	Transmission electron microscope
TET2	Tet Methylcytosine Dioxygenase 2
TMM	Trimmed M-Means
TNK	T-cell natural killer cell progenitor
TPO	Thrombopoietin
U	Enzyme unit
UCB	Umbilical cord blood

Appendix C

PRIMER SEQUENCES

Gene Symbol	Forward Sequence (5' → 3')	Reverse Sequence (5' → 3')
ATP5E	AGACTTCTGGCAGCAACGTA	TGCCCACACATCTTCACCTT
BCL2	AGTACCTGAACCGGCACCT	ACAGTTCCACAAAGGCATCC
CDC42EP2	GTCCAGCTCCTGAGACCTTG	GCACTTTGGTCTTGTCACCG
COL1A1	GACATGTTCAGCTTTGTGGACC	TGATTGGTGGGATGTCTTCGT
CYSLTR2	GCAGCTGAAAGACAGAGACCT	CCATACCTTGCATGGACCTTCT
EGR1	AGCCCTACGAGCACCTGAC	TGGGTTGGTCATGCTCACTA
ELN	TCCCGGGAGTTGGCATTTC	CAAACTGGGCGGCTTTGG
GAPDH	CCGCATCTTCTTTTGCGTCG	CCCAATACGACCAAATCCGTTG
HBP1	CCTGTGATGAACACATGGAGC	TGGTACATGCCAGATTGGGT
ITGAX	CCTACGGAACCACCATCACC	ACATGTCAGGTGCAGGGAAC
MAOA	ATGACACCAAGCCAGATGGG	AAGTCGATCAGCTTTCCGGG
NFIB	GTCCAGCCACATCATATCACAG	TTGGCAGGATCATTGTGGCTT
PTEN	TGGATTCGACTTAGACTTGACCT	ACGCCTTCAAGTCTTTCTGC
RAB13	GAGGCCGGAGATCAGGAAAC	AGGGAGCACTTGTTGGTGTT
S100A9	GGAATTCAAAGAGCTGGTGCG	AGCTGCTTGTCTGCATTTGTG
TET2	AGCAGCAGCCAATAGGACAT	TTCCATCAGGCTTGCTTCGG

SUMMARY

Cell-to-cell communication plays an essential role in regulating homeostasis in multicellular organisms. Recent evidence indicates that cells effectively communicate via extracellular vesicles (EVs), which carry bioactive cargo, such as proteins, lipids and RNA, between cells. Bone is a complex organ consisting of a broad variety of cell types living in harmony within the favorable microenvironment of the bone marrow. The establishment of a proper communication network is key to ensure not only normal bone development but also many other vital physiological processes. In this thesis, we present a thorough characterization of the biochemical content of EVs secreted by human osteoblasts, study their biological significance in communication with the cells in the surrounding microenvironment, and investigate their potential application in stem cell therapy.

In **Chapters 2**, **3** and **4** we delineate the structural and regulatory cargo of osteoblast-derived EVs with a focus on identifying the cargo overrepresented in EVs. In **Chapter 2**, we present the EV protein content by mass spectrometry. We show the diversity of EV cargo depending on the stage of osteoblast differentiation and mineralization condition. Notably, EVs secreted by non-mineralizing osteoblasts, are depleted of biomineralization-related proteins suggestive of an activity independent of matrix vesicles. Instead, they are enriched with cell adhesion-associated extracellular matrix proteins and chromosomal proteins with regulatory potential. In **Chapter 3** and **4**, we present next-generation sequencing analyses to delineate the mRNA and miRNA content of EVs secreted by non-mineralizing osteoblasts. We define the RNA cargo selectively incorporated into EVs or depleted from EVs during their biogenesis. In **Chapter 3**, we show that EV-mRNAs mostly consist of genes encoding for proteins with ribosomal activities, while they lack the genes important to carry out vital cellular processes. In **Chapter 4**, we demonstrate that EV-miRNAs mostly consist of miRNAs involved in molecular functions related to growth and proliferation, including the well-characterized regulators of early hematopoiesis.

In **Chapters 2**, **4**, **5** and **6** we focus on the role of osteoblast-EVs as a mean of communication with the surrounding cells in the bone marrow microenvironment. In **Chapters 2** and **4** we demonstrate the molecular function of osteoblast-EVs by showing their proliferative effect on bone-metastasizing prostate cancer (PC3) cells and human umbilical cord blood (UCB)-derived $CD34^+$ hematopoietic stem and progenitor cells (HSPCs). Through transcriptomics studies in **Chapters 2 & 6** we confirm that EVs alter the expression of HSPC and PC3 genes important for cellular development and growth. We use integrated bioinformatics approach to explain the biological mechanism of EV function and delineate a list of candidate regulatory EV cargo predicted to target cell growth. In **Chapter 5**, we show the therapeutic potential of osteoblast-EVs by showing their potency to expand UCB-derived $CD34^+$ HSCPs in combination with hematopoietic growth factors in *ex vivo* culture systems. Notably, we show the success of using EVs as expansion agents to preserve the repopulating activity of UCB-$CD34^+$ HSPCs, necessary for hematopoietic recovery.

In conclusion, the findings described in this thesis provide insights into the complex osteoblast-EV-mediated communication network within the bone microenvironment. Biochemical analyses combined with *omics* studies identified overrepresented pathways and biological processes important for the regulation of target cells. Furthermore, *in vitro* and *in vivo* evaluations indicate the power of an osteoblast-EV-based novel strategy for clinically relevant *ex vivo* expansion of hematopoietic progenitor cells. Thorough biochemical and genetic analyses are of utmost importance to characterize the biologically active EV components, which will open up avenues for the use of EV as therapeutic tools for the treatment of a broad range of disorders.

SAMENVATTING

De communicatie tussen cellen speelt een belangrijke en essentiële rol in de regulatie van de homeostase van meercellige organismen. Recente studies hebben laten zien dat extracellulaire blaasjes (extra-cellulaire vesicles, EV's) een bioactieve vracht zoals eiwitten, lipiden en RNA bevatten en een belangrijke rol kunnen spelen in de communicatie tussen verschillende cellen in het lichaam. Botweefsel is een zeer complex orgaan dat uit veel verschillende cellen bestaat die alle met elkaar kunnen communiceren in het beenmerg en bot. Een goede intercellulaire communicatie is niet alleen essentieel voor een goede botontwikkeling maar ook voor vele andere vitale fysiologische processen. In dit proefschrift beschrijven we 1) de karakterisatie van de inhoud van EV's die afgescheiden worden door humane osteoblasten; 2) bestuderen we de biologische effecten van EV's in de communicatie met cellen die zich in de directe omgeving van osteoblasten bevinden; 3) onderzoeken we een mogelijke toepassingen van EV's in stamceltherapie.

In **hoofdstuk 2, 3 en 4** beschrijven we welke structurele en regulerende vracht oververtegenwoordigd is in EV's die afgescheiden worden door humane osteoblasten. In **hoofdstuk 2** bestuderen we door middel van massaspectrometrie de eiwit samenstelling van EV's. In dit hoofdstuk laten we zien dat de eiwitten die aanwezig zijn in EV's afhankelijk zijn van de differentiatie fase van de osteoblasten. EV's afgescheiden door niet-mineraliserende osteoblasten bevatten minder mineralisatie verwante eiwitten. Dit toont aan dat EV's die geproduceerd worden door osteoblasten nog andere functies kunnen hebben dan alleen de vorming van matrix blaasjes. In plaats daarvan zijn EV's van niet-mineraliserende osteoblasten verrijkt met cel bindende extracellulaire matrix eiwitten en chromosomale eiwitten met een regulerende functie. In **hoofdstuk 3 en 4** onderzoeken we welke RNA moleculen zich bevinden in EV's die worden afgescheiden door niet-mineraliserende osteoblasten. De analyse van next-generation sequencing data laat zien dat RNA moleculen selectief opgenomen worden tijdens de vorming van EV's. In **hoofdstuk 3** vinden we dat EV-mRNA voornamelijk bestaat uit mRNA moleculen die coderen voor ribosomale eiwitten, terwijl genen die belangrijk zijn vitale cellulaire processen afwezig zijn. Verder zien we in **hoofdstuk 4** dat EV-miRNAs voornamelijk bestaan uit miRNAs die betrokken zijn bij de groei en proliferatie van cellen, zoals goed gekarakteriseerde miRNAs die de vroege hematopoiese reguleren.

In **hoofdstuk 2, 4, 5 en 6** hebben we vervolgens onderzocht wat de effecten van EV's zijn op cellen die zich in de directe omgeving van osteoblasten bevinden. In de **hoofdstukken 2 en 4** laten we zien dat EV's afgescheiden door osteoblasten een proliferatief effect hebben op bot gemetastaseerde prostaatkankercellen (PC3) en $CD34^{+}$ hematopoetische stam- en voorlopercellen (HSPCs) uit humaan navelstrengbloed (UCB). Transcriptoom studies in de **hoofdstukken 2 en 6** bevestigen dat EV's de expressie van HSPC en PC3 genen kunnen veranderen die een belangrijke rol spelen bij de ontwikkeling en groei van cellen. Door middel van bioinformatica analyses hebben we een lijst van kandidaat

genen geïdentificeerd die aanwezig zijn in EV's en de effecten op de celgroei kunnen verklaren. Vervolgens bestuderen we in **hoofdstuk 5** de therapeutisch potentie van osteoblast-EV's. In een *ex vivo* kweeksystemen laten we zien dat EV's , in combinatie met hematopoetische groeifactoren, $CD34^+$ HSCPs voorlopercellen kunnen expanderen. Verder is het mogelijk om beenmerg opnieuw te laten bevolken met EV-geëxpandeerde UCB-$CD34^+$ HSPC voorlopercellen, wat noodzakelijk is voor het hematopoïetisch herstel.

Kortom, de in dit proefschrift beschreven resultaten geven meer zicht op het complexe osteoblast-EV-gemedieerde communicatie netwerk in het bot. Biochemische analyses gecombineerd met *omics* studies hebben nieuwe signaal paden en processen geïdentificeerd die van belang zijn voor de regulatie van de target cellen door EV's. Bovendien hebben de *in vitro* en *in vivo* experimenten meer inzicht gegeven op een nieuwe osteoblast-EV-gebaseerde strategie voor klinisch relevante *ex vivo* expansie van hematopoëtische voorlopercellen. Grondig uitgevoerde biochemische en genetische analyses zijn van groot belang voor de bepaling van de biologisch activiteit van EV's componenten en opent nieuwe mogelijkheden voor het gebruik van EV's als therapeutische middel voor de behandeling van een breed scala aan aandoeningen.

CURRICULUM VITAE

Jess Morhayim

18.09.1984	Born in Istanbul, Turkey
2004 - 2008	B.Sc. (Honours) *Molecular Genetics* University of Toronto, Toronto, Ontario, Canada
2008 - 2010	Erasmus Mundus Master of Nanoscience and Nanotechnology M.Sc. *Molecular Bioengineering* Dresden University of Technology, Dresden, Germany M.Sc. *Nanoscience* Leiden University, Leiden, the Netherlands
2010 - 2016	Ph.D. Research Calcium and Bone Metabolism Group Department of Internal Medicine Erasmus University Medical Center, Rotterdam, the Netherlands

Ph.D. PORTFOLIO

Name:	Jess Morhayim
Institute:	Erasmus University Medical Center, Rotterdam, the Netherlands
Department:	Internal Medicine
Group:	Calcium and Bone Metabolism
Ph.D. Period:	October 2010 - September 2016
Research School:	Postgraduate School Molecular Medicine
Supervisors:	Prof.dr. J.P.T.M. van Leeuwen
	Prof.dr. J.J. Cornelissen
Co-supervisor:	Dr.ing. J. van de Peppel

Ph.D. Training Activities

Courses and Workshops

2011	Molecular medicine course
	Regenerative medicine – from bench to bedside (module 5)
	Biomedical research techniques course
	Molecular and cellular basis of regenerative medicine (module 2)
2012	European Calcified Tissue Society Ph.D. training course
2013	Workshop presenting skills for junior researchers
	Basic introduction course on SPSS
2014	Molecular aspects of hematological disorders

(Inter)National Conferences

2010	The Netherlands Institute for Regenerative Medicine Symposium, Amsterdam
	Annual Meeting of the Dutch Society for Calcium and Bone, Zeist
2011	Internal Medicine Science Days, Antwerp, Belgium
	Molecular Medicine Day, Rotterdam
	Dutch Society for Stem Cell Research Meeting, Leiden
	Erasmus Stem Cell Institute Retreat (*Oral presentation*)
	Annual Meeting of the Dutch Society for Calcium and Bone, Zeist (*Oral presentation*)
2012	Internal Medicine Science Days, Antwerp, Belgium (*Poster presentation*)
	Molecular Medicine Day, Rotterdam (*Oral presentation*)

International Society for Extracellular Vesicles Meeting, Gothenburg, Sweden (*Poster presentation*)

International Society for Extracellular Vesicles RNA Seminar, New York City, USA (*Oral presentation*)

Annual Meeting of the Dutch Society for Calcium and Bone, Zeist (*Oral presentation*)

The Netherlands Institute for Regenerative Medicine Meeting, Amsterdam (*Poster presentation*)

2013 Internal Medicine Science Days, Antwerp, Belgium (*Poster presentation*)

International Society for Extracellular Vesicles Meeting, Boston, USA (*Oral presentation*)

International Conference on Children's Bone Health Meeting, Rotterdam (*Poster presentation*)

The Netherlands Institute for Regenerative Medicine Consortium Meeting, Utrecht (*Poster presentation*)

Annual Meeting of the Dutch Society for Calcium and Bone, Zeist (*Oral presentation*)

2014 Internal Medicine Science Days, Antwerp, Belgium (*Oral presentation*)

Molecular Medicine Day, Rotterdam (*Plenary poster presentation*)

International Society for Extracellular Vesicles Meeting, Rotterdam (*Oral presentation*)

Dutch Society for Stem Cell Research Meeting, Groningen (*Poster presentation*)

European Society of Gene and Cell Therapy Meeting, the Hague (*Poster presentation*)

The Netherlands Institute for Regenerative Medicine Consortium Meeting, Rotterdam (*Poster presentation*)

Annual Meeting of the Dutch Society for Calcium and Bone, Zeist (*Oral presentation*)

2015 Internal Medicine Science Days, Antwerp, Belgium (*Poster presentation*)

International Society for Extracellular Vesicles RNA Seminar, Utrecht

Teaching Activities

2012 M.Sc. Thesis: Pierre-Yves Helleboid

"Isolation and characterization of osteoblast-derived extracellular vesicles."

2012 M.Sc. Internship: Gulistan Kocer

"Effects of osteoblast-derived extracellular vesicles on prostate cancer cells."

2014 HLO Thesis: Dennis Kloots

"Investigation of osteoblast-derived extracellular vesicle microRNA content."

Awards

Best poster award: International Conference on Children's Bone Health Meeting (2013)

Best poster award: Internal Medicine Science Days (2015)

New investigator award: European Calcified Tissue Society (2015)

Best paper award: Annual Meeting of the Dutch Society for Calcium and Bone (2015)

"Proteomic signatures of extracellular vesicles secreted by non-mineralizing and mineralizing human osteoblasts and stimulation of tumor cell growth."

Other Activities

Weekly endocrinology lectures (2010 – 2015)

Organization of the Internal Medicine LabDay (2012)

Organization of the Erasmus MC extracellular vesicle meetings (2013 – 2015)

Organization of International Conference on Children's Bone Health Meeting (2013)

Chairing a session at the Annual Meeting of the Dutch Society for Calcium and Bone (2013)

Chairing a poster session at the International Society for Extracellular Vesicles Meeting (2014)

Committee member for the best presentation award at the Annual Meeting of the Dutch Society for Calcium and Bone (2014)

Related to this thesis:

Morhayim J, van de Peppel J, Braakman E, Dudakovic A, Chiba H, van Wijnen AJ, Cornelissen JJ, van Leeuwen JP. Identification of hematopoietic regulatory networks controlled by osteoblast-derived extracellular vesicles. *In progress*.

Morhayim J, van de Peppel J, Dudakovic A, Chiba H, van Wijnen AJ, van Leeuwen JP. Molecular characterization of human osteoblast-derived extracellular vesicle mRNA using next-generation sequencing. *Submitted*

Morhayim J, van de Peppel J, Braakman E, Rombouts EWJC, ter Borg MND, Dudakovic A, Chiba H, van der Eerden BCJ, Raaijmakers MH, van Wijnen AJ, Cornelissen JJ, van Leeuwen JP. Osteoblasts secrete miRNA-containing extracellular vesicles that enhance expansion of human umbilical cord blood cells. *Submitted*.

Morhayim J, Rudjito R, van Leeuwen JP, van Driel M. Paracrine signaling by extracellular vesicles via osteoblasts. 2016. Curr Mol Bio Rep. DOI 10.1007/s40610-016-0034-6

Kim DK, Lee J, Kim SR, Choi DS, Yoon YJ, Kim JH, Go G, Nhung D, Hong K, Jang SC, Kim SH, Park KS, Kim OY, Park HT, Seo JH, Aikawa E, Baj-Krzyworzeka M, van Balkom BW, Belting M, Blanc L, Bond V, Bongiovanni A, Borràs FE, Buée L, Buzás EI, Cheng L, Clayton A, Cocucci E, Dela Cruz CS, Desiderio DM, Di Vizio D, Ekström K, Falcon-Perez JM, Gardiner C, Giebel B, Greening DW, Gross JC, Gupta D, Hendrix A, Hill AF, Hill MM, Nolte-'t Hoen E, Hwang DW, Inal J, Jagannadham MV, Jayachandran M, Jee YK, Jørgensen M, Kim KP, Kim YK, Kislinger T, Lässer C, Lee DS, Lee H, van Leeuwen J, Lener T, Liu ML, Lötvall J, Marcilla A, Mathivanan S, Möller A, **Morhayim J**, Mullier F, Nazarenko I, Nieuwland R, Nunes DN, Pang K, Park J, Patel T, Pocsfalvi G, Del Portillo H, Putz U, Ramirez MI, Rodrigues ML, Roh TY, Royo F, Sahoo S, Schiffelers R, Sharma S, Siljander P, Simpson RJ, Soekmadji C, Stahl P, Stensballe A, Stępień E, Tahara H, Trummer A, Valadi H, Vella LJ, Wai SN, Witwer K, Yáñez-Mó M, Youn H, Zeidler R, Gho YS. EVpedia: A Community Web Portal for Extracellular Vesicles Research. 2015. Bioinformatics. 31: 933-939.

Morhayim J, van de Peppel J, Demmers JA, Kocer G, Nigg AL, van Driel M, Chiba H, van Leeuwen JP. Proteomic signatures of extracellular vesicles secreted by nonmineralizing and mineralizing human osteoblasts and stimulation of tumor cell growth. 2015. FASEB J. 29: 274-285.

Morhayim J, Baroncelli M, van Leeuwen JP. Extracellular vesicles: Specialized bone messengers. 2014. Arch Biochem Biophys. 561:38-45.

Previous publications:

Porta F, Lamers GE, **Morhayim J**, Chatzopoulou A, Schaaf M, den Dulk H, Backendorf C, Zink JI, Kros A. Folic acid-modified mesoporous silica nanoparticles for cellular and nuclear targeted drug delivery. 2013. Adv Healthc Mater. 2:281-286.

Robbins N, Collins C, **Morhayim J**, Cowen LE. Metabolic control of antifungal drug resistance. 2010. Fungal Genet Biol. 47:81-93.

ACKNOWLEDGEMENTS

This thesis presents not only the final step of my academic career, but it is a milestone that represents my development in more than a decade of work in scientific research. Throughout this time, I have been given unique opportunities to meet and work with remarkable people. In this last part of my thesis, I would like to acknowledge all these people who contributed to this work via directly helping me, inspiring me or simply supporting me all along.

First of all, I would like to thank you for showing interest in my thesis, perhaps reading it thoroughly, and hopefully learning something from it…

I would like to acknowledge all the members of my Ph.D. defence committee: Prof. Hans van Leeuwen, Prof. Jan Cornelissen, Dr. Jeroen van de Peppel, Prof. Guido Jenster, Prof. Joost Gribnau, Prof. Wim Fibbe (LUMC), Dr. Gabri van der Pluijm (LUMC), Dr. Carlijn Voermans (Sanquin) and Prof. Andre van Wijnen (Mayo Clinic).

I would like to express my sincere gratitude to my supervisor Hans. Thank you so much for giving me the opportunity to join your lab, encouraging my research and providing continuous support throughout my Ph.D. research. Your guidance and enthusiasm was a great motivation for me to grow as a research scientist.

I would like to express my special appreciation and thanks to my co-supervisor Jeroen. I could not have imagined having a better advisor and mentor for my Ph.D. experience. Thank you for being there every single day throughout my time in the lab, helping me out with every experiment, and giving your feedback on my manuscripts and chapters in this thesis. I appreciate all your contributions of time, ideas, and company to make my Ph.D. experience productive, stimulating and fun.

The members of the Bone lab have been an important part of my professional and personal time at Erasmus MC. I would like to acknowledge all my fellow colleagues that I met during my five years there: Adriana, Andrea, Anke, Bianca, Bram, Cindy, Jyoti, Iris, Katja, Marc, Marco, Marijke, Marjolein, Marta, Michelle, Pui, Rodrigo, Ruben and Tanja, my students Pierre-Yves, Gülistan and Dennis, and the numerous other students who have come through the lab. I thank you for all the help, stimulating scientific discussions, and for your friendship and all the fun we have had in and out of the lab. I particularly would like to thank Rodrigo for introducing me to EVs. I also thank Bram and Marijke for their help with animal studies, Iris for cell cultures, and Cindy for help with hematology-related experiments. I cannot finish my thanks by not mentioning all the cakes we had in the Bone lab. I would not be exaggerating if I admit that I ate more cakes in five years in the lab than in my entire life.

The cord blood studies discussed in this thesis would not have been possible without the help of hematology people. My sincere thanks goes to Jan Cornelissen and Eric Braakman, who provided me with an opportunity to learn about hematopoietic stem cells and gave me access to the hematology laboratory and research facilities. Without their precious support it would not have been possible to conduct this research. I cannot thank El-

win enough for his immense help with flow cytometry analysis and all kinds of other hematology-related issues. I would like to thank Mariette for assisting with *in vivo* studies and providing cord blood. I also would like to acknowledge Marc Raaijmakers for helpful scientific discussions during our bone-hematology meetings. I also thank Ayşegül and Lucia for their help with cell cultures.

Dozens of other people have helped with the project and supported me in many ways. I would like to thank Andre van Wijnen and his team for their tremendous help with next-generation sequencing data generation and analysis, Jeroen Demmers for proteomics studies, Gert-Jan Kremers for confocal imaging, Alex Nigg for 4Pi microscopy, and Mark Bourgondien for transmission electron microscopy. I also acknowledge everyone at Internal Medicine for listening to my presentations over the five years and for the stimulating questions, which incented me to widen my research from various perspectives. I would like to acknowledge the EV community that I met at Erasmus MC, ISEV meetings and round table discussions. Thank you for productive meetings and giving me more incentive to explore the fascinating world of vesicles.

In 2003, as a young and adventurous high school graduate I decided to go abroad to get a unique education experience, and gain a new outlook and perception on life and other cultures. It has been 13 years now, and it indeed has been a life changing experience. Of course, there were challenges and cultural norms I had to adapt to, though everyone I encountered was very welcoming. Finally in 2009, as a part of an Erasmus Mundus Masters program I came to the Netherlands, which has become such an important part in my life. Not only it is where I accomplished the most important achievement in my academic career, but also where I took the most important steps of my personal life: getting married with an amazing person and becoming a mother to a handsome little boy. It is also where I met so many amazing people that made the process of being abroad less stressful and overwhelming.

I would like to acknowledge all these amazing friends, though not in any particular order…

I met Andrea on my first day in the Bone lab. It was her first day too. Andrea, during our time in the lab you were not just my colleague but also a very good friend with whom I shared so many fun memories outside of work. I would like to thank my paranymphs Tanja and Marta for their help with my defence, and most importantly for our friendship that began in the Bone lab and became ripe throughout my years at Erasmus MC. Tanja, I am so sorry that you are leaving the Netherlands. I was so looking forward to have many play dates in the upcoming years, but I know we will meet somewhere sometime somehow. Marta, it was so much fun to share the same office with you. Thank you for listening to my chitchat, excitements and frustrations… Other close friends from Erasmus MC that I would like to mention here are Adriana, Cindy and Pierre-Yves. I would never forget all the chats and beautiful moments we shared.

I feel so lucky to have met so many special people outside of Erasmus MC as well. Fabai, your friendship has been so important for me. It is heartwarming to know that

you have been there for me since the first day we met during our masters. Romina, I am so happy you decided to spend couple of years here. It was so nice for me to have family and a very close friend from back home around, especially at the beginning of my Ph.D. Eda, it was a pleasure to have met you. I am grateful for all the fun memories we shared in Rotterdam. Federica and Sourena, thank you for the fun long night chats that always helped me clear my mind after a tough week at work. I also would like to thank all the Rotterdam mamas I met in the past year. Sharing the experience of being a new mother far from home gave me so much support to stay sane and strong. Also, I would like to mention Andrew, Brooke, Dafni, Lily, Lorraine, Maggie, Pinar, Selin and Veneta, among many others. Thanks everyone for your support through good and bad times, for social activities and for making me feel here at home. I would also like to thank all of my other friends who supported me in writing, and incented me to strive towards my goal. Many thanks to all my friends from back home, all the friends I met throughout my journey around the world, and everyone who became a part of my life and filled it up with good memories.

Last but not the least, I would like to thank the most important people in my life…my family…

I take this opportunity to express the profound gratitude from my deep heart to my beloved mother Iris, father Aslan and sister Dilara. Without their love and continuous support I would not have been where I stand today.

Sizi çok seviyorum. İyi ki hayatımda varsınız!

I would like to express appreciation to my dear husband Hugo, who embarked on this journey with me. You have been my motivation to pursue a Ph.D. degree. I always enjoy our enthusiasm to think of collaboration every time we have an exciting idea popping up at a dinner table. You are always my support in the moments when there is no one else to answer my queries. You are my classmate, my colleague, my love and my family.

Te amo con todo mi corazón!

Being a mother, without doubt, is the best thing that happened to me during my time in the Netherlands. Better said it is the best thing that has ever happened to me. Many people asked me how I was going to finish my Ph.D. with a little baby in my arms. Determination and discipline is what got me through, despite my growing belly, sleepless nights and a handful baby boy. Mateo, thank you for letting me write this thesis despite all your attempts to break my laptop. You are my inspiration for the future.

Seni çok seviyorum minik aşkım benim!

"To life…"

Jess Morhayim